

Component analysis with visualization of fitting – PopShare, a Windows program for data analysis

I. DUNKL AND B. SZÉKELY

Institute of Geology, University of Tübingen, D-72076, Germany (istvan.dunkl@uni-tuebingen.de)

It is always a question whether the results what we have measured represent one population or they form a mixture of more components. In the first case the average, standard deviation and other, commonly used statistical indicators are reliable figures and describing the distribution, but in the second case these are only meaningless numbers. To judge this question numerical tests are used. We present here a computer program, which performs some tests and visualizes the distribution, the goodness of fit, and searches the components using the SIMPLEX algorithm.

Figure 1: The "rhomb-plot" where the user can input quickly by mouse clicks the supposed mean, standard deviation for component 1 and 2 and also their ratio as "User Defined Parameters".

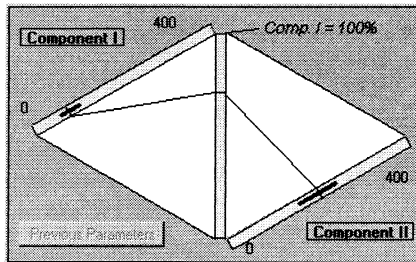


Figure 2: Results of SIMPLEX fitting (RMS: root mean square, W: weighted, K-S: Kolmogorov-Smirnov test).

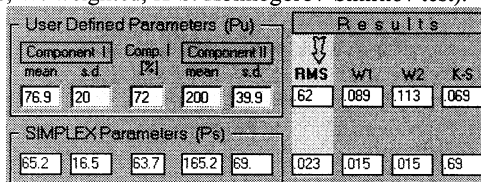
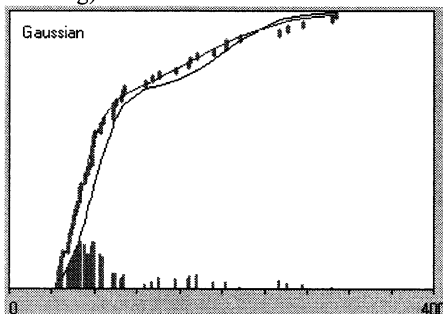


Figure 3: Graphic presentation of fitting (dots: cumulative distribution of measured data, vertical bars: residuals, thick line: fitting with User Defined Parameters, thin line: SIMPLEX fitting).



Detrital zircons from the Jack Hills metasediments, Western Australia: provenance record of the Earth's oldest material

S.J. DUNN, A.A. NEMCHIN, P.A. CAWOOD AND R.T. PIDGEON

Tectonics Special Research Centre, Curtin University, Western Australia (dunnsj@lithos.curtin.edu.au)

Detrital zircons up to 4.4 billion years old (Ga) occur in metaconglomerate from the Jack Hills metasedimentary belt (Compston & Pidgeon 1983; Mojzsis *et al.* 2001, Wilde *et al.* 2001) and are the only source of direct information about the Earth's early history. All work has so far concentrated on zircon grains extracted from a single sample of metaconglomerate with no attempt to establish either the distribution of old grains within the belt or variations in the detrital zircon age signature of the belt. The depositional environment of the sedimentary units and the character of potential source rocks is still unknown, although the time of deposition is considered to be about ~3.0 Ga, based on the youngest detrital grains found in the conglomerate.

We have extracted zircon grains from five samples representing three apparently conformable units (quartz-pebble conglomerate, quartzite and shale) and collected from both near the original sampling site and from the other end of the belt, some 70 km to the north-east.

All rock types contain various proportions of grains older than 4.0 Ga. Conglomerate and quartzite samples show age distributions similar to those reported in previous studies with the youngest detrital zircons at ca. 3.0 Ga. However, two shale samples contain a significant number of zircons with Late Archaean (2.7-2.5 Ga) as well as some grains as young as 1.9 Ga, which contradicts the existing view that the sediments have been deposited at ~3.0 Ga.

Detrital zircon age distributions suggest that the Jack Hills sedimentary belt consists of at least two distinct sequences deposited more than 1000 m.y. apart. The presence of ca. 4.2 Ga zircons in the younger sediments argues against the tectonic juxtaposition of the two parts of the sequence. Either the two temporally distinct parts of the belt were deposited in close proximity to >4.0 Ga source rocks or alternatively, the younger part of the sequence contains significant proportion of material derived from erosion of the older depositional sequence of the Jack Hills metasedimentary belt.

References

- Compston W. and Pidgeon R.T. (1983) *Nature* **399**, 252-255.
 Mojzsis S.J., Harrison T.M. and Pidgeon R.T. (2001) *Nature* **409**, 178-181.
 Wilde S.A., Valley J.W., Peck W.H. and Graham C.M. (2001) *Nature* **409**, 175-178.

The role of basalt chemical weathering on the CO₂ cycle

BERNARD DUPRE¹, CÉLINE DESSERT¹, ALINE GRARD²;
LOUIS FRANÇOIS², YVES GODDERIS¹, CLAUDE JEAN
ALLEGRE³ JÉROME GAILLARDET³.

¹ LMTG, Université Paul Sabatier, Toulouse, France
(dupre@lmtg.ups-tlse.fr)

² LPAP, Université de Liege, Belgium

³ IGP Paris Université P7

After discovering the role of runoff, T and physical erosion on chemical weathering, recent studies have shown the very important role of basalt weathering on the climate and CO₂ cycle. The aim of the presentation is to summarize the main existing arguments and to illustrate the effect of basalt's weathering.

Recent data have shown that chemical weathering of basalt is 5 or 10 time more efficient than the weathering of acidic silica rocks (granite, gneiss).

Second, a simple law is proposed by Dessert et al., (Chem. Geol. 2002

$f_w = R_f \times 18.41 \exp(0.0553 T)$ where f_w is the specific silicate weathering rate (t/km²/yr) and R_f is the runoff. This law is derived from compilation data of Iceland Reunion, Deccan, Java, Columbia, Massif Central (France) Cameroon, Parana, Sao miguel.

From these relationships and digital maps (temperature, runoff and surfaces of basalts), Dessert et al. (Earth; Planet. Sci. Lett. 188, 459-474 2002) have determined a CO₂ consumption rate of about 4.36 10¹² mol/yr, that represents between 32% and 37% of the flux derived from continental silicate determined by Gaillardet et al. (chem. Geol. 159 3-30 1999). As a consequence, the volcanic activity acts not only as a major CO₂ source, but also creates strong CO₂ sinks which cannot be neglected when attempting to improve our understanding of the geochemical and climatic evolution of the Earth.

Another example of the role of basaltic chemical weathering comes from the modelling trap eruptions such as the Deccan traps (Dessert et al E.P.S.L 188, 459-474). Two main effects are observed: first global air temperature increases during the emission of CO₂ into the atmosphere, then global climate is getting cold after the eruption. In the case of Deccan traps the global cooling effect approaches 0.5°.

The succession of basaltic emplacements that occurred during the Cenozoic may explain at least part of the climatic cooling recorded over the same period. Model simulations investigating the possibility that sharp cooling or glacial periods are linked to the formation of large basaltic provinces (Grard et al., EGS 2002), will be presented

Groundwater influences on the chemical budget of river water : clues from U isotopic ratios

S. DURAND, F. CHABAUX

CGS-EOST, 1 rue Blessig, F-67084 Strasbourg Cedex
(France)

Quantifying the influence of groundwater on the chemical budget of rivers waters remains an open question in Surface Earth Sciences. Here we propose to illustrate the potential of ²³⁴U/²³⁸U activity ratio to answer this question, with the case of the Rhine graben hydrosystem. Major and trace elements, ⁸⁷Sr/⁸⁶Sr isotopic ratios and (²³⁴U/²³⁸U) activity ratios, were analysed in the dissolved load of water samples collected in the main reservoirs, i.e. the Rhine river, its main tributaries, the shallow and deep ground-waters. Variations of major elements, trace elements and Sr isotope ratios of the water samples correlate with the lithological variations of the watersheds. By contrast ²³⁴U/²³⁸U ratios does not follow the same trend. Important variations are observed in waters draining a single lithology as illustrated with the Lauter stream, in the northern of the studied area. This stream flows on the lower Triassic sandstone. The sandstone reservoir contains numerous layers of more or less enriched clay minerals. Such a lithology allows a superposition of more or less developed aquifers. Three levels of these aquifers have been recognised and sampled. Each of them has specific U isotopic composition. The figure clearly demonstrates that U of the dissolved load of the Lauter water is influenced by contribution of these aquifers. U activity ratios of the dissolved load of the rivers does not only represent the ²³⁴U-²³⁸U fractionations resulting from the meteoritic weathering of surface rocks, but is also modified by inputs from groundwater to rivers. ²³⁴U/²³⁸U ratios become a good tracer to calculate influence of groundwater on the global chemical budget of stream water.

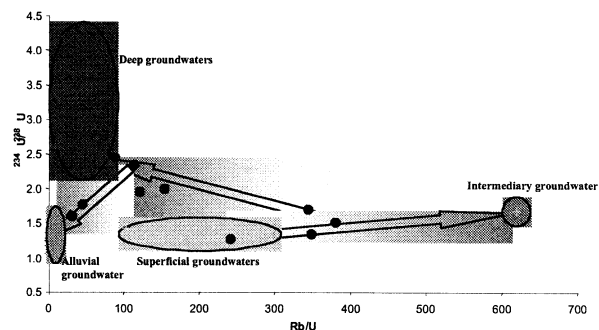


Figure : U-Sr variations in the Lauter river (a tributary of the Rhine river). Evidence from contribution of several aquifers.

Ocean paleotemperatures from ostracode Mg/Ca ratios

G.S. DWYER¹, T.M. CRONIN², AND P.A. BAKER¹

¹Division of Earth and Ocean Sciences, Nicholas School of the Environment and Earth Sciences, Duke University, Durham, NC, USA (gsd3@duke.edu)

²United States Geological Survey, Reston VA, USA (tcronin@usgs.gov)

We investigated ostracode Mg/Ca ratios as a benthic marine paleothermometer. Our research has focused on Mg/Ca ratios in the calcite shells of two common marine genera: deep-sea genus *Krithe* and shallow marine/estuarine genus *Loxococoncha*. Calibration studies, including analysis of modern and laboratory-raised specimens across a wide range of temperature and salinity conditions, confirms that *Krithe* and *Loxococoncha* Mg/Ca ratios are dominantly controlled by water temperature. We also evaluated *in vivo* effects including genus, species, gender, ontogeny, shell size, intra-shell Mg/Ca heterogeneity and possible diagenetic effects including partial dissolution and recrystallization. Phylogenetic and ontogenetic effects are indicated, including different Mg-thermodependence and intra-shell Mg distribution between *Krithe* and *Loxococoncha*. Dissolution is the dominant diagenetic effect on marine ostracode shells, but appears to have only a slight impact (decrease) on Mg/Ca ratios. Down-core applications, including results from deep and intermediate waters as well as from estuarine sites, collectively provide evidence for temperature variability at a range of timescales; from orbital to decadal. When coupled with benthic oxygen isotope records, deep-sea Mg/Ca-based temperature records allow for assessment of the timing and extent of continental ice-volume changes, whereas coupled estuarine records permit reconstruction of regional temperature and precipitation histories.

Origin of Enstatite Chondrites and Implications for the Inner Planets

D. S. EBEL¹ AND C. M. O'D. ALEXANDER²

¹ Dept. of Earth & Planetary Sciences, American Museum of Natural History, NY, NY 10024 USA (debel@amnh.org)

² Dept. of Terrestrial Magnetism, Carnegie Institution of Washington, 5241 Broad Branch Rd., Washington DC, 20015, USA (alexande@dtm.ciw.edu)

Over 90% of EC chondrules are enstatite-rich. Some enstatite was initially Fs_5 to Fs_{30} , and was reduced after formation, probably by interaction with a vapor in which reduced matrix phases were thermodynamically stable (Lusby *et al.* 1987; Weisberg *et al.* 1994). We are interested in the nature and nebular location of such a reducing vapor, in which EC minerals (e.g.- CaS, MgS) might have been stable.

Ebel and Grossman (2000) mapped dust enrichment conditions for thermodynamic stability of FeO-rich silicates using a CI chondrite dust composition. The highly unequilibrated, anhydrous, interstellar organic- and presolar silicate-bearing cluster IDPs (C-IDPs) may be closer to the primordial dust composition than CI dust, as suggested by observed C depletions, relative to solar, in dense interstellar clouds. C-IDPs are relatively reduced, with low FeO and high C contents. Alexander (2002) noted modest enrichments of C-IDP-like dust would create conditions reducing enough to stabilize EC minerals, unless ice was also concentrated. Also, recent solar photosphere measurements suggest a 25% lower O abundance than previous estimates (Prieto *et al.* 2001).

We calculated condensation using a C-IDP-like dust composition at dust enrichments of 10, 100 and 1000 times solar at $P^{\text{tot}}=10^{-3}$ bar. Oxygen is calculated from a 75% solar baseline. The dust is H-, N-free CI, with all S as FeS, and O sufficient to make rock-forming oxides of the remaining Fe, Si, Mg, etc. At 100x enrichment, CaS is stable below 1290K, and MgS below 1180K. At 1290K, modal pyroxene (Fs_0) and olivine (Fa_0) are approximately equal. Although the system tracks $f(O_2) \sim (IW-4)$ above 1720K, $f(O_2)$ drops to (IW-8) by 1290K. Surprising! Silicate FeO decreases with decreasing T.

These results suggest that at the time the asteroids were forming, the snow line was near the inner edge of the asteroid belt, the presumed location of EC parent bodies. Bodies forming inward of the snow line would have been reduced, unless during high-T processing the dust enrichments relative to gas were modest. This has implications for the terrestrial planets' inventories of highly and moderately volatile element (and water) sensitive to reducing *versus* oxidizing conditions.

References

- Alexander C.M.O'D. (2002) *LPSC XXXIII*, Abs.#1864.
 Ebel D.S. and Grossman L. (2000) *GCA* **64**, 339-366.
 Lusby D., Scott, E.R.D., and Keil K. (1987) *Proc. Lunar Plan. Sci. Conf.* 17th, *J Geophys. Res. Suppl.* **92**, E679-E695.
 Prieto C.A., Lambert D.L., and Asplund M. (2001) *Astrophys. J. Letters* **556**, L63-L66.
 Weisberg M.K., Prinz M., and Fogel R.A. (1994) *Meteoritics* **29**, 362-373.

REE, Th and U abundances in individual chondrules from Dhajala, Allegan and Bjurböle chondrites

M. EBIHARA¹, K. HAYANO¹ AND T. NOGUCHI²

¹Department of Chemistry, Tokyo Metropolitan University, Hachioji, Tokyo 192-0397, JAPAN (ebihara-mitsuru@c.metro-u.ac.jp)

²Department of materials and biological science, Ibaraki University, Mito, Ibaraki 310-8512, JAPAN

It is apparent that chondrules once experienced melting processes of the precursor material. As relict minerals are still present in chondrules of some UOCs, these chondrules may provide us information concerning the precursor materials and melting episodes. Chondrules in EOCs have experienced thermal metamorphism on their parent bodies and, hence, may help us to understand their metamorphic activities. In this study, we separated chondrules from Dhajala (H3.8), Allegan (H5) and Bjurböle (LL4) and studied them for trace element compositions and mineralogical/petrological characteristics.

Chondrules were separated mechanically, embedded in acetone-soluble resin and sawed into three portions. One portion was used for determining REE, Th and U by ICP-MS. Another portion was used for mineralogical and petrological descriptions by SEM and EPMA.

REE, Th and U abundances in Dhajala chondrules are generally unfractionated from and higher than those in the bulk sample. Eu anomaly (negative) is commonly but not ubiquitously observed. There seems no apparent correlation between REE abundances and mineral/petrological characteristics. In contrast, REE, Th and U abundances are largely variable in chondrules of Allegan and Bjurböle even though chondrule types are identical. Lanthanoids (REE) (with positive Eu anomaly) and actinoids (Th and U) are generally fractionated, with REE being relatively depleted. Our study suggests that REE, Th and U abundances in chondrules inherited those from the precursor material. During thermal metamorphism on ordinary chondrite parent bodies, REE migrated into surrounding minerals much faster than Th and U.

Halogen-derived noble gases in the Allende meteorite: A laser microprobe study

N. EBISAWA¹, R. OKAZAKI¹, K. NAGAO¹
AND A. YAMAGUCHI²

¹Laboratory for Earthquake Chemistry, Graduate School of Science, University of Tokyo, Japan
(n-ebisaw@eqchem.s.u-tokyo.ac.jp)

²Antarctic Meteorite Research Center, National Institute of Polar Research, Japan

Introduction

Micro-distribution of halogens in meteorites still remains unsolved due to the difficulty of their *in situ* microanalysis. We intend to make the matter clear with noble gas isotopes produced by decay of extinct nuclide ¹²⁹I and by neutron capture on ³⁵Cl, ³⁷Cl, ⁷⁹Br, ⁸¹Br and ¹²⁷I in space. A high sensitive mass spectrometer with a laser microprobe allows us to determine the small quantities of halogen-derived noble gases. In addition, it is convenient that we can investigate only the intrinsic halogens of meteorites independent of terrestrial contamination.

In this study, we investigated micro-distribution of noble gases in the Allende meteorite, mainly a CAI. 7-10 micrograms of meteorite material was melted with laser heating and the extracted noble gases were measured. These mass spectrometers were modified to be available for various extraterrestrial materials such as meteorites [1, 2, 3] and single micrometeorites [4].

Results and discussion

Prior to noble gas analysis, electron microprobe analysis revealed that marginal areas of the CAI were partly enriched in chlorine.

Noble gas analysis was performed in about 70 points in the CAI and neighbouring matrix. The chlorine-rich areas of the CAI have significantly high concentrations of ¹²⁹Xe than the chlorine-poor areas. Excess of ⁸⁰Kr produced by neutron capture on ⁷⁹Br correlated with the ¹²⁹Xe distribution. Several ¹²⁹Xe-rich points had relatively low ³⁸Ar/³⁶Ar ratios, which would be caused by the difference in cross section of neutron capture between ³⁵Cl and ³⁷Cl. The results show that the halogen-rich area was formed in a period when ¹²⁹I was still alive. Although we cannot determine the absolute time scale of the event when the halogens were enriched in some parts of CAIs, it must have occurred in the early stage of solar system formation.

References

- [1] Nakamura T., Nagao K. and Takaoka N., (1999), *Geochim. Cosmochim. Acta* **63**, 241-255
- [2] Nakamura T., Nagao K., Metzler K. and Takaoka N., (1999), *Geochim. Cosmochim. Acta* **63**, 257-273
- [3] Okazaki R., Takaoka N., Nagao K., Sekiya M. and Nakamura T., (2001), *Nature* **412**, 795-798
- [4] Osawa T., Nagao K., Nakamura T. and Takaoka N., (2000), *Antarct. Meteorit. Res.* **13**, 322-341

The geochemical impact of MSWI bottom ash on the environment

U. EGGENBERGER¹, R. BUNGE² AND K. SCHENK³

¹Institute of Geological Science, University of Bern, Switzerland (eggenberger@geo.unibe.ch)

²Hochschule Rapperswil, umtec, Rapperswil, Switzerland (rainer.bunge@hsr.ch)

³Swiss Agency for Environment, Forests and Landscape, SAEFL, Switzerland (kaarina.schenk@buwal.admin.ch)

Introduction

In Switzerland domestic waste without thermal treatment is no longer allowed to be stored in land fills. Consequently, the production of MSWI bottom ash has reached 650'000 tons per year, which have to be stored in special landfills. The present study is the first nation wide investigation to chemically and mineralogically characterize the bottom ash of all 27 incinerators. Special attention was also directed to the possibilities to separate metal fraction of the bottom ash using mechanical separation techniques, to recover metal fractions, to reduce landfill volume, and to evaluate possible changes to legislation for disposal.

Results and Conclusions

Regarding major elements the chemical compositions of the of the 27 bottom ash do not show big differences and are comparable to mafic/ultramafic rocks. Indicator for the different observed melting conditions can however be found using the Ca/Si ratio forming melilithes and/or anorthite. Relatively small variation is observed for conservative behaving trace elements such as e.g. Zr which is rarely used in consumer products. Volatile elements such as Pb, Hg, and Cd are found as good indicators for thermal conditions of the incineration process, and C_{org} content for reaction time and temperature. Today's legislation prescribes bulk chemical analyses and leaching tests for the classification of e.g. "inert material" (TVA, 1990). In respect to inert material thresholds, some bulk metal concentrations are significantly elevated: Pb, Zn and Cu (3'000-40'000ppm). In contrast, leaching behaviour of the bottom ash in respect to TVA tests are mostly below legislation thresholds. To obtain better information about possible long-term behaviour of the residue in the hydrosphere, also alternative leaching tests have been adopted considering buffering capacity and leachability of trace metals under defined pH conditions.

Today still large amount of metals in waste enter incinerator plants, and most of them remain unaltered in the bottom ash. Using special mechanical treatment of the bottom ash, large amounts of ferrous metals, Cu, and Al could be separated in the fraction >2mm.

References

- Technische Verordnung über Abfälle (TVA; 10. Dez. 1990); SR 814.600

Laser ablation-ICP-MS compositional profiling of chamber walls in planktonic Foraminifera; implications for Mg/Ca thermometry

S. EGGINS¹, P. DE DECKKER² AND J. MARSHALL¹

¹Research School of Earth Sciences, Australian National University, Canberra, 0200, Australia
(Stephen.Eggins@anu.edu.au, John.Marshall@anu.edu.au)

²Department of Geology, Australian National University, Canberra, 0200, Australia
(Patrick.DeDeckker@anu.edu.au)

We have profiled compositional variation through the chamber walls of individual Foraminifera using a new, high resolution, laser ablation ICPMS technique. Mg/Ca ratios are able to be measured accurately and precisely in specific shell parts (wall layers and chambers) along with simultaneous analysis of other trace elements (e.g. Mn, Zn, Sr, Ba, Cd, U) and their isotopes with detection limits to low ng/g levels in <60 seconds. The mass of material consumed by each analysis is ~20-30ng (cf. typical test mass of ~10-30µg) and replicate analyses can be made on individual chambers. The technique readily distinguishes outer crust and inner primary wall layer compositions, as well as the presence of an outermost zone characterised by Mg, Mn, Ba and Zn concentrations increasing strongly towards the surface. Exploratory studies on planktonic Foraminifera (*Globigerina* and *Neoglobobulimina* sp.) define the capabilities of our technique, highlight the inherent limitations of conventional bulk analysis methods, and provide new insights into fundamental biomineralisation processes. Mg/Ca ratios can be reproducibly measured within particular chamber wall layers to $\pm 2-5\%$ and more uniformly distributed Sr/Ca ratios to $\pm 1\%$. Inner primary wall layers of different chambers in the same test are commonly found to have distinct Mg/Ca compositions, whereas the inner portions of the outer crust on all chambers have similar and lower Mg/Ca. The strong enrichment in Mg, Mn, Ba, and Zn toward the outermost crust surface in both modern and fossil shells, suggests a significant vital effect change during the biomineralisation process. The ability to measure Mg/Ca in shell parts grown under specific seawater conditions, rather than bulk compositions integrated over the life-cycles of entire shells, may enable calibration of more accurate and precise Mg/Ca thermometers than is currently possible. The tiny amount of sample consumed also allows for subsequent $\delta^{18}\text{O}$ microanalysis of the same shell material, and the simultaneous acquisition of other trace elements presents an opportunity to further develop their potential as proxies for seawater temperature, composition, and nutrient levels.

The structure of hematite (0001) surfaces in water: STM and resonant tunneling calculations of coexisting O and Fe terminations

CARRICK M. EGGLESTON¹, ANDREW G. STACK¹, KEVIN M. ROSSO², AND STEVEN R. HIGGINS¹

¹Department of Geology and Geophysics, University of Wyoming, Laramie, WY 82071-3006 USA
(carrick@uwyo.edu)

²William R. Wiley Environmental Molecular Sciences Laboratory, Pacific Northwest National Laboratory, P.O. Box 999, MSIN K8-96, Richland, WA 99352 USA
(Kevin.Rosso@pnl.gov)

The structure of hematite (0001) surfaces is not fully understood; questions remain about the existence of Fe- and O- terminations of (0001) terraces. The presence or lack of Fe atoms at the (0001) surface that can be partially coordinated by adsorbed molecules is important for understanding a wide range of adsorption phenomena. We have imaged hematite (0001) surfaces in air and aqueous solution using STM and electrochemical STM (EC-STM), and interpreted images with the aid of a resonant tunneling model (RTM) parameterized using ab-initio calculations.

Our STM and RTM results are consistent with mixed O- and Fe-terminated (0001) surfaces (Figure 1). For surfaces that had been acid etched and extensively annealed, a periodic (period = 2.2 ± 0.2 nm) arrangement of O- and Fe-terminated domains was observed. Two different borders between domains should occur, one in which the Fe-termination is high relative to the O-termination and vice versa. These borders have significantly different heights, allowing us to conclude that the Fe-termination is topographically high on most terraces. Surface domains appear to be quite stable, with little evidence for dissolution at pH 1.

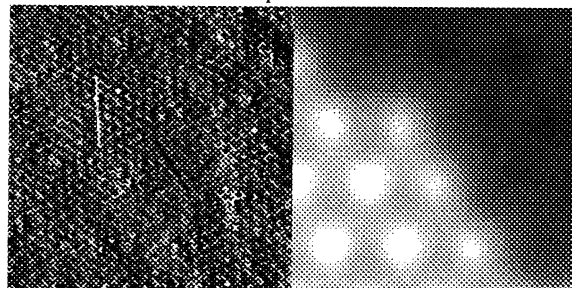


Figure 1: Two different domains in a 20x20 nm STM image of hematite (0001)(+500 mV; left) compared to an RTM calculation (2x2 nm) for +500 mV, Fe termination high.

Consistently, nonperiodic material is imaged at higher negative sample biases, and the characteristics of this material are consistent with resonant tunneling through "adsorbed" Fe atoms at the surface.

Apatite (U-Th)/He Signals of Transient Topography

T. A. EHLERS AND K. A. FARLEY

California Institute of Technology, Division of Geological and Planetary Sciences, Pasadena, CA
(ehlers@gps.caltech.edu, farley@gps.caltech.edu)

The influence of evolving topography on the exhumation history of mountain ranges has long been supposed but there have been few attempts to quantify the magnitudes of such interactions. We use a coupled atmospheric and surface process numerical model to quantify how the evolution of mountainous topography influences the cooling history of exhumed apatite (U-Th)/He thermochronometer samples.

Methods

The atmospheric model predicts orographic precipitation as a function of atmospheric moisture content, prevailing wind strength, temperature, and topographic slope (Roe et al., 2002). The coupled atmospheric and surface-process model predicts plan-form topographic evolution as a function of tectonic uplift, and processes of hill slope and fluvial erosional (Braun and Sambridge, 1997). Exhumed (U-Th)/He sample ages are calculated using multi-dimensional thermal models and a cooling-rate dependent model of helium diffusion in apatite.

Results

Model results indicate that orography is a first-order control on the topographic and exhumation history of mountain ranges. The model predicts that for a uniformly uplifting crustal block an orographically produced pulse of high erosion rates will propagate across the range in the wind direction and cause the drainage divide to migrate over time. This process of divide migration results in a trend of high to low rock exhumation rates across range in the wind direction. During the period of divide migration exhumed apatite (U-Th)/He sample ages are predicted to be youngest on the windward side of the range and increase towards the drainage divide. The topography eventually reaches steady state when erosion rates equal the exhumation rates across the orogen. Once the topography is in steady state the difference in exhumed apatite (U-Th)/He sample ages on the windward and leeward sides of the range decreases and spatial variations in ages occur only between valleys and ridges where exhumed sample cooling histories differ due to topography.

Conclusions

The coupled atmospheric and surface process model provides a climatic, geomorphic, and structural context for interpreting (U-Th)/He cooling, and cosmogenic exposure ages in areas with evolving topography. This study demonstrates that spatial variations in cooling ages can result solely from geomorphic processes and does not necessitate structurally controlled variable uplift rates.

References

- Roe, G.H., Montgomery, D.R., Hallet, B., (2002) *Geology*, 30, 143-146.
Braun, J., Sambridge, M., (1997) *Basin Research*, 9, 27-52.

Complex organics and prebiotic molecules in space

P. EHRENFREUND¹, R. RUITERKAMP¹, O. BOTTA¹,
Z. PEETERS¹, B. FOING²

¹Astrobiology Laboratory, Leiden Institute of Chemistry,
POBox 9502, 2300 RA Leiden, The Netherlands
²ESA, ESTEC-RSSD, 2200 AV Noordwijk, The Netherlands

The connection between interstellar and solar system material is discussed from the perspective of recent laboratory studies testing the spectroscopic properties and photostability of large polycyclic aromatic hydrocarbons and prebiotic molecules. We discuss the life cycle of these molecules in extragalactic environments, the galactic interstellar medium, comets and meteorites.

U and Pb isotope ratios in manganese nodules by MC-ICP-MS

S. EHRLICH., M. BAR-MATTHEWS Y. HARLAVAN AND L. HALICZ

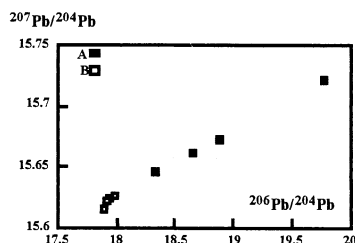
Geological Survey of Israel, 30 Malchei Israel St. Jerusalem, 95501, Israel (ehrich@mail.gsi.gov.il; matthews@mail.gsi.gov.il; y.harlavan@mail.gsi.gov.il; ludwik@mail.gsi.gov.il)

Isotope ratios of U and Pb were measured in two groups of manganese nodules from the Cambrian Timna Formation, Israel. The division into two groups was based on petrographical, major and trace element geochemistry (Bar-Matthews, 1987). The first group (A) of nodules is composed mainly of pyrolusite and hollandite, with Mn, Ba, Pb and U concentrations of 45-50%, 1-2.5%, 0.1-0.8% and 500-3500 ppm respectively. The second group (B) was formed by alteration of the former, and contains mainly coronadite, with Mn, Ba, Pb, and U concentrations of 9-30%, 0.2-5%, 1-2.5% and 60-150 ppm respectively.

Samples were dissolved in $\text{HNO}_3 + \text{H}_2\text{O}_2$ and measurements were obtained on the acid soluble fraction using the "Nu Instrument" MC-ICP-MS. Two sets of analyses were performed, with and without matrix separation. For Pb analyses, measurements were carried out with Meinhard nebulizer, and thallium ($^{205}\text{Tl}/^{203}\text{Tl}=2.3875$) was added to enable correction for mass discrimination. U was measured using an Aridus system with microconcentric nebulizer (MCN). Mass discrimination was corrected using U internal standard $^{238}\text{U}/^{235}\text{U}=137.88$.

The results obtained from the matrix-separated and unseparated samples were identical, with a slightly better (2σ) precision for the separated sample of $^{208}\text{Pb}/^{204}\text{Pb}$, $^{207}\text{Pb}/^{204}\text{Pb}$, $^{206}\text{Pb}/^{204}\text{Pb}$ 60-80ppm; $^{208}\text{Pb}/^{206}\text{Pb}$ and $^{207}\text{Pb}/^{206}\text{Pb}$ ~30ppm and $^{234}\text{U}/^{238}\text{U}$ 0.2-0.4%.

The isotopic results support the distinction between the two groups. On a $^{207}\text{Pb}/^{204}\text{Pb}$ vs. $^{206}\text{Pb}/^{204}\text{Pb}$ plot the nodules from group A have higher and variable ratios compared with the nodules of group B. Both groups fall probably on a mixing line (Fig. 1). $^{234}\text{U}/^{238}\text{U}$ in group A nodules fall close to the equilibrium values of 54.887 (Cheng et al., 2000), whereas in group B nodules the values fall usually below this value.



References

- Bar-Matthews M., (1987) *Geol. Mag* **124**, 211-229
Cheng H. et al., (2000) *Chem. Geol.* **169**, 17-33

Use of surface analysis, solid-state spectroscopy, and geochemical modelling to characterize phosphate-stabilized wastes

T.T. EIGHMY¹, B.S. CRANNELL², J.D. EUSDEN, JR.³, L.G. BUTLER⁴, AND F.K. CARTLEDGE⁵

¹ Environmental Research Group, University of New Hampshire, Durham, N.H. (taylor.eighmy@unh.edu)

² Environmental Research Group, University of New Hampshire, Durham, N.H. (bradley.crannell@unh.edu)

³ Geology Department, Bates College, Lewiston, Maine (deusden@abacus.bates.edu)

⁴ Chemistry Department, Louisiana State University, Baton Rouge, Louisiana (lbutler@lsu.edu)

⁵ Chemistry Department, Louisiana State University, Baton Rouge, Louisiana (chcart@unix1.sncc.lsu.edu)

Chemical stabilization of inorganic wastes can reduce leachability of heavy metals through formation of geochemically stable and insoluble precipitates. Understanding the immobilization reaction, the reaction products, and the leaching behaviour of the treated material is crucial for a mechanistic understanding of the process.

Our group has focused on phosphate stabilization of various MSW ashes, electric arc furnace dusts, smelter dusts, mine tailings, and metal-contaminated sediments. The approach typically characterizes both the untreated and the treated wastes before and after aggressive leaching with the Dutch NEN 7341 Availability Leach Test. A variety of bulk spectroscopic techniques (petrography, SEM-WDS, SEM-EDAX, XRD, STEM-XRM, MAS-NMR and EXAFS) are used to characterize untreated residues and metal phosphate reaction products. XPS is particularly useful in identifying surface species where leaching first occurs. SIMS can identify reaction mechanisms (sorption, surface precipitation to pre-existing phases, discrete phase precipitation) via depth profiling of discrete reactant particle agglomerates. pH-static leaching coupled with the geochemical thermodynamic equilibrium modelling with MINTEQA2 can confirm chemical stabilization and solid phase control of leaching. MINTEQA2 databases have been extensively modified to include many metal phosphate solids and ideal solid solutions for better applicability.

Immobilization mechanisms almost always involve precipitation of discrete metal phosphate crystalline solids or solid solutions. Apatite family (e.g., $\text{Ca}_5(\text{PO}_4)_3\text{OH}$) minerals for Cd and Pb and tertiary metal phosphates (e.g. $\text{Zn}_3(\text{PO}_4)_2$) for Zn, Cu, and Cd are typical reaction products; these phases are very insoluble and are present after the treated residues have been subjected to aggressive leaching. Work is ongoing on the application of apatite-based reactive barriers for waste containment and plume interception.

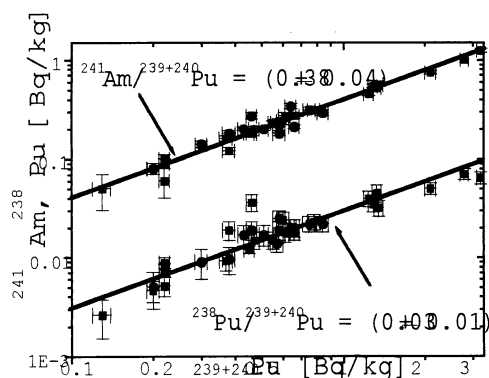
Actinide isotope analysis for determining different nuclear fallout components in soils

J. EIKENBERG¹, S. BAJO¹ AND M. RUETHI¹

¹Paul Scherrer Institut CH-5232 Villigen (PSI)
(jost.eikenberg@psi.ch)

The Swiss immission surveillance program around nuclear installation includes analyses of soil samples for various cosmic, terrestrial and particularly anthropogenic radioisotopes such as ⁷Be, ¹⁴C, ⁴⁰K, ⁸⁹Sr, ⁹⁰Sr, ¹³⁴Cs, ¹³⁷Cs, U- and Th-series decay products as well as the actinides ²³⁸Pu, ²³⁹⁺²⁴⁰Pu, ²⁴¹Pu, ²⁴¹Am, ²⁴⁴Cm. The isotopes of Pu and Am can be used to determine the fraction of hot particle fallout from different nuclear accidents, e.g. derived from surface atomic bomb tests in the 60ies or the Chernobyl accident, that occurred 16 years ago. Figure 1 shows that there is a strong correlation between ²³⁸Pu, ²⁴¹Am and ²³⁹⁺²⁴⁰Pu. The ²³⁸Pu/²³⁹⁺²⁴⁰Pu ratio of 0.03 ± 0.01 calculated via regression analysis agrees well with literature values obtained from various other sites in the northern hemisphere. For the ²⁴¹Am/²³⁹⁺²⁴⁰Pu ratio a value of 0.38 ± 0.04 was obtained. This result is within uncertainty identical to the present day ²⁴¹Am/²³⁹⁺²⁴⁰Pu ratio of 0.36 calculated via ²⁴¹Pu/²⁴¹Am progenitor/progeny relationship and additionally considering that the initial ²⁴¹Pu/²³⁹⁺²⁴⁰Pu ratio resulting from nuclear weapon testing in the 60ies was about 13. This result shows clearly that ²⁴¹Am measured in the samples analysed here can be well explained via support from decaying ²⁴¹Pu initially released during the surface A-bomb testing period meaning that contribution of heavy particles from the Chernobyl accident are not significant in Central Europe.

Figure 1: Correlation diagram with ²³⁸Pu vs. ²³⁹⁺²⁴⁰Pu and ²⁴¹Am vs. ²³⁹⁺²⁴⁰Pu obtained on Swiss soil samples from various locations.



Hydrogen-isotope geochemistry of the CM chondrites

JOHN M. EILER, NAMI KITCHEN

California Institute of Technology, Pasadena CA 91125,
eiler@gps.caltech.edu

Hydration of initially anhydrous silicates and oxides is a common and significant early solar system processes recorded by the carbonaceous chondrites. We present new data constraining the hydrogen isotope geochemistry of the CM chondrites, which are characterised by a wide range in degree of hydration. Our study makes use of a recently developed method for analysis of D/H ratios of 10^{-9} mol quantities of water released by heating small (10's of microgram) solid samples.

Data for four CM chondrites (Murchison, Mighei, Murray, Cold Bokkeveld) document a trend of monotonically decreasing matrix D/H with increasing $[\delta^{18}\text{O}_{\text{matrix}} - \delta^{18}\text{O}_{\text{whole-rock}}]$ —a measure of the extent of aqueous alteration. The upper and lower limits in matrix D/H are 0.000148 (Murchison) and 0.000125 (Cold Bokkeveld). Mighei and Murray yielded intermediate D/H ratios of 0.000143 and 0.000137, respectively. A nearly anhydrous CM chondrite (L85311) was also analysed but was not sufficiently well resolved from background to yield a reliable D/H ratio. The D/H ratios of individual altered chondrules from both Cold Bokkeveld (highly hydrated) and Murchison (modestly hydrated) are equal to one another and to that for Cold Bokkeveld matrix; i.e., altered chondrules from both H-rich and H-poor samples have D/H ratios equal to that of the most extensively hydrated matrix. Replicate analyses suggest matrix is isotopically homogeneous within any one sample.

These data are not easily reconciled with either simple (0-dimensional) or chromatographic (1-dimensional) models of reaction between water and initially H-poor rock, in part because such models generally predict hyperbolic relationships between H-isotope composition and extent of aqueous alteration rather than the linear relationship we observe. Our results could be explained if the matrices of CM chondrites contained substantial amounts of hydrogen *before* they underwent the episode of aqueous alteration responsible for their first-order geochemical and mineralogical variations, or if they are mechanical mixtures of two components that did not share the same history of hydration and/or dehydration. Finally, our data suggest the D/H ratio of water that infiltrated the CM chondrites was ca. 0.000132. This value is interpretable as a constraint on the temperature at which infiltrating water last equilibrated with the dominant H reservoir of nebular H₂; this temperature was 282 ± 50 K if the D content of water was influenced only by H₂O(v) — H₂(v) equilibrium and 390^{+110}_{-90} K if water was isotopically fractionated by formation of ice at a 'nebular snow line' before incorporation into the CM parent body. The principle source of uncertainty in these estimates is the protosolar D/H ratio (ca. 0.000034 ± 10).

Concentration and carbon stable isotope patterns of methane and DIC in deep peatlands – Implications for the microbial methanogenic pathways and gas transport

B. EILRICH¹, M. LEUENBERGER², S.J. BURNS³,
C.E. WEYHENMEYER⁴, AND P. STEINMANN¹

¹ Institut de Géologie, Université de Neuchâtel, Switzerland
(bernd.eilrich@unine.ch; philipp.steinmann@unine.ch)

² Klima- und Umwelphysik, Universität Bern, Switzerland
(leuenberger@climate.unibe.ch)

³ Department of Geosciences, University of Massachusetts
Amherst, USA (sburns@geo.umass.edu)

⁴ Lawrence Livermore National Laboratory, Livermore, USA
(weyhenmeyer1@llnl.gov)

Abstract

This study reports the results of a field study from October 1999 to August 2001 at the Etang de la Gruère (EGr) Bog in the Swiss Jura Mountains. Pore water samples were obtained in situ using diffusion chambers ("peepers") down to a depth of almost 6 m. Methane concentration of up to ca. 0.5 mM in the upper catotelm are comparable to those reported from shallow peat at other locations. Values continue to increase to almost 2.4 mM in the deep layers. The DIC concentration also generally increases with depth from ca. 1 mM in 0.5 m depth to up to 12 mM in 5 m depth. While DIC became less depleted in ¹³C with depth (ca. -22 ‰ vs. VPDB in the upper to ca. +9 ‰ in the lower catotelm), $\delta^{13}\text{C}$ values for pore water methane at EGr showed no straight trend with depth. Methane was isotopically light with $\delta^{13}\text{C}\text{-CH}_4$ values ranging from ca. -69 to -58 ‰ vs. the VPDB standard. The results indicate that CO₂-reduction represents a "background" microbial process, while the intensity of acetate splitting is much more variable depending mainly on temperature and the availability of acetate as metabolic substrate.

Significant seasonal variations can be inferred from concentration and isotope data for pore water methane in particular. These variations can be explained by the seasonal and depth-related change of the methane producing pathways: CO₂ reduction (lowest $\delta^{13}\text{C}\text{-CH}_4$ and high fractionation between CH₄ and CO₂) versus acetate splitting (higher $\delta^{13}\text{C}\text{-CH}_4$ and moderate CH₄-CO₂ fractionation). Transport processes such as pore water advection, molecular diffusion, and ebullition have a major impact on the concentration of the chemical species in depth/time space.

A numerical model adapted to the observations made at EGr indicates that gas transport by bubble formation is by far (maybe over 70 times) more efficient than diffusive transport. The discrepancies between model and field results underline the importance of the seasonality of labile organic precursor availability and over-saturation effects.

Kinetic Effects on Calcium Isotope ($\delta^{44}\text{Ca}$) Fractionation in Calcium carbonate

A. EISENHAEUER¹, N. GUSSONE¹, M. DIETZEL²,
A. HEUSER¹, B. BOCK¹, F. BÖHM¹, H. J. SPERO³,
D.W. LEA⁴, J. BIJMA⁵, R. ZEEBE⁵ AND TH. F. NÄGLER⁶

¹ GEOMAR Forschungszentrum für marine
Geowissenschaften, Wischhofstr.1-3 24148 Kiel Germany
(aeisenhauer@geomar.de)

² Technische Universität Graz, Austria

³ University of California, Davis, U.S.A.

⁴ University of California, Santa Barbara, U.S.A.

⁵ Alfred Wegener Institut für Polar und Meeresforschung,
Bremerhaven, Germany

⁶ Universität Bern, Erlachstrasse 9a 3012 Bern Switzerland

The calcium isotope ratios ($\delta^{44}\text{Ca}$) of *Orbulina universa* and of inorganically precipitated aragonite are positively correlated to temperature. The slopes of 0.019 and 0.015 ‰ °C⁻¹ are a factor of 13 and 16 times smaller than the previously determined temperature dependence of 0.24 ‰ °C⁻¹ measured on *Globigerinoides sacculifer* (Näglér et al., 2000). The observed $\delta^{44}\text{Ca}$ fractionation is positively correlated to temperature. This fractionation is opposite to the oxygen isotopic fractionation ($\delta^{18}\text{O}$) which is inversely correlated to temperature in calcium carbonate (CaCO₃). This difference in sign is explained by a model that takes into account that Ca²⁺ ions, forming ionic bonds, are affected by kinetic fractionation only whereas covalently bound atoms like oxygen are also affected by equilibrium fractionation. From thermodynamic considerations it can be shown that the slope of the enrichment factor $\alpha(T)$ is mass dependent. However, the calculated mass for *O. universa* and the inorganic precipitates is about 640 amu (atomic mass units) which is not compatible with the expected ion mass for ⁴⁰Ca and ⁴⁴Ca. To reconcile this discrepancy we propose that Ca diffusion and Ca isotope fractionation at liquid/solid transitions involves the transport of Ca²⁺-aquocomplexes (Ca[(H₂O)₆]_n²⁺) rather than pure Ca²⁺ ion diffusion. From our measurements we calculate that such a Ca²⁺-aquocomplex correlates to a hydration number of up to 33 water molecules (Ca[(H₂O)₆]_{4.6}²⁺) although alternative complexation with other anions cannot be ruled out. The strong temperature dependence of $\delta^{44}\text{Ca}$ in *G. sacculifer* but weak temperature dependence in *O. universa* suggests considerable differences in their calcification mechanisms.

References

Näglér T., Eisenhauer A., Müller A., Hemleben C., and Kramers J. (2000) The $\delta^{44}\text{Ca}$ -temperature calibration on fossil and cultured *Globigerinoides sacculifer*: New tool for reconstruction of past sea surface temperatures. *Geochemistry, Geophysics, Geosystems* 1(2000GC000091)

Organic Contaminants in Lakes: Atmospheric Exchange and Linkage to the Trophic Status of Lakes

S.J. EISENREICH¹, J. DACHS², J.E. BAKER³,
J.J. JEREMIASON⁴

¹Institute for Environment and Sustainability, JRC, European
Commission, Ispra, IT steven.eisenreich@jrc.it

²Dept. of Chemistry, CSIC, Barcelona, Spain

³Chesapeake Biological Laboratory, Solomons, MD USA

⁴J.J. Jeremiason, MN Pollution Control Agency, St. Paul, MN
USA

Air-water exchange fluxes of polychlorinated biphenyls (PCBs) and polycyclic aromatic hydrocarbons (PAHs) have been determined in small lakes (ELA, Canada), the Great Lakes (Green Bay; Lake Michigan; Lake Superior) and in the estuaries of the Mid-Atlantic States (NY-NJ Harbor Estuary; Chesapeake Bay). In systems previously contaminated by PCBs, volatilization fluxes are large and play a dominant role in aquatic losses and as sources to the regional atmosphere. Other aquatic systems near urban-industrial centers experience enhanced deposition (absorptive fluxes) resulting from elevated concentrations in urban plumes. The controls and importance of air-water exchange of PCBs and PAHs in system mass balances and inventories, and in direct contamination of aquatic food webs will be discussed with examples from these well-studied systems. Air-water exchange of organic contaminants is an important if not dominant contributor to contamination of phytoplankton, the base of the aquatic food web, and thus is closely linked to carbon cycling and trophic status. In addition, improved physical-chemical properties of organic compounds and modeling frameworks permit the re-evaluation of organic chemical fluxes first determined 5 to 15 years ago, and their relative importance to total loads.

Various graphite morphologies with a diversity of C- and N-isotopic signatures in the highly equilibrated Acapulco meteorite

A. EL GORESY¹, E. ZINNER², P. PELLAS³ (DECEASED)
AND C. CAILLET³

¹Max-Planck-Institut für Chemie, 55128 Mainz, Germany
(goresy@mpch-mainz.mpg.de)

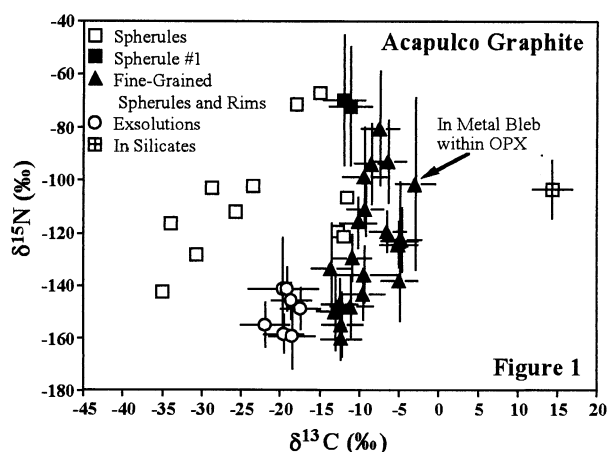
²Washington University, St. Louis, MO, 63130, USA
(ekz@howdy.wustl.edu)

³Muséum National d'Histoire Naturelle, 75005 Paris, France
(ccaillet@mnhn.fr)

Introduction

Acapulco is a highly equilibrated meteorite and a member of the acapulcoite-lodranite clan with strong chemical affinities to H-chondrites [1]. It has experienced partial melting and pervasive re-crystallization [1], a process expected to erase primordial N-isotopic signatures.

In a detailed petrographic-isotopic study of graphite in this meteorite we encountered eight different graphite morphologies, either in close vicinity or inter-grown with each other. These include spherulitic, feathery, fibrous bands, round fine-grained inclusions, exsolution veneers between kamacite and taenite, and single crystals in the silicate matrix. The C- and N-isotopic ratios ($\delta^{13}\text{C}$ versus $\delta^{15}\text{N}$) are plotted in Figure 1. Spherulitic graphite plots along a linear array with a slope of 3.25. Graphite exsolution veneers at the kamacite-taenite interface has the lightest C- and N-isotopic compositions ($\delta^{13}\text{C} = -23 \rightarrow -18 \text{‰}$, $\delta^{15}\text{N} = -159 \rightarrow -141 \text{‰}$). Fibrous graphite band around spherulitic graphite has much lighter N than the spherulitic core ($\delta^{15}\text{N} = -145 \text{‰}$ versus $\delta^{15}\text{N} = -71 \text{‰}$). A single crystal in the silicate matrix has an C-isotopic ratio completely different from all other graphite grains in Acapulco (Figure 1).



The results indicate that the individual graphite morphologies retained their pristine isotopic signatures, despite the pervasive equilibration and partial melting experienced at $T = 1200^\circ\text{C}$ by the Acapulco parent body [1].

References

[1] Zipfel J. et al., (1995), *GCA*, **59**, 3607-3627.

Geochemical response to arc-continent collision on Alor, Sunda-Banda arc, Indonesia

MARLINA ELBURG^{1,2}, JOHN FODEN¹, MANFRED VAN BERGEN³, ISKANDAR ZULKARNAIN⁴

¹Department of Geology and Geophysics, University of Adelaide, Adelaide SA5005, Australia

²Now at: Max-Planck Institute for Chemistry, PO Box 3060, 55020 Mainz, Germany (elburg@mpch-mainz.mpg.de)

³Institute of Earth Sciences, Utrecht University, The Netherlands

⁴RDCG-LIPI, Bandung, Indonesia

The island of Alor lies in the extinct sector of the Sunda-Banda arc, where collision with the Australian continent halted subduction-related volcanism. It provides us with an end member scenario of arc magmatism, where the geochemistry is dominated by input from the subducting plate.

Older lava flows and intrusives (2.5 Ma) have rather homogeneous geochemical characteristics, with only moderately 'crustal' signatures ($^{87}\text{Sr}/^{86}\text{Sr} = 0.7060\text{-}0.7066$, $^{143}\text{Nd}/^{144}\text{Nd} = 0.51261\text{-}0.51252$, $^{206}\text{Pb}/^{204}\text{Pb} = 19.1\text{-}19.2$).

The youngest volcanic deposits (1.3 Ma) show extreme isotopic variability ($^{87}\text{Sr}/^{86}\text{Sr} = 0.706\text{-}0.711$, $^{143}\text{Nd}/^{144}\text{Nd} = 0.5126\text{-}0.5122$) with Pb isotope ratios among the highest recorded for an island arc ($^{206}\text{Pb}/^{204}\text{Pb} = 19.0\text{-}19.6$; $^{208}\text{Pb}/^{204}\text{Pb} = 39.3\text{-}40$). The highest Pb isotope ratios are only found on the north coast (distal from the trench), and the extreme $^{208}\text{Pb}/^{204}\text{Pb}$ ratios reflect subduction of upper crustal material of Australian origin. Some south coast samples combine higher Sr with lower Pb isotopic characteristics, indicating that the isotopic composition of the youngest deposits cannot be explained by two component mixing of mantle and subducted sediments. The lower-Pb isotopic component resembles cordierite-bearing samples of the neighbouring island Wetar, suggesting an origin in the lower (?) continental crust.

Trace elements ratios such as Pb/Ce indicate that any influence of a fluid component in the source of the youngest volcanics is masked by the large amount of subducted continental material. High Th/Nb ratios for the high $^{206}\text{Pb}/^{204}\text{Pb}$ samples indicate that the slab to wedge transfer medium was a partial melt, but this may not be the case for the samples with lower Pb isotopic signatures.

Conclusions

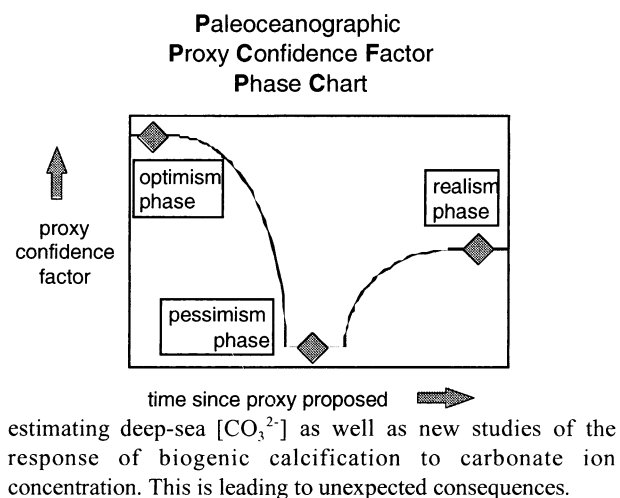
Our results show that arc-continent collision results in isotopic signatures becoming more heterogeneous, reflecting subduction of continental crust and, in the case of Alor, addition of two types of crustal material to the mantle wedge. This situation contrasts with the active part of the Sunda-Banda arc where only one type of crustal material is added to the mantle wedge, and where a fluid component plays an important role in frontal volcanoes.

Foraminiferal Mg/Ca paleothermometry: expected advances and unexpected consequences

H. ELDERFIELD

Department of Earth Sciences, University of Cambridge, Downing Street, Cambridge CB2 3EQ, England, E-mail: he101@esc.cam.ac.uk

"The oxygen isotope method of determining paleotemperatures (Urey H., *J. Chem. Soc.*, 562, 1947) is widely regarded as a tool of unique potential in the investigation of past changes in the temperature of the earth's surface." (Shackleton N.J., *Colloq. Int. Cent. Natl.*, 219, 203, 1974). That potential was first realised by Epstein S., Bushsbaum R., Lowenstam H.A. and Urey H. (*Geol. Soc. Amer. Bull.*, 62, 417, 1951; *ibid* 64, 1315, 1953) and its subsequent development has played an invaluable role in paleoclimate research. Among the newer methods for estimating paleotemperature (including faunal analysis and alkenones), Mg/Ca thermometry has the added potential, not yet realised, of providing an estimate of seawater $\delta^{18}\text{O}$. Like all proxies, it is moving through the PPCFPC (see graph). This development has the added benefit that more is being learned about $\delta^{18}\text{O}$ systematics as well as the factors controlling trace element incorporation and retention in marine biogenic carbonates. Amongst these, the influence of dissolution on Mg/Ca is a matter of current importance and has interesting links with recent ideas for



Li isotope variations in the upper mantle

T. ELLIOTT¹, A.L. THOMAS¹, A. B. JEFFCOATE¹
AND Y. NIU²

¹Department of Earth Sciences, Bristol University, Queens Road, Bristol, BS8 1RJ, UK (Tim.Elliott@bristol.ac.uk, at8581@bristol.ac.uk, A.Jeffcoate@bristol.ac.uk)

²Department of Earth Sciences, Cardiff University, Cardiff, CF10 3YE, UK (yaoling@ocean.cf.ac.uk)

A large proportion of the mantle is likely to have been enriched by recycled oceanic lithosphere, such as envisioned by the marble cake mantle. Yet definitive evidence for such recycled material, despite the host of distinctive geochemical signatures it is expected to impart, remains elusive. Partly as a consequence, alternative theories have become popular in which subducted slabs form a deep, hidden reservoir and are largely removed from our mantle sample.

A novel means to address this issue is the use Li isotopes. Alteration of the oceanic lithosphere both increases its Li concentration and ⁷Li/⁶Li. Mixing of this material back into the upper mantle should therefore elevate its ⁷Li/⁶Li and generate Li isotope heterogeneity on a small scale. New Plasma Induced Multi-collector Mass Spectrometers (PIMMS) dramatically improve the reproducibility of Li isotope measurements. Analyses with the Finnigan Neptune allow us to determine natural variations in ⁷Li/⁶Li of less than 0.5 per mil, using rapid sample-standard bracketing. Using this enhanced analytical capability, we have begun to investigate ⁷Li/⁶Li variations in well characterised basaltic glasses from the East Pacific Rise (10.5 and 11.5°N). Initial results show a significant spread in ⁷Li/⁶Li of ~1.5 per mil. The Li isotope variation correlates with ⁸⁷Sr/⁸⁶Sr and La/Sm, but not [Li] or MgO, suggesting it is a primary signature. It thus appears that a definitive signature of recycled material in the upper mantle has been gleaned.

Lipid biomarkers as a tool for the analysis of anaerobic methanotrophy in marine environments

M. ELVERT¹, H. NIEMANN¹, A. BOETIUS², T. TREUDE¹,
K. KNITTEL¹

¹Max Planck Institute for Marine Microbiology, Bremen, Germany (melvert@mpi-bremen.de, hniemann@mpi-bremen.de, ttreude@mpi-bremen.de, kknittel@mpi-bremen.de)

²International University Bremen, Bremen, Germany (a.boetius@iu-bremen.de)

Downcore lipid analysis of gas hydrate-bearing sediments at Hydrate Ridge and methane-rich sediments from the Håkon Mosby Mud Volcano (HMMV) show elevated concentrations and high numbers of diverse membrane lipids (biomarkers) of archaeal and bacterial origin. Structural and carbon isotopic analyses demonstrate the presence of a consortium of archaea and sulfate-reducing bacteria oxidizing methane under anoxic conditions. Concentrations of relevant biomarkers are clearly enriched at locations with elevated methane seepage and decreased at locations with lower methane outflow. The enrichment of consortium-specific biomarkers is directly translated into their isotopically light carbon isotopic signature. Concentrations and carbon isotopes are in good agreement with rate measurements and rRNA analyses and thus help identifying the methane oxidation zones *in situ*. Whereas high methane oxidation rates at Hydrate Ridge can be found throughout the core, methane oxidation at HMMV takes place only in a restricted zone right below the sediment surface. Small increments may, however, indicate a second *hot spot* of anaerobic methanotrophy or, on the other hand, active methanogenesis in deeper layers. Among the specific biomarkers, isoprenoids (crocetane, pentamethylcosenes) and glycerolethers (archaeol, hydroxyarchaeol) are identifiable as markers of the archaeal partner belonging to the *Methanosarcinales* group. The most dominant biomarkers of bacterial origin are monoalkylglycerolethers containing hexadecyl carbon chains and the fatty acids cis11-C_{16:1} and ΔC_{17:0}. These biomarkers can be attributed to the syntrophic bacterial partner closely related to the *Desulfosarcina-Desulfococcus* group.

Hypotheses and facts on the when, why and how of sapropel formation in the Mediterranean Sea

KAY-CHRISTIAN EMEIS

Institut für Ostseeforschung, Seestrasse 15, 18119
Warnemuende, Germany,
kay.emeis@io-warnemuende.de

Sapropels in the Mediterranean Sea are sediment layers that were deposited during periods when the deep waters of the eastern Mediterranean Sea were anoxic for several thousands of years. Anoxia was caused by enhanced water column stratification. I review the state of knowledge on three aspects of sapropel formation: the timing of sapropels and implications for the underlying climatic mechanism, the causes for stratification and geographical patterns of run-off, and the coupled chemical and biological consequences that led to enhanced organic carbon accumulation.

Differing from previous hypotheses, recent investigations on speleothems suggest that enhanced rainfall and onset of anoxic conditions were synchronous with insolation maxima. Large negative excursions in $\delta^{18}\text{O}$ in sapropels are largely accounted for by increasing SST and pooling of isotopically depleted water in the surface layer. Spatial patterns in coeval sapropels are consistent with climate processes in the low latitude catchment and of regional surface water warming associated with insolation cycles. However, much of the excess moisture apparently originated from evaporation in the Mediterranean Sea.

Regional and global temperature evolution modulated the basic sapropel rhythm and raised the threshold for full stagnation of deep water during glacials, but each insolation-related swing from cold to warm and from dry to wet conditions is expressed as a "failed sapropel" in the isotopic, chemical, and faunal records.

Increased accumulation of organic matter was a consequence both of higher productivity and enhanced preservation of organic matter. Both were caused by anoxic conditions at the sea floor. Very low (-1 to 1‰) $\delta^{15}\text{N}$ ratios in sapropels require a very light source of nutrient-N assimilated at a minimum of ten times the modern export flux. Because isochronous records show no spatial gradient in the $\delta^{15}\text{N}$, we may exclude both Ekman-type upwelling and direct riverine discharge as likely sources of nutrients. Instead it appears that phosphorus release from sediments and denitrification at a relatively shallow redox boundary resulted in an imbalanced supply of nutrients (N:P < 16:1) to the photic zone. The result was a slow assimilation of carbon during summer stratification and extensive N_2 -fixation providing the majority of the export flux from a N-limited system.

Sapropels thus result from a basic mechanism operating in all silled basins of the temperate climate zone at transitions from cool to warm climate. The robust relationship between climate, surface water properties and biological consequences seen in the Mediterranean Sea is an analog for many black shale events of the geological record.

Element contents in the ash of dropwort roots and in the soil around the roots

M. ENEL

Geological Survey of Estonia, Kadaka tee 82, 12918 Tallinn,
Estonia (enel@egk.ee)
University of Tartu, Institute of Geology, Vanemuise 46,
51014 Tartu, Estonia

Biogeochemical mapping for characterising the pollution of the environment with heavy metals and other hazardous elements has been carried out in Estonia using dropwort (*Filipendula Ulmaria*) roots as indicators. Dropwort was chosen out, because this plant met the requirements established for indicator plants. Compared with geochemical mapping of soil, biogeochemical investigations give an overview of elements which are collected from the soil that surrounds the growing plants.

The aim of this investigation was both identifying the possible pollution of soil with a biogeochemical method, and analysing soil from the same sampling points where dropwort roots were collected.

50 sample pairs collected from the same sampling points have been compared. Root samples were washed, dried and ashed at 450°C. Analysed were Cd, Cu, Fe, Mg, Mn, Pb and Zn by AAS, P by colorimetric and Nb, Rb, Sr and U by XRF method. In soil samples the same elements were analysed with the same methods.

Results will show that the elements Cd, Cu, Mg, Mn, Nb, P, Rb, Sr, Zn and U concentrate better in dropwort roots than in soil. These results show how intensively plants collect nutrient elements from the soil. It became evident that the anomalies in the analysed results can be caused by pollution in the surrounding soil, higher concentrations in bedrock but also by anthropogenic pollution.

Plants are more sensitive for identifying pollution. Plants show pollution from a whole catchment area, but soil only pollution in a certain sampling point. The heterogeneity of the soil in both vertical and horizontal layers interferes with a good comparison of the results; in this case plants are better indicators for the environment.

Biom mineralization mechanisms in foraminifera and corals and their paleoceanographic implications

J. EREZ¹, S. BENTOV¹, C. BROWNLEE², M. RAZ¹, AND B. RINKEVICH³

¹Institute of Earth Sciences, The Hebrew University Jerusalem, Israel. erez@vms.huji.ac.il

²Marine Biological Association, Plymouth, UK. cbr@mba.ac.uk

³Israel Oceanographic and Limnologic Research, Tel Shikmona, Haifa, Israel. buki@ocean.org.il

Foraminifera and corals CaCO₃ shells are highly valuable for paleoceanographic reconstructions. However, their complex biomineralization process, often cause significant deviations from expected chemical and isotopic equilibrium. Our new observations on the calcification mechanisms in foraminifera and corals are based on various microscopic techniques including light, fluorescent, spectral, confocal and electron microscopy. They show several basic features that are common for both groups: Crystal nucleation and growth are mediated by an organic matrix. The shells consist of two types of crystals, primary and secondary, which have different chemical compositions (usually more enriched in trace elements). The solution from which calcification proceed is seawater, which may be slightly modified in its ionic composition. This seawater calcification reservoir is maintained at high pH. The calcification reservoir is behaving as a semi-closed system with respect to trace elements distribution coefficients. Seawater in the calcification reservoir is replaced by intensive vacuolization in foraminifera and by tissue pumping in corals. The implications of these observations for paleoceanography are far reaching. The "good news" is that for their secondary calcification (responsible for more then 90% of the CaCO₃ in their shell), foraminifera and corals start with ambient seawater as their initial ingredient. Apparent distribution coefficients arising from this semi-closed reservoir can be modelled. Primary calcification in both groups is strongly controlled by the organism in close association with the organic matrix. The primary crystals may significantly deviate from equilibrium (especially with respect to trace elements and stable isotopes in foraminifera). The proportions between these two components and their apparent different solubility may determine the overall chemical and isotopic composition of the shell.

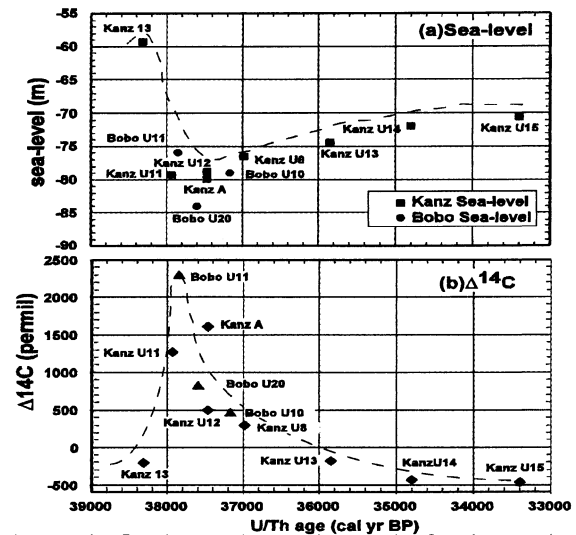
Rapid sea-level, ice-volume and radiocarbon excursions during a Heinrich event at Huon Peninsula

T.M. ESAT¹ AND Y. YOKOYAMA²

¹Research School of Earth Sciences, Australian National University, Canberra Australia (tezer.esat@anu.edu.au)

²Space Sciences, Lawrence Livermore National Laboratory, Livermore CA 94550, USA (yokoyama@llnl.gov)

We have previously demonstrated a connection between the ages of OIS-3 coral terraces at Huon Peninsula and the timing of North and South Atlantic ice-rafted debris layers and hence Heinrich events. In addition, coral radiocarbon analyses revealed large radiocarbon peaks at the same time periods which can best be explained by the stop-start behaviour of the thermohaline circulation. One of the better documented ¹⁴C peaks occurs at ≈38 ka and was derived from corals of terrace IIA, a prominent reef both at Bobongara and Kanzarua. In the figure, we have plotted the sea-level curve and excess ¹⁴C on the same time scale. The phase relationship between the various events is as follows: Just before 38.3 ka and sea-level



is at its peak. Terrace IIA crest is in place. Over the next 1000 years the sea level drops by over 20 m. The radiocarbon levels rise rapidly and reach their peak within 500 years at 37.8 ka. Presumably, the Gulf-stream slowdown occurs before 38.3 ka and by 37.8 ka the circulation is again active. The radiocarbon levels drop to previous values within about 2000 years and decline further over the next 3000 years, possibly indicating a vigorous re-start to the circulation. The data demonstrate the rapidity of the sea-level changes and by implication the rapidity with which ice-sheets can partially disintegrate and recover. Equally sharp is the 230% excess atmospheric radiocarbon pulse.

References

- Yokoyama Y., Esat T.M. and Lambeck K. (2001), *Earth Planet. Sci. Lett.* **193**, 579-587.
Yokoyama Y. et al., (2000), *Radiocarbon* **42**, 383-401.

Organic chemistry and the riddle of the pre-RNA world(s)

ALBERT ESCHENMOSER

Laboratorium für Organische Chemie, ETH Hönggerberg HCI
H309, CH-8093 Zürich, Schweiz und
The Scripps Research Institute, MB 16, 10550 North Torrey
Pines Road, La Jolla, CA 92037, USA
Eschenmoser@org.chem.ethz.ch

The lecture will survey experimental contributions to the pre-RNA-world problem from past and current organic chemistry and will focus on recent results obtained in the author's laboratory.

Os, Sr, Nd, Pb isotopic systematics in basalts and carbonatites from Fogo Island, Cape Verde

STÉPHANE ESCRIG¹, RÉGIS DOUCELANCE² & MANUEL MOREIRA

¹ escrig@ipgp.jussieu.fr

² r_doucelance@hotmail.com

Previous trace element and isotope data of basalts from Cape Verde archipelago have shown a difference between the northern and southern islands.

Here we focus on Fogo island (southern group) and report Os-Sr-Nd-Pb systematics on 17 basalts and 2 carbonatites. Except one sample, basalts present ¹⁸⁷Os/¹⁸⁸Os ranging from 0.13197 to 0.13694 and concentrations from 4.8 ppt to 28.6 ppt. Sr-Nd-Pb isotopic compositions are in the southern island range [1,2,3]. Basalts define positive correlations in lead-lead diagrams and negative correlations in Pb-Sr and Sr-Nd diagrams, significantly steeper than the classical mantle array in the latter. These correlations are interpreted as a mixing between a moderate 'high μ ' end-member and an enriched end-member identified as Sub-continental lithospheric Mantle (SCLM). Os isotopic data coupled with other systems show unexpected negative Pb-Os and positive Sr-Os correlations that imply radiogenic ¹⁸⁷Os/¹⁸⁸Os for the EMI-like end-member.

Both carbonatites present similar isotopic composition with ¹⁸⁷Os/¹⁸⁸Os = 0.17; ⁸⁷Sr/⁸⁶Sr = 0.703158; ¹⁴³Nd/¹⁴⁴Nd = 0.512930; ²⁰⁶Pb/²⁰⁴Pb = 19.5; ²⁰⁷Pb/²⁰⁴Pb = 15.597; ²⁰⁸Pb/²⁰⁴Pb = 39.189. Such compositions do not plot on the basalt correlations, precluding carbonatite fluid as the moderate 'high μ ' end-member. We rather propose a mixing between a 1.6 Ga recycled oceanic crust and lower mantle material.

Comparisons with trace element and Sr-Nd-Pb isotope data of kimberlites and lamproites suggest that the SCLM involved in Cape Verde source has encountered enrichment in incompatible elements by melt percolation. Such feature and recent works [4,5] on Canary islands lead to propose a partial melting model of SCLM that can generate the whole isotopic composition required for the enriched end-member, especially ¹⁸⁷Os/¹⁸⁸Os up to 0.14, consistent with the unradiogenic Os isotopic ratios of peridotite xenoliths.

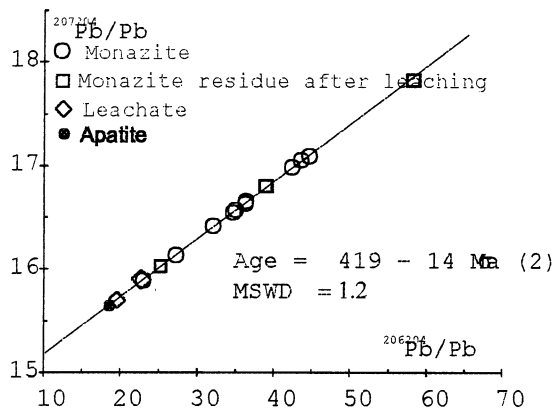
- [1] Gerlach D.C., Cliff R.A., Davies G.R., Norry M. and Hodgson N. *Geochim. Cosmochim. Acta* 52, 2979-2992. (1988)
- [2] Davies G.R., Norry M.J., Gerlach D.C. and Cliff R.A. *Geol. Soc. Spec. Publ.* 42, 231-255. (1989)
- [3] Doucelance R, Escrig S, Moreira M, Gariépy C, Kurz MD, Allègre CJ, *Geochim. Cosmochim. Acta* submitted.
- [4] Widom E, Hoernle KA, Shirey SB, Schmicke H-U. *J. Petrol* 40, 279-296. (1999)
- [5] Neumann ER, Wulff-Pedersen E. *J. Petrol* 38, 1513-1539. (1997)

Dating diagenetic monazite in mudrocks: constraining the oil window?

EVANS, J.A.¹, ZALASIEWICZ, J.A.², FLETCHER, I.³, RASMUSSEN, B.³, & PEARCE, N.J.G.⁴.

- 1) NERC Isotope Geosciences Laboratory, BGS, Keyworth NOTTM, NG12 5GG. UK (JE@nigl.nerc.ac.uk)
- 2) Department of Earth Sciences, University Road Leicester University LE1 7RH, UK (jaz1@leicester.ac.uk)
- 3) Univ Western Australia, Dept Geol & Geophys, Ctr Global Metallogeny, Crawley, WA 6009, Australia (ifletche@geol.uwa.edu.au., brasmuss@geol.uwa.edu.au)
- 4) Institute of Geography and Earth Sciences, University of Wales, Llandinam Building, Aberystwyth, SY23 3DB, Wales, (njp@aber.ac.uk)

Authigenic monazite nodules, increasingly recognised in Pre-Mesozoic mudrock successions, provide a means for dating diagenesis by exploiting trace uranium within the monazite structure. But, dating is difficult in practice because of zonation and abundant host rock inclusions. We report here a refined technique that has yielded a date of 419 ± 14 Ma 2σ MSWD = 1.2 for a 17-point Pb-Pb regression age from a Telychian (Silurian: late Llandovery c.430 Ma) mudrock from central Wales.



SHRIMP analyses of the same material are consistent with this, and additionally demonstrate concordance of the U-Pb and Th-Pb systems. These results open the door to providing robust dates for a phase of burial related diagenesis, which, in Wales, seems approximately coincident with hydrocarbon expulsion.

Determination of variations in isotope ratios of Hg

R. DOUGLAS EVANS AND PETER J. DILLON

Environmental Science Centre, Trent University,
Peterborough, ON, Canada K9J 7B8 (devans@trentu.ca,
pdillon@trentu.ca)

The question of whether Hg isotopes are fractionated to a measurable degree in natural environments by chemical, physical and biological processes remains unanswered. If isotopic signatures of Hg from various anthropogenic sources or environmental compartments are different, it may be possible to fingerprint Hg, partitioning accumulated Hg according to source.

Recent development of multicollector-ICP-MS (MC-ICP-MS) instruments makes it possible to measure isotope ratios of Hg with high precision. MC-ICP-MS has been used primarily in geological applications, and only recently has its potential for environmental applications begun to be explored. Measurement of high precision isotope ratios in environmental matrices presents a different set of challenges. Given the low concentrations of Hg in environmental media and the very small differences between ratios that we expect to find, sample introduction without contamination is a major problem to be overcome.

Mercury can be introduced to the MC-ICP-MS as a liquid, or vapour via hydride generation or directly after trapping and thermal desorption on gold traps. Each of these techniques has limitations with respect to isotope ratio measurement. We will discuss some of these limitations. Our preferred approach is the gold trapping method. As will be demonstrated, this technique minimizes potential for sample contamination. The major drawback is the necessity to work with transient signals, usually considered detrimental to measurement of high precision isotope ratios. However, our work suggests that acceptable precision can be achieved using transient signals, while maintaining the veracity of the original isotopic signature.

Hg isotopic signatures vary by more than 1‰ per AMU across a range of sample types. However, the differences are very small, and external variation among replicate samples is high. In part, this variability is attributable to the transient signals. The potential for blurring of signatures from external contamination remains a serious issue. Further work will be required to develop simple, standardized methods for Hg isotope ratio determination.

Developments in Fluorite (U-Th)/He Thermochronology

NOREEN EVANS¹, NICK WILSON², JEAN CLINE³, BRENT
MCINNES¹ AND JOHN BYRNE⁴

¹CSIRO Exploration and Mining, PO Box 136, North Ryde,
NSW 1670 Australia (Noreen.Evans@csiro.au
,Brent.McInnes@csiro.au)

²Geological Survey of Canada, 3303-33rd St. N.W., Calgary
AB, Canada T2L 2A7 (nwilson@nrcan.gc.ca)

³Department of Geoscience, University of Nevada, Las Vegas,
4505 Maryland Parkway, Box 454010 Las Vegas, NV
89154-4010 USA (jcline@unlv.edu)

⁴Department of Chemistry, Materials and Forensic Sciences,
University of Technology, Sydney, PO Box 123
Broadway NSW 2007 Australia (John.Byrne@uts.edu.au)

We report the results of (U-Th)/He dating trials on fluorite precipitated as a secondary hydrothermal mineral within Miocene tuff (12.8 Ma) at Yucca Mountain, Nevada.

Three varieties of fluorite crystals were separated from vein specimens containing 1–3 mm thick layers of fluorite. Early fluorite adjacent to the host tuff is translucent, changing gradually to colourless and finally purple transparent varieties. Several mg of 100–300 μm , inclusion-free crystals were analysed from the three varieties. The cloudy crystal layers adjacent to the tuff have (U-Th)/He ages of 9.8 ± 0.3 Ma. The clear fluorite is slightly older (11.9–15.6 Ma), whereas the purple grains consistently yield anomalously high He contents resulting in geologically unreasonable ages.

Fluorite	U (ppm)	Th (ppm)	Age (Ma)	$\pm 2\sigma$
purple	6.5	1.4	212, 41	1.1
clear	10.6	0.22	11.9, 13.8, 15.6	0.4
cloudy	12.1	0.64	9.7, 9.9	0.3

Alpha-emission correction after Farley et al., (1996). Mean U and Th concentrations given.

He diffusion experiments were carried out at Caltech on a handpicked sample of 200–350 μm colourless fluorite. The helium closure temperature for this fluorite is $60 \pm 5^\circ\text{C}$, assuming a $10^\circ\text{C}/\text{Ma}$ cooling rate. The (U-Th)/He age of 9.8 Ma for the cloudy variety of fluorite indicates that it was precipitated within 2 myr of tuff deposition. Subsequently, only meteoric fluids cooler than 35°C entered the site (Wilson et al., submitted). We suggest that the purple variety was in contact with late-stage U-rich fluids that implanted He in the fluorite margins and caused discoloration of the crystals.

Material properties and microstructure from Crystallisation of (PGE)AsS from sulphide melt

T.L. EVSTIGNEEVA, R.K.W. MERKLE, N.V. TRUBKIN

IGEM RAS, Staromonetny 35, Moscow, 109017 Russia
(evst@igem.ru)

University of Pretoria, Earth Sciences, Pretoria ;0002, South
Africa (rmerkle@postino.up.ac.za)

Amongst Platinum-Group Minerals (PGM) there are sulpharsenides of all Platinum-Group Elements (PGE) except Pd: platarsite, PtAsS; irarsite, IrAsS; hollingworthite, RhAsS; osarsite, OsAsS; ruarsite, RuAsS. The 'ideal' composition corresponds to the end members, 'PGE'AsS, but the real ones present the intermediate members of solids solutions regarding to PGE and As-S.

PGE sulpharsenides are found in basic/ultrabasic complexes with chromite or cooper-nickel sulphide mineralization, i.e. ophiolites, layered intrusions etc. Essentially all PGE sulpharsenides occur in metamorphosed rocks and ores. But the conditions of their formation remain unknown. The (PGE)AsS bearing associations could contain other PGM and basic sulphides. Very often people find the crystal of 'PGE'AsS in close association with Ni-rich sulphides, as millerite, and heazlewoodite. For example, Shetland ophiolites contain: 1) IrAsS + RuS₂+Os, 2) IrAsS + RuS₂, and 3) IrAsS + RuS₂ + Ru-bearing pentlandite (Ni>Fe). Norilisk Cu-Ni sulphide ores present other associations: RhAsS + CuFeS₂ + (Fe,Ni)₆S₇ (+Ni₈S₈), or RhAsS + CuFeS₂ + NiS + (Ni,Fe)₉S₈. It seems to be interesting to check the possibility of 'PGE' sulpharsenide formation directly from the sulphide melt containing Cu, Fe, Ni, and PGE.

Based on the composition of natural associations the preliminary experimental study was carried out in evacuated quartz ampoules. 100 mg charges of elements corresponded to the mixtures: 1) 'PGE'AsS + Po_m+Pn_{Ni}+Cp, 2) 'PGE'AsS + Cp + Bor + Pn_{Ni} + Mil, and 3) 'PGE'AsS + Cp + Tr + Pn_{Fe}, in different proportions. Charges were preheated in the argon flow (400°C), then gradually heated to 1080°C , annealed at this temperature during 76 hours, and slow cooled with the furnace. Polished sections from samples synthesized were studied with optical microscope, microprobe, and electron microscope (SEM + energy disperse analysis).

In spite of the relatively low proportion of 'PGE'AsS in the charges (~10 mol.%) some 'PGE' sulpharsenides were crystallized, i.e. RhAsS in association with Cp and Pn_{Ni}, and with Cub and Po_m, and IrAsS with Cub. The most of other PGM are dispersed in basic sulphides, but the additional study is necessary to determine the form of their occurrence: isomorphous elements in sulphide structures or tiny inclusions in sulphide matrix.

Using the composition of associated sulphides the conditions of 'PGE'AsS formation (i.e.) are discussed relative to the stability of basic sulphides. For both, RhAsS and IrAsS, lg_{S_2} is less than 10 at $T < 600^\circ\text{C}$ that is in agreement with experimental data of one of the author on the stability field of some other PGM.

Impact of the Nuclear Fuel Cycle on the Environment

R.C. EWING¹

¹Nuclear Eng. & Radiological Sciences and Geological Sciences, University of Michigan, Ann Arbor, MI, 48109, USA (rodewing@umich.edu)

The nuclear fuel cycle impacts two types of geochemical cycles: **Carbon cycle**: reduced emissions of carbon to the atmosphere as nuclear power plants replace carbon-based sources of energy. **Radionuclide cycles**: increased production of technogenic radionuclides in spent nuclear fuel (SNF). Depending on national policy, the SNF is considered a waste product, or fissile nuclides, such as ²³⁵U and ²³⁹Pu, can be recycled for further energy production. However, most fission products and the “minor” actinides (Cm, Am, Np) are generally considered waste. Unlike other energy producing systems, the by-product, fissile nuclides, can be diverted for weapons production. This paper analyzes the global impact of increased utilization of the nuclear fuel cycle.

Carbon Cycle: In Kyoto, a Framework Convention on Climate Change proposed a reduction of greenhouse-gas emissions of industrialized countries by 5 percent below 1990 levels, over the next ten to fifteen years. However, energy demands world-wide are increasing and are expected to at least double over the next fifty years. The amount of energy supplied by carbon-free sources must grow by a factor of ten to twenty by 2050 (Fetter, 2000). At present, the use of nuclear power plants avoids carbon dioxide emissions of an estimated 600 million metric tons per year. However, in order to impact carbon emissions in a significant way by 2050, electrical power production by nuclear plants would have to reach 3,300 gigawatt-years (a single GW-year is the output of a large electric power plant) (Sailor et al., 2000). Even if the installed capacity of nuclear power plants only reaches 1,000 GW, there is the potential to avoid the emission of 6 billion metric tons of CO₂. Although this number is large, it has to be evaluated in the context of carbon exchange fluxes and sinks between the atmosphere, land and oceans.

Radionuclide Cycles: Although the use of nuclear power plants to produce electricity will reduce CO₂ emissions, there will also be a concomitant increase in the production of SNF and high-level nuclear waste. In 2002, approximately 150,000 metric tons of SNF have already accumulated. One of the principal concerns is the production of technogenic radionuclides, such as the transuranium elements, particularly Pu. There is presently a global inventory of over 1,400 metric tons of Pu. At present, the annual production of spent nuclear fuel is on the order of 10,000 metric tons (containing approximately 100 metric tons of fissile Pu). A ten-fold increase in nuclear power plants will yield substantial quantities of spent nuclear fuel, approximately 100,000 metric tons per year (for comparison, the legislated capacity for the proposed geologic repository at Yucca Mountain is 70,000 metric tons of SNF).

References

- Fetter S (2000) *Bull. Atomic Scientists* July/August, 28-38.
Sailor W.C, Bodansky D, Braun C, Fetter S, van der Zwann B (2000) *Science* **288**, 1177-1178.

Landscape preservation under ice sheets

D. FABEL¹, A. P. STROEVEN² AND J.HARBOR³

¹The Australian National University, Canberra, Australia
(d.fabel@anu.edu.au)

²Stockholm University, Stockholm, Sweden (arjen@geo.su.se)

³Purdue University, West Lafayette, Indiana, U.S.A.
(jharbor@purdue.edu)

Some areas within ice sheet boundaries retain landforms that appear unmodified by glacial erosion. These relict areas have either remained ice-free islands (nunataks), or were preserved under ice. Differentiating between these alternatives has significant implications for palaeoenvironment, ice sheet surface elevation, and ice volume reconstructions.

We collected samples from what are mapped as glacially eroded and relict surfaces in the northern Swedish mountains and areas closer to the centre of maximum Fennoscandian ice sheet extent, to test whether or not the mapped relict areas have indeed been preserved. In situ cosmogenic ¹⁰Be and ²⁶Al concentrations from erratics on relict surfaces, and glacially eroded bedrock adjacent to these surfaces, provide consistent last deglaciation exposure ages (~8-13 kyr), confirming ice sheet overriding as opposed to ice free conditions. Exposure ages of 34 kyr to 61 kyr on bedrock surfaces in these same relict areas demonstrate that these areas were preserved through at least the last glacial cycle, probably as a result of frozen-bed conditions. Based on the relative decay of ²⁶Al and ¹⁰Be it can be inferred that these relict bedrock surfaces remained largely unmodified during multiple ice sheet growth and decay phases.

Subglacial preservation implies that source areas for glacial sediments in ocean cores are considerably smaller than the total area covered by ice sheets. Our results indicate that boundaries between glacially sculpted and preserved landscapes should not automatically be interpreted as former ice limits in palaeoclimatic and palaeoglaciological reconstructions. Relict areas need to be accounted for as frozen bed patches in basal boundary conditions for ice sheet models, and in landscape development models.

Biogeochemical cycling of various metals in Baldeggersee, Switzerland

D. FABIAN AND B. WEHRLI

EAWAG - Swiss Federal Institute for Environmental Science and Technology, Kastanienbaum, Switzerland
(daniel.fabian@eawag.ch, bernhard.wehrli@eawag.ch)

This study focuses on the biogeochemical cycling of Ca, Mg, V, Cr, Mn, Fe, Ni, Cu, Zn, As, Sb, Mo, and Pb in Baldeggersee, a eutrophic lake in Switzerland. Sedimentation was recorded at the deepest site of Baldeggersee (65 m) during 1994 using sediment traps. A sediment core was taken at the same site with a freeze corer five years later (1999). The sediment layer deposited in 1994 was sampled and the metal accumulation in this layer was determined. Based on this data, we established the balance of sedimentation and remobilisation (Table 1).

Table 1: Annual (1994) sedimentation found in sediment traps and accumulation in the sediment (in mg m⁻²).

	Sedimentation	Accumulation	Remobilisation
Ca	390'000	260'000	34%
Fe	32'000	27'000	16%
Mn	30'000	9'000	70%
Mg	15'000	10'000	31%
Zn	240	180	23%
Ni	150	150	0%
V	78	69	11%
Cr	64	42	34%
Cu	62	54	13%
As	52	40	22%
Pb	21	17	19%
Mo	6.1	1.7	72%
Sb	2.1	1.2	47%

The results show that the lake sediment acts as a sink for most of the metals studied. Less than 25% of the settling Fe, Cu, Ni, Zn, V, Pb, and As are remobilised. For Ca, Mg, and Cr, remobilisation accounts for one third. On the other side, the major fraction of Mn, Mo, and Sb are remobilised upon sedimentation.

References

- Fabian D., Zheng Z., Wehrli B. and Friedl G. (2001) In: *Water-Rock Interaction* (ed. R. Cidu), pp. 1071-1073. A.A. Balkema.
- Lotter A.F., Renberg I., Hansson H., Stöckli R. and Sturm M. (1997), *Aquat. Sci.* **59**, 295-303.

Combined modelling of hydrological and hydrochemical dripwater data to deduce karstic plumbing

IAN J FAIRCHILD¹, GEORGE W TUCKWELL¹, ANDY BAKER² AND ANNA F TOOTH³

¹School of Earth Sciences and Geography, Keele University, Staffs ST5 5BG UK; i.j.fairchild@keele.ac.uk

²Department of Geography, University of Newcastle-on-Tyne, UK

³Department of Geology, University of Innsbruck

Two of the incentives for improving our understanding of the vadose zone of karstic aquifers are the need to model the behaviour of pollutants and the drive to find proxy indicators for palaeoclimate in speleothems formed from dripwaters. Specifically, quantitative knowledge of karstic plumbing could generate a predictive capability. Models of karstic plumbing can be approached by combining hydrological and hydrochemical data.

Here we report on a study on data from the disused limestone mines under Browns Folly, Bathford, near Bath (UK) which contain a number of dripwater sites, associated particularly with major open joint systems. The drip sites offer a range of hydrological behaviours that fall within the seepage flow and seasonal drip categories of previous authors, and there is an overall correlation between variation in drip rate and mean drip rate. A sub-set of sites exhibit hydrological behaviour that is clearly tied to major rainfall input events. Such sites also display distinctive variations in geochemistry with drip rate. At low drip rates there is either an evidence for increased prior calcite precipitation in the aquifer above the drip (decrease in Ca), or an increase in Sr/Ca or Mg/Ca from inferred low discharge sub-sections of the aquifer, or both.

Quantitative modelling of three sites representing the full range of mean drip rates has been approached by a box modelling approach with finite time steps, initially calibrated by hydrological response to rainfall events, but tuned by the geochemical data. The results allow different conceptual models of karstic plumbing to be evaluated. In particular the relative importance of macropore flow routes through soils and fissure flow in relation to seepage flow can be determined and possible geometries of coupling of different flow routes can be assessed.

Significance of oxygen isotopic signature in magnetite [$\text{Fe}^{\text{III}}_2\text{Fe}^{\text{II}}\text{O}_4$] under Earth surface conditions: preliminary results

D. FAIVRE¹, P. ZUDDAS¹, P. AGRINIER², F. GUYOT³ AND N. MENGUY³

¹Laboratoire de Géochimie des Eaux, Université Paris 7 & IPGP, 2 place Jussieu, 75251 Paris Cédex 05 France (faivre@ipgp.jussieu.fr and zuddas@ipgp.jussieu.fr)

²Laboratoire de Géochimie des Isotopes Stables, IPGP, 4 place Jussieu, 75251 Paris Cédex 05, France (piag@ccr.jussieu.fr)

³Laboratoire de Minéralogie – Cristallographie, Université Paris 7 & IPGP, 2 place Jussieu, 75252 Paris Cédex 05, France (guyot@lmcp.jussieu.fr and menguy@lmcp.jussieu.fr)

Under present surface Earth conditions, nanoparticles of biotic magnetite are intracellularly formed in the magnetosomes of magnetotactic bacteria. Thus, magnetite nanoparticles found in carbonate globules of Martian meteorites have been related to a possible extraterrestrial life. In order to determine if oxygen isotopes can be used as a proxy of bacterial signature, inorganic magnetite has been synthesized under controlled chemical affinity conditions at temperature of 298 K, oxygen fugacity close to 0, ionic strength of 0.2 M and high solution saturation state (> 100). Total dissolved iron of stoichiometric ratio (i.e. $\text{Fe}^{\text{II}} / \text{Fe}^{\text{III}} = 0.5$) was varied to identify the role of this variable on the kinetic rate and on the oxygen isotope fractionation.

Under our experimental conditions, magnetite particles of an average dimension of 8 nm are formed only when $[\text{Fe}_{\text{tot}}]$ is higher than 9 mM while in lower dissolved iron concentration, only goethite [$\text{Fe}^{\text{III}}\text{O}(\text{OH})$] particles are formed. Oxygen isotopes fractionation, $10^3 \ln \alpha_{\text{m-e}}$, decreases by 6 times when the iron concentration increases more than one order of magnitude.

Since biotic magnetites have similar oxygen isotope signature (Mandernack et al., 1999) to our abiotic magnetite particles, we propose that bacteria may simply produce an increase of solution saturation state in the magnetosomes that, in turn, control the precipitation of magnetite nanoparticles in surface conditions.

Mandernack K. W. *et al.* (1999), *Science* **285**, 1892-1896.

Carbon isotopic composition of fatty acids in the marine aerosols from the western North Pacific: Implication for the source and atmospheric transport

JIASONG FANG¹, KIMITAKA KAWAMURA², YUTAKA ISHIMURA², AND KOUHEI MATSUMOTO²

¹Department of Geological and Atmospheric Sciences, Iowa State University Ames, IA 50011-3212, USA

²Institute of Low Temperature Science, Hokkaido University, Sapporo, Japan

Abstract – A combined molecular and isotopic approach was used in this study to reveal the source and transport of aerosols at a remote oceanic site. Fatty acid distributions and stable carbon isotopic compositions of individual fatty acids were determined in the aerosol samples collected at Chichi-Jima in the western North Pacific over a period of forty-one months. Fatty acid concentration and isotopic composition $\delta^{13}\text{C}$ (vs. PDB) exhibited temporal variations. Concentrations of fatty acids (C_{12} to C_{34}) ranged from 7.6 to 20.7 ng/m³. The concentrations of lower molecular weight (LMW) fatty acids (C_{12} - C_{19}) tend to decrease in winter and increase in summer, whereas the higher molecular weight (HMW) C_{20-34} fatty acids exhibited a reversed trend. Compound specific isotopic analysis revealed that the LMW fatty acids exhibited consistently less negative $\delta^{13}\text{C}$ values than the HMW fatty acids. However, both the LMW and HMW fatty acids displayed similar trend of temporal variations in $\delta^{13}\text{C}$, suggesting that the fatty acids experienced similar atmospheric pathways and transport processes to the remote marine atmosphere, whereas the difference in absolute $\delta^{13}\text{C}$ reflects the different sources of the fatty acids.

Modelling the sorption of metal cations on metal hydroxides: experiment vs. model.

FRANÇOIS FARGES^{1,2}, MARCO BENEDETTI³,

INGRID BERRODIER¹ AND GORDON E. BROWN JR.²

¹Laboratoire des Géomatériaux, Université de Marne la Vallée, France (farges@univ-mlv.fr)

²Department of Geological & Environmental Sciences, Stanford University, Stanford, CA 94305-2115 USA (gordon@pangea.stanford.edu)

³CNRS-ESA 7047, Université de Paris 6, Paris, France.

Modelling of the local structure around metal cations in Earth materials of environmental importance is based on thorough analyses of available spectroscopic and scattering information for these samples. However, construction of atomistic models of metal ion sorption on mineral surfaces from experimental data is not straightforward. In order to refine our understanding of sorption processes, we have developed a procedure for refining EXAFS spectroscopic data based on wavelets and Monte-Carlo modelling of the local structure around the sorbate ion. Then, electrostatic potential and bond valence considerations are used to validate and constraint the model. Finally, this model is compared with predictions from the CD-MUSIC model and with macroscopic information obtained from potentiometric titrations.

To illustrate this approach, the sorption of gold on the surface of goethite will be examined (based on the EXAFS data of Berrodier et al., 1999). Medium-range inter-polyhedral relationships were obtained from a wavelet analysis of the EXAFS spectra, which excludes spurious artefacts such as multi-electronic transitions and multiple-scattering features, and provides a correct estimate of the k -range needed to derive robust structural information from the EXAFS spectra. Then, bond valence models were constructed in 3-D and refined using Monte-Carlo-type methods to match the experimental results. Several unique models were tested by calculating effective charges on each atom using self-consistent potentials (which also include protons) with the FEFF8 code (Ankudinov et al., 1998). These bond-valence models were then refined using the CD-MUSIC package (Hiemstra and van Riemsdijk, 1996), which predicts the speciation of gold at the goethite/solution interface (110 and 021 faces). The results of this approach are in excellent agreement with potentiometric titrations up to pH 12.

Ankudinov, A.L., Ravel, B., Rehr, J.J., and Conradson, S.D. (1998) *Phys. Rev. B* 58, 7565-7576.

Berrodier, I., Farges, F., Benedetti M., and Brown, G.E., Jr. (1999) *J. Synchrotron Rad.* **S6**, 651-652.

Hiemstra, T. and van Riemsdijk, W. (1996) *J. Colloid Interface Sci* **179**, 488-508.

New concepts in XAFS analysis

FRANÇOIS FARGES^{1,2}

¹Laboratoire des Géomatériaux, FRE CNRS 2455 and Univ. de Marne la Vallée, France (farges@univ-mlv.fr)

²Department of Environmental Sciences, Stanford University, USA

The extraction of robust structural information from the x-ray absorption fine structure (XAFS, including XANES and EXAFS regions) spectra is highly dependent on the methods used to extract the desired information. We present here a variety of new methods to further reduce the XANES and EXAFS spectra.

Deconvolutions

Pre-edge, XANES and EXAFS deconvolutions (see Filipponi, 2000) are used to enhance spectral features such as electronic transitions in the pre-edge region. Application to the case of Fe in glasses suggests that Fe(II) do not form any 6-coordinated environment, but a mixture of 4-, and 5-coordinated Fe(II). Using deconvolutions, one can also show that the enhanced pre-edge (Fe-K) for ferrihydrite is related to some extra transition, which is not related to crystal-field splitting (probably a Fe-Fe transition, as in epidote: Farges, 2002). Finally, deconvolutions of the EXAFS region help to evidence multi-electronic transitions, as it will be shown for Th in zircon.

Fourier modelling of the XANES

Analysis of the XANES can now be performed using FT methods, considering single-, and multiple scattering paths of the photo-electron (Bugaev et al., 2002) to get speciation information such as for Ti in radiation damaged titanites or in silicate glasses. Despite of the intrinsic limitations, the obtained information is consistent with that obtained from pre-edge or EXAFS analysis and other methods such as scattering methods (Bugaev et al., 2002).

Principal Component Analysis

In order to get the components composing the XAFS spectra of a mixture, principal component analysis provides some statistics on the number of end members to model. By inversion, the spectra for the end members can then be derived. An application to the photo-reduction of Au on ferrihydrite will be presented as well as for Fe in glasses synthesized under variable redox conditions.

References

- Bugaev L.A., Farges F., Rusakova E.B. and Sokolenko A P (2002) *Phys. Rev. Lett.* (submitted).
 Farges, F. (2002) *Amer. Mineral.* (submitted)
 Filipponi A. (2000) *J.Phys. B (Atom., Molecul. & Optical Phys.)* **33**, 2835-2846.

Using proton-induced ³He to study He diffusion kinetics and rock thermal histories

K.A. FARLEY¹, D.L. SHUSTER¹, D.S. BURNETT¹ AND J. SISTERTSON²

¹Division of Geological and Planetary Sciences, Caltech, Pasadena, CA 91125; farley@gps.caltech.edu; dshuster@gps.caltech.edu; burnett@gps.caltech.edu
²Northeast Proton Therapy Center, Massachusetts General Hospital, Boston, MA 02114; janet_sisterson@dfci.harvard.edu

We have investigated He release kinetics by step-heating of minerals in which we introduced artificial ³He with a beam of ~150 MeV protons in a particle accelerator used primarily for cancer therapy. This process mimics cosmic-ray spallation, and produces He with a ³He/⁴He ratio of about unity. The induced helium is homogeneously distributed within the target crystals, and because it is emitted with few MeV energies, the ³He should reside in sites indistinguishable from those of radiogenic ⁴He. As a consequence it is reasonable to use ³He as a proxy for radiogenic ⁴He during step heating. The advantage of this procedure is that we can measure He diffusion coefficients from essentially any mineral, even those for which there is little or no natural He or He retention. In addition, diffusion coefficients computed using standard step-heat procedures would be erroneous if the He is not uniformly distributed within the diffusion domain. For example a slowly cooled apatite sample will have a highly rounded ⁴He concentration profile which would retard the early He release in a step heating experiment, thus yielding erroneously low apparent diffusion coefficients. By using the artificial ³He we can invert for the ⁴He concentration profile and helium diffusivity simultaneously (e.g., see Albarede, 1978). This may prove useful as a technique for narrowing down permitted rock thermal histories.

Experiments on Durango apatite reveal excellent agreement between induced ³He and radiogenic ⁴He diffusion, supporting our approach. In contrast, probable slowly cooled apatites yield ⁴He/³He ratios that rise as the step heat proceeds, consistent with rounded ⁴He concentration profiles. However in the first few steps the ³He diffusion is anomalously high; we do not yet understand the origin or implications of this phenomenon.

Insight into crust-mantle coupling from anomalous $\Delta^{33}\text{S}$ of sulfide inclusions in diamonds

J. FARQUHAR¹, B. WING¹, K.D. MCKEEGAN², AND J.W. HARRIS³.

¹Essic and Dept of Geology, University of Maryland, College Park MD 20742 USA.

²Earth and Space Sciences, UCLA, Los Angeles, CA 90095-1567 USA.

³Division of Earth Sciences, Gregory Building, University of Glasgow, Glasgow, G12 8QQ, UK.

Sulfur isotope compositions of 26 sulfide inclusions from diamonds have been measured with the Cameca IMS 1270 ion microprobe at UCLA. Inclusions were extracted from 12 diamonds from the Orapa kimberlite pipe, Kaapvaal-Zimbabwe craton, Botswana. In-house reference standards were analyzed between every 3 analyses, and estimated (2σ) uncertainty for $\Delta^{33}\text{S}$ is $\pm 0.14\%$ - adequate to document that inclusion populations from 4 diamonds have anomalous $\Delta^{33}\text{S}$ (0.55%, 0.24%, 0.41%, 0.62%). Inclusions from the other 8 diamonds yielded $\Delta^{33}\text{S} = 0.04 \pm 0.10\%$ (2σ). Preliminary EPMA analyses indicate these have an eclogite affinity.

$\Delta^{33}\text{S}$ is an excellent geochemical tracer of Archean crust-mantle interactions because it is invariant during geological processes and in bulk meteorites (Farquhar et al. 2000a). Observation of anomalous $\Delta^{33}\text{S}$ of inclusions in diamond confirms earlier assertions that some diamond sulfur derives from the surface (Chaussidon et al., 1987; Eldridge et al., 1991) and also provides new ways to study coupling between Archean mantle, crust and atmosphere. Our measurements of peridotite xenolith sulfur yield near zero $\Delta^{33}\text{S}$ ($0.03 \pm 0.06\%$ (2σ)). Mean and median of whole rock $\Delta^{33}\text{S}$ measurements for Archean sulfide (Farquhar et al. 2000b) are 0.6 and 0.3%, respectively. Regardless of whether these $\Delta^{33}\text{S}$ values reflect average Archean crust and mantle compositions, they form a framework that can be used in combination with $\Delta^{33}\text{S}$ for sulfide from diamonds to place limits on the proportions of mantle and crustal sulfur prior to trapping in diamond. This approach can be extended to the atmospheric subcycle since we attribute $\Delta^{33}\text{S}$ variations in Archean samples to 193 nm SO_2 photolysis which produces S^0 with $\Delta^{33}\text{S} = 65 \pm 4\%$ (Farquhar et al., 2001). In this context, our data indicate that all of the sulfur in these inclusions may represent subducted, but undiluted crustal sulfur and that up to 1% of the sulfur for sulfide inclusions was processed through the Archean atmosphere.

References

- Chaussidon et al. (1987) *Nature*, 330, 242-244.
 Eldridge et al. (1991) *Nature*, 55, 1697-1708.
 Farquhar J. et al. (2000a) *Geochim. Cosmochim. Acta* 64, 1819-1825.
 Farquhar J. et al. (2000b) *Science* 289, 756-758.
 Farquhar J. et al. (2001) *Jour. Geophys. Res.* 106, 32829-32839.

Crystallisation of plate spinifex texture at 1 atm. pressure in a thermal gradient

F. FAURE¹, N. ARNDT² AND G. LIBOUREL³

¹CRPG-CNRS, BP 20, F-54501 Vandoeuvre-lès-Nancy, France; f.faure@opgc.univ-bpclermont.fr

²LGCA, Univ Joseph Fourier, Grenoble, France; arndt@ujf-grenoble.fr]

³CRPG-CNRS, ENSG-INPL, BP40, F-54501, Vandoeuvre-lès-Nancy, France; libou@crpg.cnrs-nancy.fr

The spinifex zone in a komatiite flow consists of a thin upper layer of fine, randomly oriented olivine grains underlain by a thicker layer (30 cm to several metres) made up large plates of olivine oriented perpendicular to the flow top. Random spinifex is readily synthesized in dynamic cooling experiments that reproduce conditions during rapid cooling at the flow top. The coarse-grained spinifex is more problematic because the morphology of the olivine plates resembles those of dendritic crystals that grow experimentally only at high cooling rates, 50 to 100°C/hr. Cooling rates 1-3 m beneath the komatiite flow top, in contrast, are calculated to be <5°C/hr. This paradox has led to the suggestion that komatiites are hydrous magmas that crystallized in mid-crustal intrusions; a suggestion refuted by field studies that demonstrate clearly that most komatiites are extrusive.

To help resolve the problem we undertook a series of experiments in which synthetic Fe-free charges (51.9 wt. % SiO_2 , 17.4 wt. % MgO , 13.2 wt. % Al_2O_3 , 17.3 wt. % CaO) were slowly crystallized in a temperature gradient, such as exists at the top of a komatiite flow. The charges were confined in 5-cm-long graphite capsules in the upper part of a 1-atm vertical furnace (argon atmosphere) where the gradient is $\sim 20^\circ\text{C}/\text{cm}$, like that during cooling of a komatiite flow top. At cooling rates between 2 and 5°C/hr, we grew long parallel dendritic olivines whose morphologies resemble those of crystals that grow only at cooling rates $>50^\circ\text{C}/\text{hr}$ in experiments on the same starting material but without a thermal gradient. Plumose spinifex-like pyroxenes grow between the olivine crystals. These experiments demonstrate that plate spinifex texture forms naturally during cooling of ultramafic lava flows. The presence of water is not required to explain the texture.

Short scale changes in soil properties due to structural iron reduction.

F. FAVRE¹, V. ERNSTSEN², D. TESSIER³ AND P. BOIVIN¹

¹ Pedology Laboratory, ENAC, EPFL, CH-1015 Lausanne (fabienne.favre@epfl.ch) (pascal.boivin@epfl.ch)

² Geological Survey of Denmark and Greenland, DK-1350 Copenhagen K, DK (ve@geus.dk)

³ Institut National de Recherche Agronomique, 78026 Versailles, F (tessier@versailles.inra.fr)

Introduction

Cation exchange capacity (CEC) is one of the most important soil parameter, determining major retention and physical soil properties. CEC is due to cation heterovalent substitutions in the clay crystal and is therefore considered as a constant. As reviewed in Stucki (1997), structural iron (Fe_s) in the clay lattice of pure clay can be reduced, resulting in sharp changes in clay layer charge and CEC. Favre et al. (2002) reported simultaneous structural iron reduction and CEC increase in field and incubated bulk soil. Induced by bacteria, soil reduction may occur on short time and space scale. The redox-induced changes in CEC, exchangeable cations and clay particle organization in a rice-cropped vertisol with 40% of iron-bearing smectite are presented here.

Methods

Eh and pH were monitored in the field and in laboratory incubated bulk soil samples with native bacteria. Soil samples were collected in incubators at different Eh values. Structural iron reduction was assessed using chemical analysis and Mössbauer spectroscopy. Changes in clay texture and organization were observed using TEM images. Experiments were performed under N₂ atmosphere to avoid re-oxidation.

Results and discussion

CEC increased two times upon reduction. The increase was related to structural iron reduction. The CEC increase was almost balanced by Fe²⁺ and NH₄⁺ adsorption without release of other cations (see table below). Reductive dissolution of iron oxides was simultaneously observed. TEM images showed sharp changes in clay organisation, namely increase in particle thickness, elongation and stacking order.

E _H	Fe _s ^{II}	CEC	Ca _x	Mg _x	Na _x	K _x	Fe ²⁺ _x	NH ₄ ⁺ _x
[V]	[%]	[cmol _c ⁺ kg ⁻¹]						
0.4	0.1	22.6	15.1	10.2	0.5	0.5	0.0	0.2
0.0	0.8	55.0	10.8	6.8	0.1	0.4	18.3	7.1

Conclusions

These results show that structural iron reduction actually occurs in field conditions and changes major soil physical and retention properties. Structural iron and iron oxides seem to be reduced at similar redox potentials. This process is likely to occur either on large or short time and space scales in soils and sediments.

References

Stucki J.W., (1997), *Adv. GeoEc.* **30**, 395-406.
Favre F., Tessier D., Abdelmoula M., et al., (2002), *Eu. J. Soil Sci.*, **53**, 175-183.

A new method for U-Pb isotopic analyses of uranium oxide minerals by SIMS

M. FAYEK¹, L.R.RICIPUTI², AND T.K.KYSER³

¹Dept. Geological Sciences, Univ. of Tennessee, Knoxville, TN USA mfayek@utk.edu

²Oak Ridge National Laboratory, P.O. Box 2008, Oak Ridge, TN USA i79@ornl.gov

³Dept. Geological Sciences Queen's Univ., Kingston, ON, CA kysyer@geol.queensu.ca

We present a new SIMS method that combines the advantages of conventional U-Pb dating (*i.e.*, use of concordia) and *in situ* analysis, and therefore is ideally suited for the study of chemically complex and fine-grained uranium-oxides associated with uranium deposits. During SIMS analysis, differences in the chemical composition of the target phase can affect both relative ion-yields among the isotopes of a given element, and between different elements (e.g., U⁺ and Pb⁺). These matrix effects can lead to erroneous elemental and isotopic ratios determinations if not corrected (e.g., Holliger, 1991). Therefore, an ion-yield normalizing coefficient (α SIMS) that accounts for variation in relative ion-yields with chemical composition for the mineral of interest is necessary. We assembled a suite of uraninite standards that cover a range of U and Pb compositions to develop an appropriate empirical mass bias model. The ²⁰⁶Pb/²³⁸U and ²⁰⁷Pb/²³⁵U ratios measured for each standard by TIMS were compared to the ²⁰⁶Pb⁺/²³⁸U⁺ and ²⁰⁷Pb⁺/²³⁵U⁺ ratios obtained by SIMS. α SIMS varies as a function of wt% PbO, requiring two working curves to define the relationship between the ²⁰⁶Pb⁺/²³⁸U⁺ and ²⁰⁷Pb⁺/²³⁵U⁺ ratios measured by SIMS vs. the "True" ²⁰⁶Pb/²³⁸U and ²⁰⁷Pb/²³⁵U:

$$y_1 = 0.8277 x_1^{0.65}$$

$$y_2 = 0.3185 x_2^{0.58}$$

where y_1 and y_2 are "True" values and x_1 and x_2 are the ratios ²⁰⁷Pb⁺/²³⁵U⁺ and ²⁰⁶Pb/²³⁸U, respectively, measured by SIMS.

The application of this technique to unconformity-type uranium deposits in Canada, demonstrates that at the microscale these deposits preserve a temporal record of accretion and break up of supercontinents. Prior to *in situ* analyses, this detailed chronological record was obscured by the wide variability in U-Pb data obtained by micro-drilling and conventional isotopic analyses due to mixing of different generations of minerals. Only in studies that integrated a variety of crystal chemical techniques were these records less obscure. *In situ* U-Pb data demonstrate that uranium deposits can record the timing at which various continent-sized blocks came into existence and their histories of growth.

Holliger, P. (1991). SIMS isotope analyses of U and Pb in uranium oxides: Geological and nuclear applications. *8th Internat. SIMS Conf. Proc.* 719-722.

Tellurium isotopes and the origin of the solar system

M. FEHR¹, M. REHKÄMPER¹, A. N. HALLIDAY¹ AND D. PORCELLI²

¹ ETH Zürich, Dept. of Earth Sciences, 8092 Zürich, Switzerland (fehr@erdw.ethz.ch)

² Dept. of Earth Sciences, Oxford OXI 3PR, UK

¹²⁶Sn decays to ¹²⁶Te with a half-life of 0.235 Myrs. ¹²⁶Sn cannot be produced in significant amounts by the s-process; it is an r-process nuclide that is probably formed in a supernova environment. The discovery of ¹²⁶Te excesses that correlate with Sn/Te in meteorites would thus provide powerful confirmation of the theory that a supernova injected freshly synthesised nuclides into the molecular cloud from which our solar system formed, providing evidence of a trigger.

Tellurium is of additional interest because it has eight stable nuclides that are well suited for the study of nucleosynthetic isotope anomalies. The nuclides ¹²²⁻¹²⁴Te are produced only by the s-process, ^{128, 130}Te only by the r-process, ¹²⁰Te only by the p-process, whereas ^{125, 126}Te are produced by the r- and s-process. Recently, ε-level Mo isotope anomalies have been reported in bulk meteorites (Dauphas et al., 2002; Yin et al., 2002). These anomalies were inferred to be of nucleosynthetic origin because they mirrored the s- and r-process anomalies that were identified in presolar grains. Previous studies have also reported large (100%-level) Te isotope anomalies in acid-etched residues of Allende (Richter et al., 1998; Maas et al., 2001). Thus bulk carbonaceous chondrites may also display nucleosynthetic Te isotope anomalies.

In the present study, we analyzed bulk samples of the carbonaceous chondrites Orgueil (CI), Murchison (CM), ALH3100 (CM), Allende (CV) and ALH84028 (CV) for their Te isotope composition. All measurements were conducted by MC-ICPMS. The data are normalized to ¹²⁵Te/¹²⁸Te=0.22204 with the exponential law. Results are expressed in ε-units relative to a JMC Te solution. The reproducibility (2s) of the isotopic measurements for 100 ng samples of Te is typically ±4500 ppm for ¹²⁰Te/¹²⁸Te, ±140 ppm for ¹²²Te/¹²⁸Te, ±100 ppm for ¹²⁴Te/¹²⁸Te, ±30 ppm for ¹²⁶Te/¹²⁸Te and ±60 ppm for ¹³⁰Te/¹²⁸Te.

The Te isotopic compositions of all chondrites were within error identical to the JMC standard. Bulk chondrites thus preserve no resolvable evidence of the nucleosynthetic isotope anomalies found in presolar grains. Any ¹²⁶Te anomalies due to decay of ¹²⁶Sn are furthermore either too small to be resolvable or absent. This indicates that the initial abundance of ¹²⁶Sn was either very small or that Sn/Te fractionation occurred too late. The Te isotopic composition of the silicate Earth is probably dominated by the late veneer (Yi et al., 2000) and is therefore unrelated to the bulk earth Sn/Te. However, assuming the bulk Sn/Te ratios of carbonaceous chondrites reflect variable early volatile element depletions during condensation in the nebular that represent their parent bodies, we can calculate a maximum initial ¹²⁶Sn/¹¹⁸Sn of 1×10^{-4} .

Low pH protonation of bacterial cell walls: New data for *Bacillus subtilis*

JEREMY B. FEIN¹, NATHAN YEE², AND JEAN-FRANÇOIS BOILY³

¹ University of Notre Dame; Civil Engineering and Geological Sciences; Notre Dame, IN 46556 USA; fein.1@nd.edu

² School of Earth Sciences; University of Leeds; Leeds LS2 9JT, United Kingdom; nyee@earth.leeds.ac.uk

³ Swiss Federal Institut of Technology; Intitut für Mineralgie und Petrographie; CH-8092 Zürich, Switzerland; boily@erdw.ethz.ch

Previous potentiometric studies of the charging behavior of bacterial cell walls have focussed primarily on pH conditions higher than approximately 3.5. However, recent bulk metal adsorption and X-ray absorption spectroscopy data suggest that cell wall functional groups can be proton active below pH 3.5, and that surface complexes involving these functional groups can remain important under higher pH conditions. To provide constraints on the speciation of the bacterial cell wall under low pH conditions, we have conducted potentiometric titrations using the Gram-positive aerobic species *Bacillus subtilis*, covering the pH range 1.5 to 10.5.

Titration experiments were conducted using an auto-titrator assembly, with the bacteria suspended in 0.1 M NaClO₄. A thorough wash procedure was used to ensure that the cell walls were free of growth media components, and the electrolyte used was purged of dissolved CO₂ by bubbling N₂ gas through it for 60 minutes prior to the titration. The titrations were conducted in a N₂ atmosphere. Both down-pH and up-pH titrations were conducted, and full reversibility of the protonation reactions was observed over the entire pH range of the experiments.

The titration curves above pH 3.5 are consistent with those from previous studies over this pH range. However, we observed significant adsorption of protons under low pH conditions. In fact, this proton adsorption continued to the lowest pH values examined, indicating that proton saturation did not occur under any of the conditions of the experiments. Zeta potential measurements indicate that the cell wall remains negatively charged, even under the lowest pH conditions studied, and EXAFS data suggest that the low pH-active functional group is a phosphoryl site. We model our titration data using a range of electrostatic models, solving for the acidity constant and site concentration of the functional group that is active under low pH conditions. This study indicates that the cell wall of *B. subtilis* can interact with protons and metals under extremely low pH conditions, and that the nature of the surface phosphoryl sites is likely more complex than has been previously envisioned.

Steady-state $^{226}\text{Ra}/^{230}\text{Th}$ disequilibrium in hydrous mantle minerals

MAUREEN D FEINEMAN¹, DONALD J DEPAOLO¹, AND
FREDERICK J RYERSON²

¹Center for Isotope Geochemistry, Department of Earth and
Planetary Science, University of California, Berkeley, CA
94720-4767, USA (feineman@uclink4.berkeley.edu)

²Lawrence Livermore National Laboratory, PO Box 808, L-
202, Livermore, CA 94550, USA (ryerson@llnl.gov)

The short half-life of ^{226}Ra (~1.6 ka) makes it an ideal isotope for studying magmatic processes. However, observed excesses of ^{226}Ra are often larger than expected based on other U series nuclides and difficult to explain. The ^{226}Ra excesses in primitive IAB ($^{226}\text{Ra}/^{230}\text{Th} \leq 7$) are particularly large in comparison to MORB ($^{226}\text{Ra}/^{230}\text{Th} \leq 3$) and OIB ($^{226}\text{Ra}/^{230}\text{Th} \leq 1.5$) (Turner et al., 2001). The IAB super-excesses of ^{226}Ra may be a consequence of strong Ra/Th fractionation by the hydrous mantle minerals amphibole and phlogopite, coupled with a high diffusivity of Ra at mantle temperatures (calculated using the model of Van Orman et al., 2001). Partition coefficients (calculated and/or experimentally determined) suggest that equilibrium Ra/Th ratios in phlogopite (amphibole) are ca. 10000 (100) times higher than in clinopyroxene. Radium diffusion is predicted to be several orders of magnitude faster than Th in cpx. Consequently, as ^{230}Th decays to ^{226}Ra , the latter can diffuse out of cpx and into neighboring phlogopite or amphibole. The efficiency of the diffusional fractionation effect is related to the ratio of the cpx grain radius to $(D_{\text{Ra}}/\lambda)^{1/2}$. At temperatures >1000°C, the effect is significant for radii up to 1cm. Hydrous minerals present in low modal abundance can maintain large steady state $^{226}\text{Ra}/^{230}\text{Th}$ excesses (>10x equilibrium). Clinopyroxene will have complementary steady state depletions. Incipient melts may inherit the strong Ra excesses in the hydrous minerals by preferential incorporation of these early-melting phases, and hence could have Ra excesses larger than would be predicted by the ratio of Ra and Th distribution coefficients in major mantle minerals. The degree of ^{226}Ra excess in derived melts increases with ambient mantle temperature, and decreases with clinopyroxene grain size, degree of partial melting, and the time required for melt extraction. Further Ra enrichment during melt transport could contribute to the large observed ^{226}Ra excesses and hence relax the requirements for super-fast magma transport.

References

- Turner S., Evans P., and Hawkesworth C. (2001) *Science* 292, 1363-1366.
Van Orman J., Grove T., and Shimizu N. (2001) *Contrib. Mineral. Petrol.* 141, 687-703.

On-line separation of PGE

N. FELLNER AND T. MEISEL

General and Analytical Chemistry, University of Leoben, A-
8700, Austria (meisel@unileoben.ac.at)

The increase in applications for the Re-Os and Pt-Os isotope systems raised the interest of determining the other platinum group elements (PGE). In the past few years, various analytical procedures have been developed to meet the demand on analyzing platinum group elements at the sub 10 ng/g level. The well known nugget effect tends to mislead the analytical geochemist making him believe that irreproducible results are caused or dominated by this effect. The complexity of separating uncertainties due to sample inhomogeneity from deficiencies of the methods (e.g. digestion, measurements) especially close to the limit of quantification make it difficult to validate the procedure. Validations of procedures with reference materials (RM) are currently not possible since these are not adequately certified. But being able to analyze RM accurately not necessarily allows to infer that every determination of unknown samples will be correct.

Preconcentration techniques are essential for PGE determinations. Thus not only complete digestions but also an effective analyte-matrix separation is required. The use of ICP-MS is very demanding, since problems of molecular interference are often uncontrolled. Separations via ion-chromatography with anion or cation exchange resins rely on the reproducible behavior of PGE (mostly as chloro-complexes) and the interfering species on the column.

Here complete liberation of the PGEs is achieved with a high pressure asher (HPA-S). But only through the on-line coupling of a cation-exchange column to an ICP-MS it is possible to monitor molecular interferences and the completeness of the species separation. Through this procedure (HPA-S and online separation) we are now able to gain confidence on the "trueness" of analytical results of every sample analyzed. As a consequence we can now identify uncertainties due to true sample heterogeneity since reproducibilities (1s) are 2-3%rel. for Pd, Pt and Re, 6-7%rel. for Ru, Os and Ir in UB-N, a peridotite RM. The differences between the two PGE subgroups is explained by the different affinities to mineral phases e.g. homogeneous distributed interstitial base metal sulfides and PGM nuggets e.g. laurites (Ru(Os,Ir)S₂).

Biogenic evolution of microscale heterogeneity: Impact on contaminant dynamics

S. FENDORF, C. M. HANSEL, S. G. BENNER,
K. L. REVILL, P. S. NICO, AND B. C. BOSTICK

Dept. of Geological and Environmental Sciences, Stanford
University, Stanford, CA 94305 USA
(fendorf@stanford.edu)

Soils and sediments are complex assemblages of organic and inorganic material which are seldom at sustained equilibrium. Coupled biological, chemical, and physical factors dictate the evolutionary pathways of the system and result, generally, in (extreme) heterogeneity from macro- to micro-scale. Here we demonstrate the complexity that develops within simple systems composed of one reactive solid-phase and a single bacterial strain. Reductive dissolution of ferrihydrite by dissimilatory iron reducing bacteria under hydrodynamic conditions results in a complex mineral assemblage dominated by the production of goethite and magnetite—only minor quantities of green rust were noted. The principal bacterial role is in supplying an Fe(II) source: Fe(II) concentration is the dominant factor controlling the biomineralization pathway. At low Fe(II) concentration (less than 0.4 mM at pH 7), goethite is the dominant product, with magnetite being the major product at higher ferrous iron concentrations. Abiotic experiments confirm the role of Fe(II) in the mineralization process.

While similar minerals are produced in biologically active and inactive experiments, their distribution and crystal properties differ appreciably. Biogenic solids are constrained in morphology and crystal size, generally being mono-domainic and less than one-tenth the size of minerals formed under comparable abiotic conditions. Moreover, under biologically active conditions, both magnetite and goethite nucleate on ferrihydrite, leading to mixed-mineralogical assemblages. Further additives of the biological systems are exopolysaccharides (EPS) that coat and bridge minerals.

The fate of contaminants such as chromium and uranium will be impacted dramatically as a consequence of reductive biomineralization. Adsorption properties will be modified appreciably with the shift in mineralogy and the development of reactive ferrous iron bearing phases (solution, surface, and solid) will have important ramifications on reductive stabilization. For example, owing to the formation of dissolved, surface associated, and green rust bearing Fe(II), chromate reduction proceeds at a rapid rate and leads to the formation of a sparingly soluble phase. Uranium, in contrast, is controlled by completing processes, retention within magnetite zones and enzymatic reduction to U(IV).

Total Gaseous Mercury Exchange Between Air and Water Surface over Baihua Reservoir in Guiyang, China

XINBIN FENG, SHUNLIN TANG, LIHAI SHANG, HAIYU
YAN

State Key Laboratory of Environmental Geochemistry,
Institute of Geochemistry, Chinese Academy of Sciences,
Guiyang, China
(xinbin.feng@mail.gyig.ac.cn)

The exchanges of mercury between surface and air are of significance in the biogeochemical cycling of Hg in the environment, but there are still few reliable data on air/surface exchange in aquatic systems. Field measurement campaigns over lake water surface at Baihua reservoir in Guiyang, Southwestern China were conducted to measure mercury flux using a dynamic flux chamber technique coupled with automatic mercury vapor-phase analyzer from October 30 to November 4, 2001. The dynamic flux chamber is made of quartz glass, and has low blanks. Water samples were collected, and dissolved gaseous mercury (DGM), reactive and total mercury concentrations in water were measured using gold trap pre-concentration and AFS detection method. Meanwhile meteorological parameters, such as wind speed, wind direction, intensity of solar radiation, air and water temperature, and relative humidity, were monitored using a portable weather station.

Water surface is a net atmospheric mercury emission source even at cold season (autumn), and the average mercury emission rate is $3.0 \text{ ng m}^{-2} \text{ h}^{-1}$. It is shown that lake water is super-saturated in terms of dissolved gaseous mercury, which is the driving force of mercury emission from water to the air. The DGM, which is mainly in form of Hg^0 , could be formed in many processes in the water system. Demethylation, bacterial reduction from water and sediment, reduction by humic and fulvic acid in water, and photo-induced reduction in water are so far the possible processes suggested to be responsible for the formation of DGM in aquatic system. We observed a strong positive correlation between wind speed and mercury emission rate, suggesting that strong wind facilitate mercury evaporation process from the water system.

XRD-Rietveld and RMC analysis of the aging process in glauconites

S.F. BASTERO¹, L. GAGO-DUPORT¹, T. GARCÍA¹,
A. VELO¹, M.P. VILLAR² AND A. SANTOS³

¹Dept. Geociencias Marinas, Universidad de Vigo, Spain
(sbastero@uvigo.es).

²Dept. Ciencia de Materiales, Universidad de Cádiz, Spain.

³Dept. Geología, Universidad de Cádiz, Spain.

Glauconites work as open systems at seawater-sediment interface leading to simultaneous chemical and structural rearrangements on aging. A precise knowledge of this process, usually termed as *glauconite maturity*, is of interest for oceanographers and sedimentologists in order to characterize paleoenvironmental changes and to estimate sedimentary conditions for sequence stratigraphic studies.

Usual models are based on empirical markers as are the colour, K⁺ contents, distance between the 001, 020 reflections from XRD patterns, magnetic susceptibility, etc. Nevertheless, a complete characterization of evolutionary stages of glauconite must be able to relate the chemical changes taking place during the growth process with the structural variability, from a nearly amorphous initial stage to a highly evolved glauconite, as function of both the variation on stoichiometry and the structural disorder.

In this work, the aging process in glauconites has been examined using the XRD-Rietveld analysis to characterize the average structural disorder associated with several compositional variations in the glauconite formula. This was done by simultaneous constrained refinement of both the occupancy factors and the crystallite-size domains, as a measure of the crystallinity degree. The celadonite atomic coordinates were used as starting structural model. Fifty glauconite samples located at the NW of Spain continental shelf, with several maturity degrees were employed in the refinements and to perform geochemical mapping relating the space distribution of the glauconite maturity to the chemical variability.

The results show that although the rise in K⁺ in the structure is the driving variable in the ordering process this is coupled with simultaneous loss in Fe, given a progressive tendency towards the enrichment of Al³⁺ and Mg²⁺.

The previous study leads an average characterization of the ordering process. Nevertheless several local mechanisms, like layer interstratification or stacking faults due to layer rotation (Drits and Tchoubar, 1990) have been proposed. Then, to analyse detailed aspects of the local structural disorder, additional Reverse Monte Carlo (RMC) calculations based on the average structure previously obtained from Rietveld analysis have been performed.

References

- Drits, V.A and Tchoubar, C. (1990), Springer-Verlag, 284-303.
Fernández-Bastero, S., Velo, A., García, T., Gago-Duport, L., Santos, A. and Vilas, F. (2000), *J. Iber. Geol.*, 26, 233-247.

This study was supported by Spanish MCYT BTE2000-0877 project.

Sorption of Pb²⁺ on barite and crystallisation of (Ba,Pb)SO₄ in aqueous environments

Á. FERNÁNDEZ-GONZÁLEZ, Á. ANDARA, V. PEDREIRA,
M. PRIETO

Departamento de Geología, Universidad de Oviedo, Oviedo,
Spain (mafernan@geol.uniovi.es)

Sorption of lead ions on barite surface by precipitation of (Ba,Pb)SO₄ solid solutions represents a potential removal process of this contaminant in aqueous environments.

Thermodynamics models for the (Ba,Pb)SO₄-H₂O system reveal that this solid solution presents a wide miscibility gap (Kornicker et al., 1991). Moreover, the low solubility of barite compared to lead sulphate involves a strong preferential partitioning of Ba to the solid phase. However, under non-equilibrium conditions the complete solid solution series can be crystallised (Takiyama and Kozuki, 1969) and the preferential partitioning of Ba to the solid becomes less important.

We present experimental work on (i) crystallisation of (Ba,Pb)SO₄ solid solutions, and (ii) sorption of lead on barite in aqueous environments.

Crystallization experiments have been carried out by counter-diffusion of (Pb²⁺,Ba²⁺) and SO₄²⁻ in a silica hydrogel column. The gel reduces the nucleation density and favours the development of relatively large crystals. Representative single crystals of the complete solution series were obtained and the evolution of both morphology and composition during the growth process was studied.

In addition, two different kinds of sorption experiments have been performed. In a first set, Pb-containing aqueous solutions were placed in contact with barite grains in a stirred reactor to study the decrease in (Pb²⁺)_{aq} concentration as a function of time. Moreover, assuming that sorption occurs by surface precipitation of Pb-bearing solids, a second set of experiments were carried out in a gel medium. This procedure increases the size of the sorbed entities, that were then characterized as nearly two-dimensional (Ba,Pb)SO₄ crystallites that grow epitaxially onto the {001} barite cleavage surfaces.

References

- Kornicker W. A., Presta P. A, Paige C. R., Johnson R. D., Hileman O. E., Snodgrass W. J (1991), *Geochim. Cosmochim. Acta* 55, 3531-3541.
Takiyama K. and Kozuki E. (1969), *J. Electron Microscopy* 18, 93-99

Simulating partial melting and chemical fractionation in mantle dynamics models

SYLVAIN FERRACHAT¹ AND LOUISE H. KELLOGG²

¹University of California Davis, Geology Dept, Davis CA USA (ferrachat@geology.ucdavis.edu)

²University of California Davis, Geology Dept, Davis CA USA (kellogg@geology.ucdavis.edu)

Neither geophysical observations on mantle dynamics, nor geochemical measurements on basalt are able to constrain by themselves the long-term evolution of the Earth's mantle. However, combining both approaches is promising to restrain the set of possible mantle dynamics models, and to get a better understanding of mantle mixing. Here, we present the results of numerical mantle convection studies incorporating partial melting and chemical fractionation at ridges. We use the 2D-cartesian convective code ConMan (King et al 90) to carry out the calculations. We advect passive tracers with assigned chemical concentrations in U, Th, He, Pb and K. Partial melting at ridges is controlled by the local temperature and the mean previous degree of partial melting encountered by matter at a local scale (with a resolution of about 25 km). Reversely, latent heat consumption due to partial melting has a feedback on the temperature and velocity fields. The subsequent chemical fractionation yields a thin, highly degassed and enriched in incompatible elements oceanic crust, and a thicker residual lithospheric mantle. This process has a non-negligible impact on the global mixing properties in the system, since it generates an heterogeneous chemical distribution between crust and lithosphere, while smoothing the melt product relative to the source. In this presentation, we will focus on the effects of the petrologic parameters (such as the bulk partition coefficients) on the resulting long-term chemical evolution of the system. What are the chemical implications of some candidate models for the Earth's mantle dynamics (Hot Abyssal Layer (Kellogg et al 99), D" crust trapping (Christensen and Hofmann 94))?

References

- U. Christensen and A. W. Hofmann, (1994), *JGR* **99**, 19,867-19,884.
 L. H. Kellogg, B. H. Hager and R. D. van der Hilst, (1999), *Science* **283**, 1881-1884.
 S. D. King, A. Raefsky and G. H. Hager, (1990), *PEPI* **59**, 195-207.

Melt/Biotite ¹¹B/¹⁰B Isotopic Fractionation And The Boron Local Environment In The Structure Of Volcanic Glasses

G. FERRARA¹, C. FORTE², R. PETRINI³, F. SLEJKO³ AND S. TONARINI¹

¹Istituto Geoscienze e Georisorse, CNR, Pisa, Italy (g.ferrara@igg.cnr.it)

²Istituto Processi Chimico-Fisici, CNR, Pisa, Italy

³Dip. Scienze Terra, Trieste University, Italy

¹¹B/¹⁰B isotopic compositions were determined on biotite and glass from three evolved volcanic rocks belonging to the Neogene-Quaternary magmatism of Central Italy. ¹¹B MAS NMR spectra were also performed on the same glasses. In these samples the measured boron biotite-glass partition coefficient ranges between 0.004 and 0.011 indicating that boron behaves as an incompatible element during biotite crystallization. The ¹¹B MAS NMR spectra reveal the presence of trigonal BO_{3/2} units, tetrahedral BO_{4/2}⁻ sites and three-coordinated BO_{2/2}O⁻ species containing one non-bridging oxygen. The ¹¹B/¹⁰B isotopic fractionation between biotite and melt/glass was observed to be large even at magmatic temperatures and was found to be between 1.0066 and 1.00279. The measured α values are significantly higher than those calculated using the Reduced Partition Function Ratio (RPFR) values for B(OH)₃ and B(OH)₄⁻ as well as the abundance of trigonal and tetrahedral boron obtained by ¹¹B NMR spectra. Furthermore, a non-linear relationship is observed between the %BO₄ in the glass structure and the measured 1000ln α suggesting that the approximation of monomeric B(OH)₃ and B(OH)₄⁻ species contribution through ideal mixing in calculating the RPFR in polyanions probably does not apply to silicate glasses.

Barite dissolution rates measured with different methods

T. A. FEWLESS AND A. LUTTGE

Department of Earth Science, Rice University, Houston, TX
USA. [tfewless@rice.edu]

Barite (BaSO_4) is a model substance for study of crystal dissolution. Cleavage on barite's $\{001\}$ surface is perfect and can yield an atomically flat surface, making it ideal for atomic force microscopy (AFM) studies. Barite crystals are easily grown in the laboratory, eliminating the need for mechanical grinding, and making them ideal for powder experiments. The chemical structure of barite is a simple two-component system consisting of Ba^{2+} and SO_4^{2-} ions. Dissolution of this [AB] structure is significantly easier to conceptualize than other mineral systems. Barite is thus well suited for computer simulations, and lacks much of the complexity with which similar two component systems, e.g., carbonates, must contend. Therefore, barite is a perfect mineral for comparison of different experimental and analytical techniques.

Overall bulk dissolution rates are composed of various components, e.g., development of deep and shallow etch pits, as well as lateral step movement. These processes contribute to the overall rate, and must be measured using different techniques at different scales to understand their respective contributions. For example, Figure 1 shows the overall removal of material from stepwaves (29 nm) as well as localized development of deep etch pits (40 nm), and shallow, linearly coalescing etch pits (trenches, 7 nm). These processes contribute to the overall ("bulk") dissolution of 1.86×10^{-8} moles $\text{m}^{-2} \text{sec}^{-1}$.

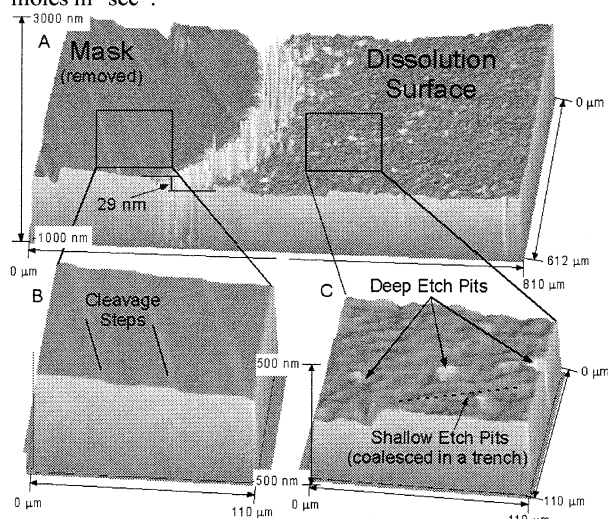


Figure 1. Barite $\{001\}$ vertical scanning interferometry (VSI) data, 4 hours, 0.05 M EDTA, pH~12, 25°C

We present rate data measured using VSI and provide comparisons to published rates from AFM and powder experiments. Our goal is to identify the causes of discrepancies between rates measured by various techniques.

Effect of agricultural activities on the mineralogy of soil clays

C-I. FIALIPS¹, D. RIGHI², AND K.N. POTTER³

¹ Los Alamos National Laboratory, EES-6, Mail Stop D469,
Los Alamos, NM 87545, USA (fialips@lanl.gov)

² HydrASA-UMR6532-CNRS, Univ. de Poitiers, Poitiers,
France (dominique.righi@hydrasa.univ-poitiers.fr)

³ USDA-Agricultural Research Service, Temple, TX 76502,
USA (potter@brc.tamus.edu)

Soils from different locations in Texas were studied by Potter *et al.* (1999) for their soil organic carbon (SOC) content and its relation to agricultural practices. More than 100 years of continuous agricultural activity has reduced SOC by more than 50% compared with untilled prairie soils. Although return to grass reverses this effect, the carbon sequestration rate is then very slow. Agricultural practices may also modify the soil clay mineralogy, and these "modified" clays could play an important role during SOC mineralization or sequestration. Our objective was to study the effects of agricultural practices on soil clays.

The cultivated (AGRI) and prairie (PRAI) soils selected for the present study are vertisols, previously studied for SOC by Potter *et al.* (1999). These soils, located near Temple (Texas), are classified as Houston Black clay (Udic Haplusterts), with large dioctahedral clay contents. Selected cores of AGRI and PRAI were split into depth segments, air dried, crushed to pass a 2-mm sieve, and suspended in water. The SOC was decomposed with H_2O_2 (30%) in the presence of a NaOAc buffer (pH5). The 0.1-0.25 μm fractions were studied by X-ray diffraction (XRD; mineralogy, charge, swelling) and Fourier transform infrared spectroscopy (FTIR; OH stretching and bending modes) after various treatments.

FTIR and XRD results indicate that dioctahedral smectites dominate the clay mineralogy of both AGRI and PRAI. NEWMOD simulations of the XRD patterns after Ca-exchange and glycolation suggest that the smectites are randomly interstratified illite/smectite with ~50% expandable layers. FTIR data established the aluminous character of the clays (intense Al_2OH bending band), and substitution of Fe^{3+} and Mg for Al was also observed (low-intensity Fe_2OH and AlMgOH bending modes). Low amounts of kaolinite and micaceous phases are present in both AGRI and PRAI, with a slightly greater micaceous component in AGRI. XRD data after K-exchange and treatment at 110°C overnight show slightly more high-charge smectite layers in AGRI than in PRAI (more irreversibly collapsed layers). Results after Li-exchange and treatment at 300°C (Greene-Kelly test) indicate that the smectite layers are predominantly beidellitic in both AGRI and PRAI, although there are slightly more montmorillonitic layers in PRAI. It is clear that agricultural practices induced only minor modifications of the clays, probably due to the low charge of the smectite layers and the short period of time involved.

Potter, K.N., Torbert, H.A., Johnson, H.B. and Tischler, C.R. (1999) *Soil Science* 10. 718-725.

Origin of methane within a subduction related high-temperature hydrothermal system and its role in risk evaluation

¹J. FIEBIG, ²S. CALIRO AND ¹J. C. HUNZIKER

¹Institut de Minéralogie et Géochemie, Université de Lausanne, BFSH 2, 1015 Lausanne, Switzerland (Jens.Fiebig@img.unil.ch)

²Osservatorio Vesuviano, via Manzoni 249, 80122 Napoli, Italy (caliro@cds.unina.it)

Introduction

The origin of methane within subduction related high-temperature hydrothermal systems (abiogenic vs thermogenic) and its role in risk evaluation is still a matter of debate. In order to address these questions we present a combined approach where fumarolic gas discharges from Nisyros volcano, Greece, are both investigated for their chemical and isotopic composition.

Discussion of results

With varying relative amounts of CH₄ and CO₂ carbon isotopic composition of both gases stays constant implying an origin from a single source. Apparent temperatures derived from carbon isotope partitioning between CH₄ and CO₂ are around 350°C and correlate well with temperatures measured directly for a deep aquifer (330-340°C, as known from two geothermal drillings). Apparent temperatures inferred from compositional data using the H₂O - H₂-CO₂-CO-CH₄-geothermometer (Chiodini & Marini, 1998) show a much larger spread, but highest temperatures again coincide with measured deep aquifer temperatures. Molar ratios of CO₂, CH₄, H₂ and H₂O at fumarolic outlet are in agreement with formation after Fischer-Tropsch CO₂ + 4H₂ = CH₄ + 2H₂O in the liquid phase, followed by adiabatic boiling and local quenching of the liquid into the vapor phase.

Conclusions

A pure inorganic reaction seems to be responsible for CH₄-formation within the high-temperature hydrothermal system of Nisyros. CO₂ and CH₄ within the deep aquifer are initially in chemical and isotopic equilibrium. Local discrepancies between the chemical and isotopic composition observed at fumarolic outlet are caused by secondary re-equilibration phenomena, such as reaction of CO to CO₂ during the ascent of the gases. These do not affect carbon isotope partitioning between CO₂ and CH₄. Since rates of isotopic exchange between dissolved CO₂ and CH₄ are unknown, the role of the carbon isotope geothermometer in monitoring volcanic-hydrothermal activity remains speculative.

References

Chiodini, G. & Marini, L. (1998) *Geochim. Cosmochim. Acta* 62, 2673-2687.

Distribution of ²³⁰Th and ²³¹Pa off SW-Africa

J. FIETZKE¹, J. SCHOLTEN¹, A. MANGINI², S. REUTER² AND P. STOFFERS²

¹Institute for Geoscience, University Kiel, D-24118 Kiel (jf@gpi.uni-kiel.de)

²Heidelberger Akademie der Wissenschaften, D-69120 Heidelberg (Augusto.Mangini@iup.uni-heidelberg.de)

The North Atlantic is one of the key areas for the formation of newly formed deep water masses (e.g. North Atlantic Deep Water (NADW)) which ventilate the world ocean basins. Changes of the formation rates are believed to influence the world climate significantly. Therefore one of the key issues in paleoceanography is the investigation of changes in the production rate of NADW in the geological past. Based on ratios of the natural radioisotopes ²³⁰Th (T_{1/2} = 75.2 ky) and ²³¹Pa (T_{1/2} = 32.2 ky) preserved in the sediments it was proposed that NADW formation rates did not change during the last glacial maximum compared to recent times. This suggestion was based on a mass balance of ²³⁰Th and ²³¹Pa for the Atlantic Ocean. Since these radioisotopes are particle reactive, areas with high particle flux, e. g. the upwelling area off SW Africa, may have an important effect on this balance.

During Meteor cruises M48/4 (2000) we investigated the distribution of ²³⁰Th and ²³¹Pa in the water column and surface sediments in the Angola and Kap basins. At 11 locations covering near shore sites as well as the open ocean, surface sediments as well as water samples (total and particulate) were obtained in up to 10 depth levels. In the Angola basin a gradual increase of ²³⁰Th concentrations with depth was observed comparable to the ²³⁰Th water-column distribution in most ocean basins. In general, concentration-depth gradients are similar in the Angola and in the Kap basins; but at the near-shore sites in the Kap basin ²³⁰Th concentrations were reduced indicating a boundary scavenging effect which is probably related to high particle flux caused by the upwelling environment off the Namibian coast. In the western Kap basin a drastic increase in ²³⁰Th concentrations of up to a factor 3 was observed in the Antarctic Bottom Water which fills the Kap basin in > 4000m water depth. It is proposed that these ²³⁰Th enriched water masses were advected from areas like the Weddell Sea where export of ²³⁰Th enriched water masses was previously observed. Both water masses and boundary scavenging control ²³⁰Th/²³¹Pa ratios preserved in the surface sediments in the area investigated. The upwelling area off Namibia seems to be an unimportant sink for ²³⁰Th and ²³¹Pa.

Calibration of the production rate of ^{36}Cl from potassium

L.K.FIFIELD¹, J.M.EVANS¹ AND J.O.STONE²

¹Department of Nuclear Physics, RSPHYSSE, Australian National University, ACT 0200, Australia:

(Keith.Fifield@anu.edu.au, Jodie.Evans@anu.edu.au)

²Quaternary Research Center and Department of Geological Sciences, Box 351360, University of Washington, Seattle, 98195-1360, USA: (Stone@geology.washington.edu)

Production of ^{36}Cl by cosmic ray bombardment of potassium at the earth's surface is higher than from any other target element. Since many rock types contain abundant potassium, an accurate value for the rate of this production is crucial for exposure-age and erosion studies that exploit the *in situ* production of ^{36}Cl in surface rocks. Here, we report a calibration of this rate, or rather rates, because there are separate contributions from spallation, muon capture, and neutron capture.

The calibration strategy was as follows:

- Select surfaces of well-known age.* Samples were collected from rock surfaces exposed by the end of the Loch Lomond Readvance glaciation in Scotland 11,600 (± 500) years ago.
- Select a potassium-rich mineral.* Mineral separates of K-feldspar were extracted from the sandstone or granite samples.
- Independently calibrate the production due to neutron capture by chloride.* Chlorine-36 was measured in quartz separates from the same rocks.
- Determine separately the production due to muon capture.* A 6m-long depth profile of ^{36}Cl in K-feldspar separates from a granite quarry at Wyangala in SE Australia was measured in order to disentangle the relative contributions from spallation and muon capture.

Samples were prepared as AgCl using standard techniques. Chlorine-36 concentrations were measured by accelerator mass spectrometry using the 14UD accelerator at the Australian National University. From these data, we deduce the following ^{36}Cl production rates from potassium at sea level and high latitude:

Spallation by fast nucleons $161 \pm 9 \text{ atom (gK)}^{-1} \text{ yr}^{-1}$
 Capture of negative muons $10.2 \pm 1.3 \text{ atom (gK)}^{-1} \text{ yr}^{-1}$

Characterisation of Sr in coral aragonite by EXAFS

ADRIAN A. FINCH¹, NICOLA ALLISON¹, STEVEN R. SUTTON^{2,3}, MATTHEW NEWVILLE³

¹Centre for Advanced Materials *and* School of Geography & Geosciences, University of St Andrews, St Andrews, Fife KY16 9AL, UK. aaf1@st-and.ac.uk

²Department of Geophysical Sciences, University of Chicago, Chicago, IL 60637, USA

³Consortium for Advanced Radiation Sources, University of Chicago, Chicago, IL 60637, USA.

We have analyzed the aragonite from *Porites lobata*, *Pavona gigantea*, *Pavona clavus* and *Montastrea annularis* corals using Sr K-edge Extended Absorption X-ray Fine Structure (EXAFS) and compared these with aragonite, strontianite and mechanically mixed standards. We seek to know the structural state of Sr in coral aragonite, specifically whether it is entirely substituted for Ca within the aragonite (single-phase), or whether submicroscopic crystals of strontianite are also present in the structure (dual phase), as suggested previously. We performed bulk analyses and compared the data with equivalent μEXAFS analyses on small ($\sim 400 \mu\text{m}^3$) analytical volumes using a microfocussed x-ray beam. As a result of the architecture of the coral skeleton, the crystals within the microanalytical volume are not randomly oriented, and the microanalytical x-ray absorption spectra show orientational dependence. However, refinement of bulk and microanalytical data provided indistinguishable interatomic distances and thermal vibration parameters in the third shell (indicative of Sr speciation). Analysis in μEXAFS mode allows the structural state of individual parts of the coral skeletal architecture to be ascertained, and the data quality is comparable with bulk analysis. The Sr K-edge EXAFS of all the coral samples refine, within error, to Sr ideally substituted in aragonite, in contrast to previous studies, in which strontianite was reported. Some samples from that study were also analyzed here. Strontianite may be less widely distributed in corals than previously thought. Coral aragonite is a Sr-supersaturated, metastable, single-phase aragonite. These observations have implications for the long-term stability of coral aragonite and the use of Sr in corals to reconstruct past seawater temperatures.

A Subduction Zone Barrier for Sediment-Derived Nitrogen

T. P. FISCHER¹, D. R. HILTON², A. M. SHAW²,
M. M. ZIMMER¹ & Z. D. SHARP¹

¹ University of New Mexico, Albuquerque, NM 87131-1116,
U.S.A (fischer@unm.edu)

² Scripps Inst. Oceanography, La Jolla, CA 92093-0244
(drhilton@ucsd.edu)

The distinct isotopic compositions of the noble gases in various terrestrial reservoirs makes them ideal for exploring deep Earth processes. Helium in particular is a powerful tracer of mantle versus crustal contributions to volatile degassing at the surface. Here we use He in combination with N-isotope systematics to trace the sources of nitrogen in subduction zones, and to address the mass balance between the input of nitrogen into the subduction zone and the output via arc volcanism. We show that nitrogen stored in sediments of the oceanic crust is efficiently recycled back to the atmosphere and is not transported into the deeper mantle. To subduct nitrogen past the zone of arc magma generation transport of nitrogen in the oceanic basement is necessary.

Investigation of the He-N₂ systematics of volcanic and geothermal gases discharging from the Costa Rican and Guatemalan segments of the Central American arc shows that 1) The majority of samples have ³He/⁴He ratios in the range 5-8 R_A indicating that both arc segments sample He primarily of mantle wedge origin; 2) nitrogen isotope systematics (and N₂/He ratios) vary considerably between Guatemala and Costa Rica. Guatemala volatiles have δ¹⁵N values in the range -0.5 to 6.3 ‰ and N₂/He ratios fall between 1,400 and 25,000 (typical range of other arc-volcanoes). Volatiles from Costa Rica, have significantly lower N₂/He values (73- 333) and mostly negative δ¹⁵N (-3.0 to 1.7 ‰). With the effects of air contamination removed, the data is interpreted as a binary mixing between mantle-derived nitrogen (³He/⁴He = 8 Ra, δ¹⁵N = -5‰) and subducted sedimentary nitrogen (³He/⁴He = 0.05 Ra and δ¹⁵N = +7 ‰). Volatiles from Costa Rica are characterised by mantle-derived nitrogen, whereas in Guatemala the subducted sedimentary contribution dominates.

To evaluate nitrogen mass balance, we determine the volatile input flux via the Central American trench by combining estimates of the volatile characteristics of localized sediments and oceanic basement with extrinsic properties such as subduction rate, arc length, sediment thickness and porosity. The flux of sediment-hosted N is 2.3 x 10⁸ mol N/yr for the Central American margin. The output is determined by combining the chemistry of the gas emissions (CO₂, SO₂, N₂) with the time-averaged SO₂ flux from the arc. This approach yields a non-air N₂ flux of 2.9 x 10⁸ mol/yr, which balances almost exactly the input flux of nitrogen via the trench. This implies that nitrogen is efficiently released from the slab and transported through the mantle wedge to the atmosphere via arc volcanism. We argue that this observation holds for arcs globally suggesting that subduction zones act as a barrier to the deeper mantle for sedimentary nitrogen.

Constraining landscape evolution of the West Antarctic rift flank of southern Victoria Land

PAUL FITZGERALD¹, SUZANNE BALDWIN², KEN FARLEY³,
LINDSEY HEDGES⁴, PAUL O'SULLIVAN⁵ AND LAURA
WEBB⁶

¹ Dept. of Earth Sciences, Syracuse University, Syracuse, NY,
13244, USA, pgfitzge@syr.edu

² Syracuse University, sbaldwin@syr.edu

³ Div. of Geological and Planetary Sciences, Cal Tech,
Pasadena, CA, 91125, USA, farley@gps.caltech.edu

⁴ Cal Tech, hedges@gps.caltech.edu

⁵ Syracuse University, posullivan@syr.edu

⁶ Syracuse University, lewebb@syr.edu

The Transantarctic Mountains (TAM) define the western flank of the intracontinental West Antarctic rift system (WARS). Cretaceous extension is distributed across the WARS, whereas extension since the early Cenozoic was concentrated along the western side of the WARS adjacent to the front of the TAM. Cenozoic geomorphic evolution of the TAM in this area has previously been summarised as escarpment retreat, formation of planation surfaces and down-cutting by fluvial processes until about the mid-Miocene. Subsequent modification of the landscape by glacial processes has been minor due to the hyper-arid polar climate. Erosion rates since rift flank formation are constrained using apatite fission track thermochronology (AFTT), (U-Th)/He dating of apatite, information from offshore drill-holes, preservation of volcanic ash, and cosmogenic surface exposure age dating. In general, AFTT constrained denudation rates in the Late Cretaceous are low but reach ~65 m/my on the inland flank of the Kukri Hills. Near the coast at Mt Barnes AFTT data indicate the onset of Cenozoic denudation at 55 Ma. Average denudation since then is ~85 m/my but at a rate of 115 m/my from 55-40 Ma. At Peak 1880 20 km inland, AFTT data suggest denudation started later at ~40 Ma, with a similar average rate. (U-Th)/He data from Peak 1880, while exhibiting considerable scatter in single grain ages due to the effects of slow cooling on zoned apatites, also suggest the onset of more rapid cooling at ~40 Ma. This younging-inland trend for the onset of early Cenozoic denudation is interpreted as escarpment retreat at a rate of ~1.5 km/my. Existing information from nearby offshore drill-holes in the WARS agree well with estimates on the amount and timing of denudation and continued slow erosion from the end of the Eocene through the Oligocene. Previously reported exposure age data indicate Miocene to present erosion rates of 0.1-1 m/my. Thus, a combination of different techniques document the history of this rift flank, its initial formation, the style and rate of geomorphic development, the overall slow and decreasing erosion rates, deposition of eroded sediment offshore, and preservation of the landscape since the mid-Miocene.

Deducing marginal marine seawater composition from biogenic carbonate and evaporites

R. FLECKER^{1,2}, S. DE VILLIERS³, I. SANCHEZ-ALMAZO³
& A. CARUSO⁴

¹School of Geographical Sciences, University Road, Bristol
BS8 1SS, UK (r.flecker@bristol.ac.uk)

²Scottish Universities Environmental Research Centre, East
Kilbride, Glasgow G75 0QF, UK

³Dept. Earth Sciences, Downing Street, Cambridge CB2 3EQ
(svil99@esc.cam.ac.uk, isabel00@esc.cam.ac.uk)

⁴Dept Geologia e Geodesia, Palermo Italy (acaruso@unipa.it)

Knowledge of the natural variability of ocean water composition has grown with the number of chemical studies published. While disentangling the controls on chemical composition of biogenic minerals remains poorly constrained, an appreciation of the range of trace element, stable and some radiogenic isotope values typical of ocean water has developed. Values outside these established ranges are commonly discarded on the pretext that they represent diagenetically altered rather than primary signals. Marginal marine settings such as semi-enclosed seas, lagoons and estuaries are subject to much more extreme chemical changes than the open ocean. Discriminating between primary and altered material from marginal marine systems is therefore difficult and controversial.

We present data from a multi-proxy study of the Late Miocene evaporite succession preserved at Eraclea Minoa, Sicily. The succession of alternating foram-bearing marls and gypsum illustrates the strong variability of the water chemistry at the time where salinity fluctuated abruptly between levels able to support a foraminiferal assemblage to those required for gypsum precipitation (130-160 g/L). Careful visual, chemical and LA-ICP-OES screening of samples permits discrimination between primary and secondary mineralisation and allows interpretation of the composition of this anomalous Late Miocene seawater around Sicily. It also reveals chemical characteristics of fluids circulating either during or after deposition. Combined chemical, faunal and sedimentological interpretation of this succession allows a better understanding of the impact of climate and the relative dominance of ocean versus freshwater influx on marginal marine systems.

Carbonate apatite at high pressure

M. E. FLEET, XIAOYANG LIU AND P. L. KING

Department of Earth Sciences, University of Western Ontario,
London, Ontario, N6A 5B7, Canada (mfleet@uwo.ca)

There is an increasing awareness of the contribution of carbonated apatite (C-OHAp, C-FAp) to bone and dental enamel, as well as in the *in vivo* remodelling of bone material. However, the structural roles of the carbonate group in apatite remain unclear. In this study, carbonate apatite (CAp) and C-OHAp and C-FAp have been synthesized in an end-loaded piston cylinder apparatus at 2-3 GPa and 1400°C, and investigated by EPMA, FTIR and C *K*-edge XANES spectroscopy and single-crystal structure analysis, to follow structural change with progressive substitution of carbonate. The composition series investigated was $(9-y)\text{Ca}(\text{PO}_4)_{2/3} + (x+y)\text{CaCO}_3 \pm [\text{CaF}_2, \text{Ca}(\text{OH})_2]$, where $x = 1$ for CAp and $x < 1$ for C-OHAp and C-FAp. Our apatites saturated in the calcite stability field at $(x + y) \approx 2.0-2.5$.

In FTIR spectra, asymmetric stretch (ν_3) bands of the carbonate group are present at about 1459 and 1539 cm^{-1} in A-type CAp ($x = 1, y = 0$); about 1409, 1453, 1504, 1539, and 1563 cm^{-1} in A,B-type CAp; about 1408, 1455, 1471, and 1546 cm^{-1} in A,B-type CAp annealed in air at 1000°C; and about 1428, 1456, 1511, 1550, and 1574 cm^{-1} in B-type C-FAp. C *K*-edge XANES spectra are characterized by a sharp absorption peak at ~ 290.2 eV and a broad peak at ~ 301.3 eV due to transition of C 1s electrons to unoccupied states of π^* and σ^* character, respectively. The area of the π^* peak increases in proportion to the amount of carbonate present.

Different from previous studies, X-ray structures of A,B-type CAp (space group $P6_3/m$) show that the channel (A) carbonate groups are deflected from the vertical plane to avoid a prohibitively short Ca2-O distance (1.74Å in the ideal structure). Also, high-pressure CAp can accommodate more than one channel (A) carbonate group per unit cell. This is possible because one of the oxygens in each group is located at the position of O(H) in OHAp but, even so, minimization of unfavourable O-O interactions results in considerable disruption in the decompressed structure. Partial decarbonation of the excess channel carbonate occurs on annealing A,B-type CAp in air at 1000°C. The B-type carbonate group is oriented close to one of the sloping faces of the vacant PO_4 tetrahedron, but tilted closer to the horizontal plane. For the full complement of Ca atoms (10 pfu), the ideal partitioning of the carbonate group between A- and B-type sites appears to be $A = [x + (y/3)]$, $B = [6 - (2/3)(9 - y)]$. However, the X-ray structures reveal that the amount of channel (A) carbonate is typically in excess of this ideal ratio in CAp because, under high pressure, carbonate is stuffed into the channel (A) sites in preference to available B sites.

Stable Equatorial Pacific Productivity over the last 1Ma

M.Q. FLEISHER, G. WINCKLER, R.F. ANDERSON,
M. STUTE, P. SCHLOSSER

Lamont-Doherty Earth Observatory, Columbia University,
Palisades, NY, US (winckler@ldeo.columbia.edu)

The large glacial to interglacial fluctuations in the atmospheric CO₂ concentration during the Pleistocene have been attributed to changes in the oceanic carbon system, i.e. ocean productivity. The Equatorial Pacific represents an important component of global oceanic productivity and, thus, is speculated to have a major influence on global climate.

Conventional wisdom has held that Equatorial productivity was substantially greater during glacials than during interglacials. Support for this hypothesis comes for example from Paytan et al. (1996) reporting that the burial rate of barite varied by a factor of 5-6 between interglacials and glacials throughout the Pleistocene climate cycles.

To test this hypothesis we present ²³⁰Th and ³He data for two cores from the central equatorial Pacific at 140W (PC 72, PC114). Both tracers represent constant flux proxies (CFP), i.e. tracers of constant supply through time, which allow us to reconstruct accumulation rates that are not biased by sediment redistribution or errors in the stratigraphy. Consequently, we use these tracers to re-evaluate the sedimentation record of paleoproductivity proxies. Normalizing the excess Ba record of the past 1Ma to CFPs eliminates the large variability in the conventional ¹⁸O-derived accumulation rates. We show that the fluctuations reported by Paytan et al. (1996) are an effect of the use of stratigraphy-derived sedimentation rates. This holds also true for the period of the Mid-Pleistocene Climate Transition (MPT, 800-560ka) for which Murray et al. (2000) inferred a major productivity increase from Ti-normalized Ba, Al and P data. Using normalization to ³He we show that the apparent maxima in the profiles during the MPT are due to a decrease in Ti, i.e. dust, and that there was no significant productivity increase during the MPT.

Re-evaluation of the Ba records with CFPs implies that the export productivity in the Equatorial Pacific was constant during the past 1Ma. The variability in the carbonate pattern in the Pacific Ocean can be exclusively attributed to variable CaCO₃ dissolution driven by changes in the paleochemistry of the deep ocean. Our study proves the unequivocal need to apply constant flux proxies (instead of stratigraphy-based sedimentation rates) to reconstruct sedimentary fluxes in the past.

References

- Murray R.W., Knowlton C., Leinen M., Mix A.C. and Polsky C.H. (2000), *Paleoceanography* 15(6), 570-592.
Paytan A., Kastner M and Chavez F.P. (1996), *Science* 274, 1355-1357.

The Origin of Solar System Organic Matter: Evidence from IDPs

G. FLYNN¹, L. KELLER², S. WIRICK³, AND C. JACOBSEN³

¹SUNY, Plattsburgh NY USA george.flynn@plattsburgh.edu

²NASA Johnson Space Center, Houston TX USA

³SUNY, Stony-Brook NY USA

Some extraterrestrial material contains organic matter, but the origin of the organic compounds has not been established. A variety of mechanisms have been proposed, with a Miller-Urey type process, producing organic matter in an aqueous process, and a Fisher-Tropsch type process operating in the Solar Nebula as two extreme cases. If the organic matter were produced by a Miller-Urey type process we would expect to see organic matter predominately in extraterrestrial samples that exhibit other evidence of aqueous processing (e.g., abundant clay minerals) while a Fisher-Tropsch type process should result in comparable amounts of organic matter in either hydrated or anhydrous samples.

The hydrated carbonaceous meteorites have %-level concentrations of organic matter, but anhydrous carbonaceous chondrites have much lower concentrations, with most of the carbon in elemental form. This observation favors a Miller-Urey type mechanism. But all anhydrous carbonaceous chondrites are depleted in volatile elements. These depletions are believed to result from either incomplete condensation or subsequent vaporization of elements more volatile than Mn. Such a process requires temperatures in excess of 1200° C, and is incompatible with the survival of organic matter.

We determined the abundance and types of carbon in anhydrous and hydrated interplanetary dust particles (IDPs) collected from the Earth's stratosphere. Many anhydrous IDPs have contents of the moderately volatile elements \geq Cl, unequilibrated minerals, and D anomalies within a few μ m of D-normal material. These features indicate many anhydrous IDPs have never been significantly heated, making them better candidates to test the origin of Solar System organics.

Scanning Transmission X-ray Microscope (STXM) carbon maps show carbon contents ranging from a few vol-% to over 90 vol-%, with comparable amounts of carbon in anhydrous and hydrated IDPs. Carbon X-ray Absorption Near Edge Structure (XANES) spectra of both anhydrous and hydrated IDPs show similar pre-edge spectra: with a strong C-ring absorption at \sim 285 eV and a carbonyl (C=O) absorption at \sim 288.5 eV. We confirmed the presence of percent-level carbonyl by oxygen XANES.

FTIR spectroscopy detected C-H stretching absorptions from aliphatic hydrocarbon at about the same strength in both hydrated and anhydrous IDPs. We compared the relative strength of C-H stretching and silicate absorptions in IDPs to mixtures of aliphatic hydrocarbon and glass, and conclude aliphatic hydrocarbon is present at the %-level in most IDPs.

Since we found organic matter of similar types and abundances in both anhydrous and hydrated IDPs, it appears that the bulk of Solar System organic matter was produced early in Solar Nebular history, possibly by a Fisher-Tropsch type process or by irradiation of carbon-rich ices.

Sangeang Api: upper plate magma chamber processes and the origin of alkaline arc lavas.

JOHN FODEN¹, MARLINA ELBURG^{1,2}, SIMON TURNER³

¹Department of Geology and Geophysics, University of Adelaide, Adelaide SA5005, Australia (john.foden@adelaide.edu.au)

²Now at: Max-Planck Institute for Chemistry, PO Box 3060, 55020 Mainz, Germany

³Department of Earth Sciences University of Bristol, Bristol BS8 1RJ, U.K.

Sangeang Api is an active alkaline volcano in the Indonesian Sunda Arc. It is composed of oxidised, potassic, Cl- and volatile-enriched, undersaturated lavas with abundant clinopyroxene-rich mafic and ultramafic xenoliths. There is strong evidence that suites of lavas and xenoliths are comagmatic and that the xenoliths are accumulative rocks in equilibrium with the Sangeang Api melts. U-Th-Ra isotope data (Turner & Foden, 2001) indicate that the melts have limited ²³⁸U/²³⁰Th disequilibrium, from slight Th- to slight U-excess, but show extreme enrichment of ²²⁶Ra relative to ²³⁰Th. Excess ²²⁶Ra might result from fractionation during dehydration and partial melting of the slab, implying very fast magmatic ascent rates. However the limited U-Th disequilibrium tends to discount this. Excess ²²⁶Ra might otherwise record very efficient fractionation in the shallow sub-arc regime, implying that melts have "seen" very large volumes of crystals.

Conclusions

Evidence for equilibrium crystallisation and for successive stages of growth and resorption of secondary amphibole and phlogopite in the xenoliths supports a model of percolation flow during waxing and waning thermal conditions. Flow varied from sluggish infiltrative grain-boundary flow to more rapid conduit flow, with periodic stagnation in interconnected small magma chambers. Periodic eruptions may then be associated with the influx of new more rapidly flowing pulses of melt migration in temporary dilatational conduits. The xenolithic clinopyroxenes invariably have relative Th-excess consistent with the D_{Th}/D_U conditions resulting when $P < 1.5$ GPa. (Wood et al., 1999). Partial melting of these clinopyroxene-rich crystal residues may periodically occur and will yield Ca-rich ankaramite liquids (Schiano et al, 2000), which at the time will show Th-excess.

References

- Schiano, P., Eiler, J. M., Hutcheon, I. D. & Stolper, E.M. (2000). *Geochemistry, Geophysics, Geosystems* **1**, 1999GC000032.
- Turner, S. and Foden, J. (2001). *Contrib. Mineral. Petrol.*, **142**, 43-57.
- Wood, B. J., Blundy, J. D. & Robinson, J. A. C. (1999). *Geochimica et Cosmochimica Acta* **63**, 1613-1620

Trace element partitioning evidence for growth of early continental crust from amphibolites, not eclogites

S.F.FOLEY¹, M. TIEPOLO² AND R.VANNUCCI²

¹ Institut für Geologische Wissenschaften, Universität Greifswald, Jahnstrasse 17a, 17487 Greifswald, Germany (sfoley@uni-greifswald.de)

² Dip. Scienze della Terra, Università di Pavia, Via Ferrata 1, 27100 Pavia, Italy

It is generally accepted that the first continental crust formed by melting of either eclogite or amphibolite, either at subduction zones or on the underside of thick oceanic crust. The compositions of early crustal gneisses and experimental studies support these interpretations, but our understanding of trace element partitioning could not distinguish between them up to now. We have investigated the trace element consequences of melting amphibolites and eclogites in various tectonic settings realistic for the Archean on the basis of new experimental trace element partitioning data sets¹⁻³. The critical tests are given by the element ratios Nb/Ta and Zr/Sm: early continental crustal gneisses (TTG gneisses) fall in the lower right quadrant with low Nb/Ta and high Zr/Sm relative to primitive mantle and modern oceanic basalts. Melting of eclogite cannot cause a decrease in Nb/Ta of melts under any circumstances (batch or pure fractional melting); Nb/Ta is *increased* substantially in melts if rutile remains in the residue. In contrast, the Nb/Ta ratios of partial melts of amphibolites depends on the Mg# [$Mg/(Mg+Fe)$] and titanium content of the amphiboles. Those with high Mg# (0.8-0.9) such as in mafic-ultramafic cumulates from primitive basaltic-picritic melts cannot fractionate Nb from Ta, whereas amphiboles with lower Mg# (30-60) can cause a dramatic *decrease* in Nb/Ta of melts.

We conclude that early continental crustal gneisses with low Nb/Ta could be produced by melting of amphibolites in a subduction zone in which fractionated basalts lead to low Mg# amphiboles during subduction. Melting of the underside of thick oceanic crust is unsuitable because of the high Mg# to be expected in the cumulate pile. Furthermore, water contents are probably very low in this environment, so that dry transition to eclogites and pyroxenites is more likely than the formation of amphibolites during metamorphism. The relative scarcity of crustal gneisses in the early Archean must reflect the rarity of conditions in which fractionated basalts could melt as amphibolites at that time.

These conclusions from trace element partitioning are consistent with those derived from experimental investigations of metamorphic reactions in picritic to komatiitic rocks which may have been common in the early Archean ocean crust⁴.

1. Tiepolo et al. 2000. *Earth Planet Sci Lett* 176, 185-201.
2. Tiepolo et al. 2001. *J Petrol.* 42, 221-232.
3. Barth et al. 2002. *Precambrian Res* 113, 323-340.
4. Foley, S.F., Buhre, S. & Jacob, D.E. 2002. This volume.

The phosphorus burial curve revisited

K.B. FÖLLMI, F. TAMBURINI, R. HOSEIN, B. VAN DE SCHOOTBRUGGE, AND K. ARN

Inst. Géologie, Univ. Neuchâtel, CH-2000 Neuchâtel
(karl.foellmi@unine.ch, federica.tamburini@unine.ch,
rachel.hosein@unine.ch, bas.vandeschootbrugge@unine.ch, kaspar.arn@unine.ch)

Phosphorus (P) serves as an element essential to life, and is closely linked to carbon (C) through photosynthesis and biogeochemical weathering. A proxy of change in the global P burial record for the last 160 million years is based on a compilation of P accumulation rates, which were calculated from systematically measured P contents in a great variety of Deep Sea Drilling Project (DSDP) and Ocean Drilling Program (ODP) cores (Föllmi 1995). Since its first publication three tests have been performed on this curve: The first test consisted in a re-examination of an important part of its early Cretaceous portion (137 to 132 myr; Valanginian-Hauterivian), which is based on relatively few data in comparison to younger parts. For this test, 575 P concentrations were measured in eight continental sections in central and southern Europe (Van de Schootbrugge, 2001). The resulting compilation correlates very well with the DSDP- and ODP-based data set, which suggests that the curve is robust for this time interval. The second test consisted in a close-up study of the last full glaciation phase. Here different P phases were analyzed in a selection of eight ODP cores using a sequential extraction method. An important result is that during this last phase of glaciation variations in P burial were coupled to climate change, albeit on a shorter time scale, in the range of the precession band frequency, and that glacial periods during this last glaciation show comparable to slightly higher P burial rates than interglacial stages (Tamburini 2001). The third test included a detailed analysis of the importance of biogeochemical weathering processes in glaciated areas. Here we selected the Rhône and Oberaar Glaciers catchments – both situated within the crystalline basement of the Aare massif (central Switzerland) –, and performed analyses on the geochemistry of the outlet waters, mineralogy of suspended material, and geochemistry and mineralogy of moraine material of different ages. One outcome is that glaciers have an important potential for increasing biogeochemical weathering rates during and especially immediately after glaciation phases (Hosein and Arn, in prep.).

Melt and source diversity under the ultra slow spreading Southwest Indian Ridge

FONT, L.¹, MURTON, B.¹, ROBERTS, S.¹, TINDLE, A.²

Southampton Oceanography Centre, European Way,
Southampton SO14 3HZ, UK. (lfm@soc.soton.ac.uk,
bjm@soc.soton.ac.uk, srl@soc.soton.ac.uk)
Earth Science Department, Open University, Milton Keynes,
MK7 6AA, UK. (A.G.Tindle@open.ac.uk)

Glassy primary melt inclusions trapped within plagioclase and olivine phenocrysts and the matrix glass of basalts of the ultra-slow spreading Southwest Indian Ridge (SWIR), (49°E - 70°E) were studied to investigate the compositional evolution of parental melts, melt extraction and magma chamber processes during ultra-slow spreading. Specifically we test the hypothesis that the depth of melting, melt fraction, the extraction and mingling of melt increments and magma residence time change as spreading evolves from rift propagation in the East to steady-state in the West.

The matrix glass compositions of the SWIR show a unique MORB composition, with high Na₂O concentrations and enriched trace element and REE concentrations compared to a typical N-MORB (Meyzen et al, 2002). The melt inclusions show variable compositions along the ridge. Towards the East they show enriched compositions and more variability in major and trace element. Two groups of inclusions can be differentiated. One shows similar compositions to the matrix glasses, with flat HREE but enriched in LREE and LILE elements. The second group shows strong depletion in HREE and enrichment in LREE and LILE. They also show strong negative anomalies in Nb, Zr and Hf. The melt inclusion compositions towards the West of the ridge appear to be more homogeneous in composition and are depleted in LREE. They do also show negative anomalies in Nb, Zr and Hf. These variations in compositions can be related to enrichments of the melts by LILE carried out by metasomatic fluids coming from the mantle. Alternatively, Nb, Zr and Hf were held back by a mantle phase when these melts were segregated.

References

Meyzen, C., Humler, E., Ludden, J., Toplis, M., Mevel, C. (2002), *Abstract, InterRidge SWIR Workshop*, 26.

Stability of hydrous minerals in subducting eclogitized crust: new experimental perspectives

J. FORNERIS¹ AND J. R. HOLLOWAY²

¹ Dept. of Geological Sciences, Arizona State University, Tempe, AZ, 85287-1404, USA (jul@asu.edu)

² Dept. of Geological Sciences, Arizona State University, Tempe, AZ, 85287-1404, USA (jholloway@asu.edu)

We have conducted experiments to study the phase equilibria of the basalt + H₂O system. The purpose of this work is to determine which hydrous phases are stable in the basaltic layer of a subducting slab and how deeply they may transport H₂O.

Previous experimental studies (Liu et al., 1996; Pawley and Holloway, 1993; Schmidt and Poli, 1998) reported contradicting results. It is possible that metastable growth of hydrous phases, such as chloritoid, occurred in the week-long runs of Schmidt and Poli (1998) as opposed to the month-long runs of Liu et al. (1996). For this reason, experiment duration for our study was either one week or one month for the same set of P and T conditions. Piston-cylinder experiments were undertaken between 2.2 GPa and 3.2 GPa at 650°C. Oxygen fugacity was buffered between 0.1 and 0.4 log units below NiNiO.

Our results show that a calcic amphibole (barroisite) is stable from 2.2 to 2.4 GPa. Above 2.4 GPa, it is replaced by a sodic amphibole (glaucofane) stable up to 2.7 GPa. Epidote is stable between 2.2 and 2.8 GPa. Chloritoid is present in week-long experiments between 2.6 and 2.8 GPa, but is not observed in the corresponding month-long experiments, except at 2.8 GPa and 650°C. At 3.0 and 3.2 GPa, neither chloritoid nor lawsonite are present in month-long experiments. Phengite is found in trace amounts from 2.2 to 3.2 GPa.

The stability field of chloritoid in our experiments is extremely reduced compared to Schmidt and Poli (1998). Metastability of chloritoid in some of their experiments is the most likely explanation for this difference, suggesting that chloritoid does not play an important role in the overall dehydration process in subduction zones.

Our results thus far show that no hydrous phases (except for trace amounts of phengite) are stable in the 3.0-3.2 GPa range at 650°C, implying that a slab following an intermediate P-T path would be completely dehydrated around 90 km depth.

References

- Liu J., Bohlen S.R. and Ernst W.G., (1996), *Earth Planet. Sci. Lett.* **143**, 161-171.
 Pawley A.R. and Holloway J.R., (1993), *Science*, **260**, 664-667.
 Schmidt M.W. and Poli S., (1998), *Earth Planet. Sci. Lett.* **163**, 361-379.

Metamorphic Monazite and the generation of P-T-t paths

G.L. FOSTER^{1&2}, R.R. PARRISH,^{1&2}
 M.S.A. HORSTWOOD.²

¹Department of Geology, Leicester University, Leicester, LE1 7RH, UK

²NIGL, The British Geological Survey, Keyworth, Nottingham, NG12 5GG, UK

Monazite is fast becoming the mineral of choice for dating amphibolite- and granulite-grade metamorphism. The thermo-barometric potential of monazite has also been recently realised with the generation of monazite-xenotime and monazite-garnet thermometers, which although complicated by assumptions of equilibrium, provide a suitable means of generating P-T-t points in a few restricted cases. In this contribution we discuss an additional, more widely applicable approach that allows a similar combination of monazite (and other U-Th bearing REE-phase) chronology with P-T.

A central aspect of the approach described here involves the chemical and textural characterisation of accessory minerals in a petrographic thin section. Simple textural relationships, such as included grains and grains restricted to rock forming mineral reaction zones, allow a first order link between accessory mineral chronology and P-T. Valuable additional constraints can also be generated through studies of accessory mineral chemistry. Monazite is particularly useful in this regard for two reasons. Firstly, metamorphic monazite appears to grow or recrystallise episodically throughout a metamorphic event, often over several millions of years. Secondly, the Y content of metamorphic monazite appears to reflect the abundance and stability of co-existing garnet; when garnet is absent or when garnet is breaking down, monazite tends to have a relatively high Y content (~2 wt%) and when garnet is growing monazite tends to have a relatively low Y content (~1 wt%). This feature is a consequence of garnets affinity for Y and can be used to link the ages of Y-distinct zones within single monazite crystals with P-T information.

By combining textural, chemical and in situ isotopic analyses of accessory minerals from a variety of orogens with P-T pseudosections (assemblage stability diagrams) we demonstrate how successful this approach can be in the determination of prograde P-T-t paths.

Ross Sea ^{226}Ra and Ba profiles measured by MC-ICP-MS.

D.A.FOSTER, M.STAUBWASSER & G.M.HENDERSON

Dept of Earth Sciences, Oxford University, Parks Road OX1 3PR (deborah.foster@earth.ox.ac.uk)

The measurement of ^{226}Ra in seawater has several potential applications in oceanography, particularly as a tracer of water masses and of groundwater input into the oceans (Moore, 1996). $^{226}\text{Ra}/\text{Ba}$ also shows potential for dating marine carbonates, but the seawater $^{226}\text{Ra}/\text{Ba}$ ratio must be known. The majority of work on ^{226}Ra in seawater has used radio decay methods such as alpha scintillation, but the poor efficiencies of radiation counters limit the precision of these measurements to about 5% (Chung, 1980), and requires a sample size of at least 20 litres. Atom counting methods such as mass spectrometry significantly reduce these limitations. Thermal Ionisation Mass Spectrometry (TIMS) has an uncertainty < 2% and requires only 40ml. However, TIMS analysis is time consuming and can be subject to organic interferences. We have developed and tested the use of multiple ion counting ICP-MS to analyse ^{226}Ra on seawater samples using a Nu instrument. We describe the potential and limitations of this approach and demonstrate that 2% (2 σ) uncertainty can be achieved on 120ml of seawater. Backgrounds across the Ra mass range are very low (<1cps) when using clean cones, but molecular interferences of ~100 cps appear on several masses if the cones are contaminated with Ba. This problem necessitates the chemical separation of Ra from Ba prior to analysis. Nevertheless, MC-ICP-MS is significantly less time consuming than TIMS.

Three water column profiles from the Ross Sea and Southern Ocean have been measured in order to assess the variability of $^{226}\text{Ra}/\text{Ba}$ in the Ross Sea and the open ocean. We measure a surface water ^{226}Ra concentration of 0.386 ± 0.014 fmol $^{226}\text{Ra}/\text{kg}$ in agreement with a value of 0.386 ± 0.0048 fmol $^{226}\text{Ra}/\text{kg}$ from the same sample analysed independently using TIMS. ^{226}Ra concentrations are relatively constant with depth, and are close to those in the open Southern Ocean measured at GEOSECS station 287 (Chung, 1980). Ross Sea $^{226}\text{Ra}/\text{Ba}$ ratios are also within error of those measured at station 287 (4.9×10^{-9} mol/mol). This similarity indicated that there is minimal discharge of ^{226}Ra into the Ross Sea, either by surface weathering or by groundwater discharge – a reassuring result for the use of Ra/Ba dating of carbonates in the area.

References

- Chung Y., Craig, H. (1980), *Earth and Planetary Science Letters*, **49**, 267-292.
Moore W. S. (1996), *Nature*, **380**, 612-614.

Experimental determination of the stability of aluminum-borate complexes in hydrothermal solutions

S. FOUQUET, B. TAGIROV, J. SCHOTT,
J. C. HARRICHOURY AND J. ESCALIER

LMTG-CNRS, Toulouse, France (tagirov@lmtg.ups-tlse.fr)

Boric acid is an important component of granite-derived fluids and thermal waters whose concentration, as measured in fluid inclusions, may reach 30 Wt% (Peretyazhko et al., 2000). To check for the formation of Al-borate species, similar to aqueous Al-silicates, a series of experiments was performed including a ^{27}Al NMR spectroscopy study at 25°C, and gibbsite and boehmite solubility measurements from 50 to 200°C. ^{27}Al spectra performed at pH=9 in Al-B solution with $m(\text{B})=0.02$ show the presence of two peaks at 80.5 and 74.5 ppm which correspond to $\text{Al}(\text{OH})_4^-$ and a single Al-substituted Q_{Al}^1 dimer, respectively. When $m(\text{B})=0.02$, a third peak appears at 69.5 ppm which can be assigned to the Q_{Al}^2 trimer. The observed chemical shifts are close to those of the Al-Si dimer and trimer (74 and 69.5 ppm, respectively; Pokrovski et al., 1998) which demonstrates the chemical similarity of Al-B and Al-Si complexes. Gibbsite and boehmite solubility was measured in weakly basic solutions as a function of boric acid concentration. Equilibrium solubility was reached within several days at $m(\text{B})=0.01-0.1$, but Al concentration increased continuously at $m(\text{B})=0.2$ due to the formation of Al-polyborates. The constant of the reaction $\text{Al}(\text{OH})_4^- + \text{B}(\text{OH})_3^0_{(\text{aq})} = \text{Al}(\text{OH})_3\text{OB}(\text{OH})_2^- + \text{H}_2\text{O}$ decreases very slowly with increasing temperature to 200°C. The log K values deduced from the solubility measurements in $\leq 0.1\text{M}$ H_3BO_3 solutions are 1.58 ± 0.10 , 1.50 ± 0.15 , 1.50 ± 0.20 , and 1.25 ± 0.10 at 50, 78, 150, and 200°C, respectively. These results demonstrate that in a solution containing ~0.5g/l of boron at 400°C and 0.5 kbar, $\text{Al}(\text{OH})_3\text{OB}(\text{OH})_2^-$ accounts for ~50% of total aluminum. At boron concentration >1g/l the formation of Al-polyborates may considerably increase aluminum transport capacity of hydrothermal fluids. *This study was supported by CNRS and RFBR (grant 01-05-64675 to BT).*

References

- Peretyazhko I.S., Prokof'ev V.Yu., Zagorskii V.E. and Smirnov S.Z. (2000), *Petrology* **8**, 214-237.
Pokrovski G.S., Schott J., Salvi S., Gout R. and Kubicki J.D. (1998), *Min. Mag.* **62A**, 1194-1195.

The climatic control of weathering in the Himalayan river system

CHRISTIAN FRANCE-LANORD¹, ALBERT GALY² AND SUNIL SINGH¹

¹ CRPG-CNRS BP 20 F-54501 Vandœuvre les Nancy (cfl@crpg.cnrs-nancy.fr)

² Earth Science Dep. Cambridge University. UK.

Physical erosion tends to favour weathering because it increases reaction surfaces in river basin. For most rivers, a rough positive correlation can be observed between chemical and physical erosions which suggests that physical erosion may exert a first order control on global weathering. Nevertheless, the Himalayan rivers, which have the highest rate of physical erosion among the major river systems, are not characterised by a remarkably high rate of chemical erosion. Depending on numbers accepted for the annual flux of sediment load, chemical erosion for the Brahmaputra and Ganga is between 3 and 7% in mass of the total erosion. Several factors explain this relatively low proportion including precipitation and transport dynamic. The comparison between the Brahmaputra and the Ganga drainages which have quite contrasted runoff (1.1 and 0.6 m/yr respectively) allow to test the importance of precipitation or runoff and transport on the efficiency of weathering in such basin undergoing very intense physical erosion.

Carbonates represent the major source of dissolved ions representing 80 to 90 % in mass of the dissolved load of the rivers. The Ganga and most of its tributaries are over-saturated with respect to carbonates and the rivers transport up to 10% of carbonate particles in their suspended load. On the contrary, the Brahmaputra carries no particulate carbonates and is under-saturated in the Assam floodplain. Carbonate particles are however carried by the tributaries including 5 % in the Tsangpo-Brahmaputra but they disappear from the sediment load of the Brahmaputra over few tenth of km in the plain. It is likely the high precipitation over Eastern Assam (5 m/yr) which allow this very efficient carbonate dissolution. Precipitation therefore acts as the controlling factor for carbonate dissolution. They are insufficient in the Ganga basin to dissolve all the particles released by erosion.

Chemical erosion of silicates is low when compared to physical erosion as it represents less than 1 % of the total erosion for both Ganga and Brahmaputra. Taking into account only Na, K and Si which are unambiguously released by silicate weathering, the specific chemical erosion of silicate is double for the Brahmaputra than for the Ganga basin. This difference is even higher if we do remove the Tibetan area of the Brahmaputra where erosion is minor. Examined in detail, chemical erosion of silicate is strongly correlated to local runoff and suggests that it is strongly controlled by precipitation rather than by physical erosion.

The Role Of Metasomatising Fluids In The Genesis Of Orogenic Magmas. A Case Study From Sardinia, Italy

L. FRANCIOSI¹, M. LUSTRINO², L. MELLUSO¹, V. MORRA¹ AND M. D'ANTONIO¹

¹ Dip. Sci. Terra, Univ. di Napoli Federico II, Naples, Italy (lufrauci@unina.it)

² Dip. Sci. Terra, Univ di Roma La Sapienza, Rome, Italy

Miocene High MgO Basalts (HMB) from Montresta (N Sardinia) and Mt. Arcuentu (S Sardinia) have been analyzed with the aim of identifying the physical state of the metasomatising agents in the mantle wedge. These rocks represent near-primary mantle melts likely not interested by crustal contamination. They show typical subduction-related trace element features: LILE (Large-Ion Lithophile Elements) enrichment relatively to LREE (Light Rare Earth Elements), with Ba/La ranging from 10 to 23. LILE and LREE are both enriched relative to NMORB-like HFSE (High Field Strength Elements).

⁸⁷Sr/⁸⁶Sr ratios range from 0.70399 to 0.70631; ¹⁴³Nd/¹⁴⁴Nd ratios ranges from 0.51260 to 0.51274 and ²⁰⁶Pb/²⁰⁴Pb from 18.609 to 18.707, ²⁰⁷Pb/²⁰⁴Pb from 15.619 to 15.661 and ²⁰⁸Pb/²⁰⁴Pb from 38.408 to 38.747.

Sr, Nd and Pb isotopic data of Sardinia orogenic basalts indicate that, in addition to the input of fluids from altered subducted oceanic crust in mantle wedge, a further component from subducted oceanic sediments is to be considered. In order to constrain if subduction components are mainly fluid or melt phases, ratios among trace elements with strongly different solid/fluid and solid/melt partition coefficients (i.e. Th/Pb, Th/Nd and Sr/Nd) have been taken in consideration. Models based on elemental (Nd/Pb) and isotopic ratios (⁸⁷Sr/⁸⁶Sr and ²⁰⁶Pb/²⁰⁴Pb) indicate that small amounts of subduction fluid components in mantle wedge can account for the geochemical and isotopic features of Sardinia basalts.

In fact, mantle source of Mt. Arcuentu magmas can be modeled considering an enrichment of a DMM source by about 0.45% MORB fluid (derived from subducted oceanic crust) and 0.05-0.08% sediment fluid; for Montresta mantle wedge the amount of subduction components is about 0.1% MORB fluid and 0.03-0.04% sediment fluid. Such low values are consistent with the lack of negative Eu anomalies. It is noteworthy that, on the basis of Sr and O isotopic modeling, other authors proposed a much larger contribution of oceanic sediments (the same utilized in this work) (2-10%) for the Mt. Arcuentu basalts.

Paleoproductivity reconstruction: The on-going quest for a quantitative geochemical tracer

ROGER FRANCOIS

The export of organic carbon from surface to deep water is one of the key aspects of the global carbon cycle controlling atmospheric CO₂ and the earth's radiation balance. A full understanding of the influence of greenhouse warming on secular changes in global climate thus requires the accurate reconstruction of this variable from the sedimentary record.

The residual organic carbon that is buried after reaching the seafloor is inadequate for this purpose, because of poor and variable preservation. Instead, indirect methods, which use geochemical or micropaleontological parameters that can be related to primary production, have been explored. In general, the main advantage of these tracers is better preservation of the productivity signal; the main drawback is that other processes, which may or may not be related to productivity, also affect this signal. One can attempt to mitigate this problem by combining different tracers of productivity that are influenced by different secondary processes, but we have yet to obtain a fully constrained system using this approach and it is becoming increasingly clear that one cannot expect to find a simple method of paleoproductivity reconstruction that would be universally applicable. Instead, different proxies will have different domains of applicability and it behooves us to clearly understand and define the limits of these domains. I will briefly review recent developments that have changed our views on the applicability of two geochemical tracers, sedimentary biogenic Ba accumulation rates and ex.²³¹Pa/ex.²³⁰Th, which were initially viewed as very promising and broadly applicable. As we gained a better understanding of their geochemistry, this initial optimism has given way to a more cautious approach towards their use for paleoproductivity reconstruction. While it is now clear that they cannot be used indiscriminately, however, they could still provide useful quantitative information under a more restricted set of environmental conditions.

Modelling the Cenozoic evolution of atmospheric CO₂

L.M. FRANÇOIS¹, J. GAILLARDET², Y. GODDÉRIS³

¹Laboratoire de Physique Atmosphérique et Planétaire,
Université de Liège, Liège, Belgium
(francois@astro.ulg.ac.be)

²Institut de Physique du Globe de Paris, Paris, France

³Laboratoire des Mécanismes de Transfert en Géologie,
Toulouse, France

In recent years, paleolevels of atmospheric CO₂ during the Cenozoic have been estimated from various proxy records, such as the ¹³C isotopic composition of marine organic matter (Pagani et al., 1999), the seawater pH recorded in boron isotopes (Pearson and Palmer, 2000; Lemarchand et al., 2000) and the stomatal density/index of fossil leaves (Royer et al., 2001). These proxy-based reconstructions provide Cenozoic evolutions of atmospheric CO₂ between two extreme scenarios: (1) CO₂ decreased from very high levels (2000-4000 ppmv) in the Paleocene-Eocene to present or lower than present values in the Miocene-Pliocene, (2) CO₂ remained relatively constant throughout the Cenozoic.

Here we present a coupled model of the carbon and boron cycles. This model includes four carbon reservoirs (ocean-atmosphere, shelf/continental carbonates, pelagic carbonates and crustal organic carbon) for which carbon content and isotopic composition are calculated. A budget is also established for ocean alkalinity, ocean boron and its isotopes. A sub-model of the ocean-atmosphere system allows a redistribution of carbon and alkalinity among the atmosphere, the surface and deep ocean reservoirs. This sub-model calculates explicitly carbonate chemistry, pH, calcite and aragonite lysocline depths, as well as discrimination of carbon and boron isotopes in physical, chemical or biological processes. Surface temperature is related to atmospheric pCO₂ through a simple parametric law.

Various weathering rate laws or scenarios of spreading rates through time are tested with this model. Organic carbon deposition is derived from the δ¹³C of ancient seawater. It is shown that it is possible to produce simulations which are broadly consistent with a variety of proxy records, such as calcite compensation depth, ¹³C isotopic fractionation of marine biology and boron isotopes changes through the Cenozoic. Interestingly, in such reconstructions, Miocene levels of atmospheric CO₂ tend to be smaller than today.

References

- Lemarchand D., Gaillardet J., Lewin E. and Allègre C.J., (2000), *Nature* 408, 951-954.
Pagani M., Freeman K.H. and Arthur M.A., (1999), *Science* 285, 876-897.
Pearson P.N. and Palmer M.R., 2000, *Nature*, 406, 695-699.
Royer D.L., Wing S.L., Beerling D.J., Jolley D.W., Koch P.L., Hickey L.J. and Berner R.A., 2001, *Science* 292, 2310-2313.

The Behaviour of ^{10}Be and ^9Be in the Arctic Ocean: Relationship to water mass distribution and particle flux

M. FRANK¹, D. PORCELLI^{1,2}, P. ANDERSSON³,
A.N. HALLIDAY¹, P.W. KUBIK⁴, B. HATTENDORF⁵, AND
D. GUENTHER⁵

¹Institute for Isotope Geology and Mineral Resources, ETH Zürich, Sonneggstrasse 5, CH-8092 Zürich, Switzerland (frank@erdw.ethz.ch, halliday@erdw.ethz.ch)

²Department of Earth Sciences, University of Oxford, Parks Road, Oxford OX1 3PR, United Kingdom (donp@earth.ox.ac.uk)

³Laboratory for Isotope Geology, Swedish Museum of Natural History, Box 50007, 104 05 Stockholm, Sweden (per.andersson@nrm.se)

⁴Paul Scherrer Institute, c/o Institute for Particle Physics, ETH Hönggerberg, CH-8093 Zürich, Switzerland (kubik@particle.phys.ethz.ch)

⁵Laboratory for Inorganic Chemistry, ETH Hönggerberg, CH-8093 Zürich, Switzerland (bodo@inorg.chem.ethz.ch, guenther@inorg.chem.ethz.ch)

The Arctic Ocean basin is confined by landmasses similar to the Mediterranean. There is only little deep water formed seasonally on the shelves of the Arctic Ocean despite the low temperatures. This is due to a freshwater lid at the surface which originates from the Arctic rivers. The deeper Arctic Ocean water masses can thus only be renewed at comparatively low rates through the only deep connection to the Atlantic Ocean, the Fram Strait. At the same time the biogenic particulate fluxes in the central Arctic Ocean are very low due to perennial sea ice cover and the organic matter produced in the surface waters is remineralised efficiently. Detrital particle fluxes from either eolian or riverine sources are also very low.

The distribution of particle-reactive natural radionuclides, (^{230}Th , ^{231}Pa) indicates differences in scavenging behaviour between the Canadian and Eurasian parts of the Arctic Basin, possibly due to different ventilation ages or lateral advection of particulate material from the shelves.

We will present the first combined dissolved ^{10}Be (cosmogenic) and ^9Be (continental sources) depth profiles from water samples of the major deep basins of the Arctic Ocean collected during the Swedish Arctic Ocean 2001 expedition. Be is 5-10 times less particle-reactive than Th or Pa and should therefore even at the low Arctic Ocean renewal rates serve as a quasi-conservative tracer for different origins of water masses (Atlantic Ocean/Norwegian Sea, Pacific Ocean, Arctic Shelves). ^9Be and Nd isotope analyses will provide complementary information on the pathways of dissolved material originating from the Arctic continents.

First results from near Svalbard indicate uniformly low ^{10}Be concentrations (500 atoms/g) over different water masses in the Eurasian part of the Arctic Basin. This suggests either small differences in initial ^{10}Be content of the mixed water masses or homogenisation through vertical processes.

Production and Isolation of Phytosiderophores

SCOTT W. FRAZIER^{1,2}, PETRA U. REICHARD^{1,3}, RUBEN KRETZSCHMAR^{1,4}, AND STEPHAN M. KRAEMER^{1,5}

¹The Institute For Terrestrial Ecology, Swiss Federal Institute Of Technology, Zurich, Switzerland

²[scott.frazier@ito.umnw.ethz.ch]

³[reichard@ito.umnw.ethz.ch]

⁴[kretzschmar@ito.umnw.ethz.ch]

⁵[stephan.kraemer@ito.umnw.ethz.ch]

The solubility of iron, a micronutrient, is far below the concentrations required by plants in well-aerated soils at circum neutral pH. Therefore, plants have developed two mechanisms to increase iron solubility so that it can be taken up by the root system. These mechanisms have been termed strategy I and strategy II. The strategy I mechanism relies on such mechanisms as the reduction of ferric iron to the more soluble ferrous state, excretion of protons from the roots, or the excretion of organic acids from the roots to increase iron solubility. The strategy II mechanism uses phytosiderophore (PS) to dissolve ferric iron in an analogous way to that of microbes who produce siderophores as an iron acquisition strategy--though this mechanism likely evolved independently between plants and microbes. PS are low-molecular weight, organic, hexadentate ligands of the Mugineic acid family (e.g. Fig. 1) that are secreted by the roots of some graminaceous

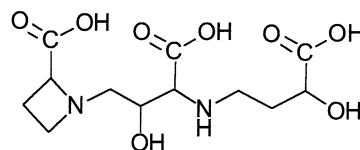


Fig.1 Mugineic Acid

plant species.

Although PS are characterized by their high affinity for Fe, these compounds also have high stability constants for other metal ions. Therefore, the specificity for this efficient iron acquisition strategy is thought to result from transporters that recognize iron-PS complexes and transport them across the plasma membrane, while excluding other metal-PS complexes. However, PS may influence the mobility of other metals in soils despite their irrelevance in plant nutrition.

Presently, studies of plant physiology regarding PS and the environmental significance of PS are hindered by a lack of PS reference material. The synthesis of PS and their isolation from root exudates are both rather involved procedures. In this presentation we will discuss details about the PS isolation procedure and how PS are involved in processes such as the ligand-promoted dissolution of iron hydroxides, the dissolution of precipitated actinides, and the adsorption of actinides to precipitated phases.

Mass Bias in ICP mass spectrometers

P.A. FREEDMAN

Nu Instruments Ltd. Wrexham, North Wales
LL13 9XS(phil@nu-ins.u-net.com)

It is well known that the uncorrected isotopic ratio measured using ICP mass spectrometers differs from the true value in a time independent manner. Experimentally it has been shown in high precision studies using multiple collector magnetic sector instruments that the following formula often applies:

$$\frac{\text{True Ratio}}{\text{Observed Ratio}} = \left[\frac{M_1}{M_2} \right]^\beta$$

with the value of β being close to 2.

We suggest that the origin of this mass bias arises from two parts, each contributing a factor of one to the beta value. The first part comes from the supersonic expansion process at the sampler, and the second from the space charge repulsion at the rear of the skimmer, in the region where the ions experience their initial electrostatic acceleration.

During the supersonic expansion process in the sampler's throat, the ion's forward motion is converted into a narrow velocity distribution, centred at a common value, equal to the velocity of the bulk argon carrier gas. The transverse velocity distribution is also narrowed, but the average velocity in this direction maintains the normal mass dependent variation. The higher transverse speeds for the lighter ions results in the lower transport efficiency of these species to the next stage of the instrument interface.

Since the distribution of the species in the expansion cone at the rear of the sampler maintains a memory of the distribution in the flame (for standard geometry's) the mass bias will alter as the torch position is changed. Similarly different elements will be ionised differently in the flame, resulting in differing spatial ionic distributions. This can result in minor variations in beta values between elements.

If no charge separation occurred at the skimmer, the transmitted ions would continue in an extremely narrow cone into the mass spectrometer, defined by the geometry of the sampler and skimmer orifices. However, the extraction voltage on the first ion optical element repels the electrons in the plasma, and accelerates the ions. These ions then experience a mutual repulsion, in this region of low acceleration potential. The heavier ions, which have a higher energy (since the forward velocity of all the species present is the same), will experience less repulsion than the lighter ions. This results in the second major contribution to the mass bias. It is to be expected that it should be possible to design an interface such that this repulsion is kept at a low enough level so that all ions which pass through the skimmer tip are transmitted into the mass spectrometer. In such a case, the overall beta value would approach unity.

Re-Os, Sm-Nd isotope- and REE systematics on komatiites and pillow basalts from the Earth's oldest oceanic crustal fragments (Isua Supracrustal Belt, W Greenland)

R. FREI^{1,2} AND B. KASTBJERG JENSEN¹

¹ Geological Institute, University of Copenhagen, Øster Voldgade 10, DK-1350 Copenhagen, Denmark
(robertf@geo.geol.ku.dk)

² Danish Lithosphere Center, Øster Voldgade 10, DK-1350 Copenhagen

Komatiites and pillow basalts from the Western and Northwestern sector of the Isua Supracrustal Belt (ISB) reveal a complex pattern of trace elements, mainly with respect to their rare earth elements (REE). The heterogeneity of LREE patterns, in combination with widely scattering $\epsilon_{\text{Nd}}[T=3.81 \text{ Ga}]$ values, indicate that the REE systematics of the samples were disturbed by one (or more) metamorphic events which took place some considerable time after the original crystallization of the Isua belt. Furthermore, LREE-rich metasomatic fluids associated with the emplacement of tonalites into the supracrustals may have significantly altered the primary trace element budget. Extreme variations in whole rock $\gamma_{\text{Os}}[T=3.81 \text{ Ga}]$ values of these rocks are favorably interpreted to derive from major metamorphic losses of Os, rather than from Re additions during fluid hydrothermal alterations. In contrast, the Re-Os isotope system remained intact in komatiite-hosted chromites from Isua and an average $\gamma_{\text{Os}}[T=3.81 \text{ Ga}]$ value of $+1.3 \pm 0.9$ indicates that these komatiites were derived from a mantle source with a time-integrated slightly suprachondritic Re/Os ratio. Our data are the first to show early Archean mantle rocks with radiogenic initial $^{187}\text{Os}/^{188}\text{Os}$ isotopic compositions. Our data do not allow to further impinge on the petrogenesis of the ISB mantle-derived rocks. Similarities of unaltered pillow basalts with Phanerozoic boninites (Polat et al., 2002) may indicate a formation in an intra-oceanic subduction zone like geodynamic process, in which extreme early (Hadean?) depletion of a mantle source by melt extraction was followed by a second stage of melting induced by enriched subduction components. Alternatively, core-mantle interaction as a plausible mechanism for the ^{187}Os enrichments in these rocks remains a valid hypothesis.

References

Polat, A., Hofmann, A.W. and Rosing, M.T., (2002), *Chem. Geol.* **184**, 231-254.

Fluid evolution and mineralogy during multi-stage hydrothermal alteration of quartz-depleted granites (episyenites)

REGINA FREIBERGER¹ & LUTZ HECHT²

¹ Institut für Mineralogie, Petrologie und Geochemie, Universität Freiburg, Albertstr. 23b, 79104 Freiburg, Germany

² Institut für Mineralogie, Museum für Naturkunde, Humboldt-Universität zu Berlin, Invalidenstr. 43, 10115 Berlin, Germany

Episyenites are quartz-depleted granitic rocks that have the chemical composition similar to syenites. Episyenites do not have a magmatic origin, but are formed through late-magmatic to subsolidus alteration. In the German Fichtelgebirge, episyenites are known from several localities, forming spatially restricted lensoid to pipe-shaped bodies within Hercynian granites. Frequently, quartz-depletion is associated with, or subsequently followed by polyphase alteration of different types (albite, chlorite, sericite, hematite, fluorite, pyrite, stilbite and secondary quartz). Episyenites may even be associated with U-, Au- or Sn-W-mineralization. Although dissolution of quartz produces a porous rock, former magmatic textures are generally well preserved. Cavities are filled with later formed minerals, including chlorite, quartz and calcite. Sharp contacts between the altered rock and the fresh granite are characteristic. Sometimes there is a small transition zone with corroded quartz. Outside the quartz-depleted zone, large alteration halos are developed (e.g. chloritization), in which no quartz dissolution is observed.

The geochemical mass transfer during episyenitization is mainly characterized by the depletion of Si, but almost all major and trace elements may show large mobility (including REE), depending on the associated and subsequent alteration type. Chlorite geochemistry shows decreasing Fe and Al^{IV} from early to late chlorite, which correlates with decreasing temperature. Fluid inclusion studies indicate that aqueous fluids causing quartz dissolution have relatively low salinities, but high homogenization temperatures (Th) with a minimum T of 200 to 300°C. Fluids causing later alteration phenomena have higher salinities and lower Th.

Discussion of quartz dissolution conditions must include changes in T, P, pH and fluid salinity, because silica solubility strongly depends on these parameters. A silica undersaturated fluid is necessary for quartz dissolution within granitic rocks. For most natural hydrothermal conditions, increasing pH, T, P and salinity leads to an increase in silica solubility. However, under low pressure, silica solubility increases slightly with decreasing temperature (above the critical point of water). The timing of quartz dissolution in relation to the emplacement of the host granitic rocks is still a matter of debate.

High precision U-series isotope measurements of East Scotia back-arc basalts using single-collector sector-field icp-ms

S. FRETZDORFF¹, C.-D. GARBE-SCHÖNBERG¹, J. FIETZKE¹, R.A. LIVERMORE² AND P. STOFFERS¹

¹Institute of Geosciences, University of Kiel, Olshausenstr. 40, 24118 Kiel, Germany (sf@gpi.uni-kiel.de)

²British Antarctic Survey, High Cross, Madingley Road, Cambridge, CB3 0ET, UK

²³⁸U-²³⁰Th disequilibrium data are particularly useful to examine the process of recent (< 350 ka) fluid input from the subducting slab into the mantle source of arc lavas. Most island-arc lavas show (²³⁸U/²³⁰Th) > 1 which has been attributed to addition of an U-rich slab derived fluid to their mantle source. Very limited data exists for the U-series isotopic composition of back-arc magmas. Because of the transitional character of most of the back-arc basalts from MORB to arc-like it is not clear if recent fluid input will dominate to control the ²³⁸U-²³⁰Th disequilibrium in the melts.

Here we present high precision U-series isotope data of an active back-arc spreading center, the East Scotia Ridge, determined with a newly developed procedure using sector-field inductively coupled plasma mass spectrometry (ICP-SFMS, Micromass PlasmaTrace 2) coupled with a desolvating micro-nebulizer sample introduction system (Cetac MCN 6000 with PFA spraychamber). The procedure involves conventional ion-exchange column separation with ²²⁹Th and ²³⁶U spikes. In general, the abundance sensitivity is critical for accurate determinations of ²³⁰Th/²³²Th ratios which are very low in rock samples (10⁻⁶). The continuously adjustable mass resolution of the PT2 instrument is advantageous for compromising abundance sensitivity (< 3 x 10⁻⁷ at 1100RP) with maximum transmission. Ionization efficiency (ions counted/ions introduced) is up to 1% (for U at 400RP) allowing precise measurements of ²³⁰Th/²³²Th with ± 2.5 (5) % (2) for 0.1 (0.01) pg ²³⁰Th. Linear working-range of the detector and wash-out protocols had to be carefully optimized to avoid analytical bias. Results for international rock standards show good accuracy within the error of accepted values ((²³⁰Th/²³²Th): TML 1.079 ± 0.008, JB-1 0.552 ± 0.006, AGV-1 0.921 ± 0.016).

The isotope ratios of the East Scotia Ridge lavas span a range in (²³⁰Th/²³²Th) and (²³⁸U/²³²Th) larger than reported of any other individual back-arc region. Most of the back-arc lavas have lower (²³⁸U/²³⁰Th) < 1 and are thus similar in composition to mid-ocean ridge basalts (MORB). Lavas from the centre and southern part of the back-arc have high (²³⁸U/²³⁰Th) ≥ 1, implying a recent addition of a U-rich slab-derived fluid.

Fluorescence Spectroscopic and Chromatographic Evidence for the Interaction of NOM and Metal Ions

F. H. FRIMMEL¹, M. DELAY² AND K. VERCAMMEN³

^{1,2,3} Engler-Bunte-Institut, Chair of Water Chemistry,
Universitaet Karlsruhe, Engler-Bunte-Ring 1, 76131
Karlsruhe, Germany

¹ (fritz.frimmel@ciw.uni-karlsruhe.de)

² (markus.delay@web.de)

³ (karlien.vercammen@ciw.uni-karlsruhe.de)

Introduction

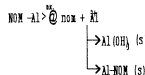
The presence of natural organic matter (NOM) in aquatic systems can strongly effect the transport of metal ions. Little is known about the influence of oxidation processes on the NOM complexing properties. As an example, the influence of photooxidation on the stability of NOM–Al complexes was investigated. The NOM sample originates from a brown water lake (Lake Hohloh, Northern Black Forest, Germany).

Experimental

The interaction of NOM and metal ions can be characterized by fluorescence spectroscopy and size-exclusion chromatography (SEC) coupled with inductively-coupled plasma mass spectroscopy (ICP-MS). Fluorescence spectroscopic techniques allow a non-destructive investigation of the metal-NOM system. Coupling of SEC and ICP-MS gives information about molecular sizes, metal distributions, and the metal mobility.

Results

At the beginning, fluorescence intensities of the NOM samples increased with increasing duration of irradiation due to cleavage of NOM molecules. Progressing irradiation and mineralization of NOM finally led to decreasing fluorescence intensities. The fluorescence signals in SEC chromatograms showed a shift towards higher elution volumes for the oxidized samples. The shift is probably attributed to the formation of smaller molecules (nom). A decrease of NOM–Al complex formation due to oxidation of NOM could be found. A shift of the Al signal towards higher molecular weight compounds indicates the formation of Al hydroxides and/or Al–NOM colloids, as pictured in the following reaction scheme:



Results of Pb and Zn will also be discussed.

References

- Kumke, M.U., Tiseanu, C., Abbt-Braun, G. and Frimmel, F.H., (1998), *J. Fluorescence*, **8(4)**, 309-318.
Vercammen, K., Schmitt, D., Frimmel, F.H., (2002), *Environ. Sci. Technol.* (submitted for publication).

Dissolution experiments and natural weathering of carbonates.

S.FRISIA¹, A.BORSATO¹, F.T.MACKENZIE², AND
R. TOMASONI¹

¹Museo Tridentino di Scienze Naturali, via Calepina 14, 38100
Trento, Italy (frisia@mtsn.tn.it)

²Dept. of Oceanography, University of Hawaii, Honolulu, HI
96822 USA (fredm@iniki.soest.hawaii.edu)

The rate of dissolution of natural dolomite and calcite, which show similar rates of weathering in the outcrops, were investigated using free-drift experiments on samples for which physico-chemical properties had been determined by scanning (SEM) and transmission (TEM) electron microscopy, EDS and ICP-AES. The surface morphology and grain-size of ground particles prior to, and after the experiments were observed by SEM, and compared with karst spring suspended sediment and naturally weathered surfaces. The experimental conditions were pH = 5.16, and T = 25°C, particle size $\phi = 90 \mu\text{m}$. Samples were precleaned in a sonic bath, and slightly acidified. The Solution pH and chemistry were measured at fixed intervals. Reactions approached steady-state after 21 hours for the limestone, and 27 for the dolomite.

Pre-reaction dolomite grain size distribution ranged from $< 10 \mu\text{m}$ to $90 \mu\text{m}$, in the same range as those of suspended sediments. Grain surfaces had ledges, macrokinks and original etch-pits. Pre-reaction calcite grains-size distribution was $90 \mu\text{m}$, and grains had smooth surfaces. The dolomite reaction rate was more rapid than that of the calcite in the first 20 hours. After 1 hour, 0.203 mol. Ca and 0.200 mol. Mg were released to the solution by dolomite, and 0.046 moles Ca were released in the limestone reaction. Only after 22 hours, were the dissolution rates of calcite and dolomite similar. Post-reaction dolomite grain surfaces show the development of etch pits located along ledges and structural defects, and deepening and intersection of original etch pits. Post-reaction calcite grain surfaces show the development of ledges, etch-pits located along twins and cleavage planes, and preferred dissolution at subgrain boundaries, as observed in naturally weathered specimens.

The rates of dissolution seem to be affected by the original surface morphologies, and the distribution of defects. Pre-reaction dolomite grains had rugged surface morphology resulting from outcropping defects (ribbon microstructures, dislocations), and high surface/volume ratio in the smaller size-fraction. Pre-reaction calcite was almost defect-free, and had less reactive sites. Average grain surface/volume ratio was smaller than in the dolomite. Higher surface/volume ratio, and number of reactive sites are probably the cause of the initial, rapid dissolution rate for the dolomite. Dissolution rate of calcite reached that of dolomite (and than became faster) once a large number of ledges were exposed to the solution during the reaction. Experimental results are consistent with the physico-chemical properties of waters from aquifers that develop in the two carbonates of the present study.

The oxidation state of iron in the lower mantle

D.J. FROST AND F. LANGENHORST

Bayerisches Geoinstitut, Universität Bayreuth, Bayreuth, Germany. (Dan.Frost@uni-bayreuth.de, Falko.Langenhorst@uni-bayreuth.de)

Determining the redox state of the lower mantle is important because it will influence processes, such as chemical diffusion, electrical conductivity and volatile speciation. Using a multianvil apparatus we have measured the partitioning of Fe^{2+} , Fe^{3+} and Mg^{2+} between magnesiowüstite and magnesium silicate perovskite in both Al_2O_3 -bearing and Al_2O_3 -free systems under variable redox conditions. In the Al_2O_3 -bearing system perovskite $\text{Fe}^{3+}/\Sigma\text{Fe}$ ratios are as high as 80%, which is over 3 times greater than for Al_2O_3 -free perovskite. The variation in the Fe^{3+} solubility with the Al^{3+} content of perovskite is non-linear.

If, as some previous studies have indicated, the influence of Al on the Fe^{3+} content of perovskite is indeed independent of the oxygen fugacity, then for a typical mantle Al_2O_3 content of 4 wt %, silicate perovskite in the lower mantle would have an $\text{Fe}^{3+}/\Sigma\text{Fe}$ ratio of approximately 70% and a bulk peridotite would have an $\text{Fe}^{3+}/\Sigma\text{Fe}$ ratio of 50 %. Upper mantle xenoliths suggest an average mantle $\text{Fe}^{3+}/\Sigma\text{Fe}$ ratio no higher than 3%, however, which would infer one of two possible scenarios for the lower mantle. Either the lower mantle contains more Fe^{3+} i.e. more oxygen, than the upper mantle or lower mantle perovskite must sequester oxygen by reducing vapour phases and through the precipitation of metallic Fe. As the vapour content of the mantle can account for only a minor proportion of the required oxygen the only feasible mechanism would be the disproportionation of FeO to produce approximately 1 wt. % metallic Fe. This metallic phase would also be supplemented by other siderophile elements. We have made a number of experiments in the presence of metallic iron in order to test this possibility. We also compare these results with analyses of inclusions found in diamonds which are considered to have formed in the lower mantle.

REE pattern of carbonaceous part of coals: a new proxy for the original plants of coals

FENGFU FU¹, TASUKU AKAGI², YUICHIRO SUZUKI³ AND SADAYO YABUKI⁴

¹Department of Environmental Sciences, JAERI, Tokai, Ibaraki 319-1195, Japan (fengfu@acl.tokai.jaeri.go.jp)

²Faculty of Agriculture, Tokyo University of Agriculture and Technology, Fuchu, Tokyo, Japan (akagi@cc.tuat.ac.jp)

³Institute for Geo-Resources and Environment, AIST, Tsukuba, Japan

⁴Division of Surface Characterization, RIKEN, Wako, Saitama 351-0198, Japan

Introduction

It is generally thought that most coals are originated from trees and peat, and some of them are from algae. However, the inference of the original plants is sometimes a difficult problem. The study on REEs in coals is expected to provide us with some knowledge about the original plants of coal.

Experiment

Coal samples of the Taiheiyo coal mine, the Ashibetsu, the Ambalut coal mine, and boghead coal were collected in this study. Each sample was divided into carbonaceous part and mineral part by treating ashed coal with 10 % acetic acid solution. REEs in each part were determined with ICP-MS.

Discussion of results

The chondrite-normalized REE patterns of the carbonaceous part of all the coals can be classified into three types. The Ashibetsu coals, the Taiheiyo coals and some of the Ambalut coals are type I, which is featured with a medium slope and no depletion in Ce (no Ce anomaly). The others of the Ambalut coals are classified into type II, which is characterized with a steeper slope (greater LREE/HREE ratio) than type I and a Ce negative anomaly. The boghead coal was classified into type III, which is featured with a smaller slope than type I and a Ce negative anomaly. Compare with the extents of the Ce anomaly and slope of the pattern of plants we have surveyed so far, we can infer that coals classified into the type I, type II, and type III are originated from peat vegetation, trees and seaweed, respectively. This correspondence is consistent with the result of maceral study.

Conclusions

The REE pattern of the carbonaceous part in coals is shown to be a good proxy for the original plants to be coalified.

Acknowledgment

This work was supported by the Sasakawa Scientific Research Grant from The Japan Science Society.

References

- Akagi T, Fu F-F, and Yabuki S. (in press). *Geochem. J.*
- Amosov I. I., and Ermakova V. P. (1955). *Otdel. Tekh. Nauk* 6, 146-156.
- Fu F-F, Akagi T., and Shinotsuka K. (1998). *Biol. Trace Elem. Res.* 64, 13-26.
- Fu F-F, Akagi T., Yabuki S., and Iwaki, M. (2001). *Plant and Soil* 235, 53-64.

Rb-Sr isotopic dating and its genetic significance to the Manaoko gold deposit, NW-Sichuan, China

S.H. FU¹ AND X.X. GU²

¹ Chengdu University of Technology, Chengdu, P.R. China
(sh-fu@263.net)

² Institute of Geochemistry, Chinese Academy of Sciences, Guiyang, P.R. China (xuexiang_gu@263.net)

Introduction

The Manaoko deposit, hosted in Triassic turbidites, is a typical micro-disseminated gold deposit. With respect to its genesis, different models have been advocated. However, there is still much controversy about the timing of mineralization.

Mineralization at Manaoko occurs commonly as scheelite bodies with distinct layering that is consistent with bedding of the host rocks. Main ore minerals include pyrite, realgar, stibnite, and arsenopyrite.

In order to constrain the timing of mineralization, Rb-Sr isotopes were measured for fluid inclusions in quartz.

Results and discussion

Rb and Sr contents in five quartz samples range from $0.731\text{--}2.702 \times 10^{-6}$ and $2.590\text{--}16.700 \times 10^{-6}$, respectively. The calculated $^{87}\text{Rb}/^{86}\text{Sr}$ and $^{87}\text{Sr}/^{86}\text{Sr}$ values vary between 0.433–1.765 and 0.71010–0.71387, respectively. The initial $^{87}\text{Sr}/^{86}\text{Sr}$ ratio of the fluids (0.7085) is consistent with the $^{87}\text{Sr}/^{86}\text{Sr}$ ratio of seawater (0.7090). The data outline an isochron age of 210–11Ma.

The Rb-Sr isotope data show that gold mineralization at Manaoko is coeval with deposition of the host sedimentary rocks. It is thus suggested that submarine sedimentary exhalative processes were responsible for formation of the deposit, accompanied by deposition of the host turbidites. Gold and associated metals were introduced by episodic exhalation of metalliferous basinal brines.

Conclusions

The timing of gold mineralization at Manaoko is consistent with deposition of the Triassic turbidites. The deposit is defined to a sedimentary exhalative (sedex) type and is similar to the recently discovered gold occurrences in the Carlin trend (Emsbo et al., 1999).

Acknowledgments

The research was supported by the National Natural Science Foundation of China (grant: 49872038) and Chinese Academy of Sciences under a special grant for young national scientists.

References

Emsbo P., Hutchinson R.W., Hofstra A.H., Volk J.A., Bettes K.H., Baschuk G.J., Johnson C.A., (1999), *Geology* 27, 59–62.

Sorption of As(V) on schwertmannite and its effect on the transformation

K. FUKUSHI,¹ T. SATO,² AND N. YANASE³

¹Graduate School of Natural Science and Technology, Kanazawa University, Kanazawa, Japan
(fukushi@earth.s.kanazawa-u.ac.jp)

²Institute of Nature & Environmental Technology, Kanazawa University, Kanazawa, Japan (tomsato@earth.s.kanazawa-u.ac.jp)

³Department of Environmental Sciences, Japan Atomic Energy Research Institute, Tokai-mura, Japan
(yanase@sparclt.tokai.jaeri.go.jp)

Introduction

At abandoned arsenic mine in Nishinomaki, Japan, water discharged from mining and waste dump area is acidic and rich in arsenic. However, arsenic in the drainage is naturally attenuated due to the sorption by the ochreous precipitates, mainly composed of schwertmannite. In the present study, synthesized schwertmannite were prepared and served for the batch sorption experiment in order to examine the mechanism of arsenate sorption. Moreover, the alteration experiment of the specimen with different arsenate content was performed to determine the role of arsenate sorption on transformation of the schwertmannite in order to understand the long-term behavior of arsenic sorbed into schwertmannite.

Experimental methods

Sorption of arsenate in the schwertmannite suspension was examined as a function of arsenate concentrations ($10^{-7}\text{M} \sim 10^{-3}\text{M}$). The suspension pH was adjusted with HNO_3 to 3.2–3.4. After 24 hours, the suspensions were filtered. The solutions were provided for the analysis of Fe, As and sulfate. The reacted solids were examined by infrared spectroscopy.

The samples contained arsenate of 0–1.0 mmol/g were prepared by the batch sorption procedure. The samples were spread onto the glass slide, dried and then placed on the airtight containers in which condition was kept vapour pressure at 50 °C. The samples after aging were characterized by X-ray diffractometry.

Results and discussion

The result of arsenate sorption experiment showed that schwertmannite sorbed arsenate up to 80 mg/g, and that the structural sulfate in schwertmannite was released to solution in response to the arsenate uptake. The result of alteration experiment showed that the schwertmannite with little arsenate transformed to crystalline iron phase after a week. On the other hand, no change in XRD patterns was observed in the samples with much amount of arsenate. The difference indicates that the transformation of schwertmannite is significantly retarded by arsenate sorption. By inhibition of the transformation, the attenuation process of arsenic in ochreous precipitates is irreversible in overall and expected to be maintained for long-term.

Reaction zones and composite veins around the metamorphosed basic dykes in the Hirao limestone, Fukuoka, Japan.

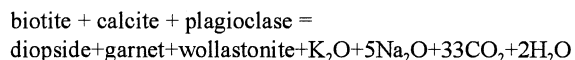
M.FUKUYAMA¹, T.NISHIYAMA¹ AND K.URATA²

¹Department of Earth Sciences, Kumamoto University, Kumamoto 860-8555, Japan (mayuko@es.sci.kumamoto-u.ac.jp, tadao@sci.kumamoto-u.ac.jp)

²Department of Geography, The Tokyo Metropolitan University (CYR00601@nifty.ne.jp)

This paper describes petrography and mass transfer analysis of the reaction zones and composite veins around the basic dykes in the Hirao limestone both of which are thermally metamorphosed by the Hirao granodiorite (Cretaceous). Reactions between the basic dykes and the limestone due to the contact metamorphism lead to the development of the reaction zones between them and the composite veins which were derived from the reaction zones by hydrofracturing and mass transfer along the fracture (Nishiyama, 1989). The peak condition of the contact metamorphism is estimated as T=650-700 °C and P<500MPa, based on thermodynamic analysis of metamorphic reactions in the Tagawa metamorphic rocks underlying the Hirao limestone.

The reaction zones consist of three zones: diopside zone, garnet zone and wollastonite zone in this order from the metabasite dyke towards the crystalline limestone. Dominant mineral assemblages of the rocks are; metabasite: biotite + diopside + plagioclase, diopside zone: diopside + plagioclase, garnet zone: grossular + plagioclase, wollastonite zone : wollastonite, and crystalline limestone : calcite. In plagioclase albite lamellae are observed in the matrix of Ab₆₂₋₇₆ plagioclase, of which compositional gap corresponds to the peristerite gap, indicating the reequilibration at approximately 400 °C. The total reaction leading to the development of the reaction zones can be modeled as:



We employed the steady diffusion model (Joesten, 1979) to analyze the stability condition of the zonal sequence and to get exchange cycles, ignoring conservation of fluid species. As a result, the stability of the observed zonal sequence depends on $L_{\text{SiO}_2\text{SiO}_2}/L_{\text{Al}_2\text{O}_3\text{Al}_2\text{O}_3}$ and $L_{\text{SiO}_2\text{SiO}_2}/L_{\text{CaO}\text{CaO}}$, but not on $L_{\text{SiO}_2\text{SiO}_2}/L_{\text{MgO}\text{MgO}}$.

A composite vein consisting of garnet, plagioclase and wollastonite comes out from the reaction zones. The vein is rich in garnet near the reaction zones and rich in plagioclase at a distance of 2meters. This change in mode may reflect the relative magnitude of diffusivity of Al₂O₃ against that of SiO₂.

The continuous growth of aqueous aluminum nanoclusters

G. FURRER¹, W.H. CASEY², B.L. PHILLIPS³

¹ ITOe, ETHZ, Grabenstr. 3, CH-8952 Schlieren, (furrer@ito.umnw.ethz.ch).

² Dept. of Land, Air and Water Res. and Dept. of Geology, UC Davis, CA 95616, USA (whcasey@ucdavis.edu).

³ Dept. of Geosciences, SUNY, Stony Brook, NY 11794-2100, USA (brian.phillips@sunysb.edu).

Introduction

The geochemistry of aluminum in natural waters and soil has been debated for decades, mainly with respect to the formation of polynuclear species and hydroxide minerals. However, it is accepted now that the tridecameric molecule AlO₄Al₁₂(OH)₂₄(H₂O)₁₂⁷⁺(aq), known as Keggin Al₁₃, can form spontaneously if acidic waters from acid-mine areas or poorly buffered soil receiving acid rain mixes with neutral surface waters (Casey et al., 2001). For many years it was thought that the tridecameric nanoclusters in aqueous solutions is decomposed rather fast and that in a first step amorphous and then crystalline aluminum hydroxide solids are formed.

Discovery

Our new findings from long-term storage experiments confirmed these assumptions, however only partially. Five slightly acidic bulk solutions containing 7 mM Al₁₃ were stored on an office desk during 11 years at room temperature, gas tight but exposed to day light. In four glass containers the solutions were still fairly clear and about 95 % of the total Al(III) has been transformed into the larger nanocluster (AlO₄)₂Al₂₈(OH)₅₆(H₂O)₂₄¹⁸⁺(aq) (Al₃₀), which contains 30 Al(III) and bears an even higher charge (18+). In one glass container the solution became very milky; approximately 30 % of the total Al(III) has been transformed into crystalline gibbsite and the other 70 % into the Al₃₀ nanocluster. The chemical structure of the Al₃₀ nanocluster has just recently been resolved (Alloche et al., 2000; Rowsell et al., 2000).

Conclusion

So far it was thought that elevated temperatures were necessary for the synthesis Al₃₀ molecule. Our finding shows that the Al₃₀ nanocluster forms spontaneously in aqueous solutions of Al₁₃ even at ambient conditions. Since this process seems to have a time constant of a couple of years, we might find even larger aluminum nanoclusters one day.

References

- Casey W.H., Phillips B.L. and Furrer G. (2001) *Reviews in Mineralogy and Geochemistry* **44**, 167-190.
 Alloche L., Gérardin C., Loiseau T., Férey G. and Taulelle F. (2000) *Angew. Chem. Int. Ed.* **39**, 511-514.
 Rowsell J. and Nazar L.F. (2000) *J. Am. Chem. Soc.* **122**, 3777-3778.

Multicomponent inverse modelling in aquatic sediments

YOKO FURUKAWA¹, J. E. KOSTKA² AND A. C. SMITH²

¹ Naval Research Laboratory Code 7431, Stennis Space Center, Mississippi 39529, USA
(yoko.furukawa@nrlssc.navy.mil)

² Department of Oceanography, Florida State University, Tallahassee, Florida 32306, USA (jkostka@ocean.fsu.edu, agold@ocean.fsu.edu)

A comprehensive understanding of chemical mass transfer in aquatic sediments requires a comprehensive tool capable of deconvoluting all major processes that are heavily interrelated. Multicomponent reactive transport modelling can be the comprehensive tool when reaction and transport parameters are adequately constrained through a sufficient number of observations and prior knowledge of their interdependency. In the present study, a multicomponent inverse model written in Matlab was applied to a saltmarsh environment heavily affected by vegetation and bioturbating organisms, located in Skidaway Island, Georgia, USA. Depth profiles of most major redox species were directly measured, and transport parameters were determined using porosity profiles (for diffusion coefficients) and the relationship between ³⁵S-determined sulfate reduction rates and pore water sulfate concentration profiles (for irrigation coefficients). Consequently, the multicomponent inverse model could be used to quantify the reaction rates. The results indicate that within the upper few millimetres of intertidal sediments, carbonate mineral precipitation takes place during the low tide periods generating small pH maxima in the immediate vicinity of sediment surface. The results also show that the *in situ* rates of iron (III) reduction determined through modelling are comparable to the rates obtained by the *ex situ* incubation procedures. Inverse modelling of reaction rates can be especially useful where forward modelling with *a priori* application of rates is difficult due to complex reaction geometry and/or rapid recycling of redox species.

No effect of hypolimnetic aeration on the P cycling of Lake Sempach: A re-evaluation of a well-accepted concept

RENÉ GÄCHTER¹ AND BEAT MÜLLER²

EAWAG, Limnological Research Center, CH-6047

Kastanienbaum, Switzerland

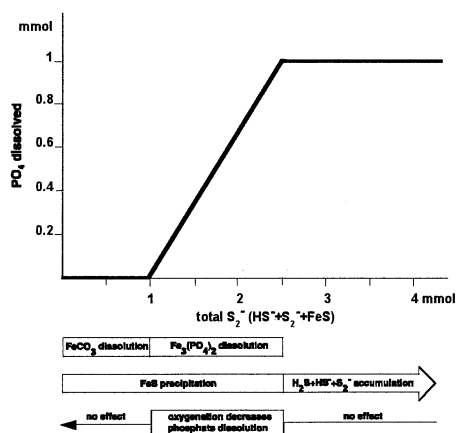
¹(rene.gaechter@eawag.ch), ²(beat.mueller@eawag.ch)

To lower the trophic state of Lake Sempach, a eutrophic lake in Central Switzerland, its external phosphorus (P) load has been decreased and its hypolimnion has been aerated. Based on more than fifteen years of experience we conclude that the reduction of the external P-load resulted in a corresponding decrease of the lake's P concentration. However, contrary to our initial expectations, increased hypolimnetic dissolved oxygen (D.O.) concentrations

1. did not affect the P release from sediments during summer, and
2. did not result in an increased permanent P-retention.

These observations warrant a re-evaluation of the well-accepted management strategy of decreasing the lake internal P cycling by maintaining an aerobic hypolimnion and sediment surface:

1. We show that irrespective of permanent oxic conditions in the hypolimnion the sediment/water interface remained anoxic during summer, due to continued high sedimentation rates of organic matter. This explains why oxygenation did not affect the temporal P release from the sediment.
2. We discuss how the Fe:P ratio of the settling seston may affect the permanent P retention as a result of oxygenation.



References

- Gächter R. and Wehrli. B. (1998), Environ. Sci. Technol. **32**: 3659-3665

Fungal influence on mineral dissolution and metal mobility: mechanisms and biogeochemical relevance

G.M. GADD

Division of Environmental and Applied Biology, Biological Sciences Institute, School of Life Sciences, University of Dundee, Dundee, DD1 4HN, Scotland, UK
(g.m.gadd@dundee.ac.uk)

In the terrestrial environment, fungi are of importance as decomposer organisms and plant symbionts (mycorrhizas), playing important roles in carbon and other biogeochemical cycles. Fungi can interact with metals and minerals in various ways depending on the metal/mineral species, organisms and environment, while metabolic activities can also influence metal speciation and mobility. Such interactions between fungi and minerals are of fundamental importance to biogeochemical cycles including those of C, N, S and P which are important elements required for plant, fungal and other microbial growth. Certain mechanisms may mobilize metals into forms available for cellular uptake and leaching from the system, e.g. complexation with organic acids, other metabolites and siderophores. Metals may also be immobilized by, e.g. sorption onto cell components, exopolymers, transport and intra- and extracellular sequestration or precipitation. Because of these properties, fungi can promote rock weathering and contribute to the dissolution of mineral aggregates in soil through the excretion of H^+ , organic acids and other ligands. They may also play an active or passive role in mineral formation through the nucleation of crystalline material onto cell walls, resulting in the formation of biogenic micro-fabrics in mineral substrates. The relative importance of such apparently opposing phenomena of solubilization and immobilization are key components of biogeochemical cycles for toxic metals, whether indigenous or introduced into a specific location, and fundamental determinants of fungal growth, physiology and morphogenesis. Furthermore, some processes are of relevance to environmental bioremediation. This contribution seeks to highlight selected physico-chemical and biochemical mechanisms by which fungi can interact with minerals and transform potentially toxic metal species between soluble and insoluble forms, and to draw attention to the biogeochemical significance of these processes.

Low-temperature reactive transport of Fe-Mg-Si-bearing solutions in sedimentary carbonate host-rock

S. GADISH¹, A. MATTHEWS¹, S. ILANI²

¹ Institute of Earth Sciences, Hebrew University of Jerusalem, 91904 Israel (sharongadish@hotmail.com; alan@vms.huji.ac.il)

² Geological Survey of Israel, Jerusalem, 95501 Israel (ilani@mail.gsi.gov.il)

The sub-surface reactive transport of solute species through carbonate (limestone/chalk) host rock is a major process of geochemical mobilization. This work studies iron and silica mineralization and dolomitization in Cretaceous limestones cut by a major tectonic fault zone (Paran tectonic line in the Negev desert of southern Israel). The aims are to understand the spatial extent, mechanism and physical conditions (temperature, fluid source) of the reactive transport process. Two groups of rocks were studied: 1) iron oxide-silica lenses located in the sub-vertical fault zone and 2) layer-parallel dolomitic bands in the carbonate rocks adjacent to the fault zone.

Laser fluorination oxygen isotope measurements on sample chips give $\delta^{18}\text{O}$ values of *ca* -5 ‰ for iron oxide (hematite/goethite) minerals in the fault-zone lenses and *ca* 25 ‰ for silica minerals (amorphous and microcrystalline quartz). A temperature of 30-40 °C is estimated from the silica-iron oxide fractionation using quartz-water and hematite-water geothermometers. The calculated $\delta^{18}\text{O}$ value of the water from which the minerals precipitated is *ca* -5 ‰, thus pointing to a meteoric groundwater source for the mineralizing fluid.

The dolomitization immediately adjacent to the fault zone is massive, but laterally spreads away from the fault zone and gradually resolves into horizontal dolomitic bands varying in thickness from less than a metre to several tens of metres and with transport distances up to 1 km from the fault zone. Impermeable clay-rich marl horizons strongly controlled layer-parallel direction of fluid movement. Field, XRD, optical and SEM microscopic studies show that almost all the dolomites are ferroan, but they are also partially coated by small iron oxide crystals and cut by iron oxide veins. These observations indicate that the lens formation and dolomitization are genetically linked processes, but that transport of Mg, Fe and Si was to some extent decoupled. The dolomitization reaction possibly created a porosity that allowed Fe-bearing solutions to continue moving through the altered rock.

The present study shows that the reactive transport is related to upward movement of fluid along the fault line and its subsequent chemical interaction with the limestone host rock. Gravitationally over-pressured meteoric water brines in the underlying sandstone aquifer were the most probable fluid source. C, O, and Fe stable isotopic studies currently in progress will shed further light on the reactive transport processes.

Diffusive Reequilibration of CaO in Olivine-Hosted Melt Inclusions

GLENN A. GAETANI¹, DANIELE J. CHERNIAK², AND E. BRUCE WATSON³

¹Geology and Geophysics, Woods Hole Oceanographic Institution, Woods Hole MA 02543

²Earth and Environmental Sciences, Rensselaer Polytechnic Institute, Troy NY 12180

Silicate melts included in olivine phenocrysts exhibit compositional variability not found in erupted lavas. Recently, there has been increased recognition of unusually CaO-rich (ultracalcic) melt inclusions, typically hosted in olivine (e.g., Kamenetsky et al., 1998, EPSL, 164, 345-352; Kamenetsky and Crawford, 1998, EPSL, 160, 115-132). Because ultracalcic liquids ($\text{CaO} \geq 14 \text{ wt\%}$; $\text{CaO}/\text{Al}_2\text{O}_3 \geq 1.0$ by weight) are exceedingly rare in the global mid-ocean ridge basalt population, these inclusions have been interpreted as partial melts of exotic mantle lithologies. To evaluate the extent to which an olivine-hosted melt inclusion preserves its initial CaO content, we determined experimentally the diffusivity of Ca in San Carlos olivine and the partitioning of CaO between magnesian olivine and basalt. The experimental results demonstrate efficient communication between a melt inclusion and the melt outside of its host crystal with respect to CaO and significant reequilibration over relatively short timescales. Therefore, the reliability of olivine-hosted melt inclusion CaO content as an indicator of mantle heterogeneity is questionable.

Diffusion experiments were carried out at 1 bar and 800-1100 °C using synthetic anorthite powder as a Ca source. Diffusion profiles in experiments carried out at $T \leq 1000$ °C were measured using Rutherford Backscattering Spectroscopy (RBS). Experiments carried out at higher T were depth profiled using Secondary Ion Mass Spectroscopy (SIMS). The Arrhenius relation for diffusion of Ca parallel to the *c* crystallographic axis of $\sim\text{Fo}_{90}$ olivine at an oxygen fugacity along the Ni-NiO buffer is:

$$D_{\text{Ca}} = 2.284 \exp(-55010/T(\text{K})) \text{m}^2 \text{s}^{-1}$$

The olivine/basalt partition coefficient for CaO was determined to be relatively insensitive to temperature at 1 bar, decreasing from 0.030 at 1225 °C to 0.027 at 1325 °C.

Diffusive reequilibration of the CaO content of an olivine-hosted melt inclusion following magma mixing was investigated by using our experimental data in the model of Qin et al. (1992, Am. Mineral. 77, 565-576) for equilibration of a 200 μm melt inclusion centered in a spherical host olivine 2 mm in diameter. The melt inclusion was assumed to have an initial CaO content of 10 wt%, while the external melt contained 14 wt% CaO. At 1225 °C, the melt inclusion will retain its original concentration of CaO for ~ 10 years, after which it increases rapidly. Following 20 years of diffusive reequilibration, the CaO content of the inclusion has increased to 11.4 wt%; after 50 years the inclusion contains 13.5 wt% CaO and by 70 years reequilibration is nearly complete.

Chemical complexity of the Kea Component preserved in West Maui lavas

AMY M. GAFFNEY¹, BRUCE K. NELSON¹ AND
JANNE BLICHERT-TOFT²

¹Dept. of Earth and Space Sciences, University of
Washington, Box 351310, Seattle, WA, 98195, USA;
agaffney@u.washington.edu, bnelson@u.washington.edu
²Ecole Normale Supérieure de Lyon, 69364 Lyon Cedex 7,
France; jblichier@ens-lyon.fr

In order to characterize the chemical variability that defines the Kea component, the depleted compositional endmember in Hawaiian shield-stage magmas, we analyzed a 250m section of valley-exposed lavas and a 400m section of well cuttings from West Maui volcano, an extreme Kea-type volcano. The stratigraphic context of the samples allows us to evaluate temporal variability in the expression of the Kea component in the West Maui lavas during the late shield-building stage.

Hf, Pb, Nd and Sr isotope compositions of the West Maui lavas show a limited range, and the depleted compositions are consistent with a significant contribution from the Kea component. ϵ_{Hf} varies from +11.5 to +13.1, and decreases slightly towards the bottom of the section. Pb isotopes were analyzed by both TIMS and MC-ICP-MS. The higher-precision MC-ICP-MS analyses resolve trends in the Pb data that are not apparent in the TIMS analyses. $^{206}\text{Pb}/^{204}\text{Pb}$ ranges from 18.39 to 18.48, and does not correlate with ϵ_{Hf} . $^{87}\text{Sr}/^{86}\text{Sr}$ and ϵ_{Nd} range from 0.703368 to 0.703661 and +6.6 to +7.6, respectively. ϵ_{Hf} correlates with ϵ_{Nd} , but does not correlate with $^{87}\text{Sr}/^{86}\text{Sr}$.

The high resolution of the new data reveals that $^{87}\text{Sr}/^{86}\text{Sr}$ – $^{206}\text{Pb}/^{204}\text{Pb}$ variability in the West Maui samples defines two subparallel trends. These are orthogonal to the trend defined by all Hawaiian shield-stage lavas, and therefore are not the result of mixing between the Kea component and the Koolau component (the relatively enriched Hawaiian endmember). We instead attribute these trends to mixing between heterogeneities within the Kea component. The two trends may share a common radiogenic endmember, but require distinct endmembers at the less-radiogenic extreme. The linear nature of the trends also requires that mixing between the two less-radiogenic endmembers is limited or non-existent. The observed positive correlation of $^{87}\text{Sr}/^{86}\text{Sr}$ and $^{206}\text{Pb}/^{204}\text{Pb}$ is consistent with predicted compositions of aged, variably hydrothermally altered oceanic crust.

Coral reconstruction of abrupt tropical cooling 8,000 years ago

M.K. GAGAN¹, L.K. AYLIFFE², H. SCOTT-GAGAN¹,
W.S. HANTORO³ AND M.T. MCCULLOCH¹

¹Research School of Earth Sciences, Australian National
University, Canberra, ACT 0200, Australia
[michael.gagan@anu.edu.au]

²Department of Geology & Geophysics, University of Utah,
Salt Lake City, UT 84112, USA

³Research and Development Center for Geotechnology,
Indonesian Institute of Sciences, Bandung 40135,
Indonesia

Establishing the relative timing and magnitude of climate change in the tropics and high latitudes provides an important means for evaluating the role of the tropics in global climate change. The largest abrupt climate change in the Holocene occurred between 8,400 and 8,000 calendar years ago, when the temperature dropped by 4–8°C in central Greenland and 1.5–3°C around the North Atlantic region. However, little is known about the nature of the so-called ‘8.2 ka cold event’ in the tropics.

We drilled a sequence of well-preserved *Porites* corals within a rapidly uplifted paleo-reef in Alor, Indonesia, with ^{230}Th ages spanning 8,400 to 7,600 calendar years before present. The corals are positioned within the Western Pacific Warm Pool, which at present has the highest mean annual temperature on Earth. Measurements of coral Sr/Ca and $\delta^{18}\text{O}$ have yielded a semi-continuous record (310 years) showing that sea-surface temperatures were essentially the same as today from 8,400 to 7,600 years ago. However, both tracers show that this period of climatic stability is interrupted by an abrupt ~3°C cooling over a period of ~100 years, reaching a minimum 8,000 years ago.

The rapid cooling of ~0.3°C per decade in the Warm Pool 8,000 years ago is nearly synchronous with abrupt cooling in the North Atlantic region, as indicated by the sudden decrease in $\delta^{18}\text{O}$ values of ice from the GISP2 ice core. This finding supports the hypothesis that abrupt climate change at high latitudes can propagate rapidly to the tropics via atmospheric teleconnections. In the case of the 8.2 ka event, initial cooling at high latitudes could serve to enhance the equator-to-pole temperature gradient and strengthen meridional atmospheric circulation and tradewind velocity in the tropics. Stronger tradewinds would increase near-equatorial upwelling, providing an efficient means for cooling the tropical ocean surface. The results suggest that the tropical ocean-atmosphere could serve to propagate abrupt climate changes between the northern and southern hemispheres without a significant time lag.

We are in the process of making high-resolution measurements of coral Sr/Ca and $\delta^{18}\text{O}$ to determine if ocean-atmosphere coupling and ENSO perturbations remain fixed during such an altered climate state.

Microchemical investigation of K-feldspar megacrysts: clues to magma dynamics in a plutonic environment.

D. GAGNEVIN¹; J.S. DALY¹ AND G. POLI²

¹ Department of Geology, University College Dublin, Belfield, Dublin 4, Ireland (Damien.Gagnevin@ucd.ie)

² Department of Earth-Sciences, Piazza Università, 06100 Perugia, Italy (Poli@unipg.it)

Aim of the study

Isotopic and multi-elemental fingerprinting of zoned feldspars have received increasing attention in order to understand the multi-stage evolution of magmas from their source to emplacement. Where whole-rock analyses fail to explain the complexity of magmatic systems, processes such as magma mixing, fractional crystallisation and crustal contamination can be recorded in individual crystals through sequential isotopic and trace element zoning (e.g. Davidson & Tepley, 1997).

We report here a detailed study of K-feldspar megacrysts from the young (7 Ma) Elba monzogranite (the Monte Capanne pluton) in the Tuscan Magmatic Province, Italy. Previous studies (e.g. Poli *et al.*, 1989) have shown the importance of magma mixing in the genesis of the Tuscan plutons. K-feldspar megacrysts occur throughout the intrusion, as well as in related enclaves and dykes. SEM investigations have revealed the occurrence of idiomorphic resorption zones within some megacrysts, corresponding to major dissolution events.

Laser Ablation ICP-MS and EPMA results

LA-ICP-MS and electron microprobe analyses of zoned megacrysts reveal trace element zoning (mainly Ba, Sr, Rb, Pb, P, Ca, Cs and LREE) with particularly large variations across growth interruptions. A great variety of zoning patterns is observed. These are compatible with a magma mixing model with repeated injections of mafic magma in the system. Trace element comparisons between K-feldspar regions coreward and rimward of resorption zones suggest that episodes of dissolution of early-formed crystals correspond to episodes of feldspar nucleation, involving complex crystal transfer between chemically distinct batches of magma. For instance, the participation of a high Rb, LREE, Cr and Pb magma with lamproitic affinities seems to be possible. The feldspar rim chemistry is compatible with a model of crystallisation of a feldspar-dominated assemblage, with a marked decrease in Sr and Ba. The role of crustal contamination and volatile components will also be discussed, with particular reference to the Cs content.

References

- Poli, G., Manetti, P. and Tommasini, S., (1989), *Per. Mineral.*, **58**, 109-126.
Davidson, J.P. and Tepley III, F.J. (1997), *Science*, **275**, 826-829.

Trace Metals and Fe-Mn Cycling

JEAN-FRANÇOIS GAILLARD¹, MARTIAL TAILLEFERT², DIDIER PERRET³, AND CHARLES-PHILIPPE LIENEMANN⁴.

¹Northwestern University, Evanston, IL, 60208-3109 USA (jfgaillard@northwestern.edu)

² Georgia Institute of Technology, Atlanta, GA 30332 USA (mtaillef@eas.gatech.edu)

³ Swiss Federal Institute of Technology, CH-1015, Lausanne (didier.perret@epfl.ch)

⁴ Institut Français du Pétrole, F-69390 Vernaison (Charles.LIENEMANN@ifp.fr)

Iron and manganese play important roles in the biogeochemical cycling of trace elements at oxic/anoxic interfaces in lakes because of the formation of hydrous oxides. The conventional view, derived from numerous laboratory experiments, is that surface complexation is the key process by which trace metals are scavenged. However, if one can find in the literature numerous measurements of bulk water dissolved and particulate concentrations, little observations have been made of individual environmental particles concentrations and, even less so, of the chemical characterization of the molecular structure of Fe, Mn, and associated trace metals. We present past and recent results of the investigation of the morphology and chemical structure of Fe and Mn oxides using analytical electron microscopy –AEM- and X-ray Absorption Spectroscopy – XAS.

Results

The observations of Fe and Mn rich particles collected at oxic/anoxic interfaces show that most often the core of the particles is constituted of biogenic organic matter. In the case of Mn these particles are associated to bacteria (Lienemann *et al.*, 1997, Taillefert *et al.*, 2002) and in the case of Fe by either microbes (Perret *et al.*, 2000) or by organic fibrils (Taillefert *et al.*, 2000). These particles contain variable concentrations of trace metals, and the oxidation state of either Fe or Mn or some other metals, e.g., Co is also variable. This indicates that these elements undergo redox reactions when associated in the inorganic/organic moieties.

Conclusions

These results stress the need to make microscopic observations and spectroscopic analyses of Fe and Mn rich particles in lakes to understand better their role in the biogeochemical cycles of metals.

References

- Taillefert M., Lienemann C.-P., Gaillard J.-F., Perret D. (2000) *Geochim. Cosmochim. Acta*, **64**, 169-183.
Taillefert M., MacGregor B., Gaillard J.-F., Lienemann C.-P., Perret D., Sthal D.A. (2002) *Environ. Sci. Technol.*, **36**, 468-476.
Lienemann C.-P., Taillefert M., Perret D., Gaillard J.-F. (1997) *Geochim. Cosmochim. Acta*, **61**, 1437-1446.
Perret D., Gaillard J.-F., Dominik J., Atteia O. (2000) *Environ. Sci. Technol.*, **34**, 3540-3546

Chemical weathering rates in the subarctics: The exemple of the Mackenzie river system

J. GAILLARDET¹, R. MILLOT¹ AND B. DUPRE²

² Institut de Physique du Globe de Paris, Paris, France, gaillardet@ipgp.jussieu.fr

³ Laboratoire des Mécanismes de Transfert en Géologie, Toulouse, France

The Mackenzie basin rivers and adjacent Pacific rivers draining the Western Cordillera have been poorly documented. These rivers are, however, unique in a weathering study perspective. Based on Sr isotopic ratios and elemental ratios, we have applied a box-model in order to derive for each soluble element the contribution of silicate/carbonate/evaporite weathering. The main conclusions are as follows.

The overall picture that emerges is that chemical denudation of silicates is weak. A significant difference is observed between the volcanic terranes of the Western Cordillera and the granitic shield of the Slave Province, but at a global scale, chemical weathering rates of silicate in the Mackenzie river system are among the lowest in the world. By contrast, carbonate weathering rates, are not different from the other places of the world. The abundance of sulfate ions in the dissolved load of rivers probably reflects the preferential dissolution of sedimentary sulfides.

The Rocky and Mackenzie mountains show silicate denudation rates similar to those of the granitic Slave Province. There is no evidence, in the Mackenzie river basin that mountains are a preferential locus of chemical weathering

The chemical weathering rates in the interior plains are enhanced by a factor of 3-4 compared to those of the mountains. This increase in chemical weathering rates is equivalent to an increase of 6 °C ! In contrast to what is observed in the other river basin having contrasted relief (Amazon, Ganges), the higher chemical denudation rates are found in the lowlands. A positive correlation between chemical weathering rates and dissolved organic carbon in the rivers is observed. We propose that the organic complexation, for example of Al, by organic matter is responsible for the release of solutes and silicate weathering enhancement.

As a whole, we do confirm, based the present data on large river system, that low temperature, in the absence of counteracting parameters, exerts a negative action on silicate weathering rates. This conclusion disagrees with those of Edmond and Huh (1997), based on the geochemistry of Siberian rivers.

References

Edmond J.M., Huh Y. (1997), in: W.F. Ruddiman (Ed.), Tectonic uplift and climate change, Plenum Press, New York, pp. 329-351.

New perspectives on the crust-mantle invariant ratio mass balance

STEPHEN J. G. GALER

Max-Planck-Institut fuer Chemie, Postfach 3060, D-55020 Mainz, Germany (sjg@mpch-mainz.mpg.de)

The mass balance of the so-called "invariant ratios" Nb/U and Ce/Pb (or Nd/Pb) between the crust and mantle (Hofmann et al., 1986) has been used to determine elemental abundances in, and sizes of mantle reservoirs. But such estimates remain very uncertain: First, the absolute abundances of the elements in question are not known very precisely in either the bulk continental crust (BCC) or the bulk silicate Earth (BSE), and second, the mass of the continental crust is only known to about 10%. By casting the mass balance in terms of the proportion of an element in the continental crust, uncertainties are diminished substantially. The reason for this is that the balance is done solely in terms of the elemental ratios in the reservoirs, and does not involve knowledge of any absolute concentrations or reservoir masses.

Using various literature Nb/U and Ce/Pb estimates for BCC, the mass balance implies the following elemental proportions in the continental crust: Nb 11 to 20% ($\pm 5\%$), U 44 to 50% ($\pm 15\%$), Ce 18 to 29% ($\pm 3\%$), and Pb 62 to 67% ($\pm 9\%$), where the errors in brackets show the effects of uncertainties in the Nb/U and Ce/Pb ratios in oceanic basalts. The elemental proportions in the "complementary mantle" (CM) follow by difference. These simple considerations suggest that the U/Pb ratios of BCC and CM are lower and higher, respectively, than that of the bulk silicate Earth, which is the reverse of what is often assumed.

Primitive mantle normalized abundances for other elements in CM can be derived via their respective ratios to Nb, U, Ce or Pb in the BCC. The resulting abundance pattern for CM is "depleted", but too enriched in highly incompatible elements, such as Ba and Rb, to be a viable depleted source for MORB. This feature is also supported by the inferred Sm/Nd ratio of CM, suggesting ϵ_{Nd} of about +3.2 in CM today, which is far lower than the ϵ_{Nd} of around +10 in the depleted mantle. These results underscore the importance of enriched mantle sources in the crust-mantle budget of incompatible elements in the silicate Earth.

ATP is a key molecule of prebiotic evolution

E.M.GALIMOV

V.I.Vernadsky Institute of Geochemistry and Analytical Chemistry, Russian Academy of Sciences, Kosygin., 19, Moscow 119991, Russia

There are several concepts which relate to origin of life with dominated role of the specific substances: "the RNA world" (Gilbert, 1986; Joyce, 1989), "the protein world" (Fox and Dose, 1977; Dyson, 1985), "the lipid world" (Segre et al. 2001), the "sugar model" (Weber, 2000) etc. Indeed, these substances played an important role in the biological evolution. However, here I stress the role of adenosine triphosphate (ATP) as necessary prerequisite of biological evolution.

I start from formulation of certain mechanism of evolving ordering. Its main feature is a consecutive disproportionation of entropy in a chain of steady state reactions. The ordering (lowering of entropy) in such a process demands chemical conjugation with a process proceeding with the production of entropy and energy supply. The best candidate is hydrolysis of ATP. This water consuming reaction is conjugated with such water releasing reactions as formation of peptide bond, oligomerization of nucleotides etc., which obviously played an important role in prebiotic evolution.

Although the organic moieties of ATP (adenine and ribose) form from simple precursors: hydrogen cyanide (HCN) and formaldehyde (HCHO) respectively, there are some barriers, which might preclude its formation. This paper deals with a geochemical model of the early Earth environment, which allows overcoming these barriers.

Unlike existing models of self-organization (e.g. Prigogine, 1983) which suggested ordering, related to essentially non-linear processes, the mechanism of disproportionation of entropy in steady state reactions admits a process proceeding not far from equilibrium, that is described in terms of linear thermodynamic of irreversible processes. The isotopic evidences in favor of such a mechanism will be presented.

It is shown that principles of evolution that can be inferred from the suggested model are in agreement with the some important features of biological evolution.

References

- Gilbert W., (1986); *Nature*. **319**, 618
 Joyce G.F., (1989), *Nature*. **338**, 217-224
 Fox S.W. and Dose K., (1977); *Molecular Evolution and the Origin of Life*. *Dekker, N.Y.*
 Dyson F.J., (1985), *Origin of Life*. *Cambridge Univ. Press. Cambridge*
 Segre D. et al., (2001), *Origins Life Evol. Biosphere*. **31**, 119-145
 Weber A.L., (2001), *Origins Life Evol. Biosphere*. **31**, 71-86
 Prigogine I., Stengers I. (1983), *Order out of Chaos*. *Heinemann, London*.

Dust settling and aggregation in the protosolar nebula

A. GALLI, J. A. WHITBY AND W. BENZ

Physikalisches Institut, Sidlerstrasse 5, 3012 Bern, Switzerland (galli@phim.unibe.ch)

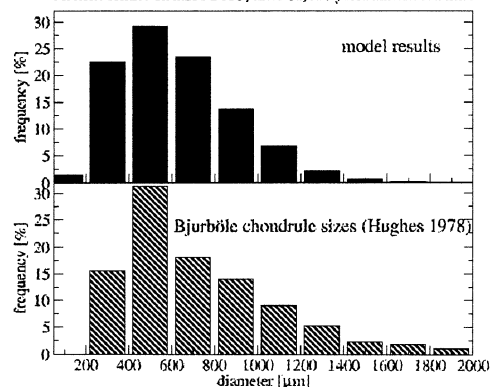
Calculations of the accretion and growth of planetesimals are currently hindered by uncertainties in the physics controlling the sticking of small particles. To better understand the lifetimes of solid particles in the early solar system we have implemented a simple one-dimensional model of dust settling and aggregation, which can be used to rapidly assess the effects of changes in physical parameters.

Chondrules, which probably constituted a major fraction of planetary material, are widely believed to have formed from precursor dust aggregates. A natural feature of our settling model is the occurrence of dust aggregates with a size-distribution appropriate for that of chondrule precursor material without appeal to more complex processes such as turbulence.

Model: We have adapted an existing model of the gravitational settling of dust in the terrestrial stratosphere for nebular conditions. The model includes both coagulation by Brownian motion and growth by collisions due to the different settling velocities of spherical particles, but does't yet incorporate any fragmentation effects. We assume an initially uniform dust/gas ratio, and follow the changes in the particle size-distribution at different heights above the nebular midplane.

Results: Using a wide range of values for the sticking coefficient, critical velocity and other parameters, our model yields approximately constant settling times of 10^5 years for 95% of the total mass of dust to fall to the midplane. This rapid settling is due to the 'rain-out' of large aggregates formed in thermal collisions and their efficient further growth. The size-distribution at the midplane has two distinct peaks after the 'rain-out' of larger particles has started: one peak corresponds to micron-sized dust, the second peak (see upper part of figure) is due to dust aggregates. Both the size of the larger particles and their mass fraction are decreasing functions of heliocentric distance due to the lower densities of gas and dust. The size-distribution of these aggregates is remarkably similar to that observed for chondrules, as shown in the figure which compares model results with chondrule sizes from the ordinary chondrite Bjurböle.

Size-frequency distribution of larger grains at midplane
 At heliocentric distance 2 AU, after 60,000 years simulation time



Isotopic composition of dissolved Mg in natural waters

A. GALY¹

Dept. Earth Sci., University of Cambridge, Downing Street,
Cambridge, CB2 3EQ, UK. albert00@esc.cam.ac.uk

Multiple collector inductively coupled mass spectrometry (MC-ICPMS) has experienced a big increase in technique and application development over the past few years. Variations in the stable isotopic composition of elements rarely studied, such as Mg, Cu, Zn, Fe or Mo are now attainable. Using this technique, natural variations in the isotopic composition of terrestrial Mg have been already found in carbonate, silicate and biological material. Here, I present preliminary results on the variation of the isotopic composition of dissolved Mg in natural waters.

27 natural waters from various geological settings (Open Ocean, continental spring, karst, lagoon, lake, and sediment) were studied. The overall variation is 4 ‰ and 2 ‰ in $\delta^{26}\text{Mg}$ and $\delta^{25}\text{Mg}$, respectively. This is more than 30 times the uncertainty of the measurements and clearly demonstrates that the isotopic composition of dissolved Mg is not unique.

The four seawater samples have indistinguishable $\delta^{26}\text{Mg}_{\text{SRM980}}$ of +2.54‰. This result is consistent with the long residence time of Mg in the oceans. Upon the twelve continental waters, only one has a heavier isotopic composition than seawater. On the other side, all the seven water coming from coastal lagoon, lake and pore-water in sediments deposited in these environments are enriched in heavy isotopes.

The isotopic composition of a dissolved element is primarily affected by 1) source/sink isotopic composition and 2) isotopic fractionation associated to dissolution/precipitation reactions. The initial source of Mg in coastal lagoon is likely to be the seawater. The positive relationship between [Mg] or Mg/Ca and the isotopic composition of the Mg left in the water is likely the result of a Mg isotopic fractionation during the precipitation of minerals. This suggests that minerals should be enriched in light isotopes and has been established for Low-Mg calcite. In coastal environment, the isotopic of dissolved Mg is primarily controlled by its uptake and associated isotopic fractionation.

Given that silicate rocks are enriched in heavy isotopes by comparison to carbonate, the few data obtained on spring water from known aquifers suggest that the Mg-isotopes in continental water may reflect the source (silicate vs. carbonate) of the dissolved Mg.

References

- Galy A., et al., (2000), *Science*, **290**, 1751-1753.
Galy A. and O'Nions R.K. (2000), *J. Conf. Abstr.*, **5**, 424-425.
Galy A., et al., (2001), *Intl. J. Mass Spectrom.*, **208**, 89-98.
Galy A., et al., (2002), *Earth Planet. Sci. Lett.*, In Press.

Ge-isotopic fractionation during its sorption on goethite: an experimental study

A. GALY¹, O.S. POKROVSKY² AND J. SCHOTT²

¹Dept. Earth Sci., U. of Cambridge, Downing Street,
Cambridge, CB2 3EQ, UK. albert00@esc.cam.ac.uk
²LMTG, UPS-OMP-CNRS, UMR 5563, F-31400 Toulouse,
France. schott@lmtg.ups-tlse.fr

Ge is generally believed to behave like Si in aqueous solution. However, unlike Si, Ge can form strong surface complexes with organic acids and iron oxides in which it increases its coordination number from 4 to 6 (Pokrovski and Schott, 1998). As a result, Ge isotopic fractionation could be associated with this process (Ge has five naturally occurring isotopes, ⁷⁰Ge, ⁷²Ge, ⁷³Ge, ⁷⁴Ge, and ⁷⁶Ge.) and used for better understanding and quantifying weathering processes. —To check this, a set of Ge sorption experiments on goethite were performed at 25°C and constant ionic strength (0.001 M) as a function of pH and Ge/goethite ratio and resulted in a fraction of adsorbed Ge ranging from 0.1 to 0.95.

The variation in the isotopic composition of Ge has been obtained by multiple collector inductively coupled mass spectrometry (MC-ICPMS). Following the method developed for Mg, solutions are introduced through into the MC-ICPMS (Nu Instruments) via a Cetac Aridus nebulizer. Isobaric interference from Ar has only been found on ⁷⁶Ge. Using this standard-sample bracketing technique, the external reproducibility of the MC-ICPMS obtained on pure Ge solution is 0.05‰/amu (2σ, n=20) on the three investigated ratios ⁷⁴Ge/⁷⁰Ge, ⁷³Ge/⁷⁰Ge, and ⁷²Ge/⁷⁰Ge.

Measured against its initial composition, the Ge left in solution after adsorption is systematically enriched in heavy isotope (up to 0.75‰/amu). In addition, the Ge-isotopic defines a single mass fractionation curve on three-isotope plots. When reported against the proportion of adsorbed Ge, all the data can be modelled by a single Rayleigh distillation.

These results have been modelled within the framework of a surface complexation approach that postulates the interaction of neutral Ge hydroxocomplexes with >FeOH° and >FeO° sites of goethite.

These preliminary data suggest that isotopic fractionation of Ge occur during its adsorption on goethite. Since goethite is a common mineral produced during weathering, Ge-isotopic composition in rivers and groundwater will be partly controlled by these adsorption mechanisms. Similar fractionation is expected to occur during Ge sorption on organic matter.

References

- Pokrovski G.S. and Schott J., (1998), *Geochim. Cosmochim. Acta*, **62**, 1631-1642.
Galy A., et al., (2001), *Intl. J. Mass Spectrom.*, **208**, 89-98.

Closure- temperature and -age of minerals

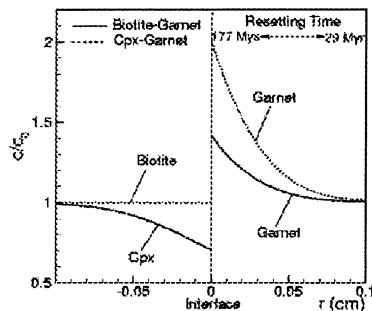
J. GANGULY^{1,2} AND M. TIRONE³

¹Bayerisches Geoinstitut, Bayreuth, Germany

²Department of Geosciences, University of Arizona, USA
(ganguly@geo.arizona.edu)

³Institut für Meteorologie und Geophysik, J.W.Goethe-Universität Frankfurt am Main, Germany
(mtirone@geophysik.uni-frankfurt.de)

Ganguly & Tirone (1999: EPSL) developed an extension of Dodson's classic formulation of closure temperature (T_C) in a mineral surrounded by a homogeneous infinite matrix so that it is applicable to the slowly diffusing systems. In addition to applying this formulation to calculate T_C to selected systems, we have, in this work, explored the effect of matrix phase on T_C . An illustration of this effect on the Nd diffusion profile in garnet (right panel) is shown below for an homogeneous infinite matrix (dashed line) and a matrix with the same D as in Grt. Conditions for the computation are taken from Ganguly & Tirone (1999: EPSL) (section 5) with $M = 1$ and partitioning between matrix and garnet = 0.5. T_C (Sm-Nd) for garnet should be significantly higher when it is surrounded by Cpx, for which $D(\text{REE}) < \text{or} = D(\text{REE})$ in Grt, than when it is surrounded by biotite.



Our REE diffusion data in almandine garnet suggest that the Sm-Nd and Lu-Hf systems should have similar T_C for similar conditions. In contrast to the T_C calculated from the diffusion data of Van Orman et al. (2002: CMP), our data yield T_C for the Sm-Nd system that is in good agreement with that derived empirically by Mezger et al. (1992: EPSL) for garnet in a granulite sample when the same grain size, cooling rate and T_0 are used. The cooling rate of a mineral can be directly retrieved from the difference between its peak metamorphic and cooling ages, as well as that between its core-age and the bulk age. In addition, it is also possible to derive the cooling rate and T_C from an isotopic concentration profile that can be measured in an ion probe.

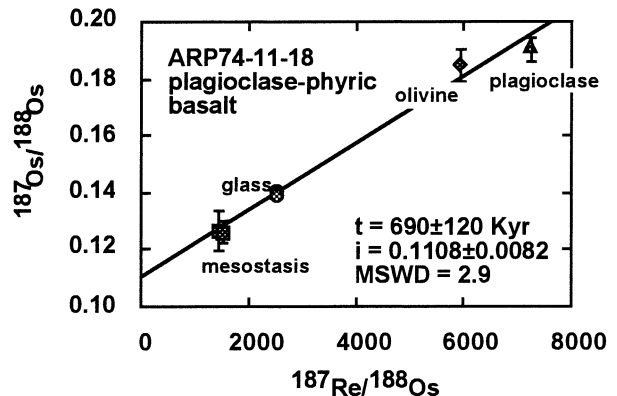
Open-system behaviour in mid-ocean ridge basalts

ABDELMOUHCINE GANNOUN¹, LOUISE E. THOMAS¹, KEVIN W. BURTON¹ AND PIERRE SCHIANO²

¹ Department of Earth Science, The Open University, Walton Hall Milton Keynes, UK (A.Gannoun@open.ac.uk; L.E.Thomas@open.ac.uk; K.W.Burton@open.ac.uk)

² Laboratoire Magmas et Volcans, Université Blaise-Pascal, 5 Rue Kessler, 63038 Clermont-Ferrand, France.
(p.schiano.@opgc.univ-bpclermont.fr)

The chemical composition of MORB provides one of the best constraints on the composition of the Earth's upper mantle. The problem remains in deciphering the mantle signal from that of melting and magmatic processes. The Re-Os isotope system potentially holds key information on the nature of the chemical signature in MORB. Partly, because (unlike the lithophile elements) Re and Os can be measured in all phenocryst phases, but also because Re/Os are highly fractionated in such phases and the details of phase equilibration are thus readily observed. This study presents high-precision Re-Os and Th-U-Ra isotope data for MORB samples from the FAMOUS region on the mid-Atlantic ridge (36°50' N). Separated phases from a plagioclase-phyric basalt yield a best-fit line corresponding to an age of 690±120 Kyr (see figure).



A first sight, this regression might be taken to represent a crystallisation age, suggesting that the Os variations in MORB glasses reflect *in-situ* post eruption radiogenic growth. However, Th-U-Ra data suggest an age of <10 Kyr for this sample. Further data from a picrite and an olivine-basalt yields Re-Os regression ages of 1.2 and 2.5 Myr, respectively, for effectively zero-age basalts. These results are consistent with assimilation of phenocryst phases just prior to eruption, in accord with chemical zonation and melt inclusions in the same phenocrysts. Taken together, these results suggest that the Os isotope variations MORB glasses, reflect assimilation, rather than *in-situ* post eruption radiogenic growth or Os isotope heterogeneities in the mantle source.

Coherency of surface protonation data - implication from modelling of dissolution experiments

J. GANOR¹, J. CAMA² AND V. METZ³

¹ Dept. Geol. & Env. Sci., Ben-Gurion Univ. of the Negev, Beer-Sheva 84105, Israel (Ganor@bgumail.bgu.ac.il)

² Institute of Earth Sciences "Jaume Almera", CSIC, Barcelona 08028, Catalonia, Spain (jcama@ija.csic.es)

³ Institut für Nukleare Entsorgung, Forschungszentrum Karlsruhe (FZK-INE), Germany (volker@ine.fzk.de)

Comparison of seven surface titration curves obtained at 25°C reveals strong discrepancies, both in the shape of the curves and in the pH of the point of zero net proton charge (pH_{PZNPC}). We suggest that the observed differences in the pH_{PZNPC} are mostly artifacts of the differences in points of reference used for the measurements of the titration. At the pH range of 3 to 9, the non-permanent surface charge of kaolinite is dominated by the surface charge of the edges, i.e., by the difference between the amount of protonated Al edges ($>AlOH_2^+$) and the amount of diprotonated Si edges ($>SiO^-$). As all the reported values of pH_{PZNPC} of kaolinite ranged from 3 to 7.5, only the edge contributes to the charge at the pH_{PZNPC} of kaolinite. Therefore, changes in the surface area ratio of the edge to that of the basal plain would not affect the pH_{PZNPC} . Hence, at equilibrium, different kaolinite samples are expected to have similar pH_{PZNPC} , although small differences in pH_{PZNPC} may result from differences in the density of ion substitution and defects on the edge surfaces. Therefore, the different titration curves may be shifted so they would have the same pH_{PZNPC} . An agreement between most of the titration curves was observed following this correction.

A prediction of the molar fraction of protonated sites was retrieved from modelling of kaolinite dissolution reaction and was compared to the protonation data obtained from surface titration. This prediction strongly agrees with the adsorption isotherm of Huertas et al. (1998), which was chosen to represent the other curves. A by-product of this comparison is that it predicts that the proton surface density on the major protonated surface site is $8 \cdot 10^{-7}$ mol m⁻² (≈ 0.5 sites nm⁻²). The excellent fitting of the surface charge prediction of our proposed model to surface charge measurements and the reasonable obtained value of the surface density strengthen both the model proposed by Cama et al. (2001) and the corrected surface protonation data.

References:

- Cama J., Metz V., and Ganor J. (2002), *Geochim. Cosmochim. Acta*, submitted.
 Huertas J. F., Chou L., and Wollast R. (1998), *Geochim. Cosmochim. Acta*, **62**(3), 417-431.

Study on the mechanism of metallogenesis of the dispersed elements Ge, Se, Cd and Tl

GAO ZHENMIN AND YAO LINBO

Open Lab. of Ore Deposit Geochemistry, Institute of Geochemistry, Chinese Academy of Sciences, Guiyang, 550002, P.R. China (zhmgao@21cn.com)

The data pertaining to the scale and grade of the selected dispersed element deposits are presented in the table:

Ore deposit	Grade ($\times 10^{-6}$)	Scale
Niujiatong Cd deposit	Average: 536 6	Large
Lincang Ge deposit	Average: 779	Superlarge
Lanmuchang Tl deposit	2000-2800	Large
Yutangba Se deposit	1258-5037	Small

It can be seen from the table that the four dispersed elements can be so abnormally enriched under certain geological conditions as to form relatively large-scale ore deposits.

Most dispersed element deposits are distributed in the southwest of China.

Their metallogenesis are discussed from the following respects.

(1) Most dispersed element deposits are formed under low temperature ($< 200^\circ\text{C}$) conditions. For example, homogenization temperatures (HT) of calcite, dolomite and sphalerite inclusions associated with sphalerite for Niujiatong deposit is $104\text{--}131^\circ\text{C}$; Lincang, HT of quartz inclusions in siliceous rocks contemporaneously precipitated with Ge is $85\text{--}88^\circ\text{C}$; Lanmuchang, HT of barite coexisting with lorandite and cinnabar is $107\text{--}194^\circ\text{C}$.

(2) It is found that many dispersed elements are concentrated as ores in the certain horizons of the strata.

(3) Ore-forming materials of the dispersed elements came from adjacent rocks of ore-host wall rocks.

(4) The nature of ore-forming fluids for the selected Cd, Ge, Tl and Se deposits are of reducibility (e.g. the ore-forming fluids responsible for the Niujiatong deposit have Eh values ranging from -0.7 to -6.3) and weakly alkaline to weakly acidic (e.g. the ore-forming fluids for the Lincang deposit have pH values ranging from 6.50-8.00).

(5) Metallogenic ages mostly dated at Cretaceous and Tertiary.

References

- Yao linbo, Gao zhenmin et al., (2002), *Science in China, Ser. D*, 2002, 32, 54-63. (in Chinese)
 Ye Lin and Liu Tiegeng, (1999), *Chinese journal of geochemistry* 18, 62-68

Oxygen isotope profile of the lower ocean crust: an in-situ study by UV-laser-ablation oxygen isotope microprobe

Y. GAO^{1,2}, J. HOEFS¹ AND J. E. SNOW²

¹ Geochemisches Institut der Universität Göttingen,
Goldschmidt Strasse 1, D-37077 Göttingen, Germany.

² Max-Planck Institut für Chemie, Abt. Geochemie Postfach
3060, D-55020 Mainz, Germany

Systematic analysis of mineral oxygen isotope compositions in gabbro has the potential to find out whether and under what conditions seawater interacts with plutonic rocks from the deeper part of the oceanic crust to constrain both the nature of oceanic crust that is recycled into the mantle through subduction, as well as the cooling history of the lower ocean crust. So we have measured 10 representative samples of gabbro from Hole 735B of Leg 176 by UV-laser oxygen isotope microprobe for the oxygen isotopic compositions of their constituent minerals.

Plagioclase-pyroxene pairs of Hole 735 B gabbro show disequilibrium pattern in the $\delta^{18}\text{O}$ space for their oxygen isotope composition. Plagioclase has an overall $\delta^{18}\text{O}$ enrichment through the depth, while $\delta^{18}\text{O}$ values of clinopyroxene show decrease with depth. The contrast behaviour between plagioclase and clinopyroxene suggests that the gabbroic crust has encountered a two-stage alteration during its cooling history. Considering the relatively unaltered constant $\delta^{18}\text{O}$ values of olivine and clinopyroxene, the modification of the O-isotope composition of plagioclase must occur at a temperature that is higher or equal to the closure temperature for O-isotopes in plagioclase but lower than that for olivine and clinopyroxene. This may reflect the melt mixing or external fluid infiltration during cooling.

Contrast to the depletion patterns of most other lower oceanic crust, Hole 735B gabbros show an enrichment of $\delta^{18}\text{O}$, this may reflect the difference in hydrothermal activation associated with different spreading rate.

References

- Fiebig, J., U. Wiechert., et al., (1999), *Geochim. Cosmochim. Acta*, V63(5), pp. 687-702.
- Wiechert, U., J. Fiebig, et al., (2002) *Chemical Geology*, 182, pp. 179-194.
- Lecuyer C. and B. Reynard, (1996), *J. Geophys. Res.*, 101(B7), pp. 15,883-15,897.
- Ito, E. and R. Clayton, (1983), *Geochim. Cosmochim. Acta*, 47, pp. 535-546.
- Gregory, R. and H. P. Taylor, (1981) *J. Geophys. Res.*, 86(B4), pp. 2737-2755.

Geochemical self-organization of mixed siliciclastic-carbonate sediments in estuarine-like systems

T. GARCÍA¹, L. GAGO-DUPORT¹, S.F. BASTERO¹, A. VELO¹, A. SANTOS² AND N. DE LA ROSA-FOX³

¹ Dept. Geociencias Marinas, Universidad de Vigo, Spain
(tatianag@uvigo.es)

² Dept. Geología, Universidad de Cádiz, Spain

³ Dept. Física Materia Condensada Universidad Cádiz, Spain

The dissipative structures concepts are usually addressed to study the evolutionary behaviour in complex, open far from equilibrium systems when they approach to a steady state configuration. This may result in the emergence of spatial and temporal macroscopic patterns expressed as functional or morphological aspects of the system. In this study, the mixing processes taking place between siliciclastic and carbonate sediments in an estuarine-like environment (Ria de Vigo, NW Spain) have been analysed following that point of view. The main goal is to evaluate how local variations in parameters, as specific solubility or grain size of minerals, result in the formation of macroscopic patterns by coupling with sediment dynamics.

The work was firstly based on an accurate study of the mineral contents in sediments from 13 gravity corers sampled every 5cm up to 25 cm. Quantification of identified phases was carried out using the Rietveld method and applied to perform both surface and deep maps, relating space-distributions of minerals. Firstly, surface maps were used to relate the specific percentage amount between mineral pairs, to the grain size distributions following defined sections of the study area. A coupled behaviour was found for the particular case of plagioclases and carbonates. This is characterized by a cross-linked distribution for the relative amounts on each mineral, indicating a straightforward relation with the grain size for the plagioclase curve and opposite for the carbonate one (García *et al.*, 2000). Secondly, the surficial and deep maps have been compared in order to evaluate the extent of preservation of the surface mineral configuration into the depth. This allows us to obtain a three-dimensional view of the chemical transformation processes in the sediment during the burial, taking into account both the diffusion and the advection mechanisms.

As a result, this study shows the existence of geochemical organised patterns which in surficial sediments manifest through opposite abundances between certain minerals from both fractions controlled by the dissolution kinetics according to the grain size, whereas with burial are driven vertically by the diffusion-reaction processes taking place during early diagenesis. As a consequence, characteristic 3D-patterns resulting from the coupling between the surface distribution and the sequence of diagenetic reactions involving clays, sulphides, feldspars and carbonates have been analysed.

References

- García T., Velo A., F-Bastero S., Alejo I., Gago L., Santos A. and Vilas F., (2000), *J. Iber. Geol.* 26, 249-269.
- Study supported by Spanish MCYT BTE2000-0877 project.

PTX properties of a natural Au-bearing hydrothermal fluid from a multidisciplinary study of fluid inclusions (Sigma deposit - Canada)

P. GAROFALO^{1,2}, C. A. HEINRICH², D. GÜNTHER³, AND T. PETTKE²

¹ Institut für Geowissenschaften -Peter Tunner Strasse 8700 Leoben -Austria (garofalo@unileoben.ac.at)

² Institut für Isotopengeologie und Mineralische Rohstoffe - ETH Zentrum - 8092 Zurich - Switzerland (heinrich@erdw.ethz.ch; pettke@erdw.ethz.ch)

³ Laboratory of Inorganic Chemistry - ETH Hönggerberg, - 8092 Zurich - Switzerland (guenther@inorg.chem.ethz.ch)

Studied samples and methods

The Sigma deposit is a large network of quartz-tourmaline-Au veins of the Archean Abitibi greenstone belt. We reconstructed the physical and chemical properties of its Au-bearing fluid using petrographically discriminated trails of fluid inclusions showing clear relations with vein quartz, tourmaline and gold. Samples were studied using microthermometry and Raman spectroscopy to determine bulk properties and identify the species in the vapour phase. Laser Ablation-ICP-Mass Spectrometry was used, for the first time for this type of deposits, to determine the concentrations of Na, K, B, and Au in the ore fluid.

Fluid inclusion data

The collected data show that ore fluid belongs to the system H₂O-NaCl-CO₂-B-Au±CH₄. Two fluids, one belonging to the system H₂O-NaCl-CO₂-Au±CH₄ and another to H₂O-NaCl-B-Au, were separately trapped within the veins as heterogeneous mixtures of liquid and vapour phases at 380-400 °C and ca. 300 bar. This pressure is significantly lower than that previously estimated for the deposit (e.g. ROBERT and KELLY, 1987). In both fluids, Au ranges between 0.5 and 5 ppm. In the liquid phase, Na is between 3900 and 31000 ppm, and K from 380 to 9500 ppm. B ranges from about 78 to 1300 ppm. We compare our results with previous data on the deposit, and propose that Au precipitated from a boiling Au-rich parent fluid.

References

Robert F. and Kelly W. C. (1987) Ore-forming fluids in Archean gold-bearing quartz veins at the Sigma mine, Abitibi Greenstone belt, Quebec, Canada. *Economic Geology* **82**, 1464-1482.

Clinopyroxene geothermobarometer for eclogites

J.G.GARTVICH¹ AND N.V. SURKOV²

¹ Institute Mineralogy and Petrography, SB RAS, Novosibirsk, Russia (julia@uiggm.nsc.ru)

² Institute Mineralogy and Petrography, SB RAS, Novosibirsk, Russia (diagrams@uiggm.nsc.ru)

Introduction

The system CaO-MgO-Al₂O₃-SiO₂ is a suitable object for the modeling. The Cpx-Gr association in the system is not divariant, and the composition of coexisting phases depends not only on temperature and pressure, but also on bulk composition of a system. The simplest geobarometer for eclogite paragenesis must consist of two equations with three parameters: the En and the CaTs contents in Cpx, and the Gross content in garnet. The experiments of coexisting Cpx and Gr in the magnesium part of system kbar were performed on the high-pressure apparatus "piston - cylinder" at T~1200 to 1585 °C, P~15 to 30 kbar.

Discussion of results

The En and CaTs content in Cpx increase with increasing pressure. The En content increases with increasing temperature but no notable changes in the CaTs content were detected. The garnet becomes more magnesium with increasing pressure and temperature. Using these data, the coefficients of two polynomials ($F=f_1+f_2x+f_3y+f_4z+f_5x^2+f_6y^2+f_7z^2+f_8xy+f_9xz+f_{10}yz$; x is the content of Gross in Gr (mol. %), y is the content of En in Cpx, z is the content of CaTs in Cpx (mol. %)) fitting the experimental composition of coexisting Cpx and Gr as a function of T and P (Table 1).

Table 1: Coefficients of polynomials.

	Temperature	Pressure
f ₁	1794.9028	97.372239
f ₂	-805.4903	-64.51706
f ₃	-1809.595	15.310452
f ₄	-774.2796	-248.6717
f ₅	3424.7345	157.20992
f ₆	-2679.645	25.737019
f ₇	-4839.156	242.51907
f ₈	1827.7546	31.650826
f ₉	5943.542	-403.9175
f ₁₀	3367.0297	173.69664
N	39	39

Conclusions

The data may be recommended for geothermobarometry of eclogites and eclogite-like rocks.

References

Boyd F.R. (1970), *Miner. Soc. Amer. Spec. Pap.*, **3**, 63-75.
Surkov N.V., (1998), *Russian Geology and Geophysics*, **11**, 1538-1551.

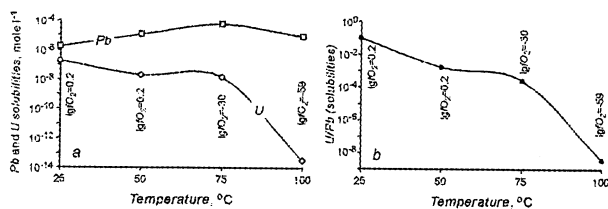
The mobility of U and Pb in cooling aqueous fluid evolving from reduced to oxidized state

O.L. GASKOVA AND Y.V. DUBLYANSKY

Institute of Mineralogy and Petrography SB RAS,
Novosibirsk, Russia (gaskova@uiggm.nsc.ru,
kyoto_yuri@hotmail.com)

Solutions that have deposited low-temperature hydrothermal minerals within the vadose zone of Yucca Mountain, Nevada were likely evolving from low to high oxidation states as the temperature of fluids decreased with time (from about 85 to less than approximately 30-50°C). Knowledge of solubilities of Pb and U in such solutions may prove important in interpreting the results of the U-Pb radiometric dating of the subject minerals. The "HCh" code (Shvarov, 1999) was used for thermodynamic modeling of the solution-mineral equilibria in the H-O-C-Ca-Si-U-Pb system. The roles of T , Eh , pH , and pCO_2 were examined.

The modeled evolution path was: from water equilibrated with silica, and dissolved CH_4 and CO_2 at equilibrium ($\lg fO_2 = -5.9$) at $T = 100$ °C, through methane-free water ($\lg CO_2 = -3.5$, $\lg fO_2 = -3.0$) equilibrated with calcium carbonate at $T = 75$ °C, to oxygenated water ($\lg CO_2 = -3.5$, $\lg fO_2 = 0.2$) buffered by calcium carbonate at $T = 50$ and 25 °C. The path depicts evolution of a hypothetical mineral-forming fluid, early portions of which represent deep-seated fluid injected into the vadose zone, after which intermixing with more-oxygenated aquifer waters and cooling occurred.



The Figure *a* shows that the solubility of Pb after a one-order of magnitude increase related to the transition from silicate- to carbonate-equilibrated fluid, steadily decreases with cooling of the fluid. Solubility of U drastically increases as the fluid evolves from hot reduced to cool oxidized one. Respectively (Figure *b*), the U/Pb solubility ratio increases by some 8 orders of magnitude.

Solubility of Pb in modeled system varies between $1.8 \cdot 10^{-6}$ and $5.5 \cdot 10^{-5}$ mole·l⁻¹ (0.4 to 11 ppm). The early reducing fluids are thus expected to carry Pb derived from deep levels of the crust, whereas late oxidized fluids would carry Pb from shallower aquifer rocks. By contrast, solubility of U in early reduced fluids is so low ($3 \cdot 10^{-14}$ mole·l⁻¹ or $7.2 \cdot 10^{-6}$ ppb) that little U from the deep levels is expected to be brought. At U-solubility as high as $1.9 \cdot 10^{-7}$ mole·l⁻¹ (45 ppb), late oxidizing fluids would be capable of mobilize U from shallow aquifer-hosting rocks.

The work was funded by the Russian Fund for Basic Research (Project 02-05-64623).

Shvarov, Y.V. (1999) *Geochem. Int.* 6, 571 – 576.

“Plum-cake” subcontinental mantle beneath SE Alps as resulting from the geochemistry of mantle xenoliths

D. GASPERINI¹, P. MACERA¹, K. MAFFEI¹, L. MORTEN²,
AND G. RIZZO²

¹Dipartimento Scienze della Terra, Università di Pisa, Italy
(d.gasperini@dst.unipi.it)

²Dipartimento Scienze della Terra e Geologico Ambientali,
Università di Bologna, Italy (morten@geomin.unibo.it)

Preliminary geochemical and petrological data on the Tertiary ultramafic xenoliths from the Veneto Volcanic Province (VVP; SE Alps, Italy) suggest the presence of a “plum-cake” mantle region at $P \cong 1.5$ -2.5 Gpa and $T \cong 1250$ °K (spl-lherzolite field). Major elements geochemistry of the spl-lherzolite and -lherzolite xenoliths reflects a depleted mantle source. Nevertheless, the VVP xenoliths are also characterized by “cryptic metasomatism”, with varied enrichment in LREE, K, Rb, Sr, and P, indicating a re-fertilized mantle source after the depletion episode(s). Their PM-normalized spiderdiagrams are comparable to those observed for the VVP alkaline basalts having a plume-related origin (HIMU-DM; Macera et al., 2002). Disregarding their mineralogy, the VVP xenoliths do not show uniform Nb and Ta anomalies, suggesting variable interactions with crustal material at depth in the mantle. Finally, the VVP mafic xenoliths display a large spread in incompatible trace elements ratios, testifying to the heterogeneity of their mantle source. These features may be explained in terms of a plume-induced metasomatism (HIMU-type mantle upwelling) on a variably depleted subcontinental lithosphere (DM) beneath SE Alps, where a not perfectly homogenized crustal component was also present. We suggest that plume material has fed the VVP upper mantle starting at least 65-60 Ma ago. Different textures shown by the VVP xenoliths, ranging in general from protogranular in the Adige Valley outcrops to porphyroclastic in the Lessini area, may be a useful tool to estimate width and intensity variation of the shallow expression of mantle diapirism beneath SE Alps at Tertiary time.

References

- Macera P., Gasperini D., Blichert-Toft J., Piromallo C., Bosch D., Del Moro A. and Martin S. (2002), *Geophys. Res. Abs.* 4, EGS02-A-06798

Multiple origin of water salinization in a coastal aquifer, south India – Geochemical point of view

N. GASSAMA¹, S. VIOLETTE², N. D'OZOUVILLE^{1&2}
AND A. DIA³

¹GéEAC, EA 2100, U. Tours, Fr (gassama@univ-tours.fr)

²UMR 7619 Sisyphe, UPMC, Paris, Fr
(violette@ccr.jussieu.fr)

³UMR 6118, GéoSciences Rennes, Fr (dia@univ-rennes1.fr)

Introduction

The coastal aquifers of the Kaluvelly basin were selected because an increase of salinity together with a drastic fall in the water level have been recorded for several years. The over-exploitation of the Vanur aquifer for irrigation purposes has modified the natural groundwater flow which is sometimes reversed and flows from the sea inland. Pumping is irregular in time and space which leads to unpredictable flow. Furthermore most wells in the area are not cased resulting in some anthropogenic mixing between the aquifers.

The aim of this work is to characterize the different water bodies involved and their seasonal evolution, and to quantify processes such as mixing and water-rock interaction. One hydrological year (2000-2001) has been monitored during dry, wet and intermediate season. Here we present the geochemical results. Results will be used for water management and planning purposes. The setting of the Kaluvelly coastal basin is characteristic of the Bengal coastal zone.

Hydrological settings

Salt may originate from multiple sources: i) seawater intrusion through the upper aquifer bordering the coast or brackish water from the swamp, during seasonal decline of the water level or throughout the year; ii) upward leakage from the charnockite aquifer caused by head differences due to the pumping; iii) vertical movement of salty irrigation water and/or of industrial output; iv) enhanced leaching of sediment beds due to drainage increase.

Results

Because of the multiple origins of the salt in the Kaluvelly aquifers, chloride alone cannot be used to discriminate between sources. In addition, the common geological origin of Vanur sandstone and charnockite increases the difficulty to distinguish between "old" Vanur waters and "young" Vanur waters mixed with charnockite waters. The geochemical tools that we applied are major and trace elements and their ratio, halide ratio, and isotopes.

Data seems to indicate that the recharge is sufficient to counteract salinity increase during the study period. A seasonal salinity fluctuation is mainly observed in the Cuddalore sandstone aquifer, where water chemistry records the influence of agriculture/industry but no direct seawater input. For the Vanur sandstone aquifer, results show that the north part is in hydraulic connection with the brackish swamp and the south part receives salty waters which can originate from the Cuddalore sandstone aquifer.

Rare gas systematics on north Atlantic basalts (33 to 45°N)

C. GAUTHERON¹ AND M. MOREIRA²

¹Laboratoire de Géochimie et Cosmochimie, IPGP, T14-15,
3ème, 4 place Jussieu, 75252 Paris

(gauthero@ipgp.jussieu.fr)

²(moreira@ipgp.jussieu.fr)

Samples from the north Atlantic ridge between 33 and 45°S of Latitude were analyzed for rare gas content and isotopic ratios by crushing and step-heating.

The total rare gas content ranges between $(0.09-49) \times 10^{-6}$, $(1-360) \times 10^{-12}$ and $(0.09-61) \times 10^{-10}$ for ⁴He, ²²Ne and ³⁶Ar respectively in ccSTP/g. The helium isotopic ratio ⁴He/³He varies between typical MORB values (80,520) and radiogenic values (108,321), (or R between 8.97 and 6.67Ra, with R the ³He/⁴He isotopic ratio and Ra the atmospheric ratio 1.384×10^{-6}). The total ²⁰Ne/²²Ne ratios vary between the atmospheric ratio and mantle like value (11.4). The total ⁴⁰Ar/³⁶Ar isotopic ratios range between 312 (air like) and 14,765.

The samples studied here do not sample the primitive Azores plume ridge interaction, but a mantle with radiogenic helium. Moreover, the ⁴He/³He isotopic ratio increases in the north as already observed by [1]. Furthermore, neon isotopic ratios show dispersion around the MORB line, but the majority of the samples have a ²¹Ne/²²Ne extrapolated ratio lower than the MORB. These results are in accord with previous neon study on this ridge [2].

The radiogenic helium isotopic composition of the basalts between 40 and 45°N is similar to the composition of Sao Miguel Island [3]. They can be explained by interaction between the ridge and the Sao Miguel source mantle, sediments, continental crust or delaminated subcontinental lithospheric mantle can be proposed for the source of Sao Miguel.

- [1] Kurz et al., 1982, Helium isotopic variations in the mantle beneath the central North Atlantic Ocean EPSL, 58, 1-14
- [2] Moreira et al., 2002, Rare gas systematics on Mid Atlantic Ridge (37-40°N) in press to EPSL
- [3] Moreira et al., 1999, Helium and Lead isotope geochemistry of the Azores Archipelago EPSL, 169, 189-205

2.0 b.y old natural nuclear wastes: the natural nuclear reactors in Gabon

F. GAUTHIER-LAFAYE¹, P. STILLE¹ AND M. DELNERO²

¹.Centre de Géochimie de la Surface – EOST- UMR7517.

Strasbourg, France.(gauthier@illite.u-strasbg.fr)

². Institut de Recherche Subatomique. CNRS/IN2P3.

Strasbourg, France. (mireille.delnero@ires.in2p3.fr)

Two billions years ago, the increase of oxygen in atmosphere and the high $^{235}\text{U}/^{238}\text{U}$ uranium ratio(>3%) allowed the formation of natural nuclear reactors on the earth. The particular geochemical conditions (low REE and B contents which are “poison” for neutrons) and the accumulation of high-grade uranium ores at Oklo initiated fission reactions which sustained for 100 000 to 500 000 years. These reactors are now considered to be good natural analogues for nuclear waste disposals. Their preservation during such a long period of time is mainly due to the geological stability of the site, the occurrence of clays surrounding the reactors and acting as an impermeable shield and the occurrence of organic matters that maintained the environment in reducing conditions, favourable for the stability of uraninite. Hydrogeochemical studies and modelling have shown the complexity of the geochemical system at Oklo (deep reactors: 100 - 400m) and Bangombé (reactor located close to the surface: 12m). It has been shown that various processes, including adsorption and precipitation, are involved in the retention of fission products and actinides. The efficiency of these processes depends on the mineralogy of the host rocks (occurrence of clays, oxides, phosphates...) and the chemistry of the groundwater. It can be shown that these parameters change with time and from one area to another. Consequently, it is of great concern to better understand the mechanisms involved during the water-rock interactions that control the water chemistry and consequently the behaviour of fission products and actinides in the natural environment for a long period of time. In this respect, the natural nuclear reactors in Gabon are ideal to illustrate the effects of time on the evolution of the geochemical processes involved in the retention/migration of fission products and actinides. In the reactors and their vicinity, the occurrence of many chemical elements with abnormal isotopic compositions (fission products and elements with high section de capture) give the unique opportunity to trace in detail the behaviour of fission products and actinides during the various geochemical processes.

Hydrological stability in carbonate aquifers over the last 250kyr as reflected by $^{234}\text{U}/^{238}\text{U}$ in groundwater, speleothems and tufa

I. GAVRIELI, M. BAR-MATTHEWS, L. HALICZ,
A. AYALON, D. GUR, A. BURG

Geological Survey of Israel, 30 Malkhe Israel St. Jerusalem, 95501, Israel (Ittai.Gavrieli@mail.gsi.gov.il; Matthews@mail.gsi.gov.il; Ludwik@mail.gsi.gov.il; Ayalon@mail.gsi.gov.il; Dafna@vms.huji.ac.il; Burg@mail.gsi.gov.il)

The main regional aquifers in the Eastern Mediterranean are set in carbonate rocks dating from Jurassic to Upper Cretaceous. $^{234}\text{U}/^{238}\text{U}$ activity ratios in groundwater emerging from these aquifers vary over a wide range, from 1.0-2.5. However, the range of values obtained in the water in each of the three regions sampled (Mt. Hermon, Galilee, and the Judea Mountains) exhibits a narrow range of values (2.21-2.48, 0.99-1.07 and 1.01-1.13 respectively). Thus, these water sources can be characterized by their $^{234}\text{U}/^{238}\text{U}$ activity ratios. Present-day speleothems and tufa associated with these waters exhibit activity ratios similar to the water from which they precipitated.

Paleo tufa and speleothems within each region were dated using the U- ^{230}Th (TIMS) method and found to cover the age range of the last 250kyr. The $^{234}\text{U}/^{238}\text{U}$ activity ratios obtained from these older samples remain similar to recent values but have a wider range. Whereas the wider range reflects the overall variation in the $^{234}\text{U}/^{238}\text{U}$ activity ratios over several glacial-interglacial intervals (Ayalon et al., 1999), the differences between the regions, remains similar to that found today. This suggests that the $^{234}\text{U}/^{238}\text{U}$ activity ratio in carbonate aquifers is determined mainly by the local hydrological and aquifer conditions (rock and vegetation type, water paths, residence time) and less by the changes in temperature and precipitation amount.

The $^{234}\text{U}/^{238}\text{U}$ ratios in the water and secondary carbonates were measured by MC-ICP-MS and compared with values derived by TIMS. Excellent precision was obtained by the MC-ICP-MS (NU instrument) with values similar within error to those determined by TIMS.

Reference

Ayalon A., Bar-Matthews M. and Kaufman A. (1999). *Holocene* **9**, 715-722.

Cosmogenic ^3He production rate: comparison of He and Be data from Himalayan samples.

ERIC GAYER¹, RAPHAEL PIK¹, CHRISTIAN FRANCE-LANORD¹, BERNARD MARTY¹, DIDIER BOURLES²,

¹CRPG, 15 rue Notre-Dames des Pauvres, 54115 Vandoeuvre-les-Nancy, egayer@crpg.cnrs-nancy.fr

²CEREGE, BP 80, Aix en provence Cedex 04.

In the framework of a more general study of erosion rates in the Himalayas, we developed the measurement and use of cosmogenic ^3He ($^3\text{He}_c$) in garnets from glacial polished surfaces and moraines in the Narayani basin, Central Nepal. As a reference we also measured ^{10}Be in coexisting quartz from the same samples. We derived cosmogenic ^3He concentrations from helium measured in garnet, correcting for inherited nucleogenic ^3He . The importance of this nucleogenic component is related to the Li concentration in garnet (about 30 ppm) and is confirmed by the ^3He content of non-exposed garnets sampled in a nearby mine. After corrections, the cosmogenic concentrations of ^3He and ^{10}Be display good linear correlation, which supports the validity of applied corrections for inherited component.

However, beside the nice correlation of cosmonucleides concentrations, the exposures ages derived from $^3\text{He}_c$ are 2.7 times higher than those derived from $^{10}\text{Be}_c$ (from < 500 yr to ~5000 yr) using the classical production rates and scaling factors. All the data being verified for possible analytical bias, this proportional factor suggests that the production rate of $^3\text{He}_c$ in these garnets is about 2.7 times higher than that of $^{10}\text{Be}_c$. Two hypothesis can be proposed to explain the $^3\text{He}_c$ and $^{10}\text{Be}_c$ difference: 1) A compositional dependence of the $^3\text{He}_c$ production rate related to garnet features. Indeed, for other phases such as olivine Licciardi et al. (GSA Bull. 2001) had shown a correspondence between $^3\text{He}_c$ exposure ages and $^{10}\text{Be}_c$ exposure ages in quartz. 2) An underestimated production rate of $^3\text{He}_c$ at high altitude, as all samples have elevations between 4000 m and 4500 m.

To address the first hypothesis we measured ^3He concentration in coexisting garnet and olivine of a kimberlite from the Lesotho Plateau, South Africa (2500 m). In this exposed rock, garnets and olivines contain the same concentration of ^3He . Other additional measurements indicate that the ^3He contained in olivines and garnets is dominated (more than 2/3) by cosmogenic ^3He . All these observations are in favour of a common $^3\text{He}_c$ production rate for olivine and garnet. These and future results from lower elevation samples will be used in assessing a possibly different altitudinal dependence of the ^3He production rate than that traditionally assumed by classical scaling.

Depletion Factor as a Paleodepth Indicator

N. GAZIT-YAARI¹, B. LAZAR² AND J. EREZ²

¹ Geological Survey of Israel, 30 malkhei Israel St., Jerusalem 95501, Israel (naama@mail.gsi.gov.il)

² The Institute of Earth Sciences, The Hebrew University of Jerusalem, Givat-Ram, Jerusalem 91904, Israel (boaz.lazar@huji.ac.il; erez@vms.huji.ac.il)

Laboratory and field studies showed that the fractionation factor (α) between atmospheric CO_2 and total dissolved carbon (C_T) may turn from the "normal" equilibrium value of ca. 1.008 to a very low value of 0.979 to 0.986. The later occurs during CO_2 invasion into solutions highly depleted in C_T and results in brine having negative $\delta^{13}\text{C}$. This phenomenon was termed as the "Baertschi Isotopic Effect" (BIE). Here we present experimental and field data that enable to predict the physicochemical conditions to the onset of BIE and formulate an expression for the minimum degree of depletion (Depletion Factor – DF) needed to turn the value of α below unity. It is suggested that the values of $\delta^{13}\text{C}$ of carbonates and organic matter from the sedimentary record of stromatolitic paleoenvironments are proxies for the depth of the ancient water body when substituted in the DF formula.

Field measurements of CO_2 invasion were conducted in two hypersaline water bodies along the northern Gulf of Aqaba, Red Sea; one, the evaporation pans of Israel Salt Company, a solar salt production plant; and the second, the Solar Lake. Both environments were highly depleted in C_T due to the intense metabolic activity of the benthic Microbial Mat Communities (MMC), the modern equivalents of stromatolites. Brine samples were taken in several places, each having different depth ranging from 5 to 50 cm. Laboratory experiments consisted of MMC taken from the Solar Lake, incubated in closed cells under different water levels and exposed to alternate light and dark conditions.

The data show that when $\text{DF}=0.09 \text{ d}^{-1}$ (depletion of 9% of the water column C_T inventory per day) the fractionation factor, α , is "normal" and larger than unity, while at $\text{DF}=0.3 \text{ d}^{-1}$ the value of α becomes much lower than unity (the onset of BIE) and C_T of the brines becomes negative. For a given environment, the water column C_T inventory is inversely correlated with water depth, hence, the shallower the water the higher the potential DF. Therefore, the $\delta^{13}\text{C}$ value of carbonates (as proxies for the isotopic composition of the brine) in stromatolitic environment can be used as depth indicator.

Fluid geochemistry of an ancient analog to the modern seafloor polymetallic massive sulfides -- Yongping super-large copper deposit, Jiangxi province, China

CHENDONG GE^{1,2} AND PEI NI³

¹ Department of Geography, University of British Columbia, Vancouver, Canada (gcd@geog.ubc.ca)

² Department of Geo and Ocean Science, Nanjing University, Nanjing 210093, China

³ Department of Earth Science, Nanjing University, Nanjing 210093, China (peini@nju.edu.cn)

Yongping super large copper deposit, occurring in middle-Carboniferous marine sedimentary rocks, is located in Jiangxi, south China. It is composed of stratiform orebody and stringer vein type orebody. Fluid geochemistry data record a typical submarine hydrothermal origin for the ore formation.

Fluid geochemistry data

This study provides first time lots of fluid geochemistry data on fluid inclusion microthermometry, REE contents, and C, H, O isotope. REE pattern of the fluid preserved in fluid inclusions in the stringer vein type ores shows clearly that it was an analog to modern submarine hydrothermal fluids. Lots of microthermometric determination of fluid inclusions indicate the ore-forming fluid have the same salinity and temperature as modern submarine hydrothermal fluid, but have been experienced a boiling event. C, H, O isotope data suggest that the ore-forming fluid have originated from seawater and joined with little magmatic fluid at the main mineralization stage.

Conclusions and discussions

Geological and fluid geochemical features of Yongping copper deposit show that it was a typical MSD type deposit. The ore formation mechanism is similar to the modern polymetallic massive sulfides in spreading zones and on top of seamounts. However, the happening of fluid boiling observed in fluid inclusions indicate that the water depth during the forming of Yongping copper deposit is much more shallower than that of most modern seafloor polymetallic massive sulfides deposits. The relative shallower environment of Yongping Copper deposit is consistent with the ore occurring tectonic environment—Hercynian-Indosinian Fault Depression in south China.

Acknowledgment

This study was supported by the NSFC of China (project number: 49733120) and state key basic research project (number: G1999043211-5).

Reference

P.A. Rona and S.D. Scott (1993). *Econ. Geol.* 88: 1935-1976
 Khin Zaw, J.B. Gemmell, R.R. Large, T.P. Mernagh and C.G. Ryan (1996). *Ore Geol. Rev.* 10: 251-278

Cw and pulse EPR: a way to gather structural information

A.U. GEHRING¹, J. GRANWEHR², AND P.G. WEIDLER³

¹ PBB, ETH Zentrum, CH-8092 Zürich (gehring@sl.ethz.ch)

² LPC, ETH Hönggerberg, CH 8093 Zürich

(granwehr@esr.phys.chem.ethz.ch)

³ FZ Karlsruhe, D-76021 Karlsruhe

(peter.weidler@itc-wgt.fzk.de)

Introduction

Electron paramagnetic resonance (EPR) spectroscopy is a powerful method to analyze binding properties, symmetry, concentration, and structural vicinity of transition metal complexes. The following two examples give an insight into the potential of EPR application.

Continuous wave (cw) EPR technique

The spectrum of V(IV) in muscovite exhibited an eight-line hyperfine-split (hfs) signal with $g = 1.939$ and $A = 18.6$ mT. Dehydroxylation of the muscovite upon heating at 650°C revealed a narrowing of the spectrum ($A = 17.5$ mT). This change can be explained by a transformation from octahedral into tetragonal-pyramidal co-ordination of V(IV).

Pulsed EPR technique

Electron spin echo envelope modulation (ESEEM) can give information on the nuclear spin environment of paramagnetic centers. V(IV) in vermiculite revealed a well resolved hfs signal (Fig. 1). The ESEEM with 20 and 40 ns pulses obtained from the central V(IV) feature near $g = 2$ position showed little modulation.

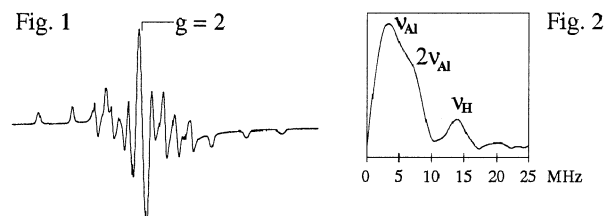


Fig. 1: cw EPR spectrum of V(IV) in vermiculite

Fig. 2: Fourier transformed ESEEM magnitude spectrum

The magnitude spectrum after Fourier transformation consisted of a broad peak at 3.4 ± 0.5 MHz with a shoulder at about 6.5 MHz, and a weaker peak at 13.9 ± 0.5 MHz (Fig. 2). The peaks indicated two different nuclear Zeeman frequencies (ν). The weak line leading to a nuclear g factor ($|g_N|$) of 5.46 ± 0.2 was characteristic of protons ($g_N = 5.5854$, natural abundance 99.985%). The maximum of the intense line corresponded to a $|g_N|$ value of 1.35 ± 0.2 which was close to those for weakly coupled nuclei of diamagnetic ^{27}Al ($I = 5/2$, 100% natural abundance, $g_N = 1.4554$). These EPR data suggest that V(IV) replaces Al(III) in the octahedral sites of vermiculite.

Further studies will show if cw and pulse EPR are an analytical tool with broad application in geochemistry.

The adsorption of Th and Pa on different particle types in dependence of the provenance of natural seawater

W. GEIBERT¹ AND R. USBECK¹

¹Alfred Wegener Institute for Polar and Marine Research, Bremerhaven, Germany (wgeibert@awi-bremerhaven.de)

We performed experiments in order to investigate the adsorption of Th and Pa on different particles in recently sampled seawater. Water from three different locations was 0.2 µm filtered. Then, four different particle types were added to the respective seawater samples at a concentration of 0.5 mg/l, and neutralized Th and Pa spikes were added. Additionally, one sample was run without particles added. Th and Pa distribution was monitored in increasing time intervals for several days.

Spike recoveries ranged from 40 to 100 % for Th and from 50 to 100 % for Pa (depending on particle type). Our recoveries are higher than previously observed in experiments with artificial seawater. The low losses to the container walls allowed the determination of distribution coefficients (K_d) for different particle types. Th on MnO_2 was found to have a K_d of $>3 \cdot 10^7$ in all water types, Pa on the same particle type $>2 \cdot 10^7$. On smectite, K_d Th was found to range between 4 and $10 \cdot 10^6$ towards the end of the experiments. K_d Pa in the same samples was 1.2 to $1.8 \cdot 10^6$. On biogenic opal particles, K_d Th was about $1 \cdot 10^6$ in two of three samples. In the water sample from the Subtropical Gyre (Argentine Basin), its K_d was found to be twice as high ($2 \cdot 10^6$) at the start of the experiment, and up to $8 \cdot 10^6$ at the end. For Pa on opal, K_d s of $0.5 \cdot 10^6$ resulted in general, with two somewhat higher exceptions ($1 \cdot 10^6$) towards the end of the experiments. The experiment with $CaCO_3$ (non-biogenic) resulted in very variable K_d s depending on the water type used for both Th and Pa.

One of the most interesting results was the large percentage of Th and Pa found in the particulate fraction when no particles were added. This must be attributed to the spontaneous formation of particles from the colloidal phase <0.2 µm, like described by Chin et al. (1998). Consequently, the temporal pattern of Th and Pa adsorption in our experiments is considered to reflect the process of colloid aggregation. A very similar pattern of aggregation in all three samples without particles added was observed, although on a different level. A strong relationship between the adsorption pattern on smectite and the aggregation pattern without particles points to a potential role of clay minerals for the uptake of dissolved organic matter (DOM) in aquatic systems, like it has been extensively described for soils.

References

Chin W.-C., Orellana M.V. and Verduco P. (1998) Spontaneous assembly of marine dissolved organic matter into polymer gels. *Nature* **391**, 568-572.

Combining control volume finite element methods with realistic fluid properties for high-resolution simulations of multiphase flow in magmatic-hydrothermal systems

SEBASTIAN GEIGER¹, THOMAS DRIESNER¹, STEPHAN K. MATTHÄI², CHRISTOPH A. HEINRICH¹

¹ETH Zürich, Isotope Geochemistry and Mineral Resources, (geiger@erdw.ethz.ch, thomas.driesner@erdw.ethz.ch, heinrich@erdw.ethz.ch)

²Dept. of Earth Science and Engineering, Imperial College, London (s.matthai@ic.ac.uk)

Realistic modelling of multi-phase fluid flow in magmatic-hydrothermal systems is very challenging because hydrological properties of fluids and rocks vary over many orders of magnitude. The governing equations for the hydrodynamics and thermodynamics in magmatic hydrothermal systems are highly non-linear and strongly coupled. Essential requirements of a numerical formulation for such a system are: (1) a treatment of the hydrodynamics that can accurately resolve complex geological structures and represent the highly variable fluid velocities herein, (2) a realistic thermodynamic representation of the fluid properties including the wide P-T-X range of liquid+vapour coexistence for the highly saline fluids, and (3) an accurate handling of the highly contrasting transport properties of the two fluids.

Recently, control volume finite element methods (CVFEM) have been successfully applied to model multiphase flow and energy transport (e.g., Forsyth 1994). CVFEM combine the best features of finite volume and finite element methods. CVFEM are mass and shock preserving, yield great geometric flexibility in 2D and 3D. Furthermore, efficient matrix solvers can be employed to model fluid flow in geologically realistic structures (e.g., Matthäi & Roberts, 1996).

We chose the system water-NaCl as a realistic proxy for natural fluids occurring in magmatic-hydrothermal systems. An in-depth evaluation of the available experimental and theoretical data led to a consistent and accurate set of formulations for the PVTXH relations that are valid from 0 to 800°C, 0 to 500 MPa, and 0 to 1 X_{NaCl} . The accuracy of the representation is probably sufficient to derive thermochemical properties of the NaCl and H₂O components for future incorporation of reactive transport schemes. Dynamic viscosities are currently approximated by the approach of Palliser & McKibbin (1998).

References

Forsyth PA (1994), *Int. J. Num. Meth. Fluids* **19**, 1055-1081
 Palliser C and McKibbin R (1998), *Transport in Porous Media* **33**, 155-171
 Matthäi SK & Roberts SG (1996), *AAPG Bulletin* **80**, 1763-1779

Effects of giant impacts on the atmosphere formation

HIDENORI GENDA AND YUTAKA ABE

Department of the Earth and Planetary Science, University of Tokyo, 7-3-1 Hongo, Bunkyo, Tokyo 113-0033, JAPAN.
genda@sys.eps.s.u-tokyo.ac.jp

The recent works on the planetary formation show that several tens of Mars-sized proto-planets are formed in the terrestrial planet region at the final stage of the planetary accretion (e.g., Kokubo & Ida, 1998). Then, collisions of Mars-sized proto-planets occur due to gravitational perturbations among the proto-planets (e.g., Chambers & Wetherill, 1998).

Mars-sized proto-planets would have a mixed proto-atmosphere composed of solar and degassed components (Abe et al., 2002). The giant impacts modify the atmosphere. For example, a large amount of atmosphere may be blown-off by the giant impacts. It has an influence on the origin and evolution of planetary volatile budget, and especially on the quantity and isotopic fractionation of noble gases. Ahrens (1990, 1993) and Chan & Ahrens (1997) concluded that almost all atmosphere is lost by the strong antipodal ground motion (~6km/s) expected for a giant impact. On the other hand, isotopic composition of the present Earth's noble gas suggests the survival of the substantial atmosphere after the giant impact (e.g., Pepin, 1997).

We have re-examined the relations between the ground motion and the amount of the lost atmosphere by calculating the spherically one-dimensional atmospheric motion for six cases of the initial atmospheric conditions. We find that the loss fraction of the atmosphere is determined by only the surface velocity irrespective of the initial atmospheric conditions. For example, when the surface velocity is 0.55 times of the escape velocity, which corresponds to 6 km/s on the Earth's condition, 30% of the atmosphere escapes. The globally averaged surface velocity is less than 6 km/s, because the planetary core focuses the shock wave energy to the antipode (Watts et al., 1991). Therefore, most atmosphere survives the giant impact. We can also apply our results to the atmosphere of the impactor planet. About 50% of the impactor's atmosphere survive the giant impact, and is brought to the target planet.

References

- Abe, Y., Genda, H. and Nishikawa, K. (2002) *this volume*.
Ahrens, T. J. (1990) In *Origin of the Earth*, Oxford Univ. Press, 211-227. Ahrens, T. J. (1993) *Annu. Rev. Earth Planet. Sci.* **21**, 525-555. Chambers, J. E., and Wetherill, G. W. (1998) *Icarus* **136**, 304-327. Chen, G. Q., and Ahrens, T. J. (1997) *Phys. Earth Planet. Interiors* **100**, 21-26. Kokubo, E., and Ida, S. (1998) *Icarus* **131**, 171-178. Pepin, R.O. (1997) *Icarus* **126**, 148-156. Watts, A. W., Greeley, R. and Melosh, H. J. (1991) *Icarus* **93**, 159-168.

The time scales of magmatic differentiation at island arcs

R. GEORGE¹, S. TURNER¹, C. HAWKESWORTH¹, C. NYE², P. STELLING² AND S. DREHER³

¹ Department of Earth Sciences, University of Bristol, Wills Memorial Building, Bristol BS8 1RJ, UK
(R.M.George@bris.ac.uk; Simon.Turner@bris.ac.uk; C.J.Hawkesworth@bris.ac.uk)

² Geophysical Institute, 903 Koyukuk Drive, University of Alaska Fairbanks, PO Box 757320, Fairbanks, Alaska, USA (cnye@giseis.alaska.edu; ftpls@uaf.edu)

³ Indiana State University, Department of Geography, Geology and Anthropology, Terre Haute, IN 47809, USA (gedreher@scifac.indstate.edu)

There is growing interest in how the time scales of magmatic differentiation might vary with magma composition and differentiation path. Available data imply differentiation times of 100's to 1000's of years for tholeiitic magmas and 1000's to perhaps 10,000's of years for calc-alkaline magmas. Numerical models can be used to predict both the rate of cooling and crystallisation in crustal magma chambers but if differentiation occurs by crystal settling, the time scale will also be controlled by the size of the crystals, their density contrast with the magma and the viscosity. Thus, the behaviour of natural systems will be complex; phenocrysts may find it hard to settle in a tholeiitic magma because the liquid line of descent yields dense, iron-rich differentiates, whilst the higher silica content and greater viscosity of calc-alkaline liquids at a similar degree of differentiation will also inhibit phenocryst-liquid separation.

The Aleutian-Alaska arc is well known for erupting both tholeiitic and calc-alkaline lavas. In order to investigate the relative roles of chemical and temporal controls on generating these contrasting liquid lines of descent we have studied tholeiitic lavas from Akutan in the Aleutian arc and Aniakchak on the Alaskan Peninsula. Akutan lavas exhibit little variation in SiO₂ or ⁸⁷Sr/⁸⁶Sr and are characterised by ²³⁸U-excesses, consistent with fluid addition to their mantle source, whereas those at Aniakchak show a range in SiO₂ and ⁸⁷Sr/⁸⁶Sr and straddle the U-Th isotope equiline suggesting that partial melting affected the U-Th isotopes after fluid addition. The lavas preserve a range in ²²⁶Ra/²³⁰Th disequilibria which suggest that the time scale of crustal residence of magmas beneath both Akutan and Aniakchak appear to be around 0-5000 years. Our interpretation is that the tholeiitic Akutan magmas underwent minimal, closed-system, compositional evolution. In contrast, calc-alkaline magmas beneath Aniakchak volcano underwent significant compositional evolution suggesting that differentiation was more time-efficient in the calc-alkaline system. The simplest explanation is that the greater density of the tholeiitic differentiates retarded crystal-liquid separation more effectively than any differences in viscosity between the two magma systems.

Chemical consequences of an impact of a comet: experimental simulation

M. V. GERASIMOV¹, YU. P. DIKOV², O. I. YAKOVLEV³, AND F. WLOTZKA⁴

¹ Space Research Inst., RAS, Moscow, Russia;
mgerasim@mx.iki.rssi.ru

² IGEM, RAS, Moscow, Russia; dikov@igem.ru

³ Vernadsky Inst. of Geochemistry, Moscow, Russia;
yakovlev@geokhi.ru

⁴ Max-Planck-Inst. for Chemistry, Mainz, Germany;
wlotzka@mpch-mainz.mpg.de

An impact of a comet into a planet is a rare but not unrealistic event. Such an impact differs from an impact of a meteorite by involvement of large quantities of volatiles. The appearance of some volatile-rich features among lunar findings was considered by some explorers as a remnant of an impact of a comet (e.g., [1]). On the other hand, a number of investigators attribute such volatile-rich lunar findings to fumarolic eruptions (e.g., [2,3]). There are some works considering mechanical issues of an impact of a comet into siliceous targets, but investigations of chemical consequences of such an impact are still lacking. There is no true experimental base which permits to identify remnants of an impact of a comet and distinguish between volatile-rich findings of cometary or another nature.

The aim of the present study was to simulate the chemistry of a spreading vapor cloud with a composition related to an impact of a comet into lunar basalts and to investigate chemical products of such an event.

Analysis of the condensed material shows that volatiles form separate phases and are concentrated mainly in the surface layer amounting there up to ~50 % by weight. Carbon was the most abundant among volatiles and was recondensed mainly as organic constituent, while carbonate bonding was also detected. Sulfur was also abundant (up to 7 wt.%) and was mainly bound in sulfides, but some S⁰ and SO₂ was present in the surface layer. It was interesting to find phosphorus in phosphate and phosphide type of bonding. The same partitioning of P into phosphates and phosphides was observed in lunar "rusty" rocks [4].

The experiment shows that an impact of a comet can result in a sufficient interaction of volatiles with silicates. The production of a wide range of various types of volatile-rich components with non-equilibrium redox states must result in a complex post-impact chemistry affecting the planetary environment. The correlation of some lunar findings with experimental results supports their possible impact origin.

Acknowledgement. This research was supported by the RFBR 02-05-64419 grant.

References: [1] El Goresy A., et al. (1973) *EPSL*, **18**, 411-419. [2] Wasson J.T., et al. (1976) *Proc. Lunar Sci. Conf. 7th*, 1583-1595. [3] Butler P., Jr. and Meyer C., Jr. (1976) *Proc. Lunar Sci. Conf. 7th*, 1561-1581. [4] Hunter R.H. and Taylor L.A. (1981) *Proc. Lunar Sci. Conf. 12th*, 253-259.

Tungsten-tin deposits in southwest of Shazand, Iran

M. GHADERI AND M.R. GHORBANI

Department of Geology, Tarbiat Modares University, Tehran
14115-175, Iran (mghaderi@modares.ac.ir)

Apart from Nezam-Abad tungsten deposit, Bamsar and Revesht are among the already discovered tungsten-tin occurrences in SW of Shazand, west Central Iran. Rare Earth Element (REE) and other trace elements in samples of scheelite (CaWO₄) from these deposits have been determined by Neutron Activation Analysis in order to constrain the composition and sources of the mineralizing fluids. The granitic and granodioritic intrusives have caused metamorphic haloes in the upper Triassic-Jurassic detrital-chemical and volcanic units. Six ore-bearing skarn horizons have been identified at Bamsar, while granodioritic intrusives host vein-type mineralization at Revesht and Nezam-Abad. Country rocks at Bamsar are mainly calcareous schists in which ore minerals occur in laminas and layers, whereas granodioritic intrusives host vein-type mineralization at Revesht and Nezam-Abad.

Revesht and Nezam-Abad scheelites have higher total REE and Na concentrations than Bamsar samples. Bamsar scheelites show flat chondrite-normalized REE (REE_N) patterns, whereas scheelites from Revesht and Nezam-Abad exhibit hump-shaped REE_N patterns with maximum REE_N concentrations displaced towards Dy. It is suggested that Bamsar scheelites have variable Eu anomalies and trivalent REE concentrations and thus appear to contain mostly Eu²⁺ and to have formed under reduced conditions (Ghaderi et al., 1999). Revesht and Nezam-Abad scheelites, on the other hand, exhibit no changes in the size of the Eu anomaly with REE concentration, implying a predominance of Eu³⁺ and crystallization under relatively oxidized conditions. Bamsar scheelites have (Ce/Lu)_N > 1 and are interpreted to have crystallized from LREE-enriched fluids, whereas Revesht and Nezam-Abad scheelites with (Ce/Lu)_N < 1 formed from LREE-depleted fluids. The elevated Na contents of Revesht and Nezam-Abad scheelites compared with Bamsar samples, suggest crystallization from hydrothermal fluids with higher Na activities.

It is suggested that Bamsar occurrence is sedimentary-diagenetic in origin, subsequent concentration happening through Late Kimmerian regional metamorphism and deformation. Considering spatial position and proximity of Bamsar ore-bearing horizons with granodioritic intrusions hosting vein-type mineralization at Revesht and Nezam-Abad, it is likely that the mineralized veins in those areas formed through assimilation of stratiform and stratabound ores by a granitoid magma.

Reference

Ghaderi M., Palin J.M., Campbell I.H. and Sylvester P.J., (1999). *Econ. Geol.* **94**, 423-437.

A lamprophyric dyke from Milakuh, SW Damghan, Iran

M.R. GHORBANI, G. ROSTAMI AND M. GHADERI

Department of Geology, Tarbiat Modares University, Tehran
14115-175, Iran (ghorbani@modares.ac.ir)

A lamprophyric rock is reported here, for the first time, from Milakuh in northern Iran. The area is a part of Alborz Structural Zone which itself is part of Alpine-Himalayan orogenic belt. Rostami (2001) in his study on the Milakuh mineral deposits, described this rock as a subvolcanic rock with intermediate to basic composition which cuts through Lower Cambrian Barut and Soltanieh Formations. Field and textural characteristics, mineralogy and geochemical composition of the rock (Table 1), all indicate its lamprophyric signature. The followings are some of these features: a) the rock appears as a dyke; b) it shows panidiomorphic texture with euhedral amphibole crystals; c) its mineral constituents and their modal proportions are: plagioclase 45%, amphibole 38%, Fe-Ti oxides 7%, calcite 6%, apatite 2%, biotite 1%; d) the rock consists of a large amount of volatile components (i.e., in fresh sample, L.O.I. is 7.25 wt%); e) it has high concentrations of LILE (e.g., Ba and Sr) and medium contents of Cr, Ni, V, Zn and Pb.

SiO ₂	TiO ₂	Al ₂ O ₃	Fe ₂ O	MnO	MgO	CaO
54.5	1.4	12.5	6.3	0.15	5.4	7.5
Na ₂ O	K ₂ O	P ₂ O ₅	L.O.I.	Total		
1.9	1.7	0.38	7.25	98.98		
Ba	Sr	Ni	Cr	V	Zn	Pb
440	700	78	80	64	84	36

Table 1: Major elements in wt%, trace elements in ppm.

Some igneous rocks from adjacent areas also appear to have lamprophyric affinities. For instance, Alavi-Naini (1972) reported an intrusive intermediate rock consisting mainly of plagioclase and biotite from Kuh-e-Vatan, some 10 km towards south of Milakuh. Lamprophyric magmatism might also have had a long history in the geological evolution of the area. Rostami (2001) found a brecciated tuff unit in horizon III of Soltanieh Formation which contains disseminated particles of fluorite. He ascribed the F-supply that crystallized as fluorite to the concurrent volcanism taking place in lower Cambrian. High F content is yet another feature of lamprophyres. Lamprophyric nature of magmatism in this part of Iran has probably been an important phenomenon in lower Cambrian (i.e., the tuff unit) which continued well in post Cambrian times (i.e., Milakuh lamprophyric dyke). This has important implications on the early stages of mantle-lower crust evolution in northern Iran.

References

- Alavi-Naini, M., (1972). Geological Survey of Iran, Report no. 23, 288p.
Rostami, G., (2001). MSc thesis, Tarbiat Modares University, Tehran, Iran, in Persian, 245p.

Effect of Fluid-Sediment Reaction on Seafloor Hydrothermal Fluxes of Solutes

E. R. GIAMBALVO¹, C. I. STEEFEL², A. T. FISHER³, N. D. ROSENBERG², AND C. G. WHEAT⁴

¹ Sandia National Laboratories, Carlsbad, NM 88220, USA
(ergiamb@sandia.gov)

² Lawrence Livermore National Laboratory, Livermore, CA 94551, USA (steefel@llnl.gov; rosenberg4@llnl.gov)

³ University of California, Santa Cruz, CA 95064, USA
(afisher@es.ucsc.edu)

⁴ University of Alaska, Fairbanks, AK 99775, USA
(wheat@mbari.org)

At a site on the eastern flank of the Juan de Fuca Ridge, basement fluid upwells through sediment before exiting to the seafloor. We used the reactive-transport code GIMRT to model the processes occurring in the sediment column (diagenesis, sediment burial, fluid advection, and multicomponent diffusion) and to estimate net seafloor fluxes of solutes. Reactive transport modeling allowed us to use pore water data to assess how reaction between upwelling basement fluid and sediment affects hydrothermal fluxes of Ca, SiO_{2(aq)}, SO₄, PO₄, NH₄, and alkalinity. GIMRT provides mechanistic descriptions of biogeochemical processes and therefore also allowed us to assess the extent to which fluid flow rate and sediment thickness control hydrothermal fluxes of solutes in this setting.

At this site the basement hydrothermal system is a source of NH₄, SiO_{2(aq)}, and Ca, and a sink of SO₄, PO₄, and alkalinity. Reaction within the sediment column increases the hydrothermal sources of NH₄ and SiO_{2(aq)}, increases the hydrothermal sinks of SO₄ and PO₄, and decreases the hydrothermal source of Ca. The effect on the hydrothermal flux of alkalinity is spatially variable.

Two series of simulations in which we varied fluid flow rate (1-100 mm/yr) and sediment thickness (10-100 m) predict that the sediment section will contribute the most to fluxes of SO₄ and NH₄ at slow flow rates and intermediate sediment thickness and to fluxes of SiO_{2(aq)} at slow flow rates and large sediment thickness. Reaction within the sediment section over a range of flow rates and sediment thickness could double the hydrothermal sink of PO₄ and could decrease (by ≤10%) the hydrothermal source of Ca.

Impact of tire-derived fuel on the chemical composition of coal-combustion products

R. GIERÉ¹, L.E. CARLETON¹, S.T. LAFREE¹,
A. ZINGG¹, AND J.K. TISHMACK²

¹ Earth & Atmospheric Sciences, Purdue University, West Lafayette, IN 47907-1397, USA (giere@purdue.edu)

² Building Services & Grounds, Purdue University, West Lafayette, IN 47907-1661 (jktishmack@purdue.edu)

Coal-fired power plants generate about 27% of the electricity consumed worldwide, and also produce large amounts of waste (ash) in addition to gaseous emissions. Several utility companies in the U.S. burn coal together with discarded automobile tires, and thus turn a major waste stream into an alternate fuel. Although this practice could lead to significant savings in coal consumption, the combustion of scrap tires may increase the concentration of some chemical elements in the coal-combustion products (CCP). To assess the chemical impact on the CCP and on the atmospheric emissions, the Purdue University power plant conducted an experiment with two different sets of fuel combusted at the same conditions (≈ 1500 °C): pure coal and a mixture of 95 wt% coal plus 5 wt% tire-derived fuel (TDF). A detailed chemical comparison was made of both types of fuel and the resulting CCP.

Compared to pure coal (sub-bituminous coal from Southern Indiana), TDF is considerably richer in Zn (133 ± 34 vs. 32 ± 43 ppm), and also has a higher S content (1.76 ± 0.91 vs. 0.57 ± 0.55 wt%). The increase in Zn is due to the high Zn content of the scrap tire chips (10936 ± 849 ppm). Most of the other 56 elements studied had similar concentrations in both fuel types. Coal contains approximately 10 wt% non-combustible mineral matter, and the combustion process leads to enrichment of many chemical components in the CCP. The levels of enrichment are different for different elements, (typically ranging between factors of 10 and >100), and also depend on the temperature at which the various ash types were collected. The bulk Zn concentrations in CCP derived from TDF, for example, are 238, 3850, and 61500 ppm in bottom ash, mechanical separator ash, and electrostatic precipitator ash, respectively. For ash derived from pure coal, these values are 68, 106, and 3450 ppm, respectively. The enrichment, however, depends also on the size of the ash particles, whereby elemental concentrations increase with decreasing size. The smallest size fraction studied (<38 μm) accounts for >25 wt% of the bulk fly ash and exhibits the highest concentrations of many trace elements (e.g., As, Cd, Cu, Pb, Sb, U, Zn). In this size fraction, the concentrations of these and several other elements are markedly higher than those in the bulk ash.

The experiment demonstrates that combustion of TDF may lead to a considerable increase in the Zn contents of CCP, particularly of the finest fly ash fraction, some of which is emitted as particulates into the atmosphere.

Progress in understanding magma chambers based on high-resolution phenocryst microprobe analysis

C. GINIBRE^{1,2} AND G. WÖRNER¹

- Abt. Geochemie, GZG, 37077 Göttingen, Goldschmidtstr. 1, Germany (gwoerne@gwdg.de)

² now at : Laboratoire de Planétologie et Géodynamique, 2, rue de la Houssinière, 44322 Nantes cedex 3 - France (catherine.ginibre@chimie.univ-nantes.fr)

Processes in magma chambers are recorded in igneous phenocrysts through major and trace element zoning. For two case studies, we combine high-resolution imaging methods (back scattered electrons) with quantitative microprobe analysis of major, minor and trace elements (Ba, Sr, Fe, Ti, Mg) in volcanic feldspars to constrain magma chamber evolution at high spatial and temporal resolution.

Tephra from the chemically zoned phonolitic Laacher See magma chamber (Germany) contains three different types of sanidine that record various growth environments: convecting main magma body, highly differentiated boundary layer (roof and walls), and movement from an early less differentiated crystallising boundary layer into the main magma body. The majority of these "phenocrysts" were not erupted in the magma in which they originally formed. Their complex inheritance rather indicates crystal dispersion and exchange between layers of the zoned magma. Trace element zoning in sanidine shows the increasing influence of a mafic magma in the convecting main magma body. In the presence of plagioclase, the ternary compositions of sanidine constrain a large temperature range from 700 °C at the wall of roof to 1000 °C at the base of the magma chamber. This suggests a possible recharge and progressive mingling with a basanitic magma as heat source and driving force for convection.

The andesitic Parinacota volcano (Chile) "Old Cone" stage" is dominated by a long differentiation history with rare recharge events. This is seen in the Sr and Fe zoning patterns of large plagioclase phenocrysts, which are characterised by oscillatory major element zoning patterns and frequent dissolution surfaces, uncorrelated between crystals. This indicates a convecting environment in the main magma body. Smaller crystals with lower trace element content at variable An content record a larger influence of a wet differentiated crystallising boundary layer. A time scale and crystal residence time of less than a few thousand year for differentiation is given by the absence of Sr-diffusion in the core.

"Young Cone" Parinacota was built after a flank collapse in less than 18 ky. Its andesitic plagioclase phenocrysts show multiple resorption. Trace element zoning indicate at least two correlated recharge events within many crystals, involving two different endmembers magmas. These are present in all eruptive stages of Parinacota volcano but recharge is at much higher frequency in the "Young Cone". Parinacota volcano is thus characterized by an increased frequency of recharge events after the catastrophic flank collapse.

Negative $\delta^{18}\text{O}$ signatures in morphologically complex zircons: evidence for Proterozoic cold-climate water/rock interaction in the Qinglongshan UHP meta-granite (Sulu terrain, China)

D. GIORGIS¹, D. RUMBLE² AND M. COSCA¹

¹ University of Lausanne, Institute of Mineralogy and Geochemistry, 1015 Lausanne, Switzerland
(david.giorgis@img.unil.ch) (mcosca@img.unil.ch)

² Geophysical Laboratory, 5251 Broad Branch Rd. N. W., Washington, D. C. 20015-1305, USA
(rumble@gl.ciw.edu)

Oxygen stable isotope analyses of bulk zircon grains and cores (isolated by air-abrasion) from ultra-high pressure (UHP) meta-granite from the Qinglongshan region of China, yield negative $\delta^{18}\text{O}$ values ranging from -0.2 to -7.3 ‰. Sample characterization using back-scattered electron and cathodoluminescence reveals a complex multistage zircon growth history. Pre-metamorphic cores contain inclusions of biotite, quartz (no coesite), K-feldspar, magnetite and apatite whereas the UHP rim overgrowths are inclusion-free. Pre-metamorphic allanite-(Ce) is chemically heterogeneous with complex internal structures and, together with the unusual zircon core morphology and inclusion-rich cores, suggests crystallization within a fluid-rich environment. The mineral inclusions in the zircon cores account for small $\delta^{18}\text{O}$ differences (0.2 to 1.0‰) between abraded and non-abraded zircons, indicating that cores and rims have nearly the same negative $\delta^{18}\text{O}$ signature. The pre-UHP metamorphic zircon cores probably acquired their negative $\delta^{18}\text{O}$ values during sub-solidus crystallization in a peculiar hydrothermal context, where rocks (or magma) interacted with cold-climate meteoric water during late Proterozoic times.

References

- Giorgis, D., Rumble, D. and Cosca, M. (2002), *Swiss Bull. Min. Pet.* (submitted).
Rumble, D., Giorgis, D., Ireland, T., Zhang, Z., Xu, H., Yui, T.F., Yang, J., Xu, Z., and Liou, J.G. (2002), *Geochim. Cosmochim. Acta* (in press).

Isotopic study of CO_2 and CH_4 out-gassed from argillites investigated for radioactive waste repository

J.-P. GIRARD¹, C. FLÉHOC¹, E. GAUCHER¹,
A. PRINZHOFER² AND J. CHAPPELLAZ³

¹ BRGM, BP 6009, 45060 Orléans, France

² IFP, BP311, 92056 Rueil-Malmaison, France

³ LGGE, BP96, 38402 Saint Martin d'Heres, France

Context and objective

The Callovo-Oxfordian (C-O) argillites, presently lying at ca. 500 m depth, in the eastern part of the Paris basin are being considered as a potential repository site for radioactive waste. As a result, this formation is the object of numerous detailed studies. One objective of on-going work is to reconstruct the chemical and isotopic signature of the argillites pore water, in order to constrain the nature and intensity of water-rock interactions that might have occurred in the past. With this purpose in mind, a methodology was designed to recover CO_2 (dissolved in pore water) and CH_4 (adsorbed on clays) gas naturally liberated from C-O core samples under vacuum in a confined inert atmosphere (N_2 or He). Stable isotope compositions of these gases were then determined by IRMS and GC-IRMS conventional techniques and provided valuable information about their origin.

Results and interpretation

CO_2 gas recovered from four cores of C-O argillites yielded reproducible and consistent isotopic compositions, averaging -6.3 ± 1.7 ‰ PDB for $\delta^{13}\text{C}$ and $+35.4 \pm 0.3$ ‰ SMOW for $\delta^{18}\text{O}$. This isotopic signature is not compatible with CO_2 sources such as atmosphere, mantle, degradation of organic matter or bacterial processes. It is best explained as reflecting isotopic equilibrium with dissolved bicarbonate (for C) and with pore water (for O). It further indicates that dissolved carbonate is of inorganic marine source and that pore water is of meteoric origin.

CH_4 gas recovered from seven C-O cores yielded $\delta^{13}\text{C}$ values ranging mostly between -53 and -43 ‰ PDB (except for one sample yielded ca. -61 ‰). These values, along with the presence of significant amounts of higher alkanes (C_2 to C_4) associated to CH_4 , suggest that adsorbed methane in the studied argillites has a thermogenic origin. Because maximum burial temperature in the C-O argillites did not exceed ca. 50°C , the thermogenic nature of methane further implies that it originated from an external source and migrated into the argillites subsequently. This agrees with the existence of accumulations of natural gas in the vicinity (about 30 km) of the sampled site.

Conclusion

The results of this study suggest that C-O argillites interacted with meteoric waters and with externally-derived gaseous hydrocarbons, and were not the locus of significant post-depositional bacterial activity. Another implication is that pCO_2 was primarily controlled by mineral equilibria.

A quantitative field based study of basalt/basaltic glass weathering and its role in carbon fixation

S. R. GISLASON¹, M. I. KARDJILOV², G. GISLADOTTIR²,
E. S. EIRIKSDOTTIR,¹ B. SIGFUSSON¹, S. ELEFSEN³
A. SNORRASON³ D. WOLFF-BOENISCH¹, E. OELKERS⁴
AND P. TORSANDER⁵

¹Science Institute, University of Iceland, Reykjavik, Iceland
(sigrg@raunvis.hi.is, ese@raunvis.hi.is, bergusi@hi.is,
boenisch@hi.is)

²Department of Geology and Geography, University of
Iceland, Reykjavik, Iceland; (marin@hi.is, ggisla@hi.is)

³National Energy Authority, Grensasvegi 9, 108 Reykjavik,
Iceland (asn@os.is, soe@os.is)

⁴Géochimie: Transferts et Mécanismes, CNRS/URM 5563--
Université Paul Sabatier, 38 rue des Trente-six Ponts,
31400 Toulouse, France, (oelkers@lmtg.ups-tlse.fr)

⁵Department of Geology and Geochemistry, Stockholm
University, S-106 91 Stockholm, Sweden

The goal of this study is the quantification of basalt/basaltic glass weathering rates and its effects on CO₂ cycling and climate. The motivation for studying basalt/basaltic glass is that due to its rapid weathering rate and widespread presence on the ocean floor and in volcanic terrains it plays a significant role in the global cycling of a large number of elements and CO₂ fixation. Moreover the role of rock weathering is especially enhanced at the end of glacial epochs, when large quantities of ground rock formed beneath glaciers become exposed to the surface environment. This study focuses on chemical and mass transport in several rivers in NE- Iceland. These rivers were chosen because they 1) drain almost exclusively basalt/basaltic glass catchments, 2) experience limited but variable biological activity, 3) drain catchments of variable glacier cover and 4) are unpolluted. The total water fluxes, total organic and inorganic dissolved and suspended load mass, and the flux of elements due to sorption onto suspended load were monitored continuously over a three year period. GIS modelling was used to assess the relative importance of climate, runoff, rock age, relief, glacier and vegetative cover on these fluxes. Overall, chemical denudation rates are dominated by runoff, rock age, aqueous F concentration and sometimes weathering of sulphides. The mechanical denudation of rocks ranges from 10 to 5000 t/km²/y; it is dominated by the glaciers, and is 20 to 10,000 times higher than that of organic matter. To assess the relative carbon fixation efficiency of the various processes, the annual carbon fixation of terrestrial vegetation was estimated using above ground yield measurements of the various plant communities and below ground vegetation ratios. Carbon fixation by chemical weathering is found to be greater than the organic carbon mechanical denudation rate, which itself is significantly greater than carbon fixation by terrestrial vegetation.

Atmospheric Mercury Deposition Rates in Ombrogenic Bogs from Southern Ontario

N. GIVELET¹ AND W. SHOTYK²

¹Institute of Geological Sciences, University of Berne,
Switzerland. (givelet@geo.unibe.ch)

²Institute of Environmental Geochemistry, University of
Heidelberg, Germany. (shotyk@ugc.uni-heidelberg.de)

To quantify the effects of human activity on atmospheric deposition of mercury in the east Canadian environment, an improved understanding of the natural concentrations, fluxes and sources of Hg is required.

Methods

Peat cores representing up to 8,000 years of organic peat accumulation were collected from three different ombrogenic peat deposits in Southern Ontario. Mercury was analysed by AAS using the protocol developed by Roos-Barraclough et al. 2002. Peat profiles were dated using ²¹⁰Pb, ¹³⁷Cs and ¹⁴C.

Fig. 1. Mercury concentration and ash content from Luther bog. Mean background Hg concentration in ombrogenic peat.

Discussion

Analysis of the Luher peat core show low and quite stable Hg concentrations, 14-32 ng g⁻¹, for most of the profile. The estimated average natural background deposition rate for Hg is about 0.7 µg Hg m⁻² yr⁻¹ (range of 0.5-1.5 µg Hg m⁻² yr⁻¹). For the upper layers (last 50 years), the accumulation rate is in a range of 4-32 µg Hg m⁻² yr⁻¹.

Conclusion

This study suggests that the atmospheric deposition rate in the upper layers of the 3 ombrogenic peat cores are 8-10 times greater than the pre-anthropogenic rate.

Reference

Roos-Barraclough et al. (2002) *Sci. Tot. Envir.* (In press)

Controls on Fe reduction and mineral formation by a subsurface bacterium

S. GLASAUER¹, P. G. WEIDLER², S. LANGLEY¹
AND T. J. BEVERIDGE¹

¹Department of Microbiology, College of Biological Sciences,
University of Guelph, Guelph, Ontario N1G 2W1, Canada

²Forschungszentrum Karlsruhe GmbH, Institute for Technical
Chemistry, D-76021 Karlsruhe, Germany

Experimental approach

Cells of *Shewanella putrefaciens* CN32, a dissimilatory Fe-reducing bacterium, were grown in defined medium under strict anaerobic conditions (Glasauer et al., 2002) in culture flasks to which nano-crystalline goethite, micro-crystalline goethite, hematite or hydrous ferric oxide (HFO) were added as electron acceptors. Cell growth, Fe metabolism, and mineral formation and partitioning were tracked over time using standard techniques (Glasauer et al., 2002).

Results

Under nutrient-limited conditions cells were unable to reduce the crystalline minerals. Reduction of HFO began within 7 d and a variety of minerals was produced. Green rust I was most frequently observed near vivianite and HFO aggregates. Vivianite appeared to form within HFO aggregates, unassociated with cells; the rate of Fe reduction influenced crystallite mean coherence lengths. Nano-crystalline magnetite and goethite (<10 nm) formed within aggregates of HFO sorbed to cells. When the $[\text{PO}_4^{3-}]$ concentration was reduced, Fe reduction was lower and nano-crystalline goethite was the only mineral detected.

Discussion and Conclusions

The inability of CN32 to reduce the crystalline Fe(III) minerals indicates that energetics of the mineral surface rather than surface area determine reducibility. In addition, $[\text{PO}_4^{3-}]$ plays a key role in mineral transformations through its influence on cell fitness and its contribution to mineral equilibria. The locations of the biogenic minerals with respect to cells reflect the ability of the bacteria to create chemical gradients. Our results highlight the microheterogeneity of mineral formation and show that both abiotic and biogenic pathways of mineral formation should be considered when modeling subsurface environments.

Glasauer, S., Langley, S. and T. J. Beveridge (2002) *Science* 295: 117-119.

Geochemical impacts of combustion wastes in reuse and disposal

F. P. GLASSER,

Department of Chemistry, University of Aberdeen, 033
Meston Building, Aberdeen AB24 3UE,
Scotland.f.p.glasser@abdn.ac.uk

Much of the world relies on thermal combustion processes for primary energy production. Combustion is also increasingly being used for volume reduction of municipal waste, perhaps with recovery of thermal energy. Much attention has been devoted to gaseous and particulate emissions arising from combustion processes but this contribution focuses on solid residues from combustion which, in the case of certain coals, may reach 30 - 40 weight %.

The presentation focuses on three aspects of combustion wastes: characterisation, disposal and prospects for reuse. Characterisation is an often neglected stage. Not only is ash very inhomogeneous but its characteristics also vary with the nature of the combustion process and fluctuate with changes in process conditions. The extent of utilization varies: some, such as coal combustion bottom ash and municipal incinerator ash are mainly landfilled. On the other hand, coal combustion fly ash and iron blast furnace slag achieve relatively high utilisation.

Landfilled materials are often strongly enriched in heavy metals. Leaching tests are usually used to determine potential for toxic or hazardous releases. But on a large scale, in landfills, the behaviour of combustion wastes is like a miniature orebody; a range of geochemical processes operate to achieve both dispersion and concentration of inorganic species. Leaching tests are useful but inadequate to characterise long-term behaviour.

Present day industrial processes do not have as their primary objective reuse or recycling of wastes: wastes are available, but the potential customer is often unable to optimise and tailor waste properties for specific uses. Clearly some compromise is needed; prospects for enhancement of the potential for reuse of wastes are discussed.

Using reactive transport modeling to characterize the record of climate change in deep vadose zones

W. E. GLASSLEY, J. J. NITAO, AND C. W. GRANT

Lawrence Livermore National Laboratory, Livermore, CA 94550, USA (glassley@llnl.gov)

Studies of deep vadose zone pore waters that evaluate chloride mass balance, and stable (deuterium and ^{18}O) and radiogenic (^3H , ^{36}Cl) isotope systematics have concluded that variations in infiltration flux can account for the observed variations in abundance of these approximately conservative tracers. It can be inferred, on the basis of these observations and interpretations, that a climate change record is preserved in these vadose zone waters. In arid regions where thick (>100 m) vadose zones persist, it has been concluded that this record may extend back more than 100,000 years. Consideration of the mechanisms that control reactive transport led to the conclusion that such climate-driven effects will also be evident as chemical reactions involving dissolution and/or precipitation of mineral phases along the flow pathway. As a result, there should also be variations in the concentrations of non-conservative chemical species that correspond to changes in the concentrations of the conservative tracers. Simulations of this reactive transport, in a regime typical of the arid Southwest U.S., demonstrate that these changes can modify pore water chemistry by factors of up to 200%, but the changes take place slowly, requiring thousands of years to achieve steady state conditions. This suggests that a very rich archive of climate change history is preserved in this type of setting. However, extracting that history is currently hampered by inadequate data for relevant rock properties. This challenge may be overcome if coordinated efforts are undertaken that exploit the power of detailed studies of isotope systematics, micro-scale rock characterization, and high performance computing.

A search for extraterrestrial amino acids in Antarctic micrometeorites

D. P. GLAVIN¹, G. MATRAJ², AND J. L. BADA³

¹Max Planck Institute for Chemistry, Mainz, Germany

(glavin@mpch-mainz.mpg.de)

²CSNSM-CNRS, Orsay-Campus, France

³Scripps Institution of Oceanography, La Jolla, CA

The delivery of amino acids by micrometeorites to the early Earth during the period of heavy bombardment could have been a significant source of the Earth's prebiotic organic inventory (Chyba and Sagan, 1992). However, one problem associated with the delivery of organic compounds by micrometeorites is that these grains can be heated to very high temperatures during atmospheric deceleration. Direct analyses of micrometeorite grains (200-400 μm) collected from Antarctic blue ice suggest peak heating temperatures from $\sim 1000^\circ\text{C}$ to 1500°C for several seconds during atmospheric entry (Toppani *et al.*, 2001). Since amino acids will begin to decompose in the solid state at temperatures in the range of 150°C to 600°C (Rodante, 1992), it is unclear whether these compounds could survive atmospheric entry on large micrometeorite grains.

In this study the acid-hydrolyzed, hot water extracts from a total of 455 Antarctic micrometeorite (AMM) grains were analyzed for the presence of amino acids by high performance liquid chromatography. Because AMMs have been found to be both petrologically and chemically similar to the CMs (Kurat *et al.*, 1994), a 5 mg sample of the CM meteorite Murchison was also analyzed. In the Murchison sample we found a high level (~ 3 ppm) of α -aminoisobutyric acid (AIB), a non-protein amino acid that is extremely rare on Earth, and is characteristic of amino acids of apparent extraterrestrial origin. In contrast, we were unable to detect any AIB in the AMMs above the 0.1 ppm level.

One possible explanation for the lack of extraterrestrial amino acids in AMMs, is that these compounds were completely destroyed and/or sublimed away from the grains during atmospheric heating. Sublimation has been proposed as a mechanism by which amino acids could survive atmospheric entry heating by vaporizing off the surface of micrometeorite grains at lower temperatures ($\sim 150^\circ\text{C}$) before they are pyrolyzed and destroyed (Basiuk and Douda, 1999). Although recent meteorite heating experiments indicate that most of the amino acids in micrometeorites are likely destroyed at temperatures $>550^\circ\text{C}$, we found that the sublimation of glycine present in micrometeorite grains may provide a way for this amino acid to survive atmospheric entry heating (Glavin and Bada, 2001).

References

- Basiuk, V. A. and Douda, J., (1999), *Pl. Space. Sci.* **47**, 577.
 Chyba, D. F. and Sagan, C., (1992), *Nature* **355**, 125.
 Glavin, D. P. and Bada, J. L., (2001), *Astrobiology* **1**, 259.
 Kurat, G. *et al.*, (1994), *Geochim. Cosmochim. Acta* **58**, 3879.
 Rodante, F., (1992), *Thermochimica Acta* **200**, 47.
 Toppani, A. *et al.*, (2001), *Meteor. Planet. Sci.* **36**, 1377.

Contrasting regional denudation patterns in southeastern Australia from apatite fission-track imaging

A. J. W. GLEADOW¹, B. P. KOHN¹, R. W. BROWN¹ AND P. B. O'SULLIVAN²

¹School of Earth Sciences, University of Melbourne, Victoria 3010 Australia (gleadow@unimelb.edu.au)

²Department of Earth Sciences, Syracuse University, Syracuse NY 13244-1070, USA (POSullivan@syr.edu)

Approximately 700 fission-track analyses on apatites from mostly granitic rocks across the states of Victoria, New South Wales and Tasmania in southeastern Australia provide a detailed low-temperature thermochronology of surface rocks across this region. In addition a number of deep drill holes and vertical sampling profiles in areas of high surface relief reveal the vertical structure of the apatite fission-track data across this region. In addition, dredge samples from the foundered continental blocks of the South Tasman Rise to the southwest of Tasmania have also been analysed, as have samples from the conjugate rifted margin of Northern Victoria Land in Antarctica.

Reconstruction of the low-temperature cooling histories of these apatites based on modelling of the fission-track age and track length data show significant variations across the region. These enable a number of distinct crustal blocks showing contrasting behaviour to be identified. Images of the evolution of these crustal blocks can be constructed by interpolation of the fission-track parameters and modelled palaeo-temperatures. Several episodes of rapid cooling can be identified in these thermal histories over the past several hundred Ma. These are reinforced by observations of significant intervals of essentially constant apatite fission-track age in many of the vertical profiles.

Assuming that the dominant control on these low-temperature cooling histories is the transport of the samples towards the surface, then quantitative reconstructions of the surface denudation history can also be obtained. These estimates can in turn be back-stacked onto the present topography and isostatically adjusted to provide reconstructions of the evolution of the landsurface through time. Analysed in this way the low-temperature fission-track thermochronology can provide estimates of sediment volumes arising from the surface denudation enabling new mass-balance calculations with sedimentary accumulations in adjacent depocentres.

The different thermal histories of the various crustal blocks in southeastern Australia are therefore interpreted as revealing contrasting denudation histories before, during and after Mesozoic to early Tertiary continental breakup in the region. No single area displays all of the denudation episodes identified.

Calibrating eolian dust accumulation rates in the central North Pacific pelagic clay province

JAMES GLEASON, TINA JOHNSON, DAVID REA, THEODORE MOORE, ROBERT OWEN AND JOEL BLUM

jdgleaso@umich.edu

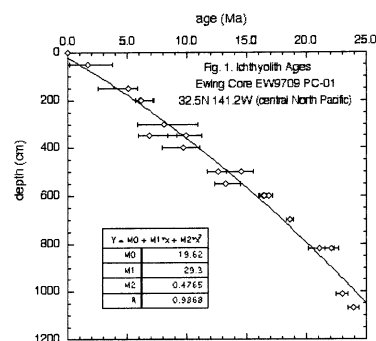


Figure 1. Age-depth curve for PC-01 red clay core, produced from ichthyolith Sr isotopic compositions.

Geochemistry of crustal samples from the Atlantis Bank Platform, SWIR

M. GLEESON^{1,2}, A.G.HUNTER², F. MCDERMOTT¹
G. PEARSON³, G. NOWELL³ A. FALICK⁴

¹Dept. Of Geology, University College Dublin, Ireland
(martina.gleeson@ucd.ie, frank.mcdermott@ucd.ie)

²The Open University in Ireland, 40 University Rd., BT7 1SU,
Northern Ireland (a.g.hunter@open.ac.uk)

³Dept. Of Geology, University of Durham, UK
(d.g.pearson@durham.ac.uk, g.m.nowell@durham.ac.uk)

⁴ SUERC, East Kilbride, Scotland (t.fallick@surre.gla.ac.uk)

This aims of this project are to determine (i) the nature of the relationship between basalts, dolerites and gabbros across the 12 Ma old Atlantis Bank Platform, (ii) the spatial relationship between magmatic and tectonic features and (iii) to compare samples from this study to those from ODP Hole 735B. To this end, major element, trace element, Sr- and Nd-isotope and O-isotope ratios have been determined on a range of basalts, gabbros and mineral separates from samples across the platform.

The ⁸⁷Sr/⁸⁶Sr ratios of leached basalts range from (0.7028 – 0.7033) whereas the leached gabbros define a narrower range in ⁸⁷Sr/⁸⁶Sr (0.7027 – 0.7028). This is comparable with the ⁸⁷Sr/⁸⁶Sr ratios of gabbros from Hole 735B which range from 0.7028 – 0.7031 (Hart et al., 1999). ¹⁴³Nd/¹⁴⁴Nd ratios are not significantly different in the basalts and gabbros, ranging from 0.51312 – 0.51317.

Oxygen isotope ratios relative to V-SMOW range from 2.8 – 6.8 ‰ in the basalts and 3.4 - 6.6‰ in the gabbros. These vary from the expected Indian Ocean N-MORB value of 5.75‰ and can be attributed to different periods of high and low temperature alteration.

Geochemically the basalts are similar to N-MORB, whereas the gabbros show very distinctive major and trace element signatures. The REEs indicate that the gabbros are cumulates and apart from EU, are more depleted than the basalts in REEs. The gabbros show a positive Eu anomaly while the basalts have a slightly negative anomaly. The major element data indicate that the gabbros have accumulated olivine and plagioclase. The data indicate that the gabbros and basalts were not formed by fractionation of a single parental magma, but were formed from different magmas. Reasons for the geochemical differences between basalts and gabbros will be discussed at this meeting.

Reference

Hart, S., Blusztajn, J., Dick, H., Meyer, P., Muehlenbachs, K. (1999). "The fingerprint of seawater circulation in a 500-meter section of ocean crust gabbros." *Geochemica et Cosmochimica Acta* 63(23/24): 4059- 4080.

Comparison of sulfide oxidation in unweathered pyritic mine tailings

M. GLEISNER AND R. HERBERT

Department of Geology and Geochemistry, Stockholm
University, SE-106 91 Stockholm, Sweden
(Magdalena.Gleisner@geo.su.se)
(Roger.Herbert@geo.su.se)

Introduction

Oxidation of pyrite in sulfide-rich mining waste is a major source of metal pollution in mining areas. This oxidation reaction depends on oxygen content, water accessibility, ferric iron concentration, temperature, pH and microbial activity. To prevent air and water intrusion into mining wastes, abandoned deposits are commonly covered with soil or water covers.

The aim of this study was to investigate and compare weathering rates and the precipitation of secondary minerals in two unweathered pyrite-rich tailings materials sampled from a soil-covered impoundment.

Materials and methods

Coarse- (silty sand) and fine-grained (silt) unweathered tailings (pyrite content 17 and 22 vol%, respectively) were sampled from the interior at two different sites in an old deposit. The deposit has been covered since 1996 with glacial till, and is located in Kristineberg (65°N 19°E), northern Sweden.

Column experiments with these samples were run for 333 days at room temperature in two water saturated columns. Aerated distilled water was pumped into the bottom of the column at a rate of 45 mL/day.

The columns were frequently sampled for pH, redox potential, anions and cations. Mineral equilibria modeling of the leachate solutions was performed with PHREEQC2 to predict the potential precipitation of secondary minerals in the columns.

Results and conclusions

Overall, the leachate from the fine tailings showed higher metal, sulfate and acidity content compared with the coarse tailings. At the start of the experimental period, pyrite oxidation rates were high (7×10^{-10} mol s⁻¹ for the coarse material and 2×10^{-9} mol s⁻¹ for the fine), but decreased by one order of magnitude towards the end of the period. The faster oxidation rate in the fine tailings is probably a result of the greater specific surface area and the higher pyrite content in this material.

Mineral equilibria modeling showed that alunite, gibbsite, ferrihydrite and kaolinite might have precipitated in the coarse material, while chalcedony, jarosite-K and kaolinite may have precipitated in the fine. The reason for this difference is primarily the lower pH level in the fine material, and differences in the silicate mineral content in the tailings samples.

Rb/Sr record of fluid-rock interaction in eclogites, Bergen Arcs, Norway

JOHANNES GLODNY¹, ALEXANDER KÜHN² AND
HÅKON AUSTRHEIM²

¹GFZ Potsdam, Telegrafenberg, 14473 Potsdam, Germany
(glodnyj@gfz-potsdam.de)

²Univ. I Oslo, Inst. for Geologi, 1047 - Blindern, 0316 Oslo,
Norway (alexander.kuehn01@gmx.de;
hakon.austrheim@geologi.uio.no)

Metamorphic reactions in the deep crust are either fluid-catalyzed, or require fluids as a reaction component. Fluid-induced rock transformations affect orogenic processes, as transformation relates to rock weakening and petrophysical changes. Isotopic dating of fluid-rock interaction therefore is a key aspect for understanding orogen dynamics. Isochron methods, in particular Rb/Sr, can provide precise ages of fluid-induced metamorphism, if, after crystallization of an equilibrated assemblage, closed system behaviour prevails.

Modally controlled closed system behaviour is presumed if shortly after equilibration fluid disappears from a rock. In a dry rock, intermineral isotope redistribution processes are drastically slowed down, and the local mode controls isotope mobility. For example a mica crystal will remain as a closed system up to very high temperatures if it is surrounded by phases with low Sr diffusivities, like garnet and omphacite. We propose that in dry rocks, Rb/Sr mineral systematics date the last metamorphic reactions rather than e.g. cooling.

The dry, granulite-facies rocks of the Lindås nappe, Bergen Arcs, Norway, were subducted to mantle depths during the Caledonian orogeny. However, eclogitization occurred only locally when fluids entered the rocks at eclogite facies conditions, at about 16-19 kbar / 650 - 750°C. Eclogite facies fluid activity resulted in metamorphic veins, surrounded by eclogitization aureolas. Overall fluid deficiency caused drying out of the eclogites shortly after the eclogitization reactions. From well-preserved vein precipitates and eclogites we obtained six Rb/Sr multimineral isochron ages, concordant at 425.2 ± 3.5 Ma, in agreement with a Sm/Nd mineral isochron age of 422 ± 10 Ma.

A second type of metamorphic veins with reaction aureolas is related to fluid infiltration during exhumation, at amphibolite facies conditions of about 8-10 kbar / 600°C. Rb/Sr multimineral isochron ages ($n = 6$) for this fluid infiltration event cluster around 412.9 ± 4.4 Ma.

The new age data, in combination with P,T conditions of metamorphism for eclogitization and retrogressive amphibolitization, allow to calculate an average exhumation rate of 2.4 mm/a in the time frame between ~425 and ~413 Ma, at a cooling rate of about 8°C/Ma. These rate estimates are independent from vague assumptions on closure temperatures and isotope diffusion parameters. The approach of dating assemblages with modally controlled closed system behaviour avoids the pitfalls of the theory of cooling ages.

Sayh al Uhaymir 094 – a new martian meteorite from the Oman desert

E. GNOS¹, B. HOFMANN², I.M. VILLA¹,
A. AL KATHIRI¹

¹Institute for Geological Sciences, Baltzerstrasse 1-3, 3012
Berne, Switzerland (gnos@geo.unibe.ch)

²Natural History Museum Bern, Bernastrasse 15, 3005 Berne,
Switzerland

Sayh al Uhaymir 094 is a 223.3 g, partially crusted, strongly to very strongly shocked melanocratic olivine-porphyrific rock of the shergottite group showing a microgabbroic texture. The rock consists of pyroxene (52.0 - 58.2 vol%) - dominantly prismatic pigeonite ($\text{En}_{60-68}\text{Fs}_{20-27}\text{Wo}_{7-9}$) associated with minor augite ($\text{En}_{46-49}\text{Fs}_{15-16}\text{Wo}_{28-31}$) - brown (shock-oxidized) olivine (Fo_{65-69} ; 22.1 - 31%), completely isotropic interstitial plagioclase glass (maskelynite; $\text{An}_{50-64}\text{Or}_{0.3-0.9}$; 8.6 - 13.0%), chromite and titanian magnesian chromite (0.9 - 1.0%), traces of ilmenite (Ilm_{80-86}), pyrrhotite (Fe_{92-100} ; 0.1 - 0.2%), merrillite ($<< 0.1\%$), and pockets (4.8 - 6.7%) consisting of green basaltic to basaltic andesitic shock glass that is partially devitrified into a brown to black product along boundaries with the primary minerals. The average maximum dimensions of minerals are: olivine (1.5 mm), pyroxene (0.3 mm) and maskelynite (0.3 mm). Primary melt inclusions in olivine and chromite are common and account for 0.1 - 0.6% of the rock. X-ray tomography revealed that the specimen contains approximately 0.4 vol% of shock-melt associated vesicles, up to 3 mm in size, which show a preferred orientation. Fluidization of the maskelynite, melting and recrystallization of pyroxene, olivine and pyrrhotite indicate shock stage S6. Minor terrestrial weathering resulted in calcite-veining and minor oxidation of sulfides. The meteorite is interpreted as paired with SaU 005/008/051. The modal composition is similar to Dar al Gani 476/489/670/735/876, with the exception that neither mesostasis nor titanomagnetite nor apatite are present and that all phases show little zonation. The restricted mineral composition, predominance of chromite among the oxides, and abundance of olivine indicate affinities to the Iherzolitic shergottites.

³⁹Ar-⁴⁰Ar dating of maskelynite suggests that SaU094 was produced during the same late Amazonian volcanic event as the other Martian shergottites Shergotty, Zagami, Los Angeles and EETA79001.

Melt freezing at the lithosphere-asthenosphere interface: Geochemical evidence from the Oman peridotites

M. GODARD¹, L. GERBERT-GAILLARD, J.-L. BODINIER

Laboratoire de Tectonophysique, UMR 5568 CNRS, ISTEEM, Cc 49, Université de Montpellier 2, Place E. Bataillon, 34095 Montpellier cedex 05, France
(¹margot@dstu.univ-montp2.fr)

Although the mantle section of the Oman ophiolite is mainly composed of extremely refractory harzburgites, some less refractory peridotites are observed in the lower mantle section. These less refractory peridotites are generally ascribed to a lower degree of melt extraction, the deeper peridotites being supposedly less affected by pressure-release partial melting. However, the Oman harzburgites do not show a gradual decrease of their refractory character from the top to the base of the mantle section, as it would be expected in this scheme. In order to better understand the origin of the less refractory peridotites in the Oman ophiolite, we carried out a whole rock major and trace element study of more than 80 peridotites, sampled along the Oman ophiolite mantle section, from the northern Fizh massif to the southern Wadi Tayin massif.

The Oman harzburgites are characterised by low clinopyroxene fractions (cpx<3%) and extreme trace element depletion (e.g., Yb = 0.08-0.35 x chondrite). Their chondrite-normalised REE patterns are steadily depleted from HREE to LREE. The less refractory peridotites display higher cpx contents (on average > 4%), higher HREE contents (Yb up to 0.8 x chondrite) and "spoon-shaped" REE patterns. Yet, these cpx-rich harzburgites are virtually indistinguishable from the other Oman harzburgites with respect to their Mg# ratios and olivine proportions. In fact, their more "fertile" character is mainly reflected in higher cpx/opx ratios and CaO content (0.25-1 wt.% for harzburgites and up to 2.6 wt.% for the more fertile peridotites). These variations suggests that they were individualised from the other harzburgites by a melt-rock reaction involving precipitation of cpx at the expense of opx.

Cpx-enriched harzburgites are unevenly distributed along the Oman ophiolite. They are found mainly in the deeper part of the massifs (Fizh, Wadi Tayin) but there is no direct correlation between their distribution and the distance to the mantle-crust transition zone. However, it should be noted that they are found in areas where lithosphere re-opening has been documented. We suggest that cpx precipitation in the Oman harzburgites underlines the lower boundary of pre-existing oceanic lithosphere thermally eroded by upwelling, partially molten asthenosphere. The occurrence of harzburgite re-fertilisation implies freezing of partial melts infiltrated across this boundary. This process would be related to the opening of the propagators identified in the Oman ophiolite.

Snowball Earth and basaltic traps

Y. GODDERIS¹, A. NEDELEC¹, Y. DONNADIEU², L.M. FRANÇOIS³, A. GRARD³ AND B. DUPRE¹

¹Laboratoire des Mécanismes de Transfert en Géologie, Toulouse, France (godderis@lmtg.ups-tlse.fr)

²Laboratoire des Sciences du Climat et de l'Environnement, Gif-sur-Yvette, France (tiphe@lscs.saclay.cea.fr)

³Laboratoire de Physique Atmosphérique et planétaire, Université de Liège, Belgique (francois@astro.ulg.ac.be)

The causes of the Neo-Proterozoic glaciations is still a matter of debate. One potential trigger for those glaciations is a major perturbation of the global carbon cycle, leading to the consumption of atmospheric CO₂, and finally to the cooling of the global climate.

The two main glacial episodes are characterized by intense rift formations. The Proto-Pacific ocean starts to open within the Sturtian stage, while the Iapetus ocean appears during the Varangian stage. In both case, the onset of rifts cutting through continental surfaces might have been coeval with the spreading of continental flood basalts. As demonstrated by Dessert et al (2001) for the K-T boundary, such events might severely impacts the long term evolution of the global climate, through intense consumption of atmospheric CO₂ by fresh basaltic surfaces, leading to non negligible global cooling at the million year timescale.

In the present contribution, we test such hypothesis using the COMBINE model (Goddéris and Joachimski, 2002), which couples a model of the C, O and P global cycles with a climatic model. We perform a study of the likelihood of the "basaltic" hypothesis, as a function of the pre-glaciation geochemical state of the exospheric system, and of the model parameters. In the case of the Sturtian glaciation, and assuming a pre-perturbation level of 280 ppm of CO₂, the onset of continental flood basalts over 8 million square km² along the equator (crossed by the Proto-Pacific rift) will drive the Earth into global glaciation 1.5 My after the event. The δ¹³C of carbonates accumulating between the start of the continental plume and the onset of the global glaciation fall by 3 to 4 ‰, in response to the degassing of large amount of mantle carbon into the atmosphere. The global glaciation is calculated to last 14 My before the PCO₂ accumulation is big enough to melt the Earth surface. This hypothesis raises the question of the cyclicity of the glaciations. Once the glaciation ends, the basaltic surface starts again to weather, and plunge the Earth into a new deep glaciation. We calculate that the interglacial episode lasts 1.7 My. The migration of the basaltic trap southward can drive the Earth out of this cyclicity. Within 30 My (two "glacial cycles"), the basaltic trap, originally located at the equator, might have migrated 3500 km southward, within the dryer tropical area. Such migration reduces the consumption of CO₂ by the basaltic surface, preventing the Earth from a new global glaciation.

Dissolution/precipitation phenomena on Ca carbonate crystals interacted with Pb²⁺ ions in aqueous solutions

A. GODELITSAS¹, J.M. ASTILLEROS¹, K.R. HALLAM²,
AND A. PUTNIS¹

¹ Institut für Mineralogie, Universität Münster, Corrensstraße 24, D-48149, Germany (athgod@nwz.uni-muenster.de, astiller@nwz.uni-muenster.de, putnis@nwz.uni-muenster.de)

² Interface Analysis Centre, University of Bristol, 121 St. Michaels's Hill, Bristol BS2 8BS, United Kingdom (k.r.hallam@bristol.ac.uk)

Introduction

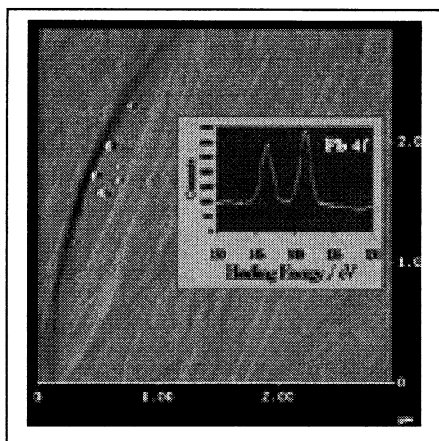
The study of the interaction of Ca carbonates with Pb²⁺ ions in aqueous solutions, as related to dissolution and sorption phenomena, plays a key role to the understanding of geochemical, environmental and technological problems in respect of natural and industrial processes.

Materials and Methods

Pure Ca carbonate (calcite and aragonite) crystals in the form of µm-sized (100-200 µm) fragments and mm-sized slices, were reacted with Pb solutions of varying concentrations. The investigation of the µm-sized samples was based on a batch-type procedure (10-1000 mg/L) using ICP, SEM-EDS, XRD and FT-IR. The mm-sized samples, interacted with slightly acidic aqueous solutions of 1000 mg/L Pb, were principally studied using a combination of surface techniques (*in-situ* / *ex-situ* AFM and XPS). Supersaturation calculations were used to evaluate the experimental results.

Results and Discussion

Fig. 1. *In-situ* AFM image of ellipsoid (10-40 Å in height) Pb carbonate nuclei developed into an oval etch-pit of the dissolved calcite surface. The relevant XPS spectrum (Pb 4f region) is also shown.



The experimental results concerning the µm-sized samples showed that Pb is intensively sorbed by the Ca carbonates while dissolution of the solids takes simultaneously place. The main sorption mechanism is the surface precipitation of Pb carbonates (hydrocerussite and cerussite).

The above chemical processes are more evident in the case of the mm-sized samples according to the AFM and XPS surface studies (see Fig.1).

Isotope constraints on brine formation in closed basin salars, NW Argentina

L.V. GODFREY, L.-H. CHAN², R ALONSO³,
T.E. JORDAN⁴, T.K. LOWENSTEIN⁵

¹Earth Env Sci, Lehigh U, Bethlehem PA (lig5@lehigh.edu)

²Geol Geophy, LSU, Baton Rouge, LA (lchan@geol.lsu.edu)

³Geol, U Salta, Salta, Argentina, (malonso@sinetis.com.ar)

⁴Earth Atm Sci, Cornell U, Ithaca, NY, (tej1@cornell.edu)

⁵Earth Env Sci, Binghamton U, NY
(lowenst@binghamton.edu)

The compositions of ⁸⁷Sr/⁸⁶Sr, δD and δ¹⁸O were determined in streams and brines located within the Hombre Muerto drainage basin in NW Argentina. Lithium isotopic compositions were also determined to trace the source of Li in the basinal brines

Hombre Muerto is a largely dry saline lake (salar) within a closed basin located at 4000 m in the Andes of NW Argentina. Most years a terminal lagoon forms at the end of the principal stream, the Rio de los Patos. Much of the drainage basin is covered by the extensive 2.03 Ma Co. Galan ignimbrite which lies on the southern edge of the basin. The eastern edge of the basin has Paleozoic basement rocks at the surface. Palaeozoic and Cenozoic sediments outcrop in the western part of the basin. The basin is heavily faulted, and basalts and dacites occur close to faults. The climate is dry and rainfall averages 100-200 mm/yr.

The range in ⁸⁷Sr/⁸⁶Sr is 0.7132 – 0.7206 with the most radiogenic compositions occurring in streams such as the los Patos that have contacted the basement rocks, even though the surface geology of their catchment is dominated by ignimbrites. The ⁸⁷Sr/⁸⁶Sr of the salar subsurface brine is similar to these streams indicating a solute source from the los Patos. In contrast the brine δ¹⁸O and δD shows no evidence of evaporation and indicates hydrologic separation between the salar brine and the terminal lagoon brine. The brine is formed by dissolution of existing evaporite minerals that precipitated in the past during wetter climate conditions when the whole salar was covered by a perennial saline lake.

Geothermally-formed travertines occur in parts of the salar, generally close to best estimates of fault traces. The ⁸⁷Sr/⁸⁶Sr of these travertines indicates a Sr source distinct from the immediate surface geology, indicating faults as a probable pathway for fluid flow.

Isotopic investigation of the sulphur and carbon cycles in sedimentary rocks from the Yangtze Platform, southern China

T. GOLDBERG¹, Q. GUO², C. LIU², M. STEINER³, and H. STRAUSS¹

¹Geologisch-Paläontologisches Institut, Universität Münster, Corrensstrasse 24, 48149 Münster, Germany (tgold@uni-muenster.de; hstrauss@uni-muenster.de)

²Institute of Geochemistry, Chinese Academy of Sciences, Guiyang 550002, China (gqjowen1@hotmail.com; liucongqiang@hotmail.com)

³Technische Universität Berlin, Ackerstrasse 71-76, 13355 Berlin, Germany (steishhb@mailszrz.zrz.tu-berlin.de)

Introduction

A well preserved Neoproterozoic and Cambrian sedimentary succession on the Yangtze platform provides an excellent setting for isotopic investigations. The principal succession exposed comprises in ascending stratigraphic order the Nantuo Formation with glacial deposits, followed by the predominantly calcareous Doushantuo and Dengying formations and black shales of the lower Cambrian Niutitang/Guojiaba Formation. Paleoenvironmental conditions range from very shallow water (evaporite deposition) across the shelf into deeper water.

The prime aspects which will be addressed during this study are: seawater chemistry, biogeochemical evolution and chemostratigraphy.

Results

Sediments of Sinian age (Nantuo, Doushantuo, Dengying formations) show low to moderate total organic carbon abundances (0.01-0.1 wt%). Organic carbon isotope values range between -33 and -24‰. In contrast, early Cambrian black shales display higher organic carbon abundances (up to 5 %) and $\delta^{13}\text{C}$ values between -35 and -30‰. Carbonate carbon isotope values are displaced by 32‰.

Highly variable $\delta^{34}\text{S}$ values for sedimentary pyrite, particularly for the early Cambrian black shales, reflect bacterial sulfate reduction, sometimes under closed system conditions. Seawater sulfate as recorded in barite and phosphorite shows sulfur isotope values around -30/-34‰.

Discussion

Based on their respective isotopic compositions, the sulphur and the carbon cycle reflect global geochemical perturbations of the ocean/atmosphere system. As such, variations in the carbon isotopic composition reflect fluctuations in the fractional burial of organic matter.

Stable isotope geochemistry of impact related alteration phases from the Woodleigh impact structure, Western Australia

GOLDING, S.D.¹, UYSAL, I.T.¹, BAUBLYS, K.A.¹, GLIKSON, A.Y.², AND MORY, A.J.³

¹ Department of Earth Sciences, University of Queensland, QLD 4072, Australia (golding@earth.uq.edu.au)

² Research School of Earth Sciences, Australian National University, Canberra, ACT 0200, Australia

³ Geological Survey of Western Australia, 100 Plain Street, East Perth, WA 6004, Australia

The Woodleigh impact structure, Western Australia has a diameter of some 120 km based on geophysical, morphometric and surface drainage evidence which makes it one of the largest Phanerozoic impact structures [1, 2, 3, 4]. Age determinations using the K-Ar systematics of impact related illitic clay minerals together with stratigraphic age constraints indicate a mid to Late Devonian age for Woodleigh and confirm its relevance to the late Devonian mass extinction [3, 4]. To constrain the post impact hydrothermal history of Woodleigh we have determined the stable isotope compositions of shocked granitoids and alteration phases in samples from the composite fault-bounded central uplift. Shocked granitoid samples from which all alteration phases have been removed ultrasonically have $\delta^{18}\text{O}$ values of 9.2 and 10.5 ‰ that are at the upper end of the normal range for granitic igneous rocks. Alteration clays and carbonates have significantly higher $\delta^{18}\text{O}$ values from 13.4 to 18.9 ‰. The coarsest clay fractions have the lowest $\delta^{18}\text{O}$ values of 13.4 and 13.6 ‰ that are interpreted to result from contamination with primary biotite and quartz. Based on the $\delta^{18}\text{O}$ values, a temperature estimate of 200°C for the formation of the Woodleigh clays and the illite-water, smectite-water and calcite-water fractionations equations [5, 6], the calculated fluid $\delta^{18}\text{O}$ values range from 6.5 to 11.7 ‰. These compositions are highly enriched in ^{18}O and overlap the fields of magmatic and metamorphic fluids. Extensive interaction at relatively low water/rock ratios with ^{18}O -rich rock types is required to explain the large ^{18}O shift as the hydrogen isotope compositions indicate water in the impact related hydrothermal system was largely of surface derivation. ^{18}O -enrichment of the country rocks may reflect shock-induced oxygen isotope fractionation [7] and/or the involvement of ^{18}O -rich condensed meteoritic components that were injected into the crater floor [2].

References: [1] Mory A. J. et al. (2000) *Earth Planet. Sci. Lett.*, 177, 119–128. [2] Mory A. J. et al. (2000) *Earth Planet. Sci. Lett.*, 184, 359–365. [3] Uysal I.T. et al. (2001) *Earth Planet. Sci. Lett.*, 192, 281–289. [4] Uysal I.T. et al. (in press) *Earth Planet. Sci. Lett.* [5] Sheppard S.M.F. and Gilg H.A. (1996) *Clay Min.*, 31, 1–24. [6] O'Neil J.R. et al. (1969) *Journ. Chem. Phys.*, 51, 5547–5558. [7] Vennemann et al. (2001) *Geochim. et Cosmochim. Acta*, 65, 1325–1336.

Effects of rapid crystallization on ^{226}Ra - ^{230}Th ages

STEVEN J. GOLDSTEIN¹, KARI M. COOPER², MARY R. REID³, MICHAEL T. MURRELL¹, KENNETH W. SIMS⁴

¹Los Alamos National Laboratory, MS K484, Los Alamos, NM 87545 (sgoldstein@lanl.gov)

²Caltech, MC 170-25, 1200 E. California Blvd., Pasadena, CA 91125 (cooper@gps.caltech.edu)

³ESS Dept., UCLA, Los Angeles, CA 90095-1567

⁴Dept. Geol. and Geophys., WHOI, Woods Hole, MA 02543

^{226}Ra - ^{230}Th disequilibria can be used to constrain ages of crystal growth that occurred within the past few hundreds of years to ~10 ka, but accurate ^{226}Ra - ^{230}Th ages must account for initial Ra incorporated into crystals during growth¹. Using Ba as a proxy for Ra, elastic-strain partitioning models can be used to predict the magnitude of fractionation which, in many cases studied to date, appears to account for the observed patterns of data¹⁻². However, Ra concentrations measured in plagioclase from the 1996 N. Gorda Ridge eruption and the 1982 addition to the 1980-86 Mt. St. Helens dacite dome are higher than would be predicted relative to Ba. These observations cannot be explained by aging of crystals, because decay of ^{226}Ra would decrease Ra concentrations compared to Ba, and could potentially indicate that elastic-strain models do not fully account for trace-element behavior in natural systems.

We suggest that this pattern of data is the result of rapid crystal growth during the final stages of magma ascent, which has been documented in the case of plagioclase microlites in the Mt. St. Helens dome³. Such rapid growth could lead to entrapment of surface enrichments of slowly-diffusing elements⁴ and could decrease the relative fractionation of highly incompatible elements like Ra and Ba. For plagioclase in the 1982 dacite, effective $D_{\text{Ra}}/D_{\text{Ba}}$ is >0.6 (compared to values of 0.15-0.2 calculated from the elastic-strain model). Assuming that plagioclase and glass in the Gorda Ridge sample are related, effective $D_{\text{Ra}}/D_{\text{Ba}}$ must lie between 0.3 and 0.6. Rapid plagioclase growth at St. Helens has been attributed to degassing, but because a similar increase in effective $D_{\text{Ra}}/D_{\text{Ba}}$ is seen in the Gorda Ridge sample despite differences in bulk composition, rapid crystal growth may be a more general phenomenon. If mineral separates in other samples include a fraction of rapidly-grown crystals, then ages calculated from ^{226}Ra - ^{230}Th disequilibria by assuming that partitioning models accurately predict $D_{\text{Ra}}/D_{\text{Ba}}$ would underestimate the average crystallization age.

¹Cooper, K.M. et al. (2001), *Earth Planet. Sci. Letts.* **184**, 703-718

²Cooper, K.M. et al. (2001) *Eos* 47, abstract #V22B-1047

³Geshwind, C.H. and Rutherford, M.J. (1995), *Bull. Volcanology* **57**, 356-370; Cashman, K.V. (1992), *Contributions Mineral. Petrol.* **109**, 431-449.

⁴Watson, E.B. (1996) *Geochim. Cosmochim. Acta* **60**, 5013-5020

Do we need a primitive mantle reservoir? An updated assessment.

STEVEN L. GOLDSTEIN¹, CHARLES H. LANGMUIR², AND YONGJUN SU¹

¹Lamont-Doherty Earth Observatory of Columbia University, Palisades, NY 10964, USA (steveg@ldeo.columbia.edu)

²Department of Earth, Atmosphere, and Planetary Sciences, Harvard University, Cambridge MA, USA

The question of whether a primitive reservoir exists within the mantle addresses a continuing enigma. The PETDB database of global MORB allows a new estimate of the composition of the upper mantle, and forms the basis of an updated assessment of where we stand on this issue.

Based on trace elements and isotope ratios of oceanic basalts, excepting volatile elements, there is little evidence for a primitive mantle component in MORB and OIB sources. Its absence is intuitively consistent with recycling of oceanic lithosphere into the lower mantle and whole mantle convection. On the other hand, a primitive mantle reservoir is supported by the presence of primordial helium and neon in some OIB, and appears to be required by most depleted mantle-continental crust mass balances. However, the presence of primordial noble gas does not require the existence of a primitive "reservoir", rather it requires that some mantle has never been degassed. Convection in the lower mantle would likely mix primitive mantle with previously depleted mantle, creating a depleted reservoir containing primordial noble gasses. Indeed, a primordial noble gas signal is strongest in OIB whose mantle sources also show Nd-Sr-Hf isotope ratios reflecting long-term depletion.

Our average MORB estimate indicates that the average upper mantle is isotopically more "enriched" than most previous estimates ($\epsilon_{\text{Nd}} \approx 8.7$). Mass balance requires that the higher the ϵ_{Nd} of the upper mantle, the lower the ϵ_{Nd} required for the lower mantle to balance the continental crust. That is, a more isotopically enriched upper mantle implies an isotopically more depleted lower mantle. We addressed the question, what conditions would eliminate the need for a primitive mantle reservoir, using Loihi as a target composition for "average lower mantle".

How difficult is it to mix away a primitive mantle reservoir? As shown by mass balances over the past 25 years, estimates of continental crust element abundances combined with reasonable estimates of its isotope ratios requires large amounts of primitive mantle. For example, recent estimates of continental crust Nd abundances combined with a mean age of 2.25 Ga raises the average lower mantle Nd isotope ratio to be only 0.8-1.7 ϵ_{Nd} units above the bulk Earth. A lower mantle without a primitive reservoir requires that there is an amount of continent-like Nd in the mantle equal to or greater than the amount in the continental crust. If this can be accommodated in continental lithosphere and EM-type OIB sources, we can dispense with the need for a primitive reservoir.

Solubility of Iron(III) and Aluminum Phosphates in Aqueous Solutions

SERGEY V. GOLUBEV,¹ ALLA V. SAVENKO²

¹ Department of Geography, Moscow M.V. Lomonosov State University, Moscow, Russia email : lanav@mail.ru

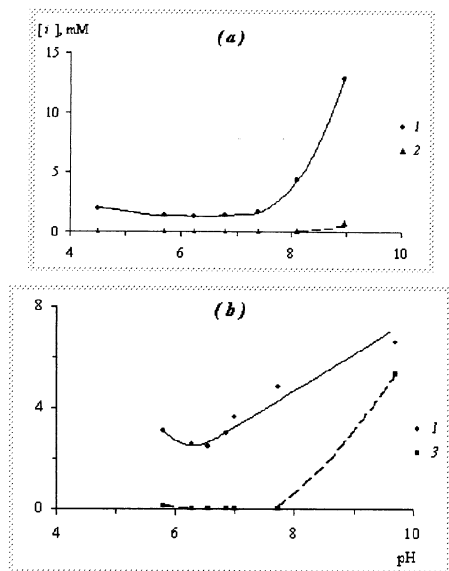
² Department of Geology, Moscow M.V. Lomonosov State University, Moscow, Russia

It is generally believed that phosphates of Fe(III) and Al are main forms of phosphorus in acid soils. However, the existing experimental data on solubility of iron and aluminum phosphates in weak acid and weak base solutions are very scarce. Our study represents a part of concerted efforts aimed at experimental investigation thermodynamic stability of these solids. For this, we studied the solubility of synthesized amorphous phases (FePO_4 and AlPO_4) in NaClO_4 - HClO_4 - NaOH - NaHCO_3 solutions with different ratio of solid/solution (m/V) at pH range 4.5-9.5 and constant ionic strength ($I=0.05$).

It was found that in our experiments solid phases FePO_4 and AlPO_4 are transformed into hydroxides of Fe(III) and Al, but with increasing m/V, the concentration of soluble components (P, Fe and Al) is defined by solubility of initial FePO_4 and AlPO_4 . A pH dependence of P, Fe and Al in equilibrium with FePO_4 and AlPO_4 is presented in Fig. 1. The solubility of FePO_4 and AlPO_4 at pH 4.5-9.5 is a several orders higher than the concentration of phosphate ions in surface and ground waters (1.5-6_10-6 M). Thus we can deduce a conclusion that phosphates of Fe(III) and Al are unstable in weak acid and weak base solutions and the phosphate phase is likely to transform to less soluble calcium phosphates.

This work is financially supported by Russian Fond for Basic Research (project 00-05-65495).

Fig. 1. The relationship between equilibrium phosphate, iron(III) and aluminum concentrations and pH value. a) solubility of FePO_4 , b) solubility of AlPO_4 . 1 – P, 2 – Fe, 3 – Al.



Metal and micro-organic pollutant partitioning between sediments and waste waters from a landfill

M.A. GONÇALVES¹, J.M.F. NOGUEIRA², C.V. PUTNIS³
AND J.FIGUEIRAS¹

¹ Dept. Geologia / CREMINER, FCUL, Ed. C2, Campo Grande, 1749-016 Lisboa, Portugal ({macg, jmvf} @fc.ul.pt)

² Dept. Química e Bioquímica, FCUL, Ed. C8, Campo Grande, 1749-016 Lisboa, Portugal (nogueira@fc.ul.pt)

³ Institut für Mineralogie, Universität Münster, Corrensstrasse 24, 48149 Münster, Germany (putnisc@uni-muenster.de)

Stream sediments in the vicinity of a landfill environment were collected and analysed for their metal and micro-organic pollutant content. These sediments were mechanically sieved into two different size fractions (<63 μm and 63-90 μm). Analytical methods used included bulk chemical analysis, XRD, SEM, sequential extraction of metals (Tessier *et al.*, 1979; Hirner, 1992), and Solid Phase Extraction (SPE) of organic compounds (Nogueira *et al.*, 2001). Surface and ground waters were also sampled and analysed. A high content of metals such as Cu, Zn and Pb was found, showing a decreasing concentration gradient down-stream away from the landfill facility. SEM observations determined that for some of these metals (Zn in particular) part of this behaviour could be due to the presence of artificial alloys. It also showed that most of Cu is concentrated at the mineral surfaces. The combined studies of sequential extraction and SPE showed that metals are preferentially bound to the organic pollutants present in the sediments. These compounds are responsible for 70-80% adsorption of Cu, 50-70% for Zn, 40-60% for Pb and 20% for Ni. This behaviour seems to relegate the presence of specific mineral types to a secondary role in these systems. The different size fractions of sediments do not show any remarkable difference in their composition and in metal distribution among different adsorption modes. Even considering that clay minerals have been shown to be present in both size fractions at least some difference should be apparent. The identification of micro-organic pollutants is currently being done by GC-MS both in the sediments and in the surface polluted waters that directly interacted with these sediments. Preliminary results also indicate that such interaction albeit important is rather limited, and that polluted waters may still carry significant concentrations of harmful substances, and these being easily transferable to the hydrological cycle.

References

- Hirner A.V., (1992), Intern. J. Environ. Anal. Chem., **46**, 77-85.
Nogueira J.M.F., Teixeira P., and Florêncio M.H., (2001), J. Microcolumn Sep., **13**, 48-53.
Tessier A., Campbell P.G.C., and Bisson M., (1979), Anal. Chem., **51**, 844-851.

Pb-Pb age of earliest megascopic, eukaryotic algae bearing Vindhyan sediments, India

K. GOPALAN¹, S. SARANGI¹ AND S. KUMAR²

1. National Geophysical Research Institute, Hyderabad 500 007, India (postmast@csngri.ren.nic.in)
2. Geology Department, Lucknow University, Lucknow, India (surendra100@hotmail.com)

Considered to be the earliest known megascopic, photosynthetic eukaryotic algae, fossils of *Grypania spiralis* of similar size and morphology occur in India, China and USA but from sites of widely different ages – 1.0 Ga, India (Kumar, 1995); 1.4 Ga, China (Du and Tian, 1986); 1.8 Ga, Montana (Walter et al., 1976) and 2.1 Ga, Michigan (Han and Runnegar, 1992). As the only site representing the younger limit of such an extended *Grypania* biozone, the *Grypania* bearing Indian site must be directly and reliably dated.

We have therefore taken up Pb-Pb dating of carbonates from the *Grypania* bearing Rohtas Formation of the Lower Vindhyan Semri Group in the Son Valley (Kumar, 1995). Sixteen chips (~ 1 g each) from a small carbonate slab near Katni show a spread of ²⁰⁶Pb/²⁰⁴Pb ratios from 26.8 to 35.6 to yield a well defined Pb-Pb isochron (MSWD = 1.3) corresponding to an age of 1615±58 Ma (1σ). In good agreement with the inferred ages for the Rohtas Formation (Rasmussen et al., 2002; Ray et al., 2002), this result pushes the record of *Grypania spiralis* in India back by about 500 my and hence restricts its biozone to between 1500 and 2100 Ma.

References

- Du R. and Tian H.Li., (1985), *Precamb. Res.* **29**, 5-10
 Han T. M. and Runnegar B., (1992), *Science*, **257**, 232-235
 Kumar S., (1995), *Precamb. Res.* **72**, 171-184
 Rasmussen B., Bose K., Sarkar S., Banerjee S., Fletcher I.R. and McNaughton N.J., (2002), *Geology*, **30**, 103-106
 Ray J.S., Martin M.W., Veizer J. and Bowring S.A., (2002), *Geology*, **30**, 131-134
 Walter M.R. and Oehler J.H., (1976), *J. Paleontol.* **50**, 872-881

Regulation and assembly of extracellular polymeric substances by the facultative metal reducing bacterium *Shewanella oneidensis* strain MR-1

Y.A. GORBY, J. MCLEAN, G. PINCHUK, E. A. HILL, AND ALICE DOHNALKOVA

Pacific Northwest National Lab, Richland, WA
 (yuri.gorby@pnl.gov)

Production of extracellular polymeric substances by *Shewanella putrefaciens* strain MR-1 was examined under controlled conditions in continuous cultures using a chemically-defined medium with electron donor limitation. Cells produced EPS under aerobic conditions with dissolved oxygen concentrations ranging from 1 to 100 % of air saturation. Cells grown anaerobically with fumarate as the sole terminal electron acceptor did not produce visible assemblages of cells and no detectable EPS. Excess Ca²⁺ (provided as 0.7 mM CaCl₂) promoted the assembly of the EPS in aerobically grown cells while deficiency in Ca²⁺ inhibited the formation of the EPS matrix. The distribution of negatively charged sites on cell surfaces and within EPS matrix was examined by TEM using positively charged nanogold particles (1.4 nm diameter) as electron-dense contrasting agents. Cells that did not produce an EPS matrix (i.e., cultured anaerobically with high Ca²⁺ concentration and cells grown aerobically with low Ca²⁺ concentrations) exhibited a heterogeneous charge distribution similar to those described for *S. algae* strain CN32 (Sokolov et al., 2000). Cells that did produce an intact EPS matrix (i.e., cells cultured aerobically with sufficient amounts of Ca²⁺) were poorly labelled with cationically-charged gold particles. However, all of the gold particles were bound by charged sites within the EPS matrix. Negatively charged sites (on cell surfaces and within the EPS) served as nucleation and growth sites for mixed Fe(II)/Fe(III) mineral phases when Fe(II) was added to anaerobic cell suspensions. These oxide phases were tentatively identified as a high-Fe(II)/Fe(III) ratio form of green rust. These results have important implications to the fate and transport of cations in aerobic/anaerobic transition zones in natural subsurface sediments and groundwaters and to the formation of highly redox-reactive minerals (green rusts) in iron reducing environments.

References

- Sokolov, I., Smith D.S., Henderson G. S., Gorby Y. A., and Ferris F. G., (2000). *Environ. Sci. Tech.* **35**, 341-347.

Glacier Erosion Factory: Using $^{26}\text{Al}/^{10}\text{Be}$, soils, and geomorphology to study relief development

J.C. GOSSE AND J. WILLENBRING

Dept. Earth Sciences, Dalhousie University, Edsell Castle
Circle, Halifax, Nova Scotia, Canada B2V 1P8
(john.gosse@dal.ca, jwillenb@is2.dal.ca)

Quantifying the influence of glaciers on landscapes of active and ancient orogens has been elusive because of the difficulty in (1) linking erosion rates and processes, and (2) extrapolating measured erosion rates over the duration of one or more glaciations and over the scale of a mountain range.

Hypothesis

In orogens with high plateaus, ice caps may reach an equilibrium state that maintains a non-erosive condition where the ice is frozen to its bed. Among other variables, the rate of achieving this equilibrium depends on the permeability and hydrological character of the substrate and the thickness of ice cover (and indirectly the size of the plateau). Ice cap outlets drain through plateau-dissecting valleys. The outlet lobes are thicker and flow faster under convergent flow, maintaining wet-based conditions and inducing glacial erosion by several mechanisms. Relief is increased during glaciations as valleys are deepened but summits are unscathed.

Initial test results

Cosmogenic nuclide exposure history results in Atlantic Canada partly test the validity of this hypothesis. The Torngat Mountains and Long Range Mountains, with up to 1600 m relief, have broad coastal summit plateaux. The post-glacial valleys maintain their glacial form although incipient post-glacial stream incision is evident ubiquitously. The plateaux and valleys have been covered with ice as recently as the Younger Dryas (^{10}Be ages on erratics on all dated Torngat summits fall within the YD chron). However, bedrock surfaces on the summits record as much as 600 kyr of exposure history (minimum duration based on $^{26}\text{Al}/^{10}\text{Be}$ on summit tor-like features; the ratio indicates burial, probably by non-erosive ice). Despite being glaciated 11 ka, summit soils also indicate antiquity with anomalous abundances of gibbsite and kaolinite relative to soils on valley sides and bottoms, and geomorphic indicators of weathering (gnammas, weathering rinds) are strongest on the plateau summits. Furthermore, on the flanks of the plateaux ^{10}Be concentrations in bedrock increase with altitude, reflecting the increasing importance of wet-based erosive processes lower in the valley. Absence of inheritance in valley bottom bedrock implies glacial erosion rates ~ 2 m per 20 kyr in the valleys (negligible erosion on the summits).

Geodynamics implications

We propose that until the plateaux are diminished by valley widening and lateral migration of headwalls, glaciers can generate relief in hypsometrically-immature orogens.

On early solar system chronology

M. GOUNELLE AND S. S. RUSSELL

Department of Mineralogy, The Natural History Museum,
Cromwell Road, London SW7 5BD, UK (mattg@nhm.ac.uk)

Extinct short-lived radionuclides such as ^{26}Al , ^{53}Mn , ^{182}Hf and others have been extensively used as chronometers for a variety of early solar system processes (see references in [1]). The possibility of building a coherent chronology relies on the assumption that short-lived radionuclides were homogeneously distributed in the accretion disk. This assumption was not unreasonable when the nebula was thought to be hot, well-homogenised, and when the extinct radionuclides were thought to come from a late-stage star such as a supernova [2]. Recent data from a diversity of fields question these assumptions. Here we review new data and ideas on extinct radionuclides, and critically discuss the possibility of building an early solar system chronology.

Astronomical observations of accretion disks around protostars of solar type suggest that the nebula was cold. Building on these observations, a new model for the formation of chondrites has been developed by Shu et al. [3], in which most of solar system matter is thermally processed close to the sun, and ejected to the cold accretion disk *via* an "x-wind".

The isotopic homogeneity of the accretion disk is questioned by FUN CAIs that contain much lower levels of short-lived radionuclides such as ^{26}Al than normal CAIs [2]. The strong dependence of ^{53}Mn abundance with heliocentric distance also supports the view of a heterogeneous distribution of short-lived radionuclides in the accretion disk [4]. This heterogeneity can be explained in the context of the x-wind model [5], where short-lived radionuclides and their host phases (CAIs) are formed close to the Sun and tossed to asteroidal distances by a fluctuating x-wind.

The discovery of ^{10}Be in CAIs [6] has cast a shadow on a supernova origin for short-lived radionuclides. This isotope cannot form in stars, although Cameron has recently suggested ^{10}Be could form in a supernova jet [7]. The presence of ^{10}Be in CAIs is however readily explained by irradiation [8] based on the x-wind model [5], which can also account for the production of ^{26}Al , ^{41}Ca and ^{53}Mn .

From these data, a new picture of the solar system is emerging, where some of the short-lived radionuclides (^{10}Be , ^{26}Al , ^{41}Ca , ^{53}Mn) were distributed heterogeneously in the accretion disk. For these short-lived radionuclides, homogeneity in the disk is not satisfied. Early solar system components were instead a mixture of irradiated and un-irradiated material, and using short-lived isotopes as a chronometer will depend on how characterising their initial microscopic and macroscopic distribution in early asteroids.

- [1] Hutchison et al (2001) *Phil Trans. Roy. Soc. A* **359**,1351ff
[2] Cameron *MAPS* **30**,13 [3]Shu et al (1997) *Science* **277**,1475 [4]Lugmair and Shokolyukov (1998) *GCA* **62**, 2863 [5] Shu et al (2001) *ApJ* **548**,1029 [6] McKeegan et al (2000) *Science* **289**,1334 [7] Cameron *ApJ* **562**, 456 [8] Gounelle et al. (2001) *ApJ* **548** 1050

In-situ Cu and Fe isotope evidence for inorganic and organic components in the HYC Pb-Zn ores

S. GRAHAM¹, W.L. GRIFFIN¹, S.E. JACKSON¹, M.R. WALTER¹, G.A. LOGAN² AND N.J. PEARSON¹

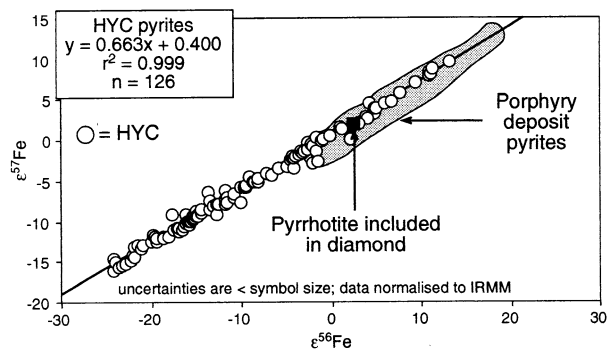
¹GEMOC Key Centre and Aust. Cent. Astrobiol., Dep. Earth and Planetary Sciences, Macquarie University, Sydney, Australia, 2109. (sgraham@laurel.ocs.mq.edu.au)

²Geoscience Australia, Petroleum and Marine Division GPO Box 378, Canberra, Australia, 2601

Ore deposition in the 1640 Ma HYC deposit (northern Australia) took place in a shallow marine setting, is syngenetic, and related to brine fluids moving through a sub-basin. The polycyclic hydrocarbon distribution within the deposit is consistent with a large thermal gradient and suggests that ore deposition is linked to interaction between the hydrothermal fluid and organic matter in the sediment at a temperature below 300°C (Chen, pers. comm). We have obtained in-situ Cu and Fe isotope data for pyrite and chalcopyrite from the same samples studied by Chen and colleagues and one higher-T sample, close to where the fluid entered the system, that span a lateral distance of ~1500m.

Figure 1 shows a linear relationship between $\epsilon^{57}\text{Fe}$ and $\epsilon^{56}\text{Fe}$ values in pyrites from HYC. The $\epsilon^{57}\text{Fe}$ values vary between -24 and +13 and overlap values found in magmatic porphyry-deposit pyrite. Chalcopyrite $\epsilon^{65}\text{Cu}$ values vary between +0.1 and +16.

Figure 1: Fe 3-isotope diagram



$\epsilon^{65}\text{Cu}$ and $\epsilon^{57}\text{Fe}$ values from the two highest-T ore samples (500 m apart) initiate a trend of increasing $\epsilon^{65}\text{Cu}$ and $\epsilon^{57}\text{Fe}$ values with distance that is interpreted to represent thermochemical sulfate reduction (TSR). This trend is consistent with the lighter isotopes being removed from the fluid first. The lower-T ores yield large ranges in both $\epsilon^{65}\text{Cu}$ and $\epsilon^{57}\text{Fe}$ on either side of the extrapolated TSR trend. We interpret these ranges as a result of living bacteria preferentially using molecules with light Cu and Fe isotopes, causing them to drop out of solution in the ore zone. This interpretation is supported by mass balance considerations; there are equal proportions of heavy and light $\epsilon^{57}\text{Fe}$ values above and below the TSR trend.

Spatially-averaged erosion rates from cosmogenic nuclides in sediments: Ten years later

DARRYL E. GRANGER

Department of Earth and Atmospheric Sciences, Purdue University, West Lafayette, IN, USA, 47907-1397

The technique of determining spatially-averaged erosion rates from cosmogenic nuclides was first presented in a series of talks in 1992 and 1994, and later published by Brown et al. (1995), Bierman and Steig (1996), and Granger et al. (1996). This cosmogenic technique was touted as a method for measuring erosion rates over a 10^3 to 10^5 year timescale for which there was no reliable alternative. For the first time the erosional impacts of land use, climate, and tectonics could be routinely measured. Ten years later, with contributions from numerous researchers, we can evaluate this technique's impacts on geomorphology.

Recognition of natural variability

Cosmogenic nuclides have better quantified the range of erosion rates both within and across different tectonic environments. For example, erosion rates in the stable Appalachian Plateau are very slow (1-3 m/My) while the tectonically active northern Apennines erode much faster at 600 m/My. Comparison with fission track exhumation rates and sedimentary basin fills imply that these areas have maintained similar erosion rates for millions to tens of millions of years.

Erosion rates through time

Disequilibrium between cosmogenic erosion rates and modern sediment yields can be due to land use, climate change, or natural episodic sediment delivery to streams.

One way to distinguish among these causes is by examining changes in erosion rate through time, by analysing cosmogenic nuclides in buried sediments that retain their erosional inheritance (e.g., in terraces, lakes, or caves).

Landscape Evolution

The concept of a steady-state landscape, where erosion rates are uniform over space and time, is intellectually appealing but difficult to demonstrate in reality. Perhaps the greatest contribution of cosmogenic nuclides is that it is no longer sufficient to ask whether steady-state landscapes exist. Instead, our research should be driven to explain the natural variability that we observe in terms of erosional processes, climate, and tectonics, and to carefully quantify the changes in erosion rate through time.

Origin and dynamics of Fe- and Mn-crusts in the sediments of Lake Baikal

L. GRANINA

Limnological Institute, Russian Academy of Science, Irkutsk, Russia (liba@lin.irk.ru)

The setting

Iron-manganese crusts were studied at six regions of Lake Baikal. They exhibit different sedimentation rates ranging from 0.8 mm yr⁻¹ at the Selenga Delta down to about 0.2 mm yr⁻¹ at Academician Ridge. Enriched Fe-Mn layers were found at the sediment-water interface at the Selenga Delta, and the Southern and Central Basins. In the North Basin of Lake Baikal and at Academician Ridge buried layers with very high concentrations of Fe- and Mn oxides were found.

The analysis

We measured pore-water profiles with dialysis plates and whole-core squeezing. From these data we obtained estimates of diffusive Fe²⁺ and Mn²⁺ fluxes into the enriched layers. By comparing the actual fluxes on the accumulated amount of Fe and Mn oxides in the layers we obtained estimates of the in-situ accumulation time of the enriched layers. These values could then be compared with the average sediment age calculated from published sedimentation rates at the different sites.

Results

Both methods yield similar estimates for the dynamics of Fe-Mn-crust formation in the sediments of Lake Baikal. Table 1 compares the accumulation time t_{acc} with the age in the enriched layer t_{age} calculated from the Mn data for different characteristic sites.

Site (core no.)	t_{acc} [years]	t_{age} [years]
Selenga Delta (core 94-08)	30	80
Southern Baikal (94-02)	80	50
Central Baikal (94-09)	390	170
Northern Baikal (94-10)	2200	680
Academician Ridge (94-11)	8100	5000

There is a good correlation between the penetration depth of oxygen into the sediment and the depth and extension of the enriched layers. They can therefore be considered as redox fronts. The crusts are enriched with Fe and Mn by factors of 10-100 compared with background levels in deeper sediment layers. Recently we have shown that P and As were strongly enriched in the Fe-fraction of these layers, while Mo and Cd preferentially accumulated in the Mn fraction (Müller et al. 2002).

Reference

Müller B., Granina L., Schaller T., Ulrich A. and Wehrli B. (2002) *Environ. Sci. Technol.* **36**, 411-420.

Studies of Archaean prokaryotic mat ecology, Belingwe Belt, Zimbabwe

N.V. GRASSINEAU¹, E.G. NISBET¹ AND C.M.R. FOWLER¹

¹Department of Geology, Royal Holloway, University of London, Egham, UK. (nathalie@gl.rhul.ac.uk, e.nisbet@gl.rhul.ac.uk, m.fowler@gl.rhul.ac.uk)

Detailed study of biological material in Archaean formations from the 2.7Ga Belingwe Greenstone Belt, Zimbabwe, has led to reconstructions of early microbial ecology. The work has been based on petrographic study of sedimentary facies, and on high resolution stable isotope analysis by CF-IRMS.

Sulphur and carbon analyses have been carried out on two very carbon- and sulphur-rich black shales of the Manjeri formation from three different drill cores. The overall results show remarkable isotopic heterogeneities. The range of $\delta^{13}C_{reduced}$ from -34.8 to -6.5‰, in samples with up to 18% carbon, indicates the signature of both rubisco and methanogenic archaea. Anoxygenic photosynthesis may also be recorded. In the S-isotope record on the same samples the large isotopic range within small distances (the largest spread in sulphur fractionation yet measured in an Archaean sequence) appears to record both sulphate reduction and sulphide oxidation parts of a sulphuretum cycle ($\delta^{34}S$ from -23.7‰ to +16.7‰). These rocks are the freshest Archaean biogenic material yet found and the isotopic diversity obtained can only be explained as the accidentally preserved products of microbial consortia.

This study has been extended by analysing also the carbonate and reduced carbon on different stromatolitic formations from the Belingwe Greenstone Belt and the 3.0Ga Steep Rock Group (Canada). The values obtained shows well established photosynthetic processes. Some results from the 3.5Ga Barberton Greenstone Belt, South Africa (collaboration with J. Kramer and C. Siebert), are also presented. Carbon isotopic compositions are around -20‰, might imply organic processes, and $\delta^{34}S$ measured are in a narrow range between 0 and +2‰.

The isotopic and sedimentary facies analyses identify microbial consortia and map out the prokaryotic Archaean ecosystem at 2.7Ga. Microbial mat consortia depend both on photosynthetic and non-photosynthetic processes. The results imply that hyperthermophile communities are of considerable antiquity, though it is not possible yet to show that they preceded photosynthesis. They also show a well established biological sulphur cycle. The extended study on earlier formations indicates that any microbial processes which were occurring at 2.7Ga might have been different in Early Archaean.

Mafic and ultramafic xenoliths from the Kaapvaal Craton (South Africa): trace element evidence for mantle magmatic and metasomatic processes.

M. GREGOIRE¹, D.R. BELL², A.P. LE ROEX²

¹UMR 5562, Observatoire Midi-Pyrénées, 14 Av. E. Belin, 31400, France, France (michel.gregoire@cnes.fr)

²Department of Geological Sciences, University of Cape Town, Rondebosch 7701 South Africa (drb@geology.uct.ac.za and alr@geology.uct.ac.za)

Kimberlite magmas from four well known kimberlite localities on the Kaapvaal craton (Bultfontein, Jagersfontein, Monastery and Premier) have sampled numerous mantle garnet lherzolites in addition to garnet harzburgites. The Bultfontein kimberlite has also sampled two main groups of phlogopite-rich mafic xenoliths which represent deep mantle segregations from high alkaline melts. The first group corresponds to MARID rocks characterised by the mineral association Mica-Amphibole-Rutile-Ilmenite-Clinopyroxene and the second group consists of PIC rocks characterised by the mineral association Phlogopite-Ilmenite-Clinopyroxene. The two groups are clearly distinguished from one another by the major element composition of their phlogopite and ilmenite, by the trace element content of their clinopyroxene and by their Sr and Nd isotope ratios. The combined major and trace element variations are interpreted to indicate a genetic relationship between the PIC rocks and Group I kimberlite magma, and between the MARID rocks and Group II kimberlite magma. The trace element compositions of clinopyroxenes of garnet lherzolites which are probably purely metasomatic are characterised by enrichment in LREE and LILE and by a relative depletion in Ti, Nb, Ta, and to a lesser extent Zr and Hf, i.e. the high field strength elements. But the LREE enrichment and the depletion in Nb and Zr (Hf) are less in the clinopyroxene of the group 1 variety than in those of the group 2 garnet lherzolites. Our study suggests that the melts responsible for the metasomatic imprints observed in the two groups of garnet lherzolites are probably high alkaline mafic silicate melts. Clinopyroxenes of group 1 that have trace element similarities to PIC rocks appear to have crystallized from, or been completely equilibrated with, a metasomatic agent related to Group 1 kimberlite magma. The case of the group 2 clinopyroxenes is more ambiguous and we consider three possible ways to explain their formation: 1. By an ancient metasomatic event, such as that recorded in harzburgitic inclusions in diamond or Mg-rich garnet peridotites, 2. By the remobilization of such ancient cratonic mantle in the form of low degree melts that may give rise to both MARID xenoliths and associated metasomatism, 3. By the infiltration and metasomatism of the lithosphere by MARID and/or group II kimberlite-like melts derived from external sources.

Antimony and lead pollution in the soil of shooting ranges

M. GRESCH, P. OSCHWALD, I. RYTZ, P. SYDLER, B. WETTSTEIN, B. MERGENTHALER, T. RICHNER, W. ATTINGER, A. GRÜNWALD, A. BIRKEFELD, U. WINGENFELDER AND G. FURRER

ITOE, ETHZ, Grabenstr. 3, CH-8952 Schlieren (greschm@student.ethz.ch), (oschwaldp@student.ethz.ch), (irytz@student.ethz.ch), (sydlerp@student.ethz.ch), (wettsteb@student.ethz.ch), (mbianca@student.ethz.ch), (attinger@ito.umnw.ethz.ch), (gruenwald@ito.umnw.ethz.ch), (birkefeld@ito.umnw.ethz.ch), (wingenfelder@ito.umnw.ethz.ch), (furrer@ito.umnw.ethz.ch)

Introduction

In Switzerland, virtually every village has one or several shooting ranges. In average, there is one shooting range per 3'000 inhabitants. Due to noise abatement regulations, many old shooting stands will be abandoned in the next years. Public concern arises with respect to future risks for soil, ground water, animals and humans. Most attention should be given to Pb and Sb in the gun bullets (approximately 75 and 2 % weight, respectively), which readily disintegrate in oxic soil environments. Polluted sites typically contain 10-50 tons Pb and 0.2-1.0 tons Sb.

Results

Among the resulting Pb(II), Sb(III) and Sb(V) species, Sb(OH)₆⁻ is probably the most mobile species under typical soil conditions. However, a lot of Sb is found to be adsorbed to poorly crystalline iron hydroxides. Antimony can easily be mobilised when the iron solids are dissolved. We also found that elution of polluted soil material from shooting ranges with pure water causes substantial leaching, even after a series of 45 treatments with neutral water (Mergenthaler and Richner, 2002).

Conclusion

In general, we can state that Sb pollution in shooting ranges bears a higher long-term risk for the ground water quality than Pb pollution. However, lead contamination in the top soil of shooting ranges can acutely affect health of animals and humans upon oral uptake of contaminated soil material.

References

- Mergenthaler B. and Richner T. (2002), *Diploma theses*. ETH Zurich.
 Gresch M. and Wettstein B. (2002), *Student research project*. ETH Zurich.
 Oschwald P., Rytz I. and Sydler P. (2002), *Student research project*. ETH Zurich.

The Natural Production of Organohalogen Compounds

GORDON W. GRIBBLE

Department of Chemistry, Dartmouth College, Hanover, New Hampshire, 03755 USA grib@dartmouth.edu

More than 3600 organohalogen compounds, mainly containing chlorine and/or bromine, are either produced by living organisms or are formed during natural abiogenic processes such as volcanoes, forest fires, and geothermal processes. The ocean is the greatest single source of natural organohalogens and myriad sponges, corals, seaweeds, tunicates, nudibranchs, bacteria, and other marine organisms produce such compounds. Terrestrial plants, fungi, lichen, bacteria, and insects are also significant producers of organohalogen compounds. Nearly all types of organic compounds are represented, including alkanes, aromatic hydrocarbons, phenols, pyrroles, indoles, fatty acids, terpenes, peptides, steroids, alkaloids, acetogenins, furans, and dioxins. Some of the halogenated byproducts of the mammalian immune system, which uses chlorine and bromine to fight infection, have been identified. Dioxins are now recognized to have several natural sources. The first examples of natural bioaccumulative compounds have been discovered in seabirds. Clearly, nature employs halogen as a basic building block to construct essential molecules for survival of the particular organism. The notion that these thousands of unique organohalogens are isolation artifacts or are the result of anthropogenic activities can now be dismissed. This presentation will discuss recent developments as to the origin and abundance of these natural halogenated chemicals.

Geochemical Characteristics of the Mantle Plume at the Eifel

E. GRIESSHABER¹, S. NIEDERMANN², U. SCHULTE¹, P. MÖLLER² AND P. DULSKI²

¹ Inst. f. Geol. Min. Geophys., Ruhr-Universität Bochum, erika.griesshaber@ruhr-uni-bochum.de, ulrike.schulte@ruhr-uni-bochum.de

² GFZ Potsdam, Telegrafenberg, Potsdam, nied@gfz-potsdam.de, pemoe@gfz-potsdam.de, dulski@gfz-potsdam.de

Introduction

The Eifel with its Tertiary and Quaternary volcanic fields is not only the youngest volcanic province in Central Europe but also one of the most geodynamically active area between the European Alps and the North Sea. These geodynamic phenomena are triggered by the presence of a mantle plume, which has been identified as a columnar low P-velocity anomaly in the upper mantle with a lateral contrast of up to 2 %. This structure is about 100 km wide, it extends to at least 400 km depth and is equivalent to about 150-200 K excess temperature (Ritter et al. 2001). One of the surface expressions of volcanism and geodynamic activity is the presence of numerous mineral and CO₂-gas rich springs and dry CO₂-gas emanations.

Results and Discussion

At present the Eifel districts are among the major CO₂-gas producing regions in Europe. There is an overabundance of CO₂-gas rich springs, which cover a much larger area than the Tertiary and Quaternary volcanism. Isotopic compositions of carbon, helium, neon and argon, as well as REE, anion and cation concentrations have been determined in highly CO₂-gas rich groundwaters following a cross-section covering both the rim and the central part of the mantle plume. In general, the isotope and concentration data show distinct geochemical differences between the East and the West Eifel districts, with considerably higher enrichments of the mantle signature in the West Eifel than in the East Eifel. Furthermore, rare gas isotope data provide unambiguous evidence for the presence of a plume type noble gas component in CO₂-gases from the southern section of the West-Eifel, as their Ne isotopic signature is similar to that of the Hawaiian plume. In contrast, MORB-like noble gas signatures prevail in the East- and the Hocheifel. Another important feature is the extensive occurrence of CO₂ emanations outside of the volcanic West Eifel. Thus, even though CO₂ and magmas might originate from similar mantle depths, CO₂ at the Earth's surface often serves as a better indicator for active mantle processes than volcanism because it is produced at the very beginning of melting, well before melt segregation occurs, and the ascent of CO₂-gas to the surface is not stopped at the crustal base due to loss of buoyancy (Griesshaber et al 2002).

Griesshaber E., Nüsslein M., Baumüller D. and Job R. (2002): Carbondioxide fluxes from the mantle plume in the Eifel. Manuscript in preparation.

Ritter J.R.R., Jordan M., Christensen U.R. and Achauer U. (2001): Earth Planet.Sci.Lett., 186, 7-14, 2001.

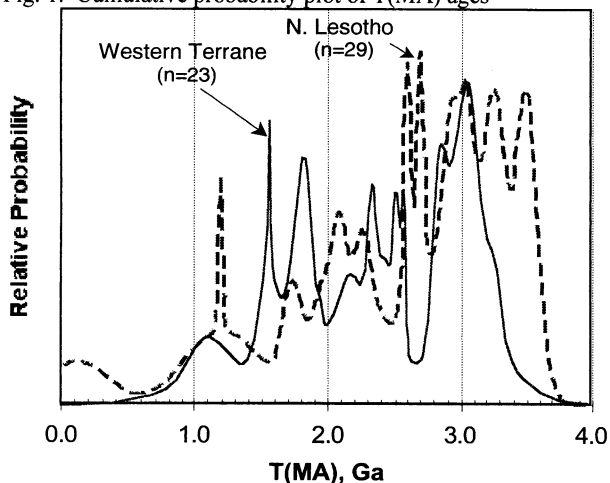
***In situ* Re-Os dating of sulfides in Kaapvaal xenoliths**

W.L. GRIFFIN, S.Y. O'REILLY, N.J. PEARSON AND
S. GRAHAM

GEMOC Key Centre, Earth and Planetary Sciences, Macquarie
University, NSW 2109, Australia (bill.griffin@mq.edu.au)

In situ Re-Os isotopic analyses (Pearson et al., 2002) have been obtained on >100 sulfide grains exposed by serial sectioning of xenoliths from N. Lesotho (n=10), and from Finsch (n=5) and Kimberley (n=7), representing the subcontinental lithospheric mantle (SCLM) beneath the SE Terrane (SET) and the Western Terrane (WT), respectively, of the Kaapvaal Craton. Sulfides can be broadly divided into two groups: (1) high Os, low Re/Os and Pt/Os, $\gamma_{Os} < 1$; (2) low Os, low to high Re/Os, high Pt/Os, γ_{Os} to +300. These correspond to the "enclosed" and "interstitial" groups of Alard et al. (2000), but both types may occur enclosed in primary silicates, reflecting recrystallisation in the SCLM. The age distribution of sulfides with $^{187}Re/^{188}Os < 0.08$ and $Pt/Os < 0$, interpreted as MSS residual from melting or crystallised from sulfide melts show distinct differences between the terranes (Fig. 1). The SET data extend to older ages, mirroring the differences in maximum crustal age. Distinct spikes at 2.7-2.8 Ga in the SET, and 2.4-2.5 Ga in the WT, reflect the time when each terrane joined the craton. The abundance of mid-Proterozoic ages in the WT relates to the rifting and compression of the western margin of the Kalahari Supercraton during this time. The peak of Archean ages in each locality overlaps only the oldest whole-rock ages of xenoliths from that locality. Whole-rock analyses of our samples give similarly mixed ages, reflecting the presence of >1 sulfide generation. These data push back the mean age of SCLM stabilisation for each terrane, and indicate the potential for correlating specific episodes of SCLM modification with crustal events on a terrane scale.

Fig. 1. Cumulative probability plot of T(MA) ages



References

- Alard et al. (2000) *Nature* **407**, 891-894
Pearson et al. (2002) *GCA* **66**, 1037-1050

Extreme unradiogenic Os isotopes in Hawaiian mantle xenoliths: implications for mantle convection

M. GRISELIN^{1,2} AND J.C. LASSITER^{1,3}

¹Max Plank Institut für Chemie, Postfach 3060, D55020
Mainz, Germany

²(griselin@mpch-mainz.mpg.de)

³(lassiter@mpch-mainz.mpg.de)

We have examined Os-isotope variations in a suite of lherzolite xenoliths from Salt Lake Crater (SLC; Oahu, Hawaiian Islands) in order to better constrain the extent and origin of Os-isotope heterogeneity in the oceanic lithosphere. Os-isotopes in the SLC xenoliths span a large range ($0.113 < ^{187}Os/^{188}Os < 0.129$) and extend to significantly less radiogenic values than previously reported in Abyssal Peridotites (AP, average $^{187}Os/^{188}Os = 0.125$). The samples also display a positive correlation between Pt/Os (0.9 - 2.7) and $^{187}Os/^{188}Os$.

We consider 3 options to explain the unradiogenic Os composition of the SLC xenoliths:

1- Xenoliths could sample sub-continental lithospheric mantle (SCLM). Such unradiogenic values have not previously been reported from oceanic settings but are common in SCLM xenoliths. However, at present there is no evidence to suggest that the Hawaiian xenoliths sample rafted or subducted SCLM (the olivine mode-composition correlation in the SLC xenoliths is similar to the trend defined by oceanic peridotites).

2- The SLC xenoliths have historically been thought to sample the oceanic lithosphere. However, their unradiogenic Os composition contrasts with the radiogenic values reported for AP. Although seawater alteration may have elevated the AP $^{187}Os/^{188}Os$, this process alone cannot account for the difference in average Os-isotopic composition between the SLC xenoliths and AP. $^{187}Os/^{188}Os$ values in other OIB xenoliths and leached Cr-spinel from AP are still significantly higher than in the SLC xenoliths. Another possible explanation for this discrepancy is that shallower portions of the oceanic upper mantle (i.e., the top of the melting column as sampled by AP and other OIB xenoliths) have had the $^{187}Os/^{188}Os$ values elevated through interaction with radiogenic melts. This hypothesis is supported by positive correlations between Pt/Os and $^{187}Os/^{188}Os$ observed in the SLC xenoliths and in some AP suites. This hypothesis would require either the presence of a large radiogenic component such as pyroxenite veins or disequilibrium melting at the grain scale.

3- Alternatively, the SLC xenoliths could derive from the Hawaiian plume. P-t estimates from a recent petrographic study of garnet-bearing SLC xenoliths are consistent with a high pressure (transition zone) origin of the xenoliths [1]. Previous isotopic studies [e.g., 2] showed that a recycled oceanic crust component is present in the Hawaiian plume. The Hawaiian xenoliths could represent a recycled piece of ~2 Ga old depleted oceanic lithosphere, i.e. the counterpart of the recycled oceanic crust.

Colloid-Facilitated Transport of Pollutants: Phenomena and Modeling

D. GROLIMUND¹, K. BARMETTLER², AND
M. BORKOVEC³

¹Swiss Light Source and Waste Management Laboratory, Paul Scherrer Institute, CH-5232 Villigen, Switzerland

²Swiss Federal Institute of Technology Zurich, Institute of Terrestrial Ecology, CH-8652 Schlieren, Switzerland

³Analytical and Biophysical Environmental Chemistry, University of Geneva, CH-1211 Geneva 4, Switzerland

Colloidal particles are being increasingly recognized as key components within geologic and aquatic environments. Such particles are involved in a broad variety of environmentally relevant processes. In subsurface systems, however, a considerable number of these processes have hazardous consequences. For example, colloidal particles are suspected to contribute to the mobility of pollutants by acting as mobile carriers. Recent field and laboratory studies pointed out the possible importance of this additional transport mechanism [e.g., 1, 2]. Therefore, considering potential hazardous incidents due to mobilized colloidal particles should represent a critical task in risk assessment of any subsurface contamination problem, in the development of remediation strategies, as well as in recharge and waste water management. However, available knowledge concerning the physical and chemical characteristics of such environmental colloids as well as the processes determining their release and mobility in natural porous media is still limited.

In order to judge or predict the susceptibility of a subsurface system to the phenomena of enhanced contaminant transport by mobile colloidal particles, a detailed understanding of the following processes is required: (i) the generation of mobile colloidal particles, (ii) the life-time of these particles within the system, and (iii) the association of the contaminant with the mobile particles.

In the present paper various aspects of the diverse problem of enhanced contaminant transport by *in-situ* mobilized colloid particles will be addressed. The discussion will be based on a comprehensive set of laboratory-scale experiments, which were performed in order to investigate relevant fundamental processes such as particle mobilization, particle deposition and transport as well as multicomponent (colloid-facilitated) contaminant transport phenomena. The resulting knowledge about mechanism and dynamics of each process obtained by these individual experimental investigations were compiled and incorporated into an extended contaminant transport model. This model was used to simulate and analyze or predict complex contaminant transport experiments where *in-situ* mobilized colloidal particles have been proven to be a dominant transport pathway for environmental pollutants.

[1] Grolimund D. et al., (1996), *Env. Sci. Technol.*, **30**, 3118.

[2] Kersting A.B. et al., (1999), *Nature*, **397**, 56.

Spatial and temporal trends for sediment-associated metal contamination in the Seine River Basin (France)

C. GROSBOIS¹, M. MEYBECK², A. HOROWITZ³

1. Laboratoire LASEH, Univ. de Limoges. 123 av. A.

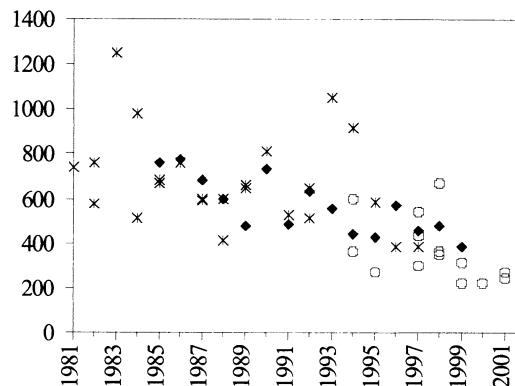
Thomas, Limoges, France (cecile.grosbois@unilim.fr)

2. Laboratoire Sisyphe, UMR 1367, 4 Place Jussieu, Paris, France (meybeck@biogeodis.jussieu.fr)

3. US Geological Survey, 3039 Amwiler Road, Atlanta, GA USA (horowitz@usgs.gov)

Since 1981, a multiple sample media approach (bed sediments-BS, recent flood deposits-RFD, trapped and filtered suspended matter-SPM).has been used to determine spatial and temporal sediment-associated trace element trends. These programs span more than 20 years, and cover the entire Seine River Basin (SRB). The SRB displays a wide range of sediment-associated trace element concentrations. In the early 1980's, the SRB probably was among one of the most anthropogenically impacted basins in the world. Trace element maxima, observed in BS surveys, correspond to contamination factors of 247 for Hg, 93 for Cd, 57 for Cu, 30 for Pb and 22 for Zn, throughout the SRB. Since the early 1980's, there has been a marked decline in the concentrations of all these trace elements, both upstream and downstream of Paris (Figure 1) as well as at the mouth of the Oise River. This substantial improvement probably can be attributed to a generalized reduction in trace element inputs from both industrial and domestic sources. One of the most marked examples of this reduction was observed in the trace element composition of discharges from the Seine Aval plant, the world's 2nd largest wastewater treatment facility. Upstream of Paris and at the mouth of the Marne River, temporal declines in sediment-associated trace element concentrations are not as marked. This probably results because anthropogenic impacts (population densities, industrialization, agriculture impacts) always were lower in this area of the SRB, relative to the Metropolitan Paris.

Figure 1: Temporal changes in sediment-associated Zn concentrations (mg/kg) at Poses, the last lock on the Seine River prior to the estuary, in various sample media [SPM (♦), BS (stars), RFD (O)]



Sorting out contributions from slab and mantle wedge in arc magmas

TIMOTHY L. GROVE¹

¹Dept. of Earth, Atm. And Planetary Sci., Massachusetts Institute of Technology, 54-1220, Cambridge, MA 02139, USA, tlgrove@mit.edu

The trace element abundances and isotopic compositions in primitive lavas from the Mt. Shasta region, N. California are used along with estimates of pre-eruptive H₂O contents and constraints from experimental petrology to infer the contributions from the mantle wedge and subducted slab. Approximately 90 wt. % of the major elements of the primitive Shasta region lavas are derived from the mantle wedge. In contrast, > 99 wt. % of the large ion lithophile (LIL) and the light rare earth elements (LREE) are contributed by an H₂O-rich component derived from the subducted oceanic lithosphere. Critical to the modelling are estimates of the pre-eruptive water contents. In the Shasta region lavas contain from <1 to >10 wt. % H₂O. Evidence from experimental petrology indicates that the high H₂O content lavas were extracted as melts from a harzburgitic residue at shallow mantle depths (30 km). Magmatic water content and modelled trace element abundances in the mantle source are used to carry out a mass balance for the relative contributions from the slab-derived fluid-rich component. Estimated fluid-rich component compositions are characterized by strong light rare earth element (LREE) enrichments ([La/Gd]_N = 3 to 7) and variable heavy rare earth element (HREE) depletions ([Dy/Yb]_N = 1 to 3). Sr and Ba abundances vary by approximately a factor of 2.5 among the fluid compositions. The calculated isotopic composition of the fluid-rich component is bimodal. One component has ⁸⁷Sr/⁸⁶Sr = 0.7028 and εNd = +8, and is most similar to a MORB source. The second component has more radiogenic ⁸⁷Sr/⁸⁶Sr = 0.7038 and εNd = +1 and is most similar to a sediment. The major elements in the fluid-rich component are: H₂O (~55-68 wt. %), Na₂O (~25-33 wt. %) and K₂O (~5-13 wt. %). The fluid-rich component could be either a supercritical fluid or a low-degree melt of slab eclogite that has reacted with the overlying mantle wedge. Although the slab beneath Mt. Shasta is inferred to be hot (~600 – 650 °C), the calculated fluid-rich components do not resemble a pure slab melt. These fluid-rich components probably represent a mantle-wedge-modified mixture of fluids and/or melts from a heterogeneous source (serpentinized mantle, altered basalt, and sediment).

Influence of H₂O on the development of spinifex textures in komatiites

TIMOTHY L. GROVE¹, STEPHEN W. PARMAN¹, PALLAVI NUKA¹, MAARTEN DEWIT² AND JESSE DANN¹,

¹Dept. of Earth, Atm. And Planetary Sci., M.I.T. 54-1220, Cambridge, MA 02139, USA, tlgrove@mit.edu

²Dept. of Geol. Sci., Univ. of Cape Town, Rondebosch 7700, South Africa

We performed cooling rate experiments to evaluate the role of variable crucible size and magmatic H₂O on the development of olivine spinifex textures. Experiments were cooled from the dry and wet liquidus at rates between 100 and 3 °C/hr. Increasing crucible volume decreases the number of nucleation sites and leads to the growth of spinifex olivine at anhydrous conditions. The presence of H₂O increases growth rate and decreases nucleation rate dramatically, and also promotes the development of spinifex textures. When experiments are compared to field exposures of spinifex in the 3.5 Ga Komati formation, evidence supports conductive cooling at the upper chill margin. One set of experiments used a variety of sizes and types of crucibles: olivine single crystals, MgO, Al₂O₃, AuPd and Pt capsules and loops, varying from 0.01 to 60 ml in volume. Decreasing crucible volume promotes heterogeneous nucleation of liquidus olivine by increasing the surface area available for heterogeneous nucleation sites. In small volume capsules (0.01 – 0.7 ml) at anhydrous conditions hundreds of small (0.1 to 1 mm) equant and hopper olivine crystals grew at slow cooling rates (3 °C/hr). In the 60 cc crucible, where surface area is at the minimum, we produce 18 to 33 mm x 0.3 mm branching spinifex-like olivine crystals at slow (3 °C/hr) cooling under anhydrous conditions. We also carried out cooling rate experiments at 200 MPa, H₂O-saturated. In the hydrous cooling experiments spinifex-like olivine crystals develop, even in the small capsule volume. In a 0.04 ml AuPd alloy capsule, seven 5 x 0.2 mm olivines filled the melt volume. Previous explanations of olivine spinifex textures in komatiites have called upon large amounts of superheat and rapid cooling to produce spinifex textures. At Barberton the komatiite chill margins contain equant olivine microphenocrysts, indicative of emplacement at supercooled conditions. The coarsest and largest spinifex crystals (300 to 500 μm long) grow in the slowest cooled centers of cooling units (2 m from the upper chill). The field observations eliminate rapid cooling from superliquidus temperatures as a mechanism for spinifex formation. Large crystals will grow at slow cooling rates if nucleation rate is lowered and growth rate is enhanced. The presence of H₂O accomplishes this by depolymerising melt structure and decreasing melt viscosity. Moreover, the large amount of H₂O dissolved in the komatiite melt lowers the liquidus and enhances undercooling in the cooling units when the magma is emplaced at a lower pressure at its site of final solidification.

Rare earth element geochemical constraints on the genesis of the Woxi W-Sb-Au deposit, South China

X. X. GU¹, O. SCHULZ², F. VAVTAR² AND J. M. LIU³

¹ Institute of Geochemistry, Chinese Academy of Sciences, Guiyang, P.R. China (xuexiang_gu@263.net)

² Institute of Mineralogy and Petrography, University of Innsbruck, Innsbruck, Austria (franz.vavtar@uibk.ac.at)

³ Institute of Geology and Geophysics, Chinese Academy of Sciences, Beijing, P.R. China

Introduction

The Proterozoic turbidite-hosted, laminated, stratiform W-Sb-Au ores of the Woxi deposit in South China have been the subject of continued debate in regard to the timing of mineralization. Early workers considered the ores to be a distal portion of magmatic systems, while later researchers have argued for a synmetamorphic replacement origin.

Mineralization at Woxi occurs predominantly (>70 %) as stratiform ore layers and subordinately as stockwork veinlets. The former consists of rhythmically interbedded, well-laminated stibnite, scheelite, quartz, pyrite and silty clays, whereas the latter occurs immediately beneath the stratiform ores and is characterized by numerous quartz + pyrite + gold + scheelite stringer veinlets subvertical to the overlying ore layers (Gu et al., 2002).

Rare earth element geochemistry is used here to demonstrate that a synsedimentary exhalative (sedex) origin is likely for the Woxi deposit.

Results and discussion

Stratiform ores, individual quartz bands and clay bands exhibit a wide range of ΣREE (4-200 ppm), Eu/Eu^* (0.6-1.1), and $\Sigma\text{LREE}/\Sigma\text{HREE}$ (3.6-14.2). However, their REE-patterns are comparable overall with the host rocks.

Fluid inclusions in banded quartz have a uniform REE-pattern, with low but variable ΣREE (3-116 ppm), LREE enrichment ($\Sigma\text{LREE}/\Sigma\text{HREE} = 6-16$), and insignificant Eu-anomalies ($\text{Eu}/\text{Eu}^* = 0.9-1.2$). In contrast, fluid inclusions in stringer quartz display a marked HREE enrichment ($\Sigma\text{LREE}/\Sigma\text{HREE} = 0.18$). Except for no negative Eu anomaly, the general pattern for the average fluid is similar in the shape to those of the average banded ore in the deposit, the banded tourmaline-rich exhalative rocks at Sullivan, the stratiform sedimentary exhalites of the Dachang Sn-polymetallic ore deposit in Guangxi, and seawater.

Conclusions

The rare earth element geochemistry provides strong evidence for a synsedimentary exhalative model whereby the stratiform ores formed from metalliferous basinal brines episodically released along diffuse feeder zones.

References

Gu X.X., Schulz, O., Vavtar, F., Liu, J.M., and Zheng, M.H., (2002), *Arch. f. Lagerst.forsch. Geol. B.-A.* 23, 210 p.

Thorium and protactinium sorption on silica and carbonate

CELINE GUÉGUEN AND LAODONG GUO

International Arctic Research Center, University of Alaska Fairbanks, AK 99775, USA (celine@iarc.uaf.edu)

Thorium (Th-234, Th-230, and Th-228) and protactinium (Pa-231) are naturally occurring radionuclides in the U/Th decay series. Due to their particle-reactive nature, these isotopes have long been used as tracers in geochemical and oceanographic investigations, such as organic carbon export fluxes, ocean circulation, boundary scavenging, and paleoproductivity. However, the interactions of Th(IV) and Pa(IV, V) with marine particles and their scavenging pathways in the ocean are not well understood. Whether the adsorption or removal process is a non-selective or selective reaction and whether there is fractionation on Pa/Th ratio due to different particle types or chemical composition are important questions needed to be addressed for better use Th and Pa as geochemical tracers.

Radiotracers, Th-234 and Pa-233, were used in batch experiments to examine the adsorption processes of Th(IV) and Pa(IV, V) on amorphous silica and calcium carbonate in artificial seawater. Aliquots of the suspensions were filtered (0.4 μm polycarbonate filter, Millipore), and Th-234 and Pa-233 activities were measured in the filter-retained particles and in the filtrate. Systematic experiments were performed to evaluate the effects of kinetic and pH on sorption processes.

The sorption kinetic of Pa-233 on silica was faster than that of Th-234, while the sorption on carbonate was faster for Th-234 than for Pa-233. While there was a fractionation of Pa/Th on silica surfaces, fractionation of Th/Pa on carbonate was much significant. In other words, Th(IV) seems preferentially sorb on carbonate surfaces and silica had higher affinity for Pa. Results on the effect of pH showed that, for the same solid phase, optimal sorption occurred at lower pH, with a sorption edge at lower pH for Th than for Pa. However, the maximum adsorption for both Th and Pa are all at $\text{pH} > 7$ on both silica and carbonate. These results suggest that the nature of sorbent, and adsorption time could affect the distribution of Th and Pa, whereas in the natural seawater pH range, the pH effects on Th and Pa sorption were minor.

Origin of lamprophres in the Xikuangshan Antimony Deposits, Hunan, P.R. China: evidence for combined trace element with Sr and Nd isotope studies

GUIQING XIE^{1,2}, AND RUIZHONG HU¹

¹Open laboratory of ore deposit geochemistry, Institute of geochemistry, C. A.S., China(xieguiq@sohu.com)

²Graduate School, C. A. S., China

Introduction

The Xikuangshan antimony deposits located in Hunan province, the center part of China, which have about 2110,000 ton total Sb metal reserves, is the largest Sb deposits in the world till now. The lamprophres located at the east part of mine are only outcropped igneous rocks in the mine districts, little work has been done on its origin in the previous work. The article will discuss genesis of lamprophres through trace element and Sr and Nd isotope studies.

Discussion

The lamprophres studied were formed ca 120Ma ago, simultaneous last stage mineralization(124.1±3.7Ma,Sm-Nd of hydrothermal calcites), and are considered to be closely related to antimony mineralization in the Xikuangshan deposits. The MORB-normalized spidergrams of sample studied are characterized by enrichment high field element, depleted Nb-Ta and non depleted Ti, strong enrichment Th and weak enrichment Ce ,being similar to spidergrams of volcanic arc basalt, their tectonic setting probably are destructive plate boundaries of within continent. The rare-earth element of sample studied have characteristics of high total contents (375-531ppm) and non-distinct Eu anomalies (0.85-0.98) and enriched LREE. The isotopic contents of sample have high ⁸⁷Sr/⁸⁷Sr (0.7098-0.7109) and low ¹⁴³Nd/¹⁴⁴Nd(0.51205-0.51244).

Conclusions

Combining trace element and isotope geochemistry with geological history, the lamprophres studied in the area result from partly melting of enrichment REE and HSFE fluid related to subduction metasomatic mantle, mixing with little underlying granite and limestone compositions.

References

- Guiqing Xie, Jiantang Peng and Ruizhong Hu ,et al, (2001),Acta Petrologica Scinica,4,629-636.
Jiantang Peng, Ruizhong Hu and Yuanxian Lin,et al, (2002), Chinese Science Bulletin,12.

Origin of lamprophres in the Xikuangshan Antimony Deposits, Hunan, P.R. China: evidence for combined trace element with Sr- and Nd- isotope studies

GUIQING XIE^{1,2}, AND RUIZHONG HU¹

¹Open Laboratory of Ore Deposit Geochemistry, Institute of Geochemistry, C. A.S., China(xieguiq@sina.com)

²Graduate School of the Academy of Chinese Academy of Sciences, China

Introduction

The Xikuangshan antimony deposits located in Hunan province, the center part of China, which have about 2110,000 ton total Sb metal reserves, is the largest Sb deposits in the world till now. The lamprophres located at the east part of mine are only outcropped igneous rocks in the mine districts, little work has been done on its origin in the previous work. The article will discuss genesis of lamprophres through trace element and Sr- and Nd- isotope studies.

Discussion

The lamprophres studied were formed ca 120Ma ago, simultaneous last stage mineralization(124.1±3.7Ma,Sm-Nd of hydrothermal calcites), and are considered to be closely related to antimony mineralization in the Xikuangshan deposits. The MORB-normalized spidergrams of sample studied are characterized by enrichment high field element, depleted Nb-Ta and non depleted Ti, strong enrichment Th and weak enrichment Ce ,being similar to spidergrams of volcanic arc basalt, their tectonic setting probably are destructive plate boundaries of within continent. The rare-earth element of sample studied have characteristics of high total contents (375-531ppm) and non-distinct Eu anomalies (0.85-0.98) and enriched LREE. The isotopic contents of sample have high ⁸⁷Sr/⁸⁷Sr (0.7098-0.7109) and low ¹⁴³Nd/¹⁴⁴Nd(0.51205-0.51244).

Conclusions

Combining trace element and isotope geochemistry with geological history, the lamprophres studied in the area result from partly melting of enrichment REE and HSFE fluid related to subduction metasomatic mantle, mixing with little underlying granite and limestone compositions.

References

- Guiqing Xie, Jiantang Peng and Ruizhong Hu ,et al,(2001),Acta Petrologica Scinica,4,629-636.
Jiantang Peng, Ruizhong Hu and Yuanxian Lin,et al,(2002),Chinese Science Bulletin,12.

Combined Sr and Cs exchange in a natural clinoptilolite

MICKEY E. GUNTER¹ AND JENNIFER L. PALMER²

¹ Department of Geological Sciences, University of Idaho, Moscow ID 83844 USA (mgunter @ uidaho.edu)

² Journal of the American Chemical Society, 315 South 1400 East, Salt Lake City UT 84112 USA (jlpalmer @ hotmail.com)

Introduction

The natural zeolite, clinoptilolite, $(\text{Na,K})_6\text{Al}_6\text{Si}_{30}\text{O}_{72} \cdot 20\text{H}_2\text{O}$, is useful in industry for its cation exchange capabilities. Because of its selectivity for certain cations, clinoptilolite has been used for the removal of Cs and Sr from low-level radioactive waste solutions. Since its opening in 1985, British Nuclear Fuels' Site Ion Exchange Effluent Plant (SIXEP) has been responsible for the removal of ⁹⁰Sr and ^{134,137}Cs from radioactive cooling-pond waters by use of clinoptilolite filtering beds. The clinoptilolite does not achieve full exchange with Sr and Cs before Sr breakthrough occurs (Sr stops exchanging with the clinoptilolite), making Sr the limiting factor in the life of the exchange beds.

Experimental design

A clinoptilolite-rich rock from the Mud Hills formation near Barstow, California was used in this study to determine the exchange behavior of clinoptilolite in the presence of varying concentrations of a mixture of Sr and Cs at varying temperatures and times. Twenty samples were generated by placing 4 g of clinoptilolite in contact with 100 mL of 0.01 M $\text{SrCl}_2 \cdot 6\text{H}_2\text{O}$ and 0.01 M CsCl. An additional 20 samples were generated by placing 4 g of clinoptilolite in contact with 0.001 M $\text{SrCl}_2 \cdot 6\text{H}_2\text{O}$ and 0.001 M CsCl. Samples were then treated at 5, 21, 50, and 90°C for 0.5, 5, 24, 240, and 720 h. Samples were vacuum-filtered to remove solids. Twenty DI samples were also created by adding 4 g of clinoptilolite to 100 mL deionized water and storing them for the same period of time and at the same temperatures. Sample solutions were analyzed for the outgoing cations Na^+ , K^+ , Mg^{2+} , and Ca^{2+} and for remaining Sr^{2+} by ICP-AES. Solutions were also analyzed by AAS for the remaining Cs^+ .

Results and conclusions

Significant concentrations of Na and K are removed from the mineral in the DI samples, and to greater extents with time and temperature. In the 0.01 and 0.001 M samples, monovalent cations leave the mineral to greater extents with time and temperature, whereas divalent cations leave the mineral to greater extents with decreasing temperature. None of the outgoing cations occur in the solutions in concentrations as high as are available in 4 g of clinoptilolite. However, within 720 h of treatment, approximately all of the Sr and Cs in the original solutions is either absorbed into or adsorbed onto the mineral. Clinoptilolite exhibits a selectivity for Cs over Sr. Overall exchange of cations increases with increasing time and temperature.

Isotope ratio measurements on transient signals by an online coupled HPLC-MC-ICP-MS system

I. GÜNTHER-LEOPOLD, B. WERNLI AND Z. KOPAJTIC

Paul Scherrer Institut, Laboratory for Materials Behaviour, 5232 Villigen PSI, Switzerland (guenther@psi.ch; beat.wernli@psi.ch; zlatko.kopajtic@psi.ch)

Introduction

Coupling of sample introduction devices necessary for chemical speciation (Krupp et al., 2001), sample preconcentration (Evans et al., 2001), separation of the sample matrix or removing of interferences (Röllin et al., 1996) leads to transient signals, often of short duration. However, the best precision for isotope ratios is obtained using steady-state signals of several minutes or longer.

The objective of the study was to determine the precision and accuracy of isotope ratios on transient signals which are achieved by online coupling of a high performance liquid chromatography (HPLC) to a multicollector inductively coupled plasma mass spectrometer (MC-ICP-MS).

Experimental

A Dionex HPLC system (GS50, 25 µl injection loop, 0.25 ml/min flow rate) was connected to the MC-ICP-MS "Neptune" (ThermoFinnigan). Since the MC-ICP-MS at the Paul Scherrer Institut will be mainly used for the characterisation of nuclear fuel samples the study was restricted to transient signals of U (main component in nuclear fuels) and Nd (burn-up monitor). Samples containing U or Nd in different concentrations were injected via a Rheodyne valve and eluted with 1 M HCl or with a gradient of α-hydroxyisobutyric acid, respectively. Typical transient signals for both elements last about 30 to 60 s.

Results and discussion

The precision and accuracy of the U and Nd measurements as a function of the elemental concentration and the integration time will be presented in comparison with results achieved on steady-state signals of the same intensity for both elements. The discussion of the results will be focussed on the question if the simplification of the sample preparation procedure (especially for nuclear materials: high risk of contamination, high dose rate for the operator) obtained by the coupling is offset by a reduction in precision resulting from measurements of short transient signals.

References

- Evans R.D., Hintelmann H. and Dillon P.J., (2001), *J. Anal. At. Spectrom.* **16**, 1064-1069.
 Krupp E.M., Pécheyran C., Meffan-Main S. and Donard O.F.X., (2001), *Fresenius J. Anal. Chem.* **370**, 573-580.
 Röllin S., Kopajtic Z., Wernli B. and Magyar B., (1996), *J. Chromatogr. A* **739**, 139-149.

High precision measurement of Ti isotopes in terrestrial and extraterrestrial materials

Y. GUO¹, A. MAKISHIMA^{1,2}, X.K. ZHU¹, N.S. BELSHAW¹, R.K. O'NIONS¹ AND S. S. RUSSELL³

¹ Department of Earth Sciences, Oxford University, Parks Road, Oxford, OX1 3PR, UK (Yueling@earth.ox.ac.uk)

² Institute for Study of the Earth's Interior, Okayama University at Misasa, Tottori-ken, 682-0193, Japan

³ Department of Mineralogy, The Natural History Museum, Cromwell Road, London, SW7 5BD, U.K.

Ti is an element of considerable geochemical and cosmochemical importance. But its isotope system remains largely unexplored due to the lack of suitable analytical techniques. Here we report high precision results of Ti isotopes in both terrestrial and extraterrestrial material, of Ti isotopes using MC-ICPMS.

To avoid potential matrix effects and isobaric interferences, a three-column procedure has been developed for Ti purification. The first column uses an anion exchange resin, where Ti, Zr and Hf are separated from the other major and trace elements. In the second column, Ti is separated from Zr and Hf using U/TEVA resin. Trace amounts of Al and P are further removed using the same anion exchange resin in a third column.

After chemical purification, Ti isotope ratios are measured using a Nu Instruments MC-ICPMS with a standard-sample bracketing approach. Solutions of standard and samples are introduced into the mass spectrometer through a Cetac MCN6000 desolvation nebulizer in 0.1M HF. The Ti isotope results are expressed in ϵ units which are deviations in parts per 10⁴ from the Ti isotope reference material:

$$\epsilon^x\text{Ti} = \left(\frac{{}^x\text{Ti}_{\text{sample}}}{{}^x\text{Ti}_{\text{standard}}} - 1 \right) \times 10000$$

where ${}^x\text{Ti}_{\text{sample}}$ and ${}^x\text{Ti}_{\text{standard}}$ are measured ratios of ${}^x\text{Ti}/{}^{46}\text{Ti}$ for the sample and the standard, respectively, and x denotes a mass number of 47, 48, 49 or 50. The long-term repeatability (2SD) is 0.4, 0.6, 0.7 and 0.8 ϵ units for $\epsilon^{47}\text{Ti}$, $\epsilon^{48}\text{Ti}$, $\epsilon^{49}\text{Ti}$ and $\epsilon^{50}\text{Ti}$, respectively.

A number of natural samples have been analysed, including basalts, mantle xenoliths, loess, and bulk chondrites and achondrites. An overall variation of ca. 15 $\epsilon^{50}\text{Ti}$ units has been observed. When plotted on a multiple isotope diagram, the Ti isotope results of the natural materials fall on the same lines with those resulting from instrumental mass fractionation. This correlation is consistent with theoretical expectation if the Ti isotope composition of the analysed materials evolved from a single isotopically uniform source in a mass-dependent manner.

The new techniques reported here makes possible for the first time the measurement of both mass-dependent fractionation and anomalies of Ti isotopes to high precision. The project in progress will make further investigation of Ti isotope compositions in meteoritic materials of chondrules and CAIs. Those results are expected to provide important new insights into processes of early solar system evolution.

Geochemical Information of Ore fluid from Fluorite in Qinglong Antimony Deposit, Southwest Guizhou, China

WANG GUOZHI^{1,2} HU RUIZHONG¹

1. Open Laboratory of Ore Deposit Geochemistry, Institute of Geochemistry, C A S, Guiyang, 550002, China (Wanguozhi66@163.net)

2. Chengdu College of Technology, Chengdu, 610059, China

Geologic Setting

The Qinglong antimony deposit is located on the platform near the northwest margin of Youjiang Basin, southwest Guizhou, China. Stratabound antimony and paragenetic fluorite deposits were found on paleokast surface between lower and upper Permian.

REE and Sr Isotope Geochemistry

The fluorite is origin of hydrothermal processes. The REE partition pattern for the fluorite shows depleted LREE, enriched MREE and HREE, and negative anomaly for Ce (Ce: 0.46~0.76). From early to final stage fluorite, the REE content decreased from (11.62~26.538) $\times 10^{-6}$ to 6.911 $\times 10^{-6}$ and enriched more LREE, Eu developed from negative anomaly (ϵ_{Eu} : 0.72~0.89) to positive anomaly (ϵ_{Eu} : 4.47). The reduced and oxidized conditions were responsible for the negative and positive Eu anomaly, respectively. The fact that Ce anomaly did not change with oxidized and reduced condition implies that ore fluid is basin fluid, which inherited negative Ce anomaly of seawater.

$^{87}\text{Sr}/^{86}\text{Sr}$ of two fluorite samples (0.71038, 0.70829) were much different from that of their host rock (0.73733), it indicated that ore fluid is introduced fluid.

Organic Geochemistry

Biomarkers such as normal alkane, isoprenoid alkane, terpane and sterane in extract of bitumen from the fluorite inclusions are similar to that in extract of kerogene (pyroclastic rock) from the Permian Linghao Formation in Youjiang Basin. It suggested that ore fluid was from Youjiang Basin.

Conclusion

Mineralization is related to lateral migration of basin fluid from Youjiang Basin to platform, there is an obvious change from reduced condition to oxidized condition from early to final mineralization stage.

Reference

Moller P., (1976), Mineral. Deposit. 11:111-116

SIMS study of $^{11}\text{B}/^{10}\text{B}$ in immiscible borosilicate glasses

A.A. GURENKO¹, I.V. VEKSLER¹, R. THOMAS¹,
A. MEIXNER¹, A.M. DORFMAN² AND D.B. DINGWELL²

¹ GeoForschungsZentrum Potsdam, Germany
(agurenko@gfz-potsdam.de)

² IMPG Ludwig-Maximilian University, Munich, Germany
(Dingwell@lmu.de)

Samples and objectives

In silicate melts B can form trigonal and tetrahedral species. Isotopic effects due to changes in B speciation are poorly constrained at high, magmatic temperatures. Our recent study of liquid immiscibility in the $\text{SiO}_2\text{-B}_2\text{O}_3\text{-Al}_2\text{O}_3\text{-CaO-Na}_2\text{O}$ system (Veksler et al., 2002) at 900-1350 °C employed centrifuge phase separation. Two immiscible melts were separated in distinct layers and quenched to glasses. According to electron microprobe analyses, one of the melts is composed mostly of SiO_2 with 12-20 wt% B_2O_3 , while the other is enriched in CaO and Na_2O , and contains 25-35 wt% B_2O_3 . Raman spectroscopy revealed strong differences between the conjugate melts in polymerisation and B speciation. The goal of the SIMS study was to evaluate the effects of two-liquid immiscibility and B speciation on $^{11}\text{B}/^{10}\text{B}$ in the conjugate glasses.

Analytical method

The centrifuged samples were analysed using the Cameca IMS 6f at the GFZ Potsdam. They were sputtered with a O⁻ primary beam ~10–15 µm in diameter, at 12.5 kV and ~0.3-0.5 nA. Secondary ions of $^{11}\text{B}^+$, $^{10}\text{B}^+$ and $^{30}\text{Si}^+$, accelerated at 10 kV, were analysed at a mass resolution $M/\Delta M \sim 1650\text{--}1700$ using a 150 µm contrast aperture. A 750 µm field aperture restricted the analysed area to the central part of the sputtered crater. Most measurements included 50 cycles. Typical internal precision (1σ counting statistic) was 0.5‰ for $^{11}\text{B}/^{10}\text{B}$ ratios, and 0.1‰ for $^{10}\text{B}/^{30}\text{Si}$ and $^{11}\text{B}/^{30}\text{Si}$ ratios. The external reproducibility assessed by replicate measurements of NBS610 and GB4 reference glasses was on average 1.1‰ for $^{11}\text{B}/^{10}\text{B}$, and 2.5‰ for $^{10}\text{B}/^{30}\text{Si}$ and $^{11}\text{B}/^{30}\text{Si}$. SIMS results were checked by comparison with TIMS data for two selected samples

Matrix effects

We observed strong matrix effects, which showed correlation with the molar $(\text{Na}+\text{Ca})/(\text{B}+\text{Al}+\text{Si})$ of bulk glass compositions. The matrix effects were effectively suppressed by using -60 V offset.

Conclusions

With matrix effects removed, $^{11}\text{B}/^{10}\text{B}$ in all the glasses were the same, within the analytical uncertainty. We did not observe any significant two-liquid $^{11}\text{B}\text{-}^{10}\text{B}$ fractionation.

References

Veksler I.V., Dorfman A.M., Dingwell D.B. and Zotov N. (2002) *Geochim. Cosmochim. Acta*, in press.

$\delta^{44}\text{Ca}$, $\delta^{18}\text{O}$ and Mg/Ca ratios Reveal Sea Surface Temperature (SST) and Sea Surface Salinity (SSS) Variations during the Emergence of the Central American Isthmus

N. GUSSONE¹, A. EISENHAEUER¹, G. HAUG²,
R. TIEDEMANN¹, A. MÜLLER¹, A. HEUSER¹, B. BOCK¹
AND TH.F. NÄGLER³

¹ GEOMAR Forschungszentrum für marine
Geowissenschaften, Wischhofstr.1-3 24148 Kiel Germany
(ngussone@geomar.de)

² Department of Earth Science ETH, Sonneggstrasse 5, CH-8092 Zürich Switzerland

³ Isotopengeologie, Mineralogisch-petrographisches Institut,
Universität Bern, Erlachstrasse 9a 3012 Bern Switzerland

$\delta^{18}\text{O}$ values increased by about 0.5 ‰ relative to the equatorial East Pacific values since about 4.6 Ma as a consequence of the emergence of the Central American Isthmus and the restricted surface water exchange through the Panama Strait the Caribbean. This increase in $\delta^{18}\text{O}$ can be interpreted either as an increase in Caribbean sea surface salinity (SSS) or a decrease in sea surface temperatures (SST) (Haug et al 2000).

In order to evaluate this problem we measured the $\delta^{44}\text{Ca}$ and Mg/Ca ratios on *G. sacculifer* (Site 999) as two independent SST proxies. Although differences concerning absolute temperature calibration exist, the general pattern of both SST proxy records is very similar indicating a SST decrease of about 2 to 3 °C between 4.4 and 4.3 Ma followed by an increase of about 2 to 3 °C between 4.3 and 4.0 Ma.

Correcting the $\delta^{18}\text{O}$ record for this temperature change and assuming that changes in ice volume are negligible, the planktonic $\delta^{18}\text{O}$ -salinity signal decreases by about 0.4 ‰ between 4.5 and 4.3 Ma and increases by about 0.9 ‰ between 4.3 and 4.0 Ma in the Caribbean. We interpret therefore that the salinity of the Caribbean increased by about 1 ‰ in response to the emergence of the Isthmus. However, today the salinity contrast between the Caribbean and the Pacific is about 2 ‰. This larger difference can be explained by a decreased salinity of the East Pacific by about 1 ‰, due to enhanced precipitation after the closure of the Isthmus.

References

Haug, G., Tiedemann R., Zahn, R. Ravelo, A.C. (2001) Role of Panama uplift on oceanic freshwater balance. *Geology*, **29**, 3, 207-210

Näglér T., Eisenhauer A., Müller A., Hemleben C., and Kramers J. (2000) The $\delta^{44}\text{Ca}$ -temperature calibration on fossil and cultured *Globigerinoides sacculifer*: New tool for reconstruction of past sea surface temperatures. *Geochemistry, Geophysics, Geosystems* **1**(2000GC000091)

Chemical fractionations induced by irradiation in early solar materials : results from laboratory experiments

F. GUYOT¹, H. LEROUX², P. CARREZ², P. CORDIER²,
AND L. LEMELLE³

¹ IPGP, LMCP UMR 7590 4 place Jussieu 75005 Paris, France (guyot@lmcp.jussieu.fr)

² LSPES UPRESA 8008. Université des sciences et techniques de Lille, 59655 Villeneuve d'Ascq, France

³ Laboratoire des sciences de la Terre. ENS Lyon. 46, allée d'Italie 69007 Lyon, France

Mineral phases from circumstellar environments are subjected to irradiation by energetic particles (ions, electrons, photons). Irradiation induces fractional volatilization of chemical elements in silicates; if large scale directional flow occurs, such as predicted by numerous models in the early solar system, then large scale chemical fractionations occur.

In series of electronic irradiation experiments carried out in both transmission and scanning electron microscopes at 300 kV and 30 kV respectively on olivines and pyroxenes, complex differential volatilization regimes have been evidenced as a function of electron fluences and accelerating voltages (Ph. Carrez et al., Phil Mag A, 2001, 81, 2823-2840; L. Lemelle, L. Beaunier, S. Borensztajn, M. Fialin, F. Guyot; an experimental study of the destabilization of olivine single crystal by 30 keV electron irradiation : a possible mechanism of space-weathering affecting interplanetary dust and planetary surfaces, submitted manuscript).

In most regimes at 300 kV, the order of electron-induced elemental loss from the silicate matrix is O>Mg>Si>Fe. An important mechanism related to that behaviour observed in the case of olivine irradiation at 300 kV is the creation of abundant Frenkel pairs in the material. In other regimes, particularly at lower accelerating voltages, the relative irradiation-induced volatilization order is O>Si>Mg,Fe.

We show that these results, particularly those obtained at 300 kV accelerating voltage, can be understood by combined effects of dielectric properties and bonding energies in the silicate materials which allow to derive tentative majority chemical trends in strongly irradiated materials in the early solar system characterized by:

- chemical reduction due to oxygen loss resulting in metal formation
- preferential loss of magnesium and enrichment in silicon, resulting in increasing the pyroxene to olivine ratio
- enrichment into high field strength lithophile elements
- depletion into alkaline and earth-alkaline elements.

Reactive Transport in Fractured Saprolite: Determining Diffusive Mass Transfer and Surface Reaction Kinetics Parameters

J. P. GWO¹, M. A. MAYES², AND P. M. JARDINE²

¹University of Maryland, Baltimore County, Baltimore, Maryland, USA (jgwo@umbc.edu)

²Oak Ridge National Laboratory, Oak Ridge, Tennessee, USA (mayesma@ornl.gov and jardinepm@ornl.gov)

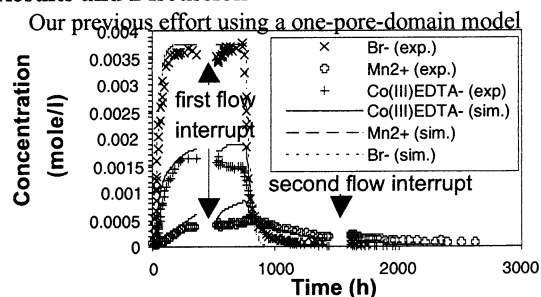
Diffusive Mass Transfer and Surface Reactions

Column miscible displacement experiments with flow interruptions have been used to determine diffusive mass transfer parameters for non-reactive tracers. These parameters, if corrected for the effect of molecular size, may be used to discern the contribution of diffusive mass transfer from that of surface reactions to solute breakthrough in fractured saprolite.

Methods

Simultaneous non-reactive and reactive tracer injections were performed on an undisturbed saprolite soil column obtained at Oak Ridge National Laboratory (Mayes et al., 2001). On the basis of our prior findings, this research uses a two-pore-domain reactive transport model to determine both diffusive mass transfer parameters and kinetic rate coefficients of surface reactions. The public domain HBGC123D code (<http://hbgc.esd.ornl.gov>) was modified to include both intra- and inter-domain mass transfer processes.

Results and Discussion



Our previous effort using a one-pore-domain model is shown above. The model clearly cannot explain the decrease of tracer concentration during flow interruptions and the tailing of tracers. The effect of inter-domain mass transfer on tracer breakthrough and its contribution relative to that of surface reactions will be discussed once we have the complete analysis of laboratory and modelling data.

Reference

- Mayes, M.A., P.M. Jardine, I.L. Larsen, S.C. Brooks, and S.E. Fendorf, 2001. Multispecies transport of metal-EDTA complexes and chromate through undisturbed columns of weathered fractured saprolite. *J. Contam. Hydrol.* 45, 243-265.